THE STRUCTURE OF HIGH SPEED FLUID JETS AND THEIR USE IN CUTTING VARIOUS SOIL AND MATERIAL TYPES

D. A. Summers, et al

Missouri University

Prepared for:

Army Mobility Equipment Research and Development Center

30 April 1975

The Structure of High Speed Fluid Jets and Their Use in Cutting Various Soil and Material Types

Final Report

by

D.A. Summers and J.L. Zakin

April 30, 1975

U.S. Army Mobility Equipment
Research and Development Center
R & D Procurement Office
Fort Belvoir, Virginia 22060

Contract Number DAAK02-74-C-0006

Rock Mechanics and Explosives Research Center
University of Missouri-Rolla, Rolla, Mo. 65401

FOREWORD

This report was prepared by the Rock Mechanics and Explosives Research Center, University of Missouri-Rolla, Rolla, Missouri under USAMERDC Contract No. DAAK02-74-C-0006. It was administered under the technical direction of Dr. David Heberlein. Mr. Arnold F. Harpine was the Contracting Officer.

This report is a summary of the work recently completed under this contract for the period from August 13, 1973 to September 30, 1974.

This program was carried out in part at the test facility of the McCartney Manufacturing Company, Inc., of Baxter Springs, Kansas. We are indebted to Mr. O.M. Walstad, Vice President of the company, for his assistance, advise, and encouragement and to his staff for their co-operation.

Appreciation is also extended to Dr. I. Radin, Mr. S.H.R. Raghavan and Mr. M. Hanshaw who assisted with the experimental aspects of the program. Components of the test equipment were constructed by Mr. B. Hale, Senior Laboratory Mechanic, including the nozzles used in the UMR components of the study.

The assistance of Mr. P.L. du Brow of Nalco Chemical Company is also acknowledged.

The fact that certain products referred to herein were used in this investigation is not to be considered an endorsement of these products by either the University of Missouri-Rolla or the U.S. Army.

SUMMARY

This report describes an investigation into the effect of fluid additives upon the structure of high speed water jets, and the resulting change in the cutting ability of the jets when such additives are used.

A literature review indicates that the effects of change in jet viscosity and surface tension upon jet structure are reduced with increase in jet velocity, and that while increasing jet viscosity improves jet cohesion, it reduces jet cutting ability. For this reason the study was directed towards the effect of viscoelastic additives, polymerized ethylene oxide and polyacrylamides, the results from which were compared with results from nonionic soaps and guar gum. The viscoelastic additives were found to give improved jet cohesion. Photographic analysis of jet structure indicated that the most cohesive jet was the polymerized ethylene oxide; however, tests on various soil types suggested that a Nalco polyacrylamide was superior for that application.

Cutting tests on soils indicated that, for effective soil removal at a distance of 6 ft. from the nozzle, a nozzle diameter in excess of 0.04 in. should be used, and meaningful results could then be achieved with jet pressures of 2500 p.s.i.

TABLE OF CONTENTS

LIST OF ILLUSTRATIONS

List of Illustrations (cont.)

List of Illustrations (cont.)

List of Illustrations (cont.)

List of Illustrations (cont.)

List of Illustrations (cont.)

List of Illustrations (cont.)

LIST OF TABLES

CHAPTER 1

Introduction

The use of water to remove natural and artificial barriers is as old as the earth itself, but its value as a simple yet effective tool has been demonstrated as recently as the Yom Kippur War of 1973. Interviewed in Al Akhbar, the Egyptian Chief of Staff, Lieutenant-General Shazli is quoted as follows:

> Dayan had made his statement (that any Egyptian attack across the Suez Canal would be finished in twenty-four hours), I believed on the basis of calculations that our engineers would need twenty-four hours to establish bridges and that heavy equipment (such as a substantial Egyptian tank force) could not be got across the canal inside forty-eight hours--allowing enough time for the arrival at the front of the Israeli armoured reserves...
>
> The problem was the sand barrier. To make a single hole about twenty feet across in this barrier (the minimum to get tanks through easily) would, we calculated, mean removing about 1,500 cubic yards of sand. And, we needed to open sixty such holes, on the east bank--90,000 cubic yards of sand. You must also remember that we ourselves had built a sand embankment over the past six years to guard against a surprise enemy attack. This doubled our problem.
>
> "Our first idea was to use explosives," Shazli said. Ismail adds the detail: "In the course of our experiments for breaking down these barriers we had tried guns of all calibres but we did not get what we hoped for." Shazli continued: "We stuck to explosives until mid-1971, when a young officer in the engineers suggested that we use water under pressure. This proved to be a superior method, making it possible for us to open holes in a period of three to five hours." With bulldozers or explosives it would have taken twice as long. (Ref. 1).

Water has been in use as an excavating tool from the time of the Ancient Egyptians (Ref. 2), but it has only been since 1852 that the jets have been produced under an artificial head, rather than using the force of gravity as a power source (Ref. 3). Hydraulic mining or "booming"

has been used to extract minerals from surface deposits since that time and within the last 50 years water jets have also been used to extract coal and other materials in underground mines (Ref. 4).

Mining operations have, in general, used low pressure (up to 2,000 p.s.i.), high volume (200 gal./min.) flows which have allowed the monitor and operator to be located up to 40 ft. from the coal being mined. This has a particular advantage in mining where the removal of the supporting coal will lead to the eventual collapse of the roof. The remote location of the jet source thus makes the method inherently much safer.

In surface work where the equipment must be made more mobile, while at the same time retaining the distance of throw, flow rates may be lower and pressures may be higher. In order to improve jet stability and, thus, increase the effective distance of the jet, chemical additives have been employed. The addition of 200 p.p.m. of the high polymer, Polyox (polymerized ethylene oxide), has been successfully used for example by the New York Fire Department to increase the performance of fire hoses (Ref. 5). There have been a number of studies of the variables affecting jet structure for low pressure jets. Some of these will be reviewed in the Appendix. The structure and stability of water jets at higher pressures has been studied in less detail.

The use of water jets to wash away earthen embankments illustrates one application of military importance. A second application is as an innovative means of exposing and potentially neutralizing landmines. A recent development of the Israeli Army is a device which can lay up to 1,000 mines to depths of 1 to 1.5 ft. in an hour (Ref. 6), requiring that equipment be developed which can match this in terms of mine exposure if not neutralization.

The need for improved jet coherence is apparent if one considers that for military use the nozzlemust be held at some distance from the target surface to provide a measure of protection from any mine detonation. At the same time the vehicle must be self contained and must, therefore, use the minimum amount of fluid necessary. These requirements led to inclusion of studies of the effects of addition of polymers and other additives to high pressure water jets in this work.

CHAPTER 2

Jet Structure Studies

Background

Previous investigators of coherent length of turbulent liquid jets emerging into stagnant air have generally reported results in the form:

$$\frac{L_B}{D\ WE^{1/2}} = \frac{C}{RE^n}$$

where L_B is breakup length of the jet, D is the nozzle diameter, WE = Weber number =

$$\frac{DV^2\rho}{\sigma}$$

(ρ is density, σ is surface tension and V is jet velocity at the nozzle), RE = Reynolds number =

$$\frac{DV\rho}{\mu}$$

(μ is jet fluid viscosity), and C and n are constants. Reported values of n are 0 in the plateau region (below 40,000 Reynolds number) (Ref. 7), 3/8 in the intermediate region (Ref. 8) (between 40,000 and 100,000 or higher Reynolds number)* and 2 at higher Reynolds numbers, above 80,000 (Ref. 9).

The variables affecting the coherent length are: (1) nozzle design, (2) nozzle diameter, (3) nozzle pressure (or fluid velocity), (4) jet fluid properties (density, viscosity, surface tension and viscoelasticity), (5) properties of the ambient fluid, (6) the steadiness of the jet flow, and (7) nozzle velocity.

In the present study two nozzle designs were used, a conventional design in the experiments at UMR with pump pressures of 2,500 to 10,000 p.s.i. as described in Appendix I and II and a proprietary design in the experiments

*Miesse proposed the value of 5/8 based on data for RE = 10^4 to 3.3×10^5, but the bulk of it is between 4×10^4 and 10^5.

at McCartney* at pump pressures of 20,000 to 45,000 p.s.i. All jet studies were made with water jets extruding into ambient air. A number of additives which impart viscoelastic properties to the fluid were studied (Table I.) These additives have relatively small effects on water surface tension or viscosity at the concentrations used and practically no effect on density. The jets were not pulsed other than by the variations in pressure induced when the driving pistons of the pumps changed direction and the nozzles were clamped stationary.

Thus, in this study the variables examined were nozzle diameter and pressure and the viscoelastic properties of the jet fluid.

Measurement Techniques

Previous research on jet structure has mainly been concerned with studies at lower jet velocities and little research has been carried out at the higher velocities associated with jet pressures above 4,000 p.s.i. and especially above 10,000 p.s.i. The jet disruption at such velocities is normally brought about by aerodynamic forces which are initiated at the nozzle exit. The jet is eroded from the outer surface radially inward and the central core is generally concealed behind the shroud of atomized fluid already separated from the jet surface.

Previous investigators have tried several techniques in order to penetrate this barrier with the emphasis in Soviet literature being given to the electrical contact method which is described in Appendix I. A critique of this technique is given in this Appendix, based on contemporary Soviet research and the conclusions drawn are reinforced by the results of Heubner's work on charged liquid jets (Ref. 10). The major criticism is that jet stability is reduced with application of a charge to the jet, an effect induced in part because charging a jet induces lateral velocity components within the jet structure. For this reason it was decided that the electrical contact method would not provide satisfactory results.

Leach and Walker (Ref. 11) have studied jet structure using high speed photography using spark, flash tube and x-ray illumination. Of the three methods, the speed photography with a flash tube gave the greatest detail. All jet coherence measurements at

*McCartney Manufacturing Company, Baxter Springs, KS.

Table I. Additives Tested

Additive	Manufacturer	Composition	Molecular Weight*	Intrinsic Viscosity deciliters/gram	Comments
Polyox FRA	Union Carbide Co. P.O. Box 8004 S. Charleston, WV 25303	polyethylene oxide	7×10^{6}**	9.5	-
Separan AP 273	Dow Chemical Co. Midland, Michigan 48640	polyacrylamide	7×10^{6}	25.6	anionic due to presence of some copolymer
Separan AP 30	Dow Chemical Co. Midland, Michigan 48640	polyacrylamide	2.7×10^{6}	19.6	slightly anionic due to presence of some copolymer
Nalco B129	Nalco Chemical Co. 6216 W. 66th Place Chicago, IL 60638	polyacrylamide	-	-	-

Table I.(cont.)

Additive	Manufacturer	Composition	Molecular Weight*	Intrinsic Viscosity deciliters/ gram	Comments
Nalco 625	Nalco Chemical Co. 6216 W. 66th Place Chicago, IL 60638	polyacrylamide	-	-	emulsion: one phase is polymer dispersed in oil which is dispersed in water. Dissolves rapidly in contact with large amounts of water.
Polyhall 654	Stein-Hall & Co. 605 3rd. Ave. New York, NY 10016	polyacrylamide	$4\text{-}5 \times 10^6$	24.6	-
Jaguar A-20D	Stein-Hall & Co. 605 3rd. Ave. New York, NY 10016	guar gum	220,000	-	natural vegetable hydrocol-loid, resists mechanical degradation

Table I.(cont.)

Additive	Manufacturer	Composition	Molecular Weight*	Intrinsic Viscosity deciliters/ grams	Comments
Alfonic 1214-60	Continental Oil Co. P.O. Box 727 Westlake, LA 70669	$C_{12}H_{25}(OCH_2CH_2)_6OH$	-	-	non-ionic surfactant
α-Naphthol (1 part)	Eastman Kodak Co. Rochester, NY 14650	$C_{10}H_7OH$	-	-	complex soap
Cetyltrimethylammonium bromide (2 parts)	Eastman Kodak Co. Rochester, NY 14650	$CH_3(CH_2)_{15}N(CH_3)_3Br$	-	-	complex soap

* from manufacturer's literature

** the sample had a low intrinsic viscosity indicating that it had degraded to a much lower molecular weight in storage.

McCartney were made using high speed photography with a single flash stroboscopic source placed to give either front or back lighting. Details of the experimental technique are given in Appendix II.

In addition, pressure profile measurements were made at UMR at fixed locations down the jet axis. Details of this method are given in Appendix II.

In the following section selected pressure profile results and photographic results are shown to illustrate the trends observed with variations in nozzle diameter, pressure and jet fluid additives.

Results and Discussion

1. Pressure Profile Measurements

a. Pure Water Jets.* Figures 1 to 6 show pressure profile measurements of water jets at various standoff distances. Ordinate lengths equivalent to 1,000 p.s.i. and (jet profile) distances of 0.1 in. are shown on the figures.

Examination of Figures 4 to 6 obtained with a 0.06-in. diameter nozzle shows that increased nozzle pressure caused a significant increase in impact pressure at all standoff positions. In general jet coherency was good, with profiles generally less than 0.1 in. in diameter. Similar measurements on the 0.04-in. jet show much lower impact pressures at all standoff positions. In fact, no significant readings could be obtained at distances greater than 18 in., even at 10,000 p.s.i. jet pressure. At 18 in. there is little effect of nozzle pressure on impact pressure indicating jet disruption.

From these results we can conclude that for these jet diameters and high jet Reynolds numbers (about 260,000 to 450,000), pressure and especially nozzle diameter have significant effects on jet impact pressure and presumably on jet coherent length. The implications of this in terms of Equation 1 will be discussed at the end of this chapter.

The maximum impact pressure value decayed with distance. The data were fit with equations of the form $x=ax^b$ and $y=ae^{bx}$ where y is maximum impactpressure in k.s.i. and x is standoff distance from the nozzle in inches. The

*All jet fluid used at UMR also contained 8 percent Dromus B soluble oil, recommended by the pump manufacturer as a lubricant.

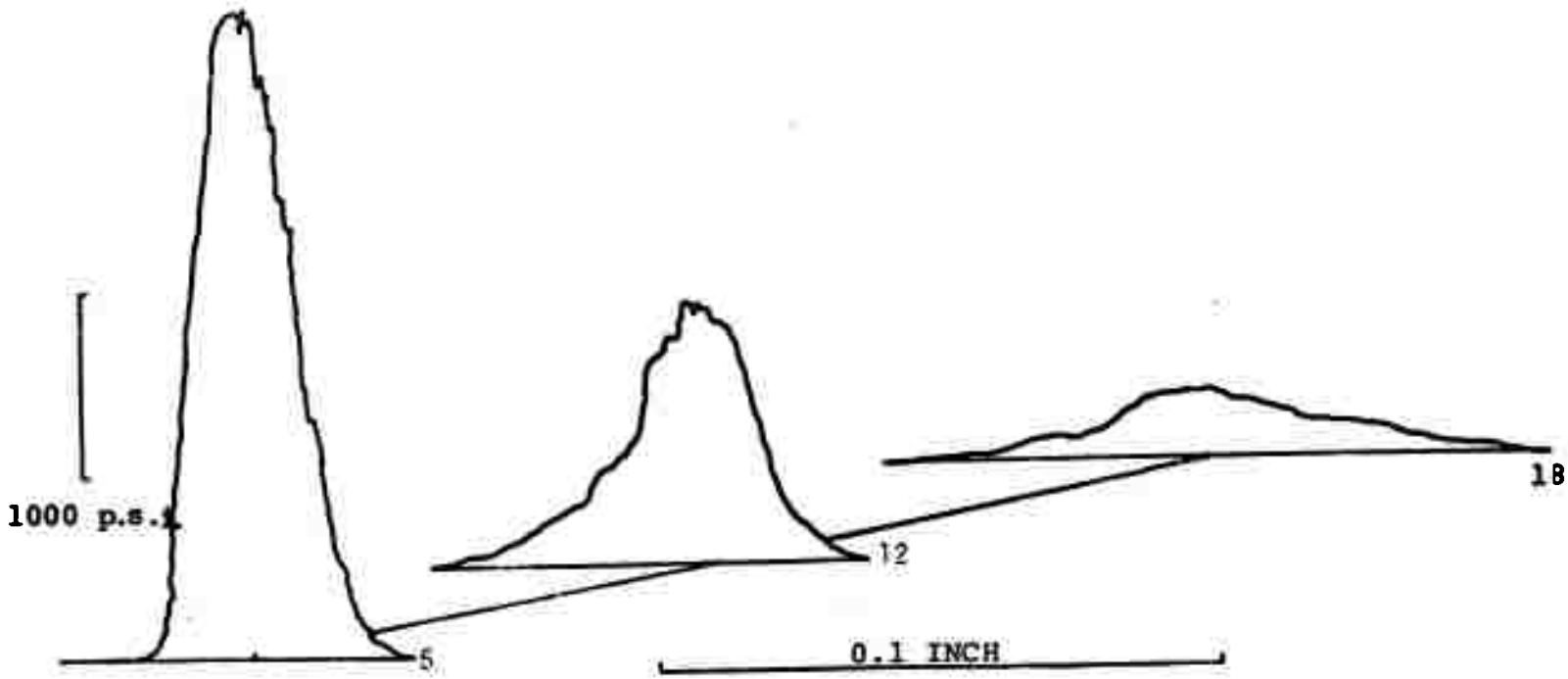

.02-in. probe
6000 p.s.i. .04-in. nozzle

Figure 1. Impact pressure profiles at various distances.

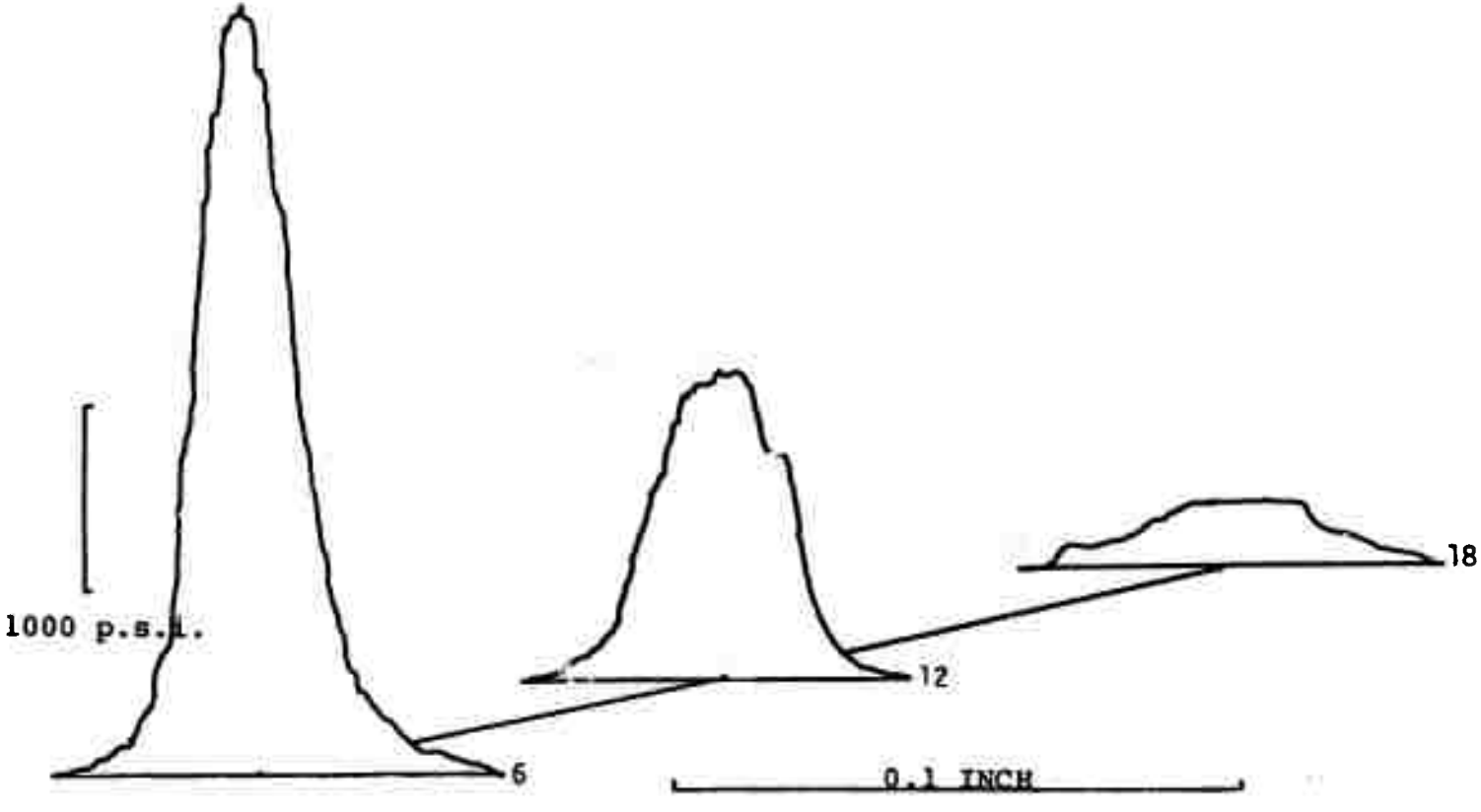

.02" probe
8000 p.s.i. .04" nozzle

Figure 2. Impact pressure profiles at various distances

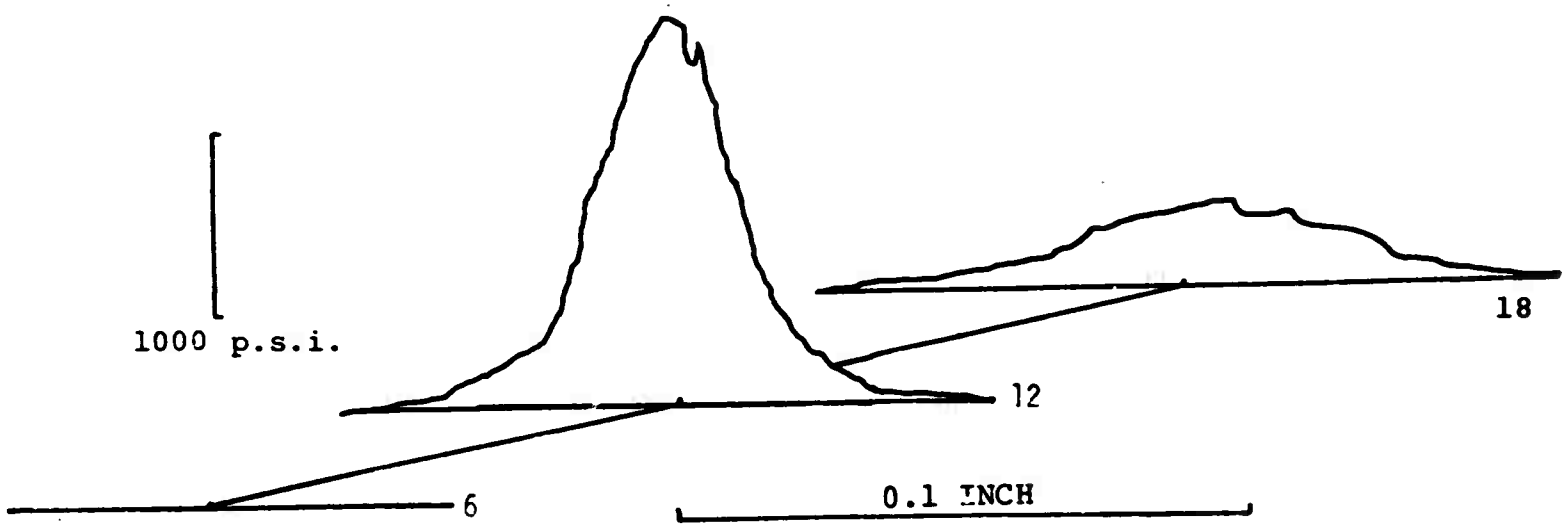

.02" probe
10,000 p.s.i. .04" nozzle

Figure 3. Impact pressure profiles at various distances

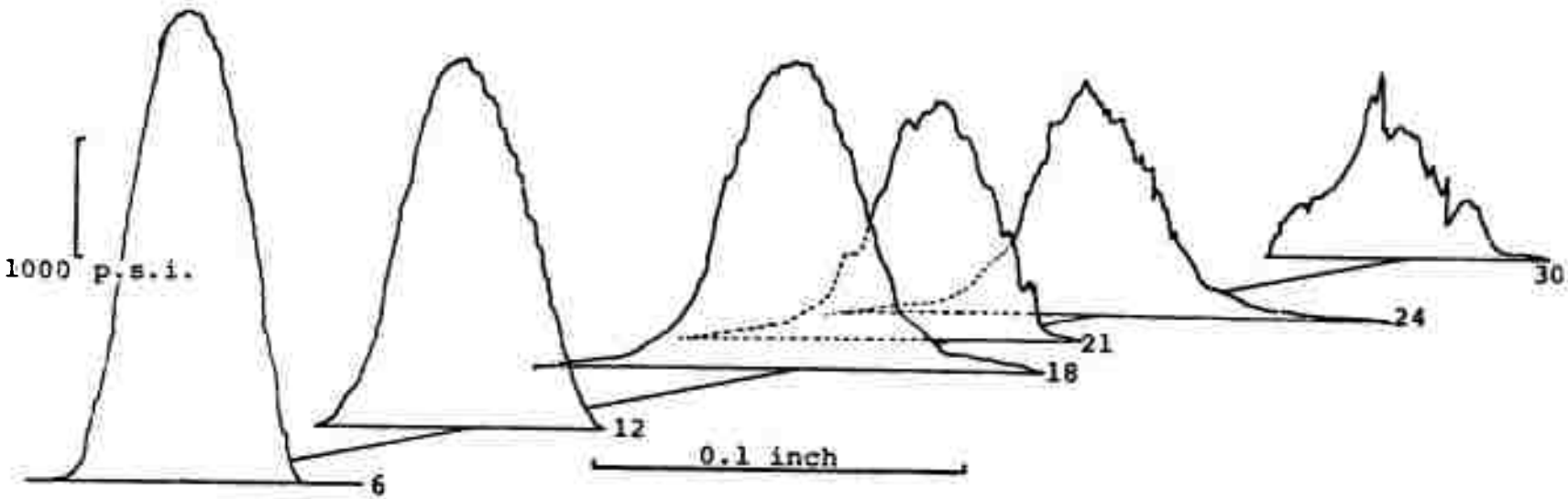

.02" probe
4000 p.s.i. .06" nozzle

Figure 4. Impact pressure profiles at various distances

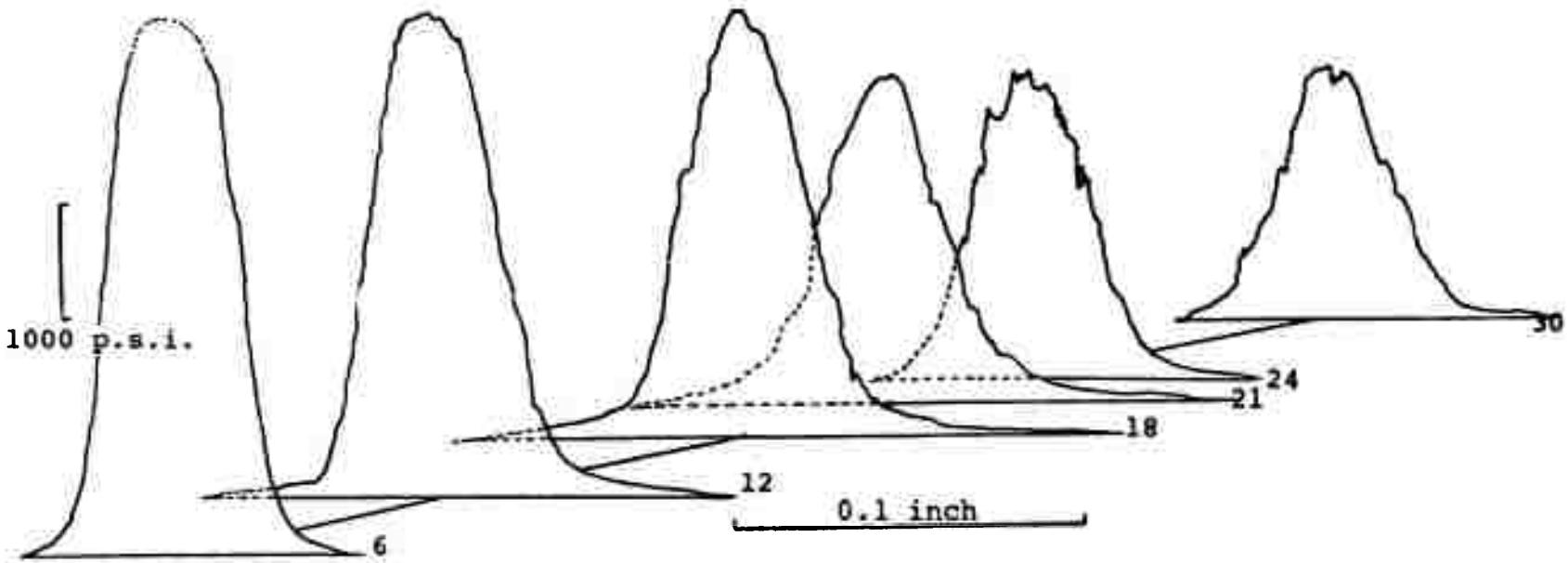

.02" probe
6000 p.s.i. .06" nozzle

Figure 5. Impact pressure profiles at various distances

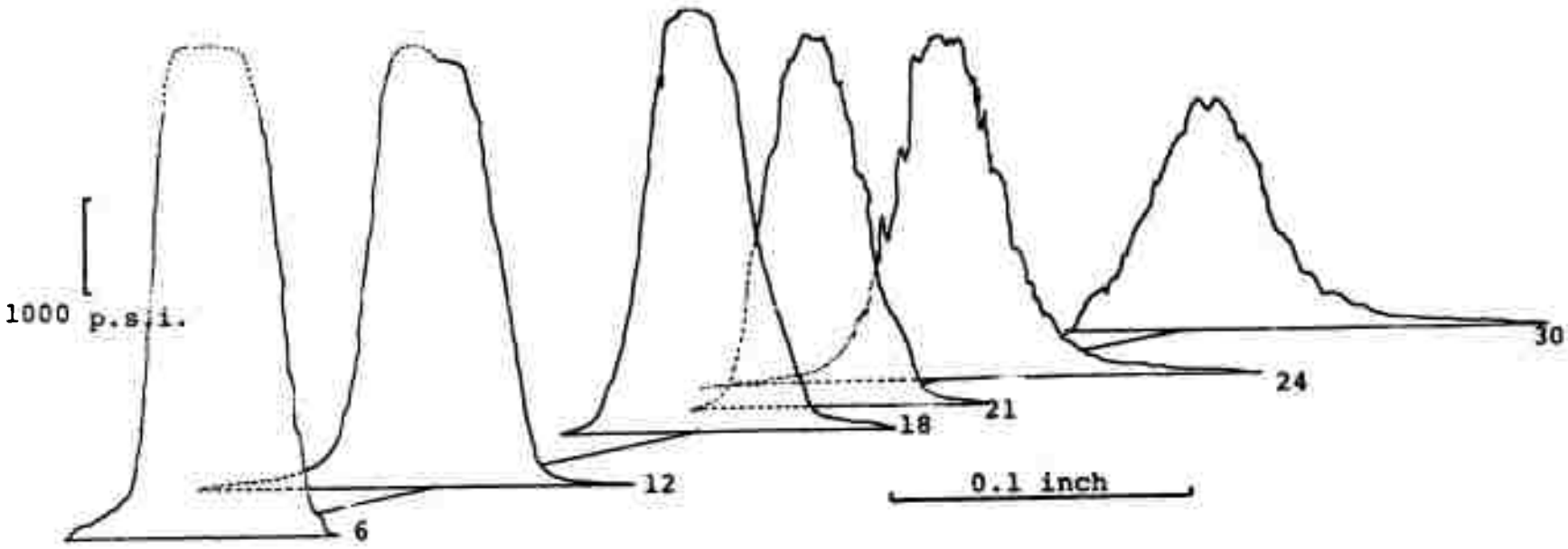

.02" probe
8000 p.s.i. .06" nozzle

Figure 6. Impact pressure profiles at various distances

latter equation gave a better fit for the data. Values of the constants "a" and "b" for the second equation are listed in Table II along with correlation coefficients. Both "a" and "b" vary with nozzle diameter. Values of "b" appear to be relatively independent of pressure as are values of "a" for the 0.06-in. nozzle. The latter may reflect the fact that the 0.06-in. jet was coherent throughout the range of standoff distances whereas the others were not.

If the analysis is carried a stage further, then a pressure effect does become apparent at points where jet disruption is postulated. The same regression function was calculated based on only three adjacent readings for each pressure and nozzle diameter set. By comparing the 6-, 12-, and 18-in., the 12-, 18-, and 24-in. and the 18-, 24-, and 30-in. data, an indication of change in the relationship with distance could be obtained (Table 2b). For data from the 0.06-in. diameter nozzle the changes are not great and no firm conclusions can be drawn, presumably because the jets are coherent throughout the standoff ranges studied. However, for the 0.04-in. nozzle diameter where jet disruption is postulated at the 18-in. station, it can be seen that the higher pressure jets decay more rapidly than those of smaller pressure. The same is true at the larger standoff distances for the 0.05-in. nozzle.

b. Jets with Viscoelastic Additives. In these early experiments, two high polymer additives were added to the jet fluid to determine their effect on the pressure profiles. The characteristics of the two additives, Stein Hall Jaguar AD 200 and Dow Separan AP 30 are listed in Table I. Their effect on the pressure profiles are shown in Figures 7 to 18.

The 0.04-in. -diameter jet was used for these measurements since jet coherence with this diameter was poor at 18 in. with water alone as the fluid, thus allowing improvements in jet coherence to be readily observed. No significant improvement was observed for the 100 p.p.m. Jaguar solutions at 6,000, 8,000, or 10,000 p.s.i. However, at a concentration of 500 p.p.m. Jaguar pressures attainable at 24 in. exceeded those at 18 in. at 100 p.p.m. at all three nozzle pressures. Some further improvement was observed with 2,500 p.p.m. Jaguar solutions but the changes were not marked. Solutions of 50 p.p.m. Dow Separan AP 30 gave impact pressures up to 24 in. which were a little lower than the 500 p.p.m. Jaguar solutions but which were far larger than the 100 p.p.m. Jaguar solutions. The AP 30 is a much higher molecular weight polymer than the Jaguar,

Table II.

a) Values for the constants in the expression $y = ae^{bx}$ describing decay in maximum jet pressure, y in k.s.i., with distance from the nozzle, x in inches, for pure water jets.

Nozzle diameter (inches)	Nozzle pressure (k.s.i.)	a	b	Correl. Coeff. R
0.04	6	11.68	-.19	.99
	8	15.20	-.21	.99
	10	40.10	-.25	.99+
0.05	4	6.39	-.06	.97
	6	8.85	-.07	.98
	8	18.84	-.14	.91
0.06	4	4.66	-.038	.99+
	6	5.72	-.032	.98
	8	6.23	-.029	.94

The Correlation coefficient, R, is calculated as:

$$R = b\left[\frac{n\Sigma x^2 - (\Sigma x)^2}{n\Sigma (\ln y)^2 - (\Sigma \ln y)^2}\right]^{1/2}$$

Table II

b) Values for the constants when three adjacent values only are considered.

Readings		Stations		Stations		Stations	
Nozzle diameter	Nozzle Pressure	6-12-18		12-18-24		18-24-30	
		a	b	a	b	a	b
04	6	11.68	-.19				
	8	15.20	-.21				
	10	40.10	-.25				
05	4	4.93	-.046	5.74	-.056	13.1	-.10
	6	6.82	-.053	9.17	-.072	16.6	-.10
	8	6.85	-.050	15.10	-.103	27.76	-.25
06	4	4.53	-.035	4.59	-.037	5.08	-.041
	6	5.01	-.019	6.57	-.038	7.28	-.042
	8	5.20	-.013	5.79	-.022	10.34	-.049

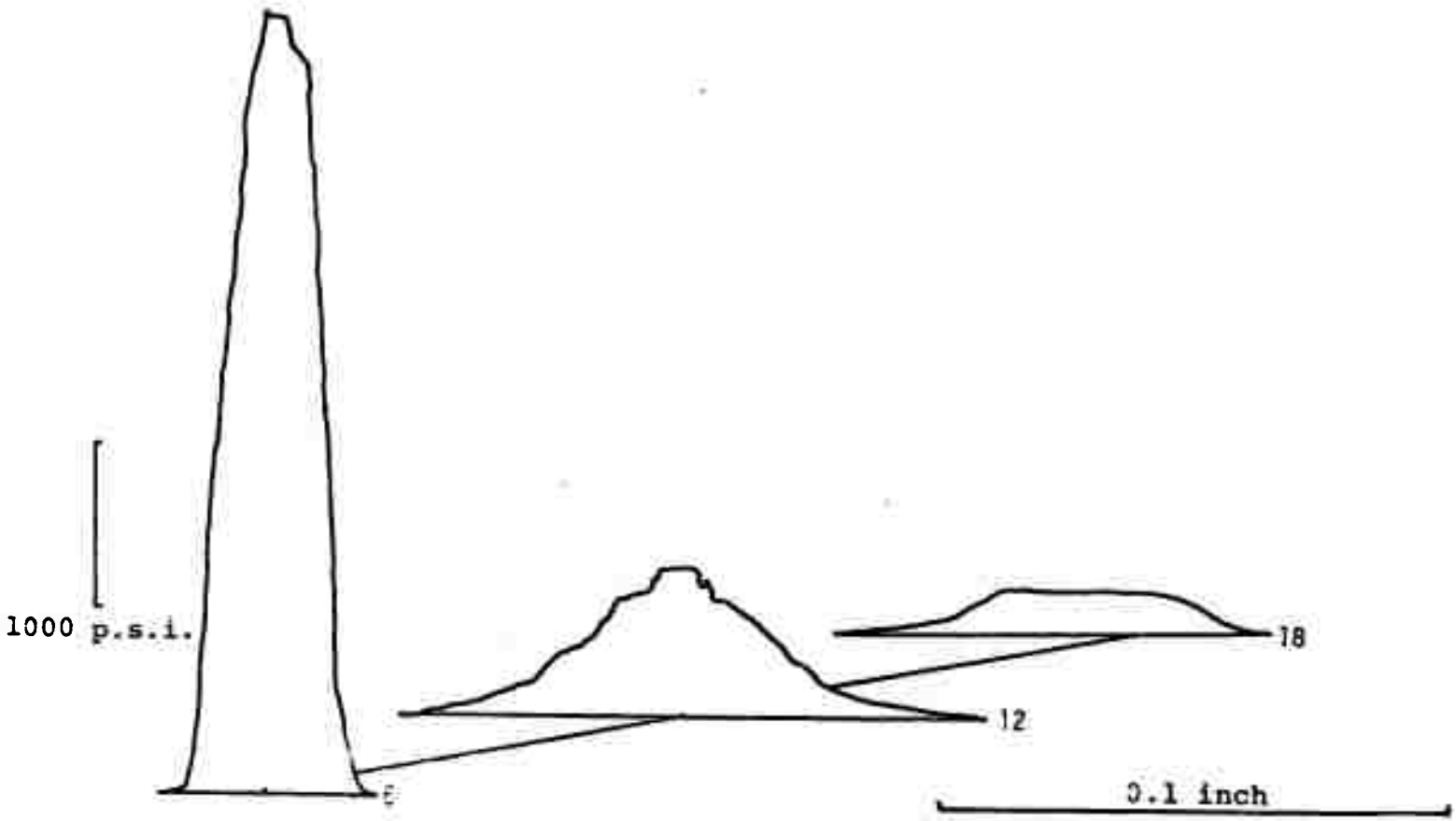

.02" probe
6000 p.s.i. .04" nozzle
+100 p.p.m. Jaguar

Figure 7. Pressure profiles at various distances

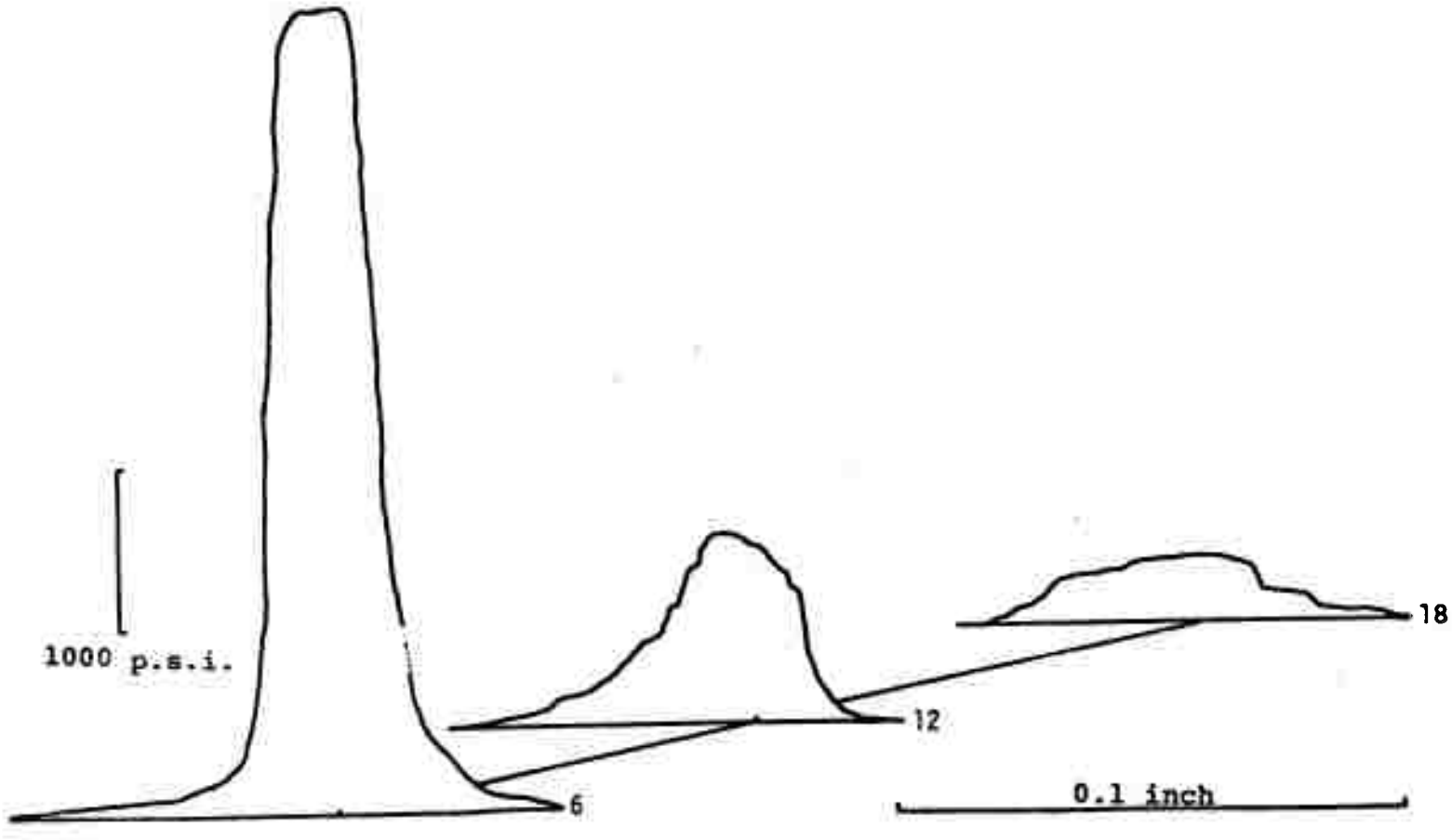

.02" probe
8000 p.s.i. .04" nozzle
+100 p.p.m. Jaguar

Figure 8. Pressure profiles at various distances

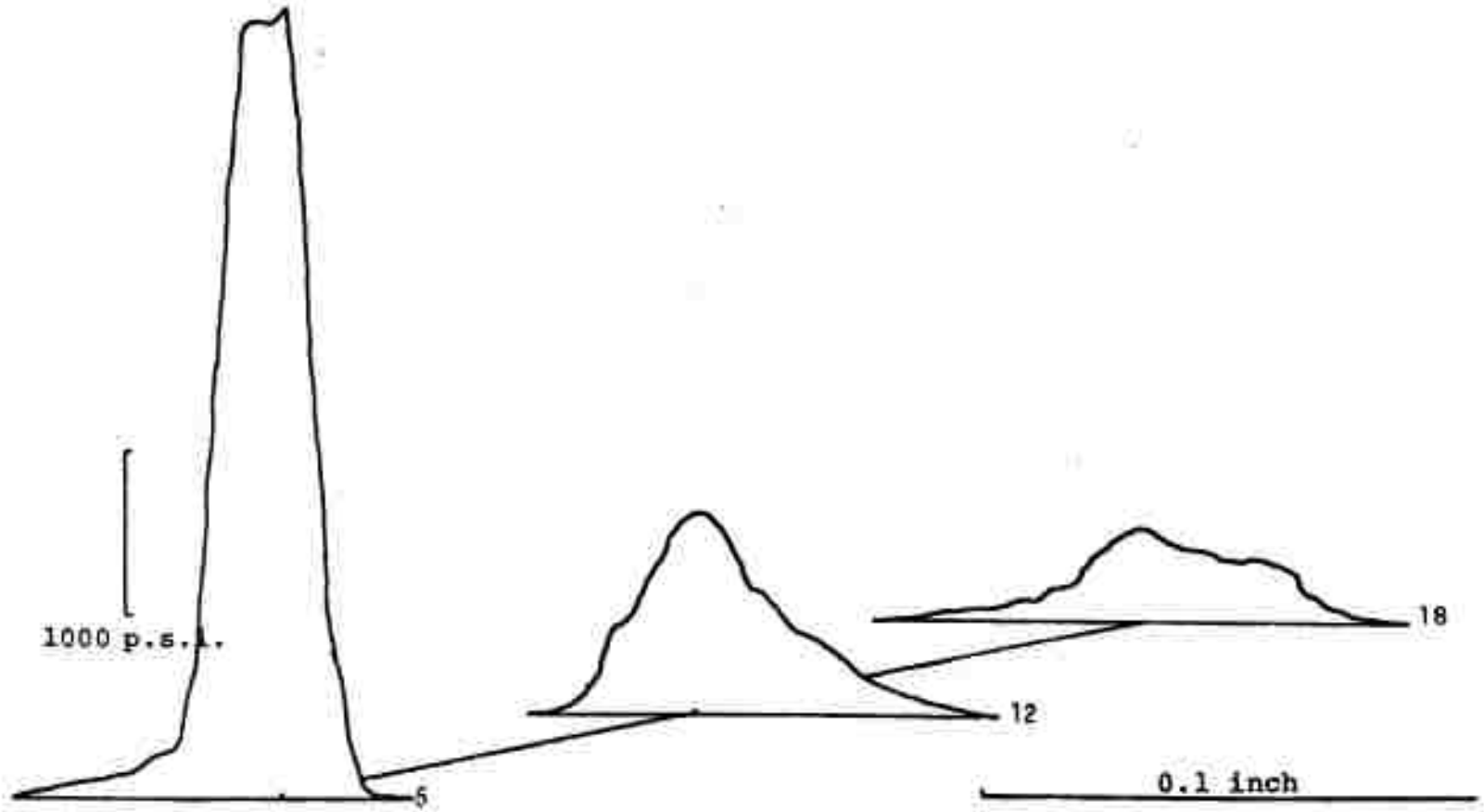

.02" probe
10,000 p.s.i. .04" nozzle
+100 p.p.m. Jaguar

Figure 9. Impact pressure profiles at various distances

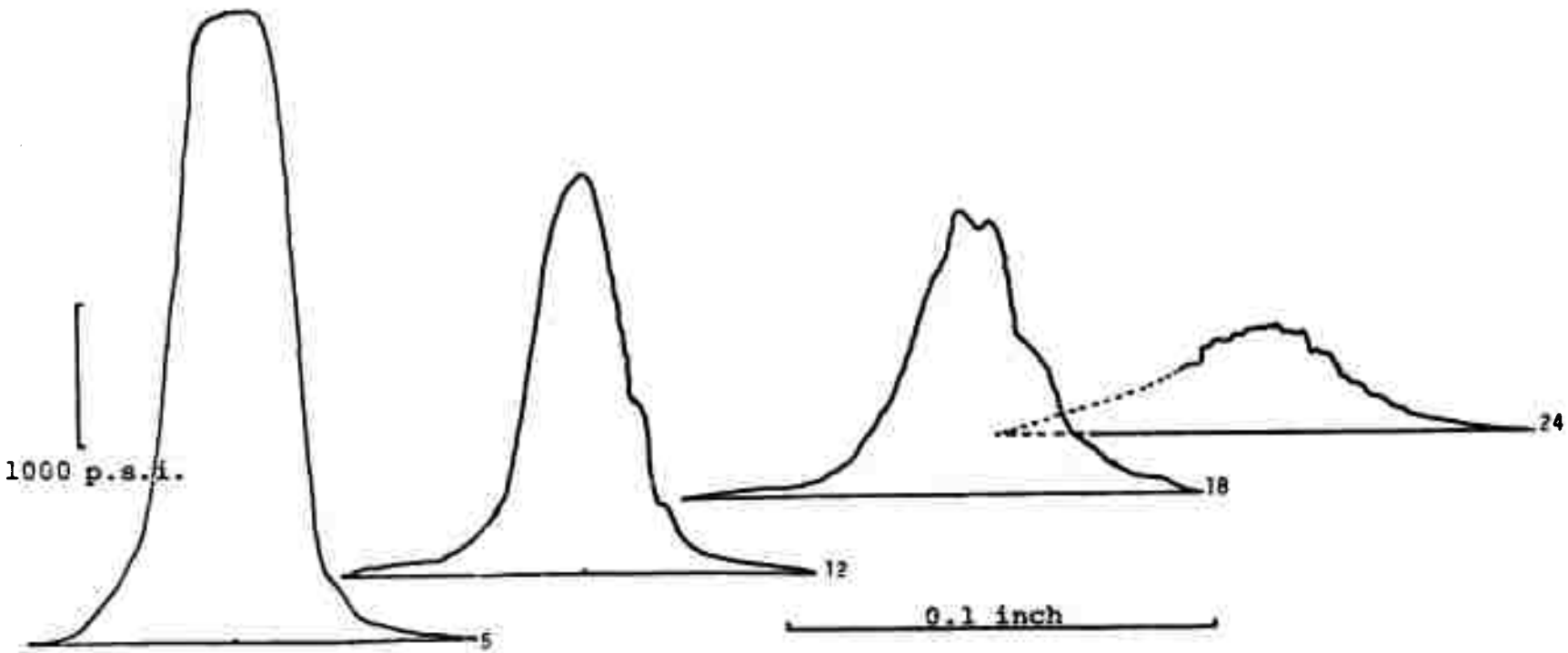

.02" probe
6000 p.s.i. .04" nozzle
+500 p.p.m. Jaguar

Figure 10. Impact pressure profiles at various distances

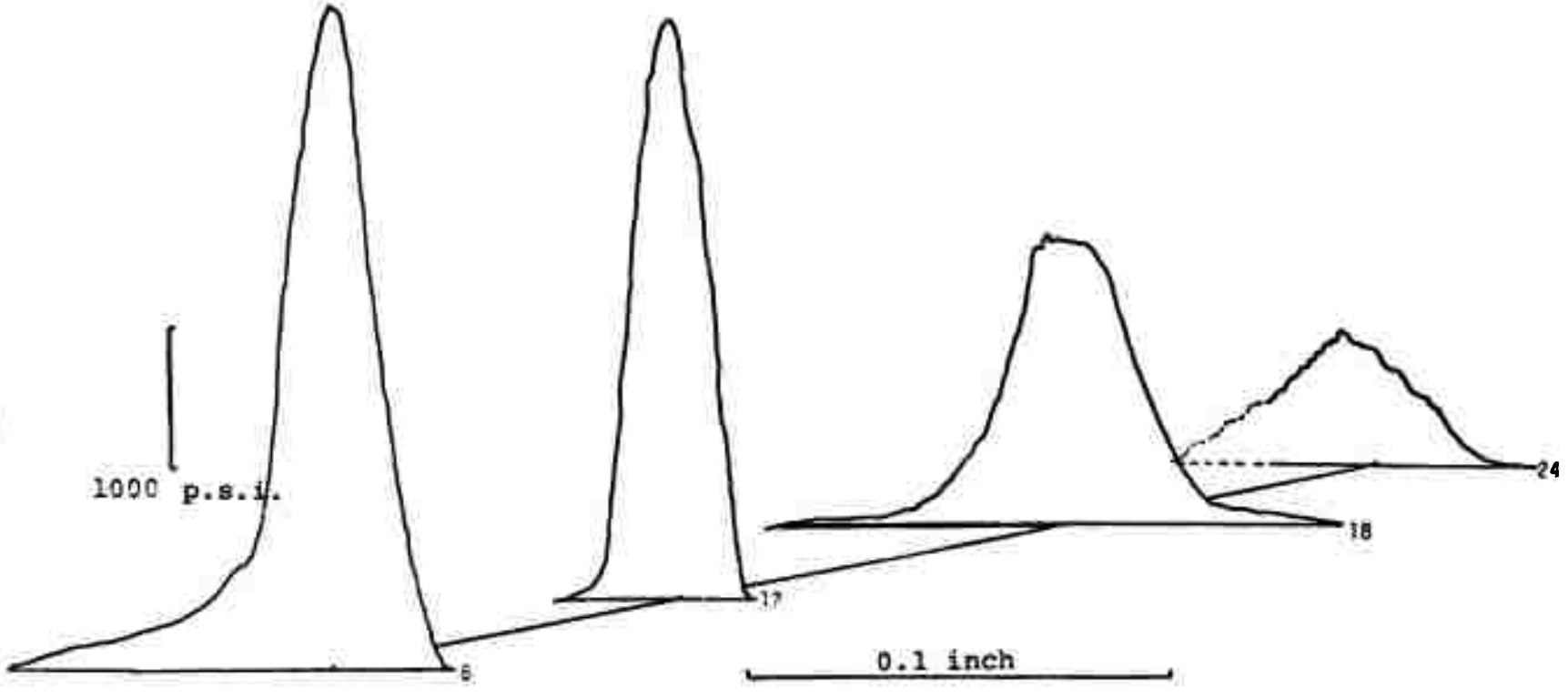

.02" probe
8000 p.s.i. .04" nozzle
+500 p.p.m. Jaguar

Figure 11. Impact pressure profiles at various distances

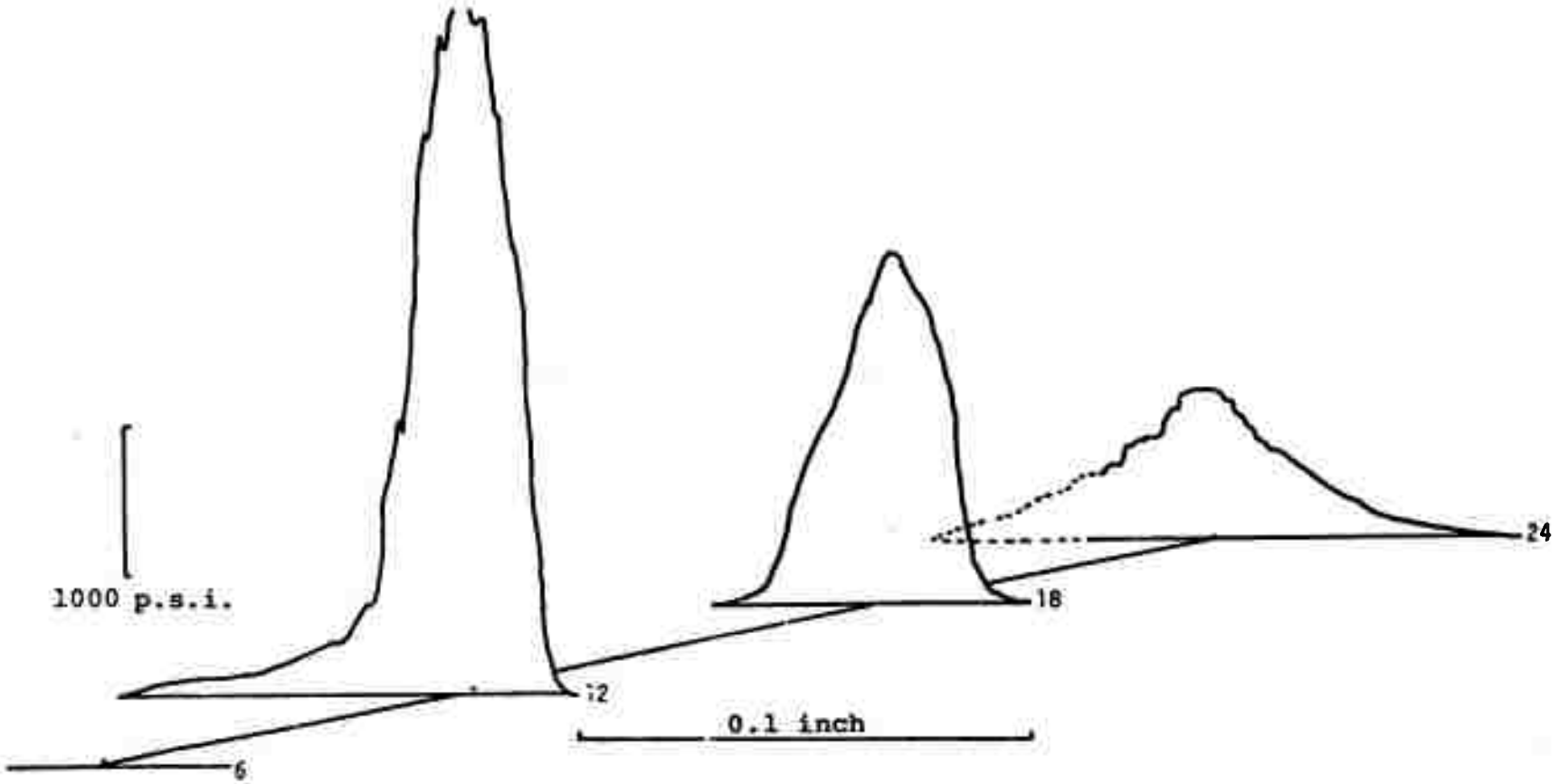

.02" probe
10,000 p.s.i. .04" nozzle
+500 p.p.m. Jaguar

Figure 12. Impact pressure profiles at various distances.

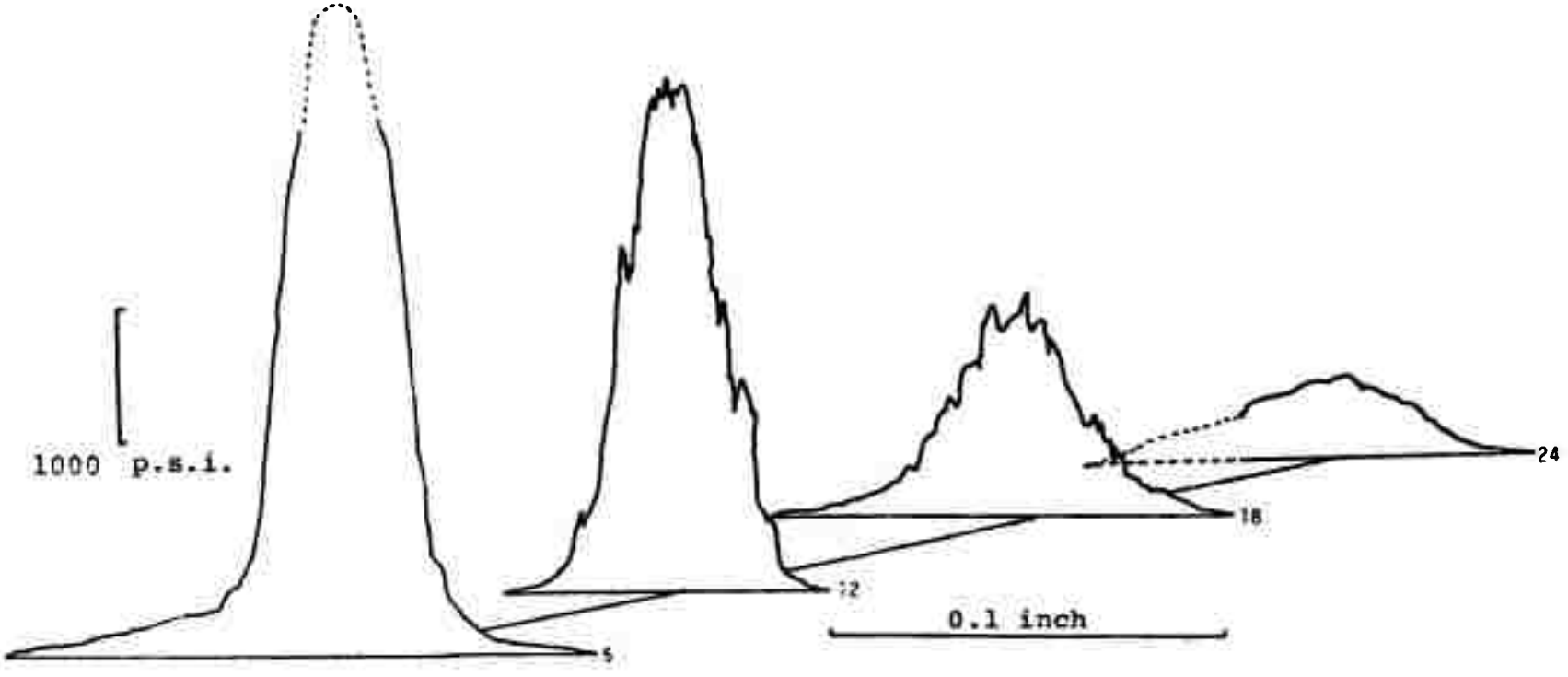

.02" probe
6000 p.s.i. .04" nozzle
+2500 p.p.m. Jaguar

Figure 13. Impact pressure profiles at various distances.

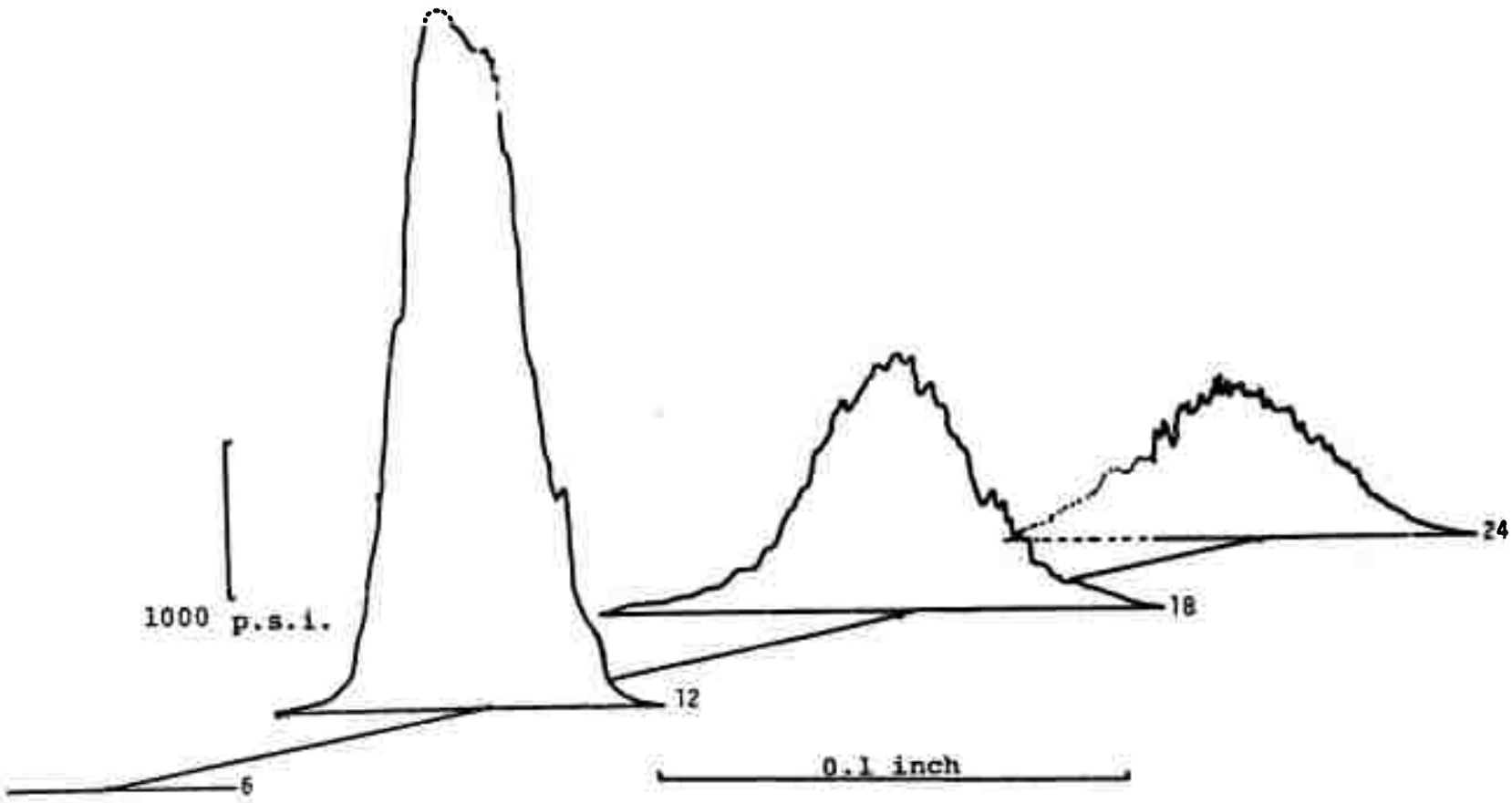

.02" probe
8000 p.s.i. .04" nozzle
+2500 p.p.m. Jaguar

Figure 14. Impact pressure profiles at various distances.

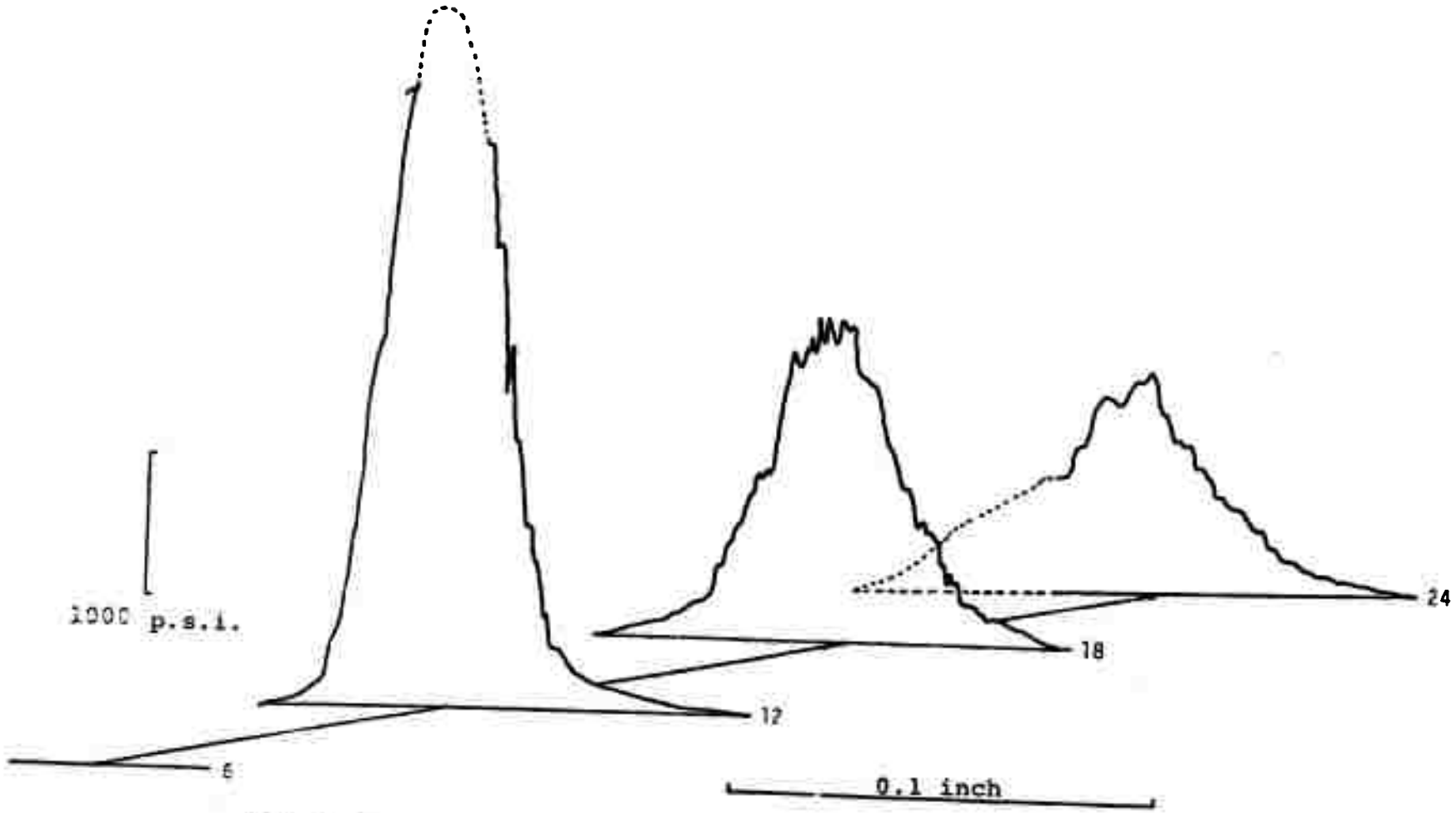

.02" probe
10,000 p.s.i. .04" nozzle
+2500 p.p.m. Jaguar

Figure 15. Impact pressure profiles at various distances.

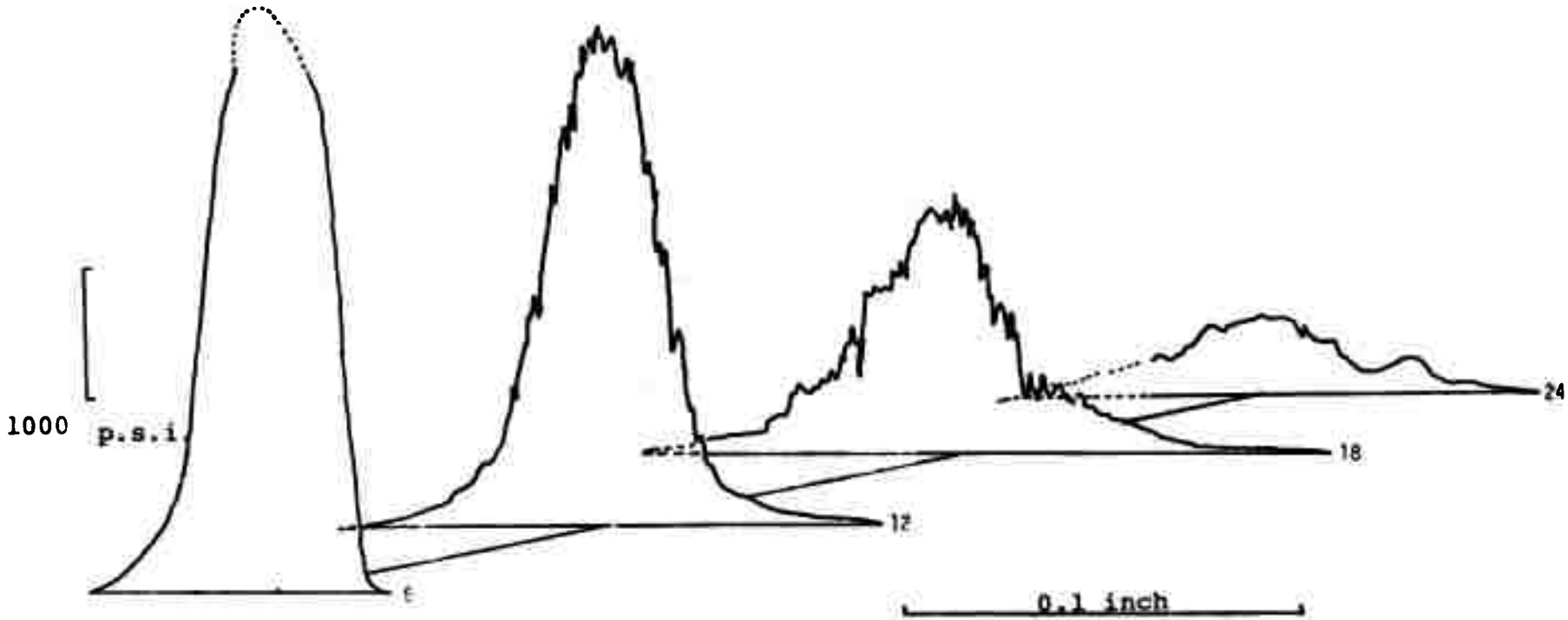

.02" probe
6000 p.s.i. .04" nozzle
+50 p.p.m. Dow AP 30 Polyacrylamide

Figure 16. Impact pressure profiles at various distances

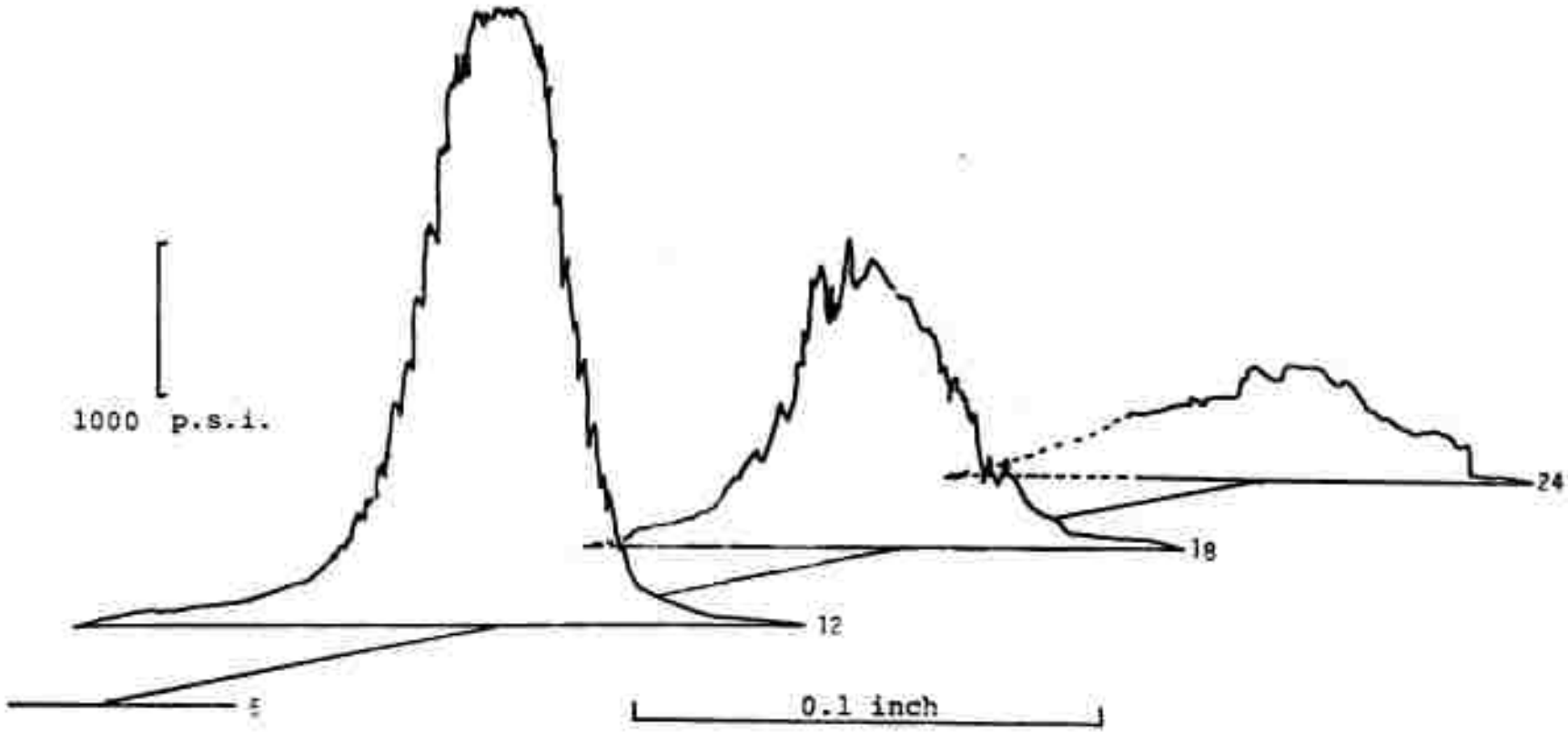

.02" probe
8000 p.s.i. .04" nozzle
+50 p.p.m. Dow AP 30 Polyacrylamide

Figure 17. Impact pressure profiles at various distances.

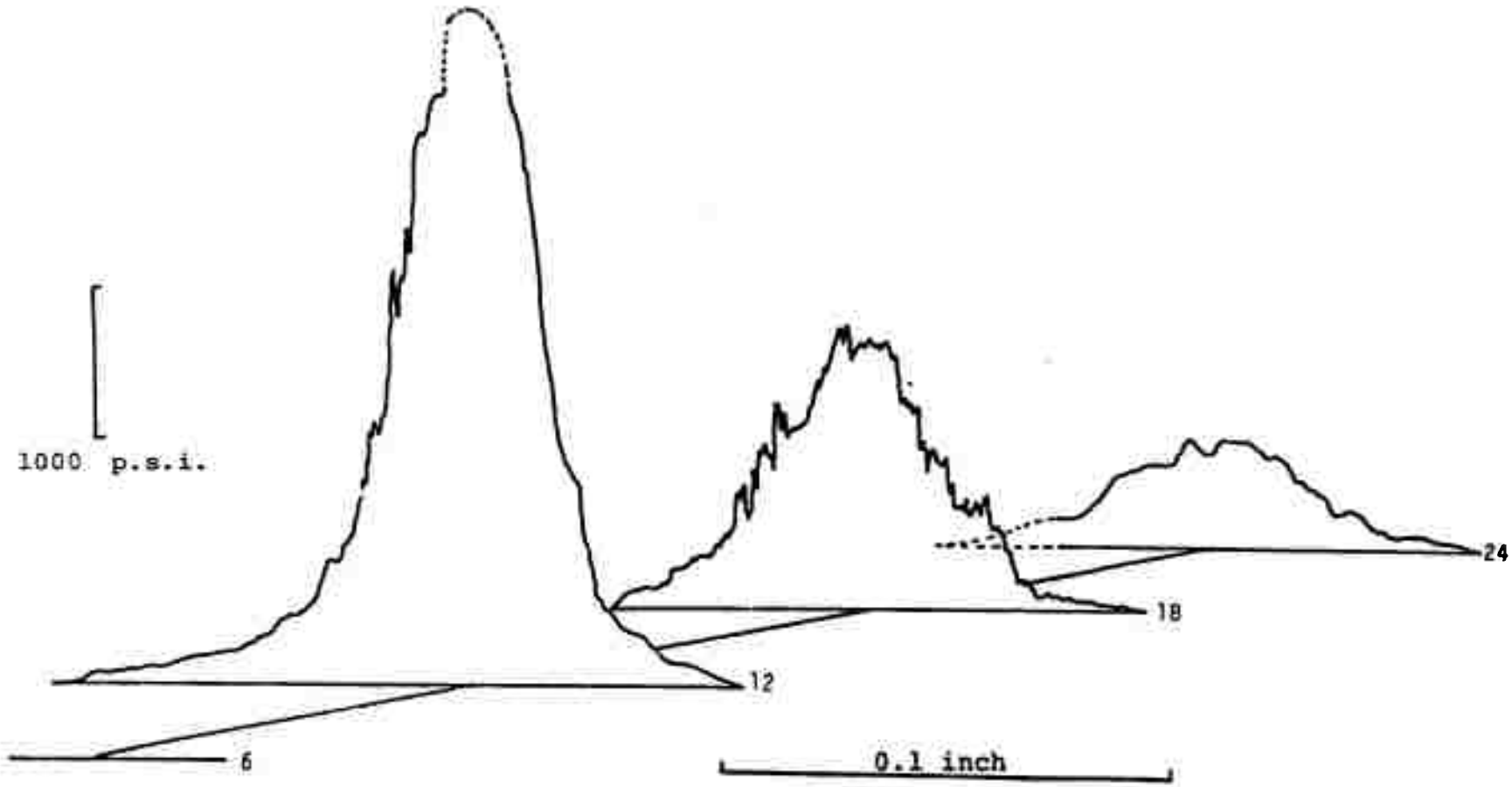

.02" probe
10,000 p.s.i. .04" nozzle
+50 p.p.m. Dow AP 30 Polyacrylamide

Figure 18. Impact pressure profiles at various distances.

and its (polyacrylamide) molecular structure is much more flexible than the Jaguar (guar gum-cellulose type chain) and, thus, imparts a greater viscoelastic character to the water solution at much lower concentrations than the Jaguar.

2. Photographic Studies

a. Pure Water Jets.* Figures 19 to 21 show back-lighted photographs of water jets using the McCartney 0.005- and 0.010-in. nozzles at 20,000 and 45,000 p.s.i. Other photographs with these nozzles were taken at 30,000 p.s.i. and with a 0.012-in. nozzle at all three pressures, but are not shown.

In rating the jet photographs for jet coherency, the back-lighted photographs were used wherever possible as these showed more detail of the jet structure and the coherence length could be more easily observed than with the front-lighted photographs where the atomized shroud made estimation of jet diameter and location of the end of the coherent jet difficult.

In the evaluation of the photographs taken of the jets in this aspect of the program two criteria of judgment, axial length and radial dispersion, were considered. These criteria were not always complementary and, as a result, an average rating, based on both results, was used. Although the criteria of judgment were somewhat subjective, due to variations in the quality of the photographs obtained, independent rankings by the two authors were in sufficient agreement that the conclusions described below could be drawn.

The relative ratings of the jet coherencies for water are listed in Table III. A rating of 1 was given to the most coherent and a rating of 9 to the least coherent jet. Also listed are the nominal Reynolds Numbers of the jet at the nozzle based on water density and viscosity.

Comparisons between the pure water photographs showed clear differences between the 0.005-in. jet and the two larger diameter jets. The structures of the 0.010- and 0.012-in. jets were more alike. The 0.010- and 0.012-in. jets were always coherent for a greater length than the 0.005-in. jets. The effect of pressure was not as obvious. Only small differences were observed as pressure was raised

*For the work at McCartney the water contained no other additives unless so stated.

Table III. Effect of Nozzle Size and Pressure on Jet Coherency

Pressure k.s.i.	Nozzle Diam in.	Nominal Reynolds Number	H_2O	Polyox 500	AP273 500	AP273 150	AP30 500	Nalco 625 1500	Nalco B129 500	Polyhall 654 500	Jag 500	Alfonic 1000
45	.012	210,000	2	2	6	6	4	2	4	2	4	3
30	.012	172,000	3	3	1	3	1	1	3	1	6	1
20	.012	140,000	4	1	2	2	3	4	1	3	5	2
45	.010	175,000	1	6	3	4	2	6	6	6	3	4
30	.010	143,000	-	4	5	5	5	3	5	5	2	5
20	.010	117,000	5	5	4	1	6	5	2	4	1	6
45	.005	87,500	8	9	8	8	9	9	9	7	8	7
30	.005	71,500	7	8	9	9	7	8	8	8	9	8
20	.005	58,500	6	7	7	7	8	7	7	9	7	9

Note:
The ranking was effected by ordering the photographs such that "1" denotes the "best" jet and "9" the "worst."

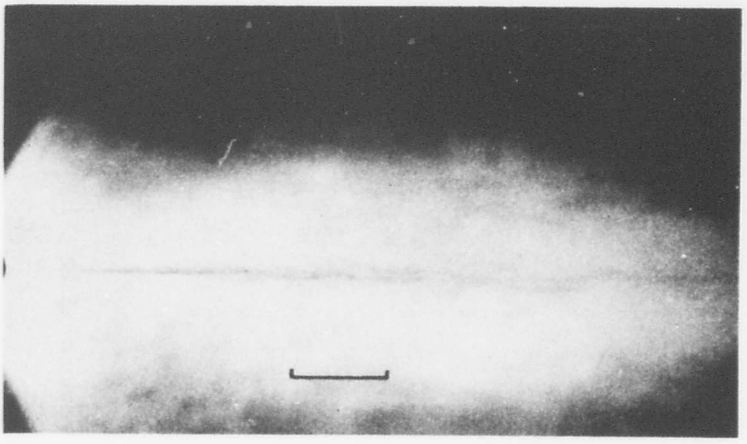

a) water at 20 k.s.i. 0.005-inch nozzle

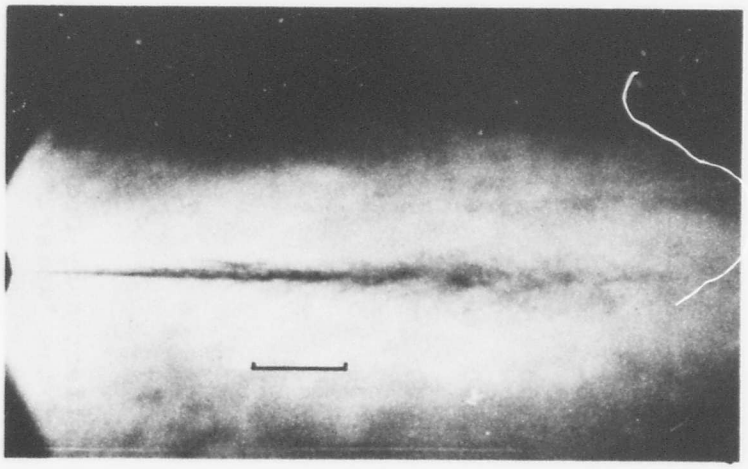

b) water at 45 k.s.i. 0.005-inch nozzle

Figure 19. Backlit photographs of fluid jets.
(The scale indicates a 1-inch length)

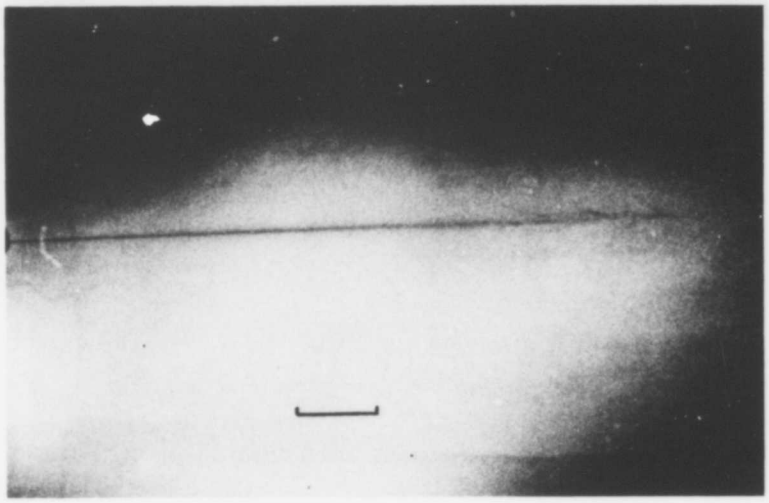

c) 500 p.p.m. Polyox 20 k.s.i. 0.005-inch nozzle

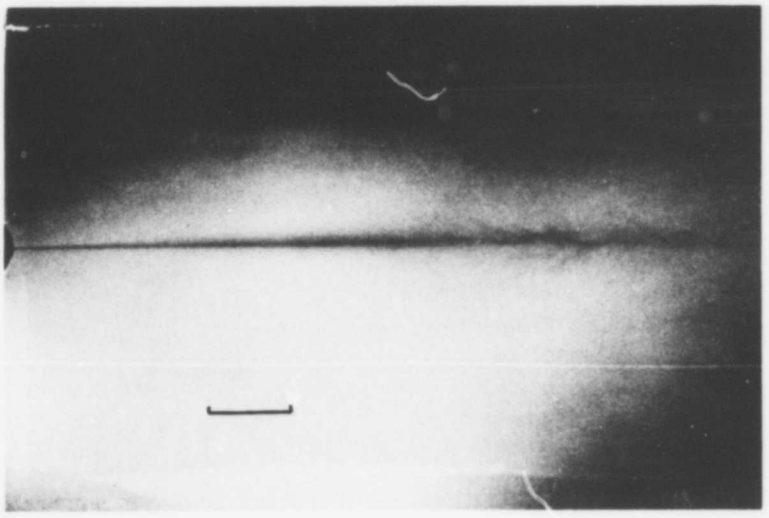

d) 500 p.p.m. Polyox 45 k.s.i. 0.005-inch nozzle

Figure 19. Backlit photographs of fluid jets (the scale indicates a 1-inch length)

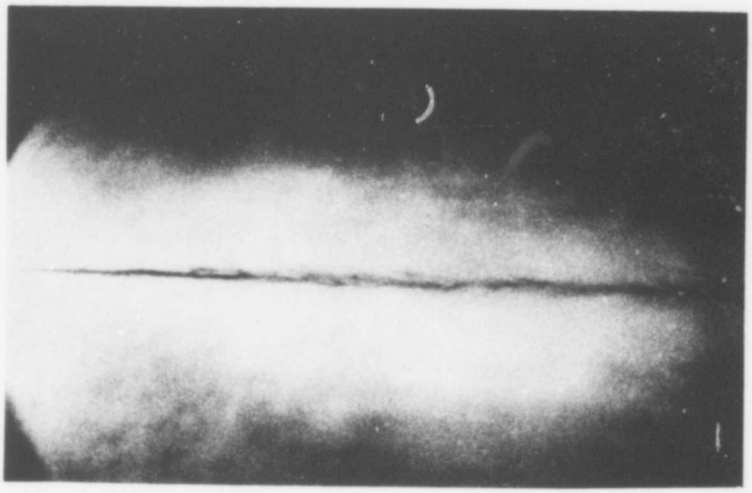

a) from the nozzle 20 k.s.i. jet, 0.01-inch nozzle

b) from 15 inches 20 k.s.i. jet, 0.01-inch nozzle

Figure 20. Backlit pictures of a water jet at pressure. (The scale indicates a 1-inch length)

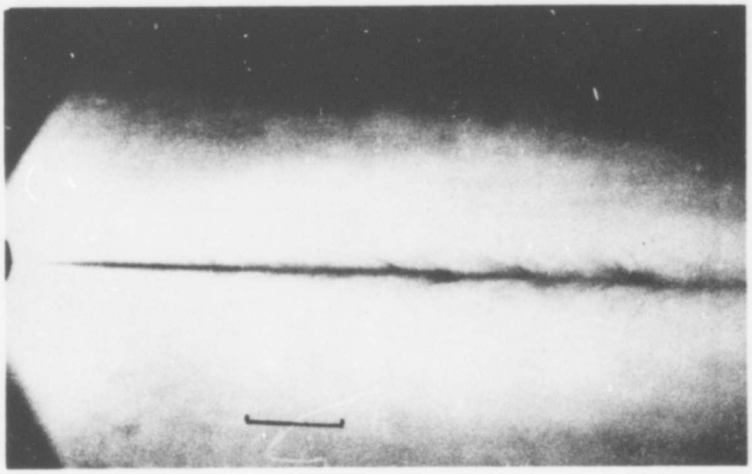

c) from the nozzle 45 k.s.i. jet, 0.01-in. nozzle

d) from 15 in., 45 k.s.i. jet, 0.01-in. nozzle

Figure 20. Backlit pictures of a water jet at pressure. (The scale indicates a 1-in. length).

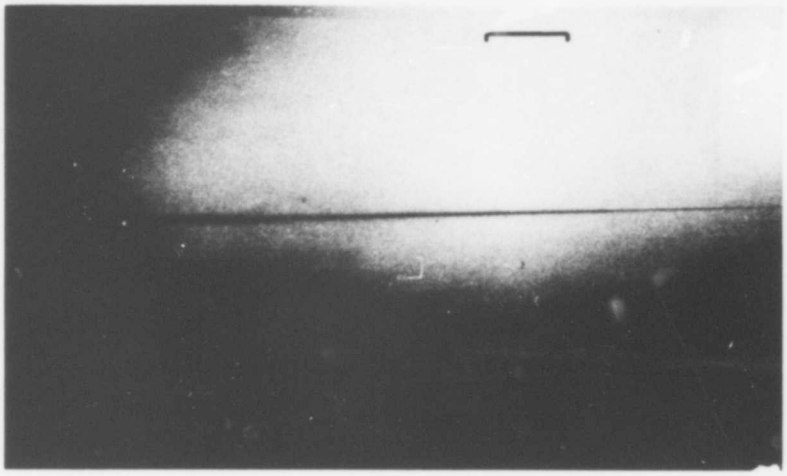

a) from the nozzle 20 k.s.i. jet, 0.01-in. nozzle

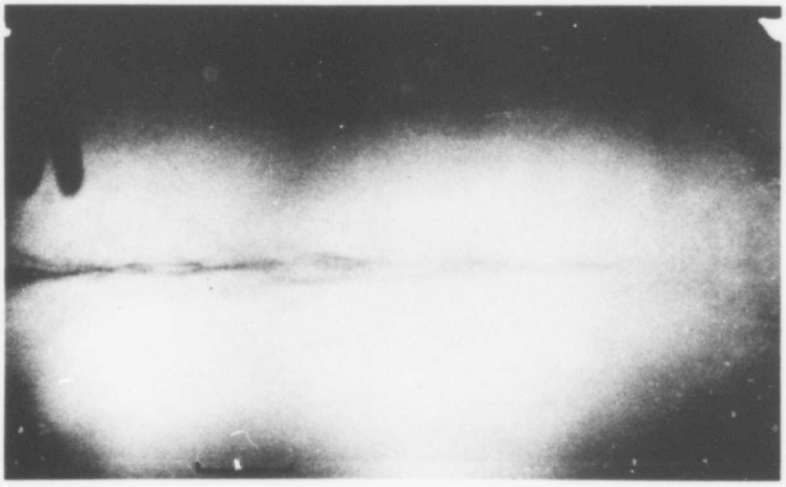

b) from 15 in. 20 k.s.i. jet, 0.01-in. nozzle

Figure 21. Backlit pictures of a 500 p.p.m. Polyox content fluid jet. (The scale indicates a 1-in. length).

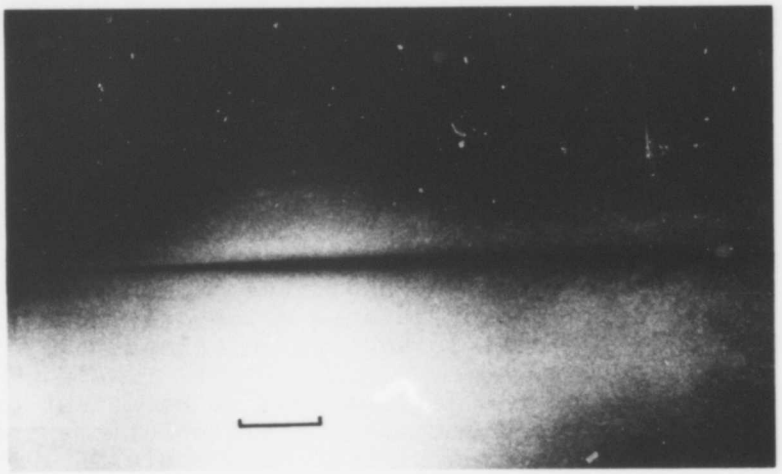

c) from the nozzle 45 k.s.i. jet, 0.01-in. nozzle

d) from 15 in. 45 k.s.i. jet, 0.01-in. nozzle

Figure 21. Backlit pictures of a 500 p.p.m. Polyox content fluid jet. (The scale indicates a 1-in. length).

from 20,000 to 45,000 p.s.i. The two larger nozzles had slightly better coherence at the higher pressures, but the trend was reversed for the smaller nozzle.

Jets With Viscoelastic Additives

Similar photographs at each of the nine test conditions were taken with water to which viscoelastic additives had been added. The additives used and the concentration levels are listed in Table IV. The additives chosen were high polymers and soaps or surfactants which are known to be effective drag reducers in aqueous solutions.

Photographs of the jet obtained at each test condition (pressure and nozzle diameter) for all solutions and water were rated relative to each other on a scale of 1 to 28. A rating of 1 was for the best jet and 28 was worst. These ratings are listed in Table V along with an average rating for each solution. From these ratings the most effective additives and their optimum concentrations could be selected for earth moving or other studies.

The most effective additive from the combined results of all nozzles and pressures was Polyox FRA at a concentration of 500 p.p.m. Polyox FRA at a concentration of 1,500 p.p.m. was only slightly less effective. The next most effective additives were Polyhall 654, at a concentration of 500 p.p.m., Dow Separan AP 273, at a concentration of 150 p.p.m., and Nalco B129 at concentrations of 150 and 500 p.p.m. These polyacrylamide polymers have very high molecular weights and are more resistant to mechanical degradation than the Polyox. Separan AP 30, a similar polymer from Dow, was less effective probably because it has a lower molecular weight. Presumably, it would be more effective at concentrations well above 500 p.p.m.

The Nalco 625 contains a polyacrylamide similar to B129 which is dispersed in oil which is then emulsified in water (about 1/3 polymer). It was a little less effective than B129 at equal solid concentrations. This may have been due to mechanical degradation of the polymer in forming the emulsion or it may have been due to incomplete solution of the polymer after the emulsion was dispersed in water. In subsequent discussion with the manufacturer, it was determined that the emulsified batch obtained was below the normal standard for this product. The convenience of using this type of product in field situations warrants further studies with it.

Table IV. Chemical Additives Tested in Program at McCartney

Additive	Concentrations Used		p.p.m.
Polyox FRA	100	500	1500
Nalco B129	50	150	500
Nalco 625 (liquid)*	150	450	1500
Dow Separan AP273	50	150	500
Polyhall 654	50	100	500
Dow Separan AP30	50	150	500
α Naphtholplus Cetyltrimethyl-ammonium Bromide	50	150	500
Alfonic 1214-60	1000	5000	10,000
Jaguar A20D	100	500	2,500
Water			

*Nalco 625 (liquid) contains 1/3 solid polymer additive.

Table V. Ranking of Chemical Additive Effectiveness In Improving High Pressure Jet Coherence

	Nozzle Diam.	0.005"			0.010"			0.012"			Ave.	Rank Based on Average
	Pressure (k.s.i.)	20	30	45	20	30	45	20	30	45	Rating	Rating
Polyox	100 p.p.m.	3	8	3	5	4	27	25	25	28	14.4	14
	500 p.p.m.	5	1	1	2	1	2	2	15	1	3.4	1
	1500 p.p.m.	1	7	13	1	2	1	24	10	2	7.1	2
Nalco B129	50 p.p.m.	13	5	12	17	15	22	8	19	7	13.1	12
	150 p.p.m.	2	4	14	13	12	5	17	5	8	8.9	6
	500 p.p.m.	6	12	16	4	7	3	7	14	13	9.2	7
AP273	50 p.p.m.	12	16	15	18	9	4	12	10	9	11.9	11
	150 p.p.m.	7	3	7	3	5	8	15	13	10	7.9	4
	500 p.p.m.	18	19	22	8	8	10	6	[illegible]	5	11.6	9
Polyhall 654	50 p.p.m.	4	6	6	23	11	13	4	3	4	8.2	5
	100 p.p.m.	15	18	10	20	13	6	10	9	3	11.7	10
	500 p.p.m.	10	7	4	6	14	18	1	1	6	7.6	3
AP 30	50 p.p.m.	25	20	23	25	26	20	11	22	16	21.1	26
	150 p.p.m.	17	14	27	11	20	24	21	23	23	20.2	24
	500 p.p.m.	27	24	26	7	3	9	3	4	14	13.3	13
αN & CTAB	50 p.p.m.	20	25	25	26	23	17	5	2	12	17.6	18
	150 p.p.m.	19	15	18	21	28	19	13	8	18	17.8	19
	500 p.p.m.	21	26	20	22	16	21	20	12	21	20.0	23
Nalco 625* (liquid)	150 p.p.m.	23	11	19	24	25	23	19	15	19	19.9	22
	450 p.p.m.	9	13	9	12	17	12	22	23	15	14.9	16
	1500 p.p.m.	14	17	17	10	2	11	9	7	11	11.0	8
Alfonic	1000 p.p.m.	8	10	2	14	22	15	14	21	24	14.6	15
	5000 p.p.m.	11	23	8	15	19	14	16	18	17	15.8	17

Table V (Continued).

	Nozzle Diam.	0.005"			0.010"			0.012"			Ave.	Rank Based
	Pressure (k.s.i.)	20	30	45	20	30	45	20	30	45	Rating	on Average Rating
Alfonic (cont.)	10,000 p.p.m.	22	27	21	16	24	16	18	20	22	20.8	25
Jaguar	100 p.p.m.	16	2	11	27	10	25	28	21	27	18.7	20
	500 p.p.m.	24	22	5	9	6	26	27	27	25	19.1	21
	2,500 p.p.m.	26	21	24	28	15	28	26	25	26	24.7	28
Water		28	28	28	19	18	7	23	17	20	21.2	27

*Nalco 625 (liquid) contains 1/3 solid polymer additive.

Note:
The ranking was effected by ordering the photographs such that "1" denotes the "best" jet and "28" the "worst."

In general, high molecular weight polymers are more effective in causing drag reduction than low molecular weight polymers. The molecular weight of a high polymer is related to its intrinsic viscosity, [η], by the Mark Houwink relationship

$$[\eta] = KM^a \qquad (2)$$

where [η] is intrinsic viscosity in deciliters/gram, M is molecular weight in grams/gram mole and K and a are constants for a particular polymer solvent system. Exact values of K and a for the polyacrylamides studied are not known because the polymer compositions are not given exactly. However, the measured values of intrinsic viscosity listed in Table I give a rough indication of the relative molecular weights of the polyacrylamides. These measured intrinsic viscosities suggest that the molecular weights obtained from the manufacturers listed in Table I are only nominal.

Polyox (polyethylene oxide) polymers have very flexible molecular structures and are probably the most effective drag reducing agents known but are very sensitive to chemical or mechanical degradation. The FRA sample tested here degraded a great deal in storage as shown by the low measured intrinsic viscosity. Nevertheless, at 500 and 1500 p.p.m. it gave the best jet coherence. Higher molecular weight polyethylene oxide polymers would probably be effective at concentrations of 100 p.p.m. or even lower.

Comparison of the average effectiveness ratings of the polyacrylamides indicate that high molecular weight polymer, sometimes even at lower concentrations (Separan AP 273), favors better jet coherence and that in many cases an optimum concentration was observed. However, the rating scale was not precise enough to draw detailed conclusions and is primarily useful for selection of additive systems for further study and for screening out ineffective additives.

The much lower molecular weight Jaguar AD 20, which also has a less flexible molecular structure, was the least effective of the polymers studied. It is also far less effective as a drag reducing agent than any of the other polymers.

The lowest concentration of Alfonic 1214 (1000 p.p.m.) was comparable in average effectiveness to the least effective of the polyacrylamides. Higher concentrations of Alfonic 1214 were still less effective and it is possible

that greater effectiveness could be obtained at a lower concentration of the additive.

Alfonic 1214 is effective as a drag reducer at temperatures above 35°C (Ref. 12). It forms agglomerates when its solutions are heated to a temperature near their cloud point, about 42°C. The exit temperatures of jets in the McCartney and Rolla experiments were 35-45°C. These agglomerates have very high molecular weights, probably in the millions, which impart viscoelastic character to the solutions making them effective drag reducers. The solutions are quite stable for more than five days.

The complex soap formed from combinations of α Naphthol and cetyl trimethyl-ammonium bromide (1:2 ratio) also forms large agglomerates in solution which are effective as drag reducers (Ref. 13). These chemicals are expensive, however, and they lose their effectiveness at temperatures above 40°C or after three days storage in solution at room temperature. This system was ineffective at all three concentrations tested probably because of the high temperature of the jet leaving the nozzle (35-45°C).

The results of both the pressure profile and the photographic studies show that polymer additives can have a significant effect on jet coherence of high pressure jets. Photographic studies of low pressure, large diameter (fire hose) jets (Ref. 14) show that small scale turbulent eddies on the jet surface are dampened when polymer additives are present. These eddies give rise to surface disturbances which promote atomization and the effect of the dampening is, thus, to reduce atomization. The mechanism by which they dampen these high frequency disturbances is not clear, but one hypothesis offered to explain the drag reduction effects of these same polymer solutions may be germane. It has been suggested that the high extensional viscosity of these high polymer solutions hinders the growth of high frequency, small scale eddies as well as their movement away from the turbulence generation region. A similar dampening effect may occur in turbulent jets of high solutions.

For some of the more effective polymer solutions, the effects of nozzle size and pressure on jet coherence were examined. Photographs were rated in order as for the water jets and the results listed in Table III.

The trends observed are similar to those found for pure water jets. In all cases the 0.010- and 0.012-in. diameter jets were more coherent than the 0.005-in. jets. The effect of pressure was not large and there was no consistent trend

to the small variations observed, i.e., in some cases higher pressure gave better jet coherence, in others it was poorer.

Thus, in this range of Reynolds Numbers (about 60,000 to 210,000) there is an effect of jet diameter on jet coherence but little apparent effect of change in jet pressure.

Rewriting Equation 1 in terms of the variables L_B, D and V, we obtain:

Case 1: For n = 0 or no Reynolds number dependency (plateau region)

$$L_B \alpha D^{1.5} V^{1.0} \quad (3)$$

Case 2: For n = 5/8 (Ref. 8)

$$L_B \alpha D^{7/8} V^{3/8} \quad (4)$$

Case 3: For n = 2 (Ref. 9)

$$L_B \alpha D^{-0.5} V^{-1.0} \quad (5)$$

Case 4: For n = 1

$$L_B \alpha D^{0.5} V^{0} \quad (6)$$

The results of Lienhard and Day (Ref. 9) shown in Figure 22 suggest a plateau region up to about 35 to 40,000 Reynolds Number followed by a transition region to about 60,000 or even 100,000 Reynolds Number. Miesse (Ref. 8) reported an n value of 5/8 for data ranging from 10,000 to 340,000 but mostly below 100,000. A value of 5/8 below 100,000 is consistent with the results in this figure. Lienhard and Day claimed n = 2 for their results in the Reynolds Number range of 80,000-160,000.

The results described herein for the photographic studies, which are in the range of Reynolds numbers from 60,000 to 210,000, show a definite diameter effect but little effect of jet pressure ($V \alpha P^{1/2}$). This suggests an n value near unity as in Case 4. However, the pressure profile studies where Reynolds Number ranged from about 260,000 to 450,000 indicated that both pressure and jet diameter were affecting jet coherence. It follows then that in this high Reynolds Number region n must be less than unity and may well be approaching zero giving a second plateau region.

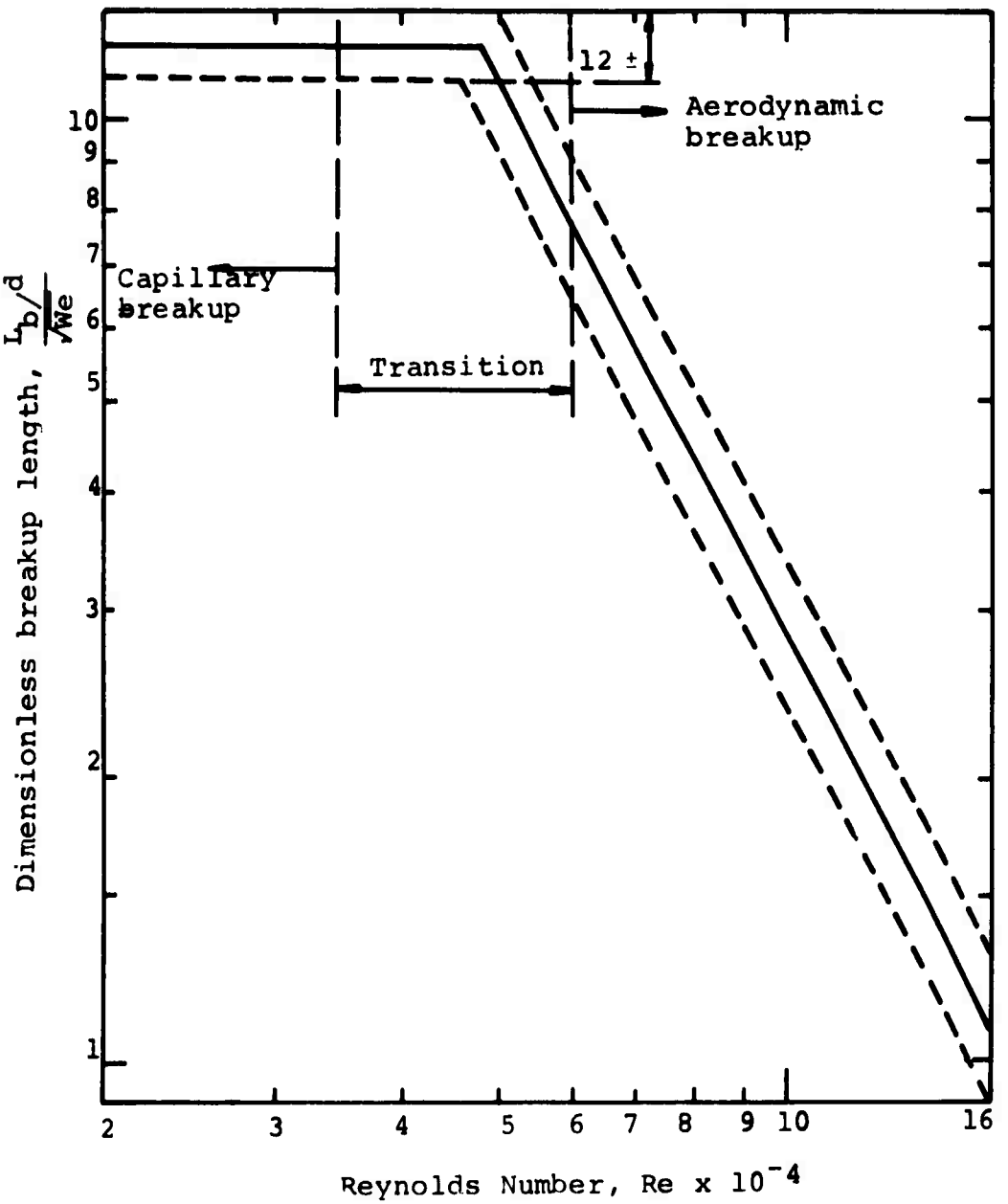

Figure 22. The effect of Reynolds Number on the form of jet breakup.

This conclusion has also been suggested by Phinney (Ref. 15).

We can conclude that the relative importance of pressure effects or nozzle diameter effects on jet coherence depends on the Reynolds Number range of interest and optimum design of systems for practical use must take this into account.

There is a need for more precise measurements covering a wide range of Reynolds Numbers to establish the form of Equation 1 (value of n) in the various regions.

CHAPTER 3

Jet Cutting of Various Soils and Materials

Background

The previous use of water jets for moving earth and for cutting various materials is described in Appendix I. An important part of the present research was a study of the effect of polymer additives on soil cutting and the effect of nozzle size, nozzle pressure, and traverse speed on the cutting of wood and plexiglass.

Soil Cutting

Three differing soil types were tested in this program which was carried out at McCartney and at UMR: a sand, a loam, and a Missouri red clay. The soils were obtained from a contractor in the Rolla area.

Because of the configuration of the test equipment at McCartney, it was necessary to traverse the soil samples under the jet nozzle rather than the converse, and for this purpose a special carriage was constructed. The carriage was filled with soil and traversed under the jet at a speed of approximately 60 ft./min. The procedure is described in Appendix II.

Initial tests indicated that cutting with the jet very close to the surface (1.25 in.) had little apparent effect since, while the jet was effectively penetrating the soil, the narrowness of the cut and the swirling of soil behind the jet effectively resealed the slot. Two distances for test, nominally 12 and 22 in. were, therefore, chosen for the series of tests. In order to account for variations in soil compactness in the field, two soil conditions were studied: loose and unconsolidated material, and soil packed and consolidated with a block of wood and a mallet. Nominal densities of these materials are listed in TableVI. It should be noted in passing, that where the soil was compacted in layers, the jet sometimes exploited these layers, peeling back a single layer of soil up to a distance of 1 in. from the traverse line. This occurred where the jet found an easier path between the layers rather than rebounding from the impact zone.

High pressure tests (30,000 p.s.i.) at the two standoff distances using a 0.012-in. nozzle were carried out on three soils (clay, loam and sand) in two stages of soil compactness

Table VI. Results of Soil Cutting Tests at McCartney

Fluid	Stand-off Dist. (in.)	Clay				Loam				Sand			
		Compact		Loose		Compact		Loose		Compact		Loose	
		Depth	Width	Depth	Width	Depth	Width	Depth	Width	Depth	Width	Depth	Width
Water	10	0.5	0.75	2.0	3.0	1.0	5.0	2.5	5.0	1.0	3.5	3.0	2.0
	22	-	-	1.5	5.0	-	-	0.5	5.0	3.0	5.5	2.5	4.0
Nalco 625 (1500 p.p.m. =833 p.p.m. solid)	10	1.0	0.07	0.75	2.5	2.0	0.25	1.5	3.0	1.5	3.0	2.5	1.5
	22	0.37	0.13	2.5	3.5	0.5	0.07	3.0	5.0	4.5	4.25	4.5	4.0
Polyox FRA (500p.p.m.)[1]	10	1.25	0.25	1.25	2.0	1.75	0.25	1.0	4.0	2.5	2.0	2.0	2.5
	22	-	-	2.75	6.0	0.07	0.25	2.5	6.0	2.0	3.5	3.0	5.5
Polyhall 654 (500p.p.m.)[1]	10	0.75	1.0	1.5	3.5	2.0	0.25	2.25	4.0	3.0	2.0	2.5	2.5
	22	-	-	2.0	5.0	0.13	0.25	3.0	6.0	3.0	5.5	4.0	4.0
Dow AP273 (450p.p.m.)[1]	10	1.25	0.25	1.25	2.0	1.5	2.0	1.5	4.75	1.5	3.0	1.5	3.75
	22	0.13	0.13	3.5	6.0	-	-	5.0	6.0	1.87	4.0	2.0	6.0

1. Pressure = 30,000 p.s.i. nozzle diameter = 0.012 inches
2. Tabulated values are in inches
3. The depth values were measured above the collapsed and refilled slot, thus achieved depth was, during cutting, up to 2 inches deeper than that finally measured in loose material.

Table VI.(Continued).

4. Moisture Content:

Clay	17.1%
Loam	13.1%
Sand	3.2%

5. Soil Density (lb./ft.^{3}):

	Uncompacted	Compacted
Sand	80.0	97.2
Loam	67.7	112.1
Clay	68.9	106.8

with water and with solutions of 1500 p.p.m. Nalco 625 (500 p.p.m. polymer additive), 500 p.p.m. Polyox FRA, 500 p.p.m. Polyhall 654 and 450 p.p.m. Dow Separan AP273 as the cutting fluid.

Results from the test series carried out at 30,000 p.s.i. and 0.012-in. nozzle diameter are shown in Table VI. In these experiments, the measured slot widths are a more accurate measure of how the jet performed than the measured depths because the loosened soil tended to resettle to a depth of up to 2 in. inthe slot due to the vertical impact of the jet.

The results of these experiments show that the jets considered are generally quite effective in removing sand, compact or loose,and loose clay and loam. They are generally not as effective in compacted clay or loam. (See Figure 23 in which the lower part with the narrow slot is compacted loam and the upper part with the wide trench is the uncompacted loam.) At the 22-in. standoff distance, the polymer solutions are generally more effective than the water. Pure water is generally more effective at the 10-in. standoff distance. These effects are illustrated in Figures 24 a,b,c and d. The latter results may be due to a narrower divergence angle of the polymer solutions compared to water, which lowered the efficiency of soil removal at the 10-in. position although the instantaneous jet penetration might be greater with the additives present. At 22 in. the coherence of the water jet was poor and the energy retained by the jet was low while the improved coherence provided by the polymer solutions caused them to be more effective.

While these results clearly show the benefit to be obtained by the use of polymers in the fluid in maintaining jet cohesion at large standoff distances, a second conclusion can also be drawn. At the 10-in. standoff the polymer jet retains more energy than the water jet but is less effective because the energy is concentrated within a small area. Thus, for maximum effectiveness in removing soil a certain degree of jet disruption would appear advantageous. The amount of jet disruption which is most effective for soil removal has not previously been investigated although the phenomenon has been recently discussed (Ref. 16) and this is, therefore, an important area for further study.

Thus, to sum up for these experiments, the jets most effectively cut sand and were least effective in clay. Compacted clay and loam were more difficult to remove than loose material as the jet cut only a thin slot in the compacted material. This would be a problem where the jets

Figure 23. Loam cut by a 500 p.p.m. Polyhall, 30 k.s.i. 0.012-in. diameter jet at 10-in. standoff, showing the change where the loam changes from compacted, nearest the camera, to uncompacted.

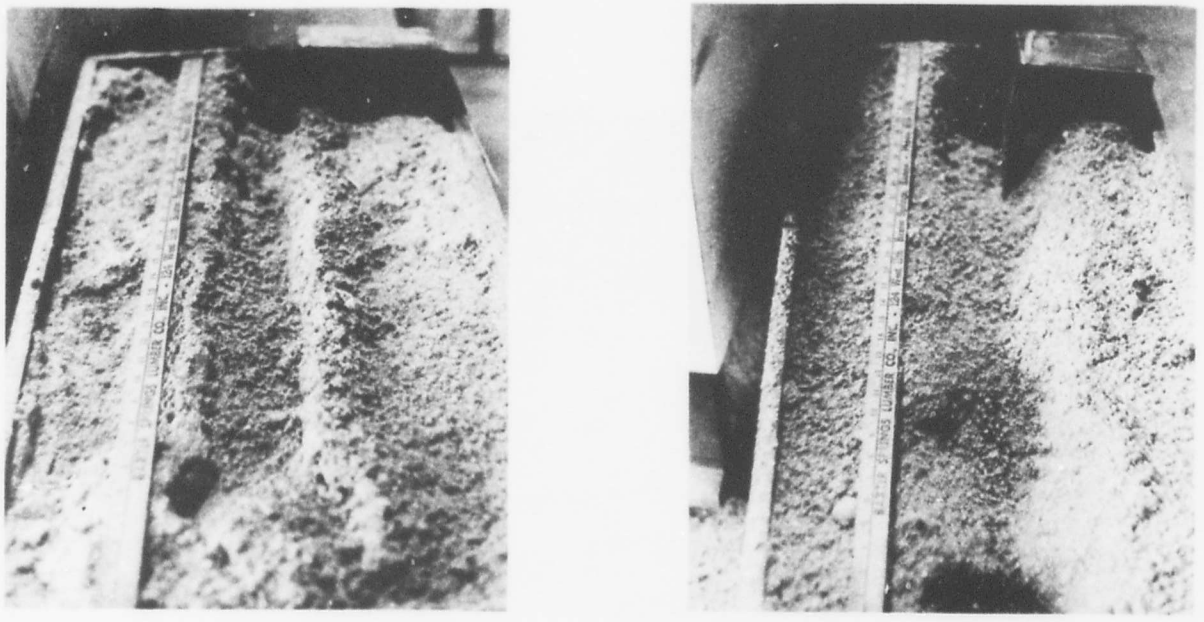

a) sand cut by water from 10 inches b) sand cut by water at 22 inches

Figure 24. Sand, compacted in the half nearest the camera, cut by a 30 k.s.i., 0.012-in. diameter jet for two jet fluids and two standoff distances.

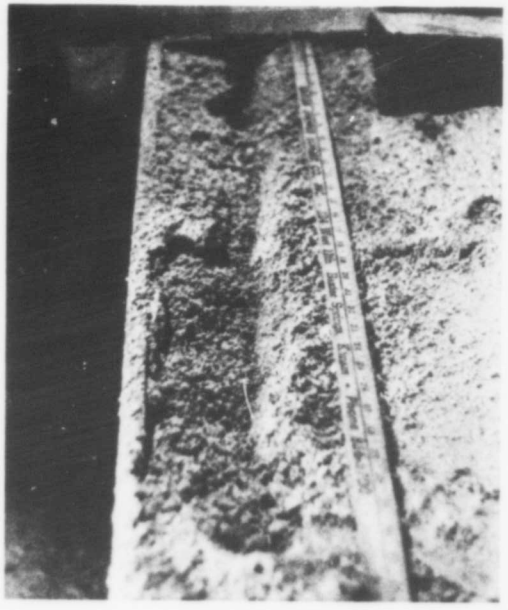

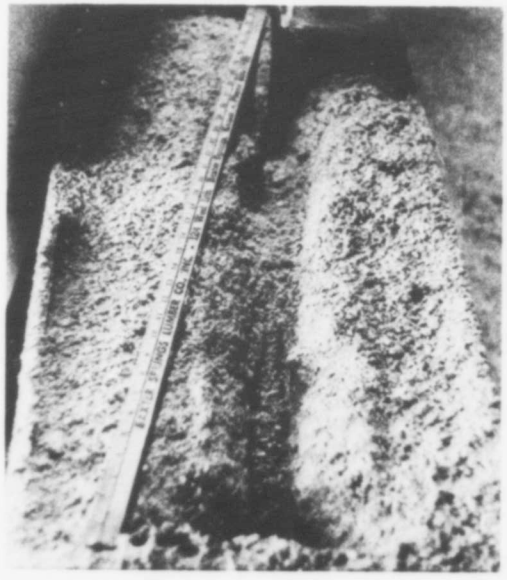

c) sand cut by Nalco from 10 inches d) sand cut by Nalco at 22 inches

Figure 24. Sand, compacted in the half nearest the camera, cut by a 30 k.s.i., 0.012-in. diameter jet for two jet fluids and two standoff distances.

are to be used for soil clearance over a suspected mine field. As noted above, in all material, the vertical orientation of the jet reduced the effectiveness of removal since the channel cut by the jet was then partially filled by subsequent ejecta.

In a further effort to evaluate the effects of jets on soil, another experiment was done at the UMR facility in which a nozzle and a feed pipe were attached to a rotatable coupling. The feed pipe was bent so that the nozzle directed the jet at a forward angle to the soil target held in a metal frame 5-1/2 ft. away (Figure 25). The test series was carried out in two parts: first, using a water and soluble oil fluid, and second, with the addition of 500 and 1000 p.p.m. (solid concentration) of Nalco BX-254, a similar polymer to the Nalco 625 used at the McCartney test facility.

Tests were originally planned over a range of nozzle diameters and a range of jet pressures. Preliminary tests, however, indicated that the jet would not reach the target material unless a 0.03-in. or larger nozzle diameter was used, smaller jets being totally disrupted before impact on the target. At 0.06-in. nozzle diameter, the plunger and liner assembly in use provided sufficient flow for a maximum jet pressure of 2,500 p.s.i. Tests with water were accordingly carried out with two traverse speeds, 3 ft./sec. and 6 in./sec., traversing the nozzle manually over the 18-in. wide test frame. The same three soil types were used (uncompacted) as in the experiments at McCartney. In these tests, the soil type made much less difference in the results (Table VII) than had previously been observed. However, for the polymer solutions the measured depths do not show the true penetration depth of the jet because, while the water jet impact generated an ejecta spray including soil and water which was thrown beyond the target area, the polymer solution jet stream did not create a large rebound spray which could carry material beyond the target area. Instead, the material resettled filling part of the slot formed (Figure 26). It is believed that this difference in fluid behavior is due to the high extensional viscosity of the polymer solution.

In the tests where the Nalco chemical was added to the fluid, the jet cohesion was noticeably improved, jet atomization not being initiated for a distance of over one foot with the 0.06-in. diameter nozzle, and for 9-in. with the 0.05-in. diameter nozzle for the 1,000 p.p.m. solution. Because the pump was a fixed displacement type producing

Table VII. Average Slot Dimensions for Soil Traverse Tests Carried Out at University of Missouri-Rolla

Nozzle Diameter 0.06 in., Nominal Jet Pressure 2500p.s.i. Distance 5 ft. 6 in.

	LOAM				SAND				CLAY			
	6 in./sec.		3 ft./sec.		6 in./sec.		3 ft./sec.		6 in./sec.		3 ft./sec.	
	Depth	Width	Depth	Width	Depth	Width	Depth	Width	Depth	Width	Depth	Width
Water	2.3	4.1	2.1	3.8	1.5	4.0	1.8	3.9	2.6	3.9	1.6	4.2
Nalco BX 254 500 p.p.m. (solid)	1.6	4.4	1.2	4.0	1.65	4.2	1.75	5.0	1.55	4.6	1.85	3.2
Nalco BX 254 1000p.p.m. (solid)	1.1	3.8	0.9	2.6	1.6	5.4	1.55	3.7	1.25	4.2	0.75	3.8

Notes:

1. The values given are in inches
2. Moisture content:

Clay	17.1%
Loam	13.1%
Sand	3.2%

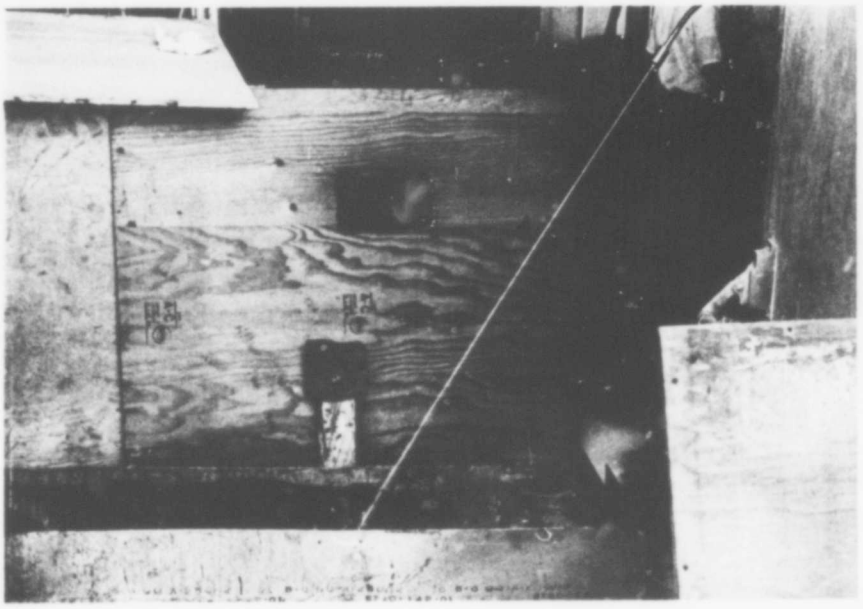

Figure 25. Experimental arrangement in Rolla (protective cover removed and pressure reduced for photograph).

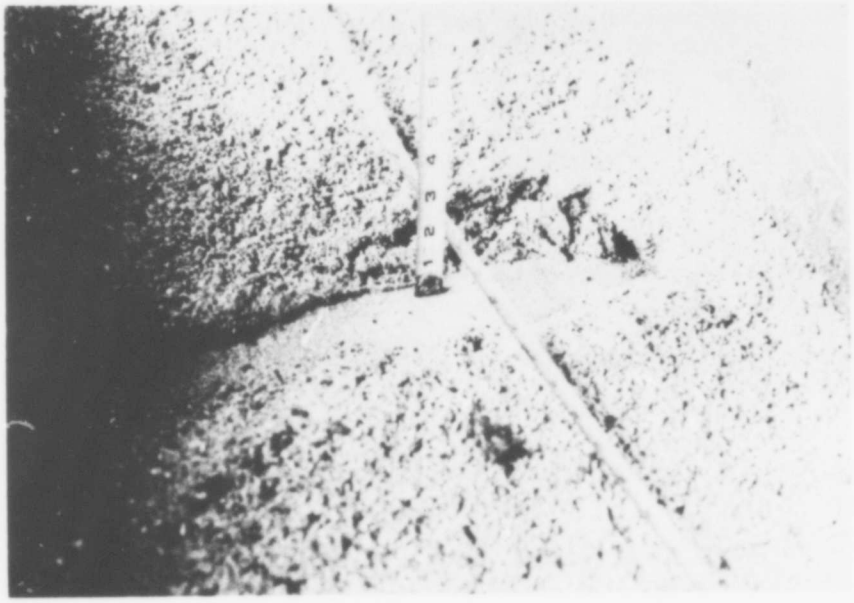

Figure 26. Flow of sand under impact at jet velocity of 6 in./sec., 0.06-in. diameter nozzle 2,500 p.s.i. at 5-1/2 ft. standoff distance.

4 g.p.m., the drag reduction of the polymer reduced jet pressure below that measured accurately by the gauge to a level of approximately 2,000 p.s.i. While this was sufficient to cut the target material, as noted above the cohesion of the fluid kept the material in the slot to a greater degree than the water alone and subsequent settling of the soil gave small measured depths of cut although the initial penetration of the soil was greater.

Smaller nozzles were also used in this phase of the program with Nalco polymer in order to determine whether jets from such nozzles could effectively cut at a distance of 5-1/2 ft. For an 0.035-in. nozzle diameter, the jet was totally disrupted as it left the nozzle. Examination of the nozzle showed that the nozzle inlet orifice was slightly larger than the pipe inner diameter which generated a turbulent condition at the interface. The importance of an exact match on this plane was, thus, clearly shown. At 0.03-in. nozzle diameter and 3000 p.s.i. pump pressure the jet retained sufficient energy at 5-1/2 ft. to move surface material on the target surface, but the depth of penetration was below 1/2 in. As jet pressure was increased to 4,000 p.s.i. the jet was distrupted to the point that no effect was observed on the target surface.

Because water from the impacting jet was retained around the impact point fluidizing the material which flowed back into the cavity, tests were run at higher traverse speeds. Short test runs, where the water jet was gyrated over the test surface, were carried out on sand (Figure 27) and clay (Figure 28). Although the jet rapidly cleared material to a depth of 4 in., the test frame was too small for this type of test since the ejecta had very little throw and was retained by the sidewall of the frame and consequently flowed back into the excavated hole.

When 500 p.p.m. (solid polymer) of Nalco BX 254 was added to the water, it was noted that the impacting fluid was not penetrating into the walls of the trench to as large an extent after impact and that, in consequence, the walls of the cut were more stable. Thus, it was found possible to make three adjacent passes over sand and soil, cutting to a depth of over 4 in. before the walls collapsed, refilling the hole to a depth of 2 in. (Figure 29 shows results after 6 passes).

In considering the logistics of any field use of water jets for soil removal over land mines certain limiting parameters can be assumed. For example, the carrying capacity of the vehicle, say 1000 gal. will probably preclude

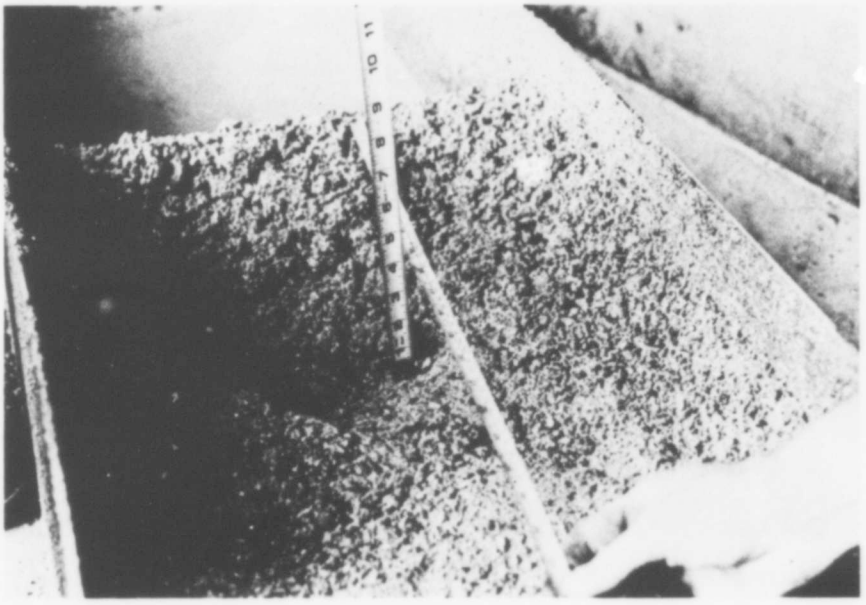

Figure 27. Results of a gyratory jet traversed over sand (2,500 p.s.i., 0.06-in. diameter, 5-1/2 ft. standoff distance).

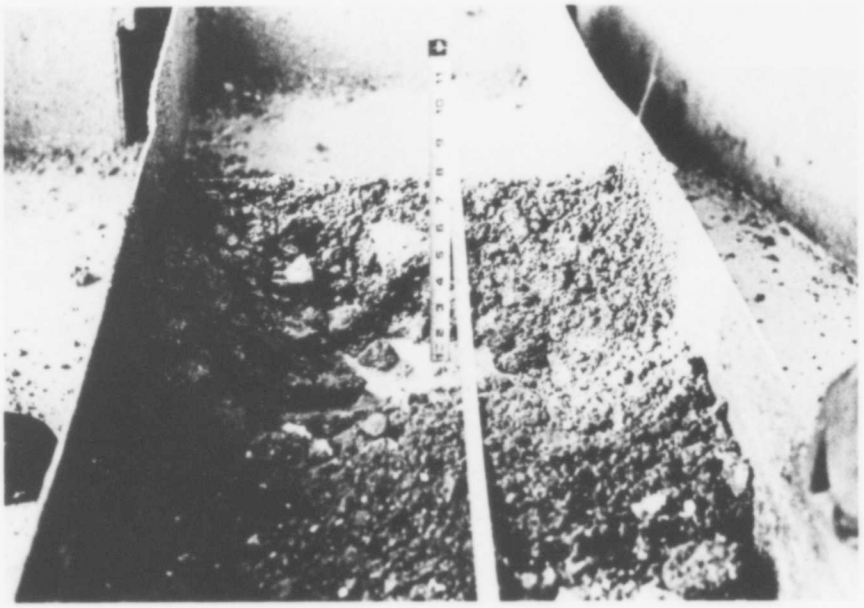

Figure 28. Results of a gyratory jet traversed over clay (2,500 p.s.i., 0.06-in. diameter, 5-1/2 ft. standoff distance).

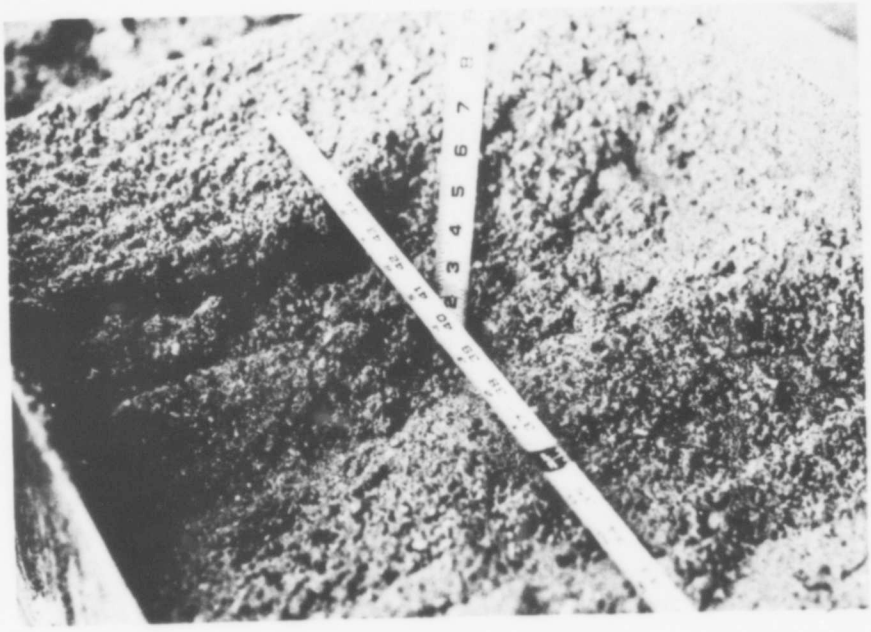

Figure 29. Result of six adjacent passes at 3 ft./sec. over sand (500 p.p.m. Nalco in a 2,000 p.s.i., 0.06-in. jet at 5-1/2 ft. standoff distance).

use of very high flow rate jets (of the order of 200 g.p.m.). If continuous operation is required, a flow rate of 10 g.p.m. maximum can be anticipated. If two or three nozzle systems are used concurrently to allow a reasonable forward advance speed while the jet sweep runs perpendicular to the line of advance, this will limit nozzle sizes to a maximum of 0.03- to 0.06-in. diameter, depending on jet pressure.* For this size of nozzle at a standoff distance of 5 to 6 ft., these last experiments suggest that at operating pressures of 2,000 to 5,000 p.s.i., the jet would reach the target. While not apparent in the results in Table VII the use of long-chain polymers assisted the cutting effect in that it reduced jet breakup and the wetting of the target material, so that the cavity created was more stable. An exhaustive study to find optimum polymer types and concentrations to give jet coherence sufficient for target penetration while at the same time having the ability to carry ejecta away from the impact point needs to be made utilizing standardized tests.

Of major interest, but not examined in this study, is the effect of lateral traverse speed on jet stability. It has been shown (Ref. 17) that the addition of polymers enhances jet stability under these conditions but experiments were carried out only at low traverse velocities. The effect of polymer addition on jet stability at high traverse speeds in the pressure range from 2,000 to 5,000 p.s.i. at nozzle diameters from 0.03- to 0.06-in. at standoff distances up to 6 ft. would, therefore, be a worthwhile continuation of this study.

Cutting of Wood and Plexiglas

A sufficient amount of results was available in the literature (Appendix I) to describe the effects of water jets in cutting wood and Plexiglas. A small program to observe the effect of change in test parameters was, however, carried out. The samples were clamped on a frame and traversed under the jet nozzle by an hydraulically driven ram. Feed rate was varied, as were nozzle diameters and pressure of the jet, but standoff distance was held constant at zero inches. Previous work by Summers (Ref. 18) demostrated the advantages of using polymer additives in jet cutting.

The results of the tests carried out (Table VII, Figures 30 to 33) show the need to use as large a nozzle diameter

*An 0.03-in. nozzle will deliver approximately 1.2 g.p.m. at 2000 p.s.i. and 2.0 g.p.m. at 5,000 p.s.i. The 0.06-in. nozzle delivers four times as much fluid at each pressure.

Table VIII. Results of Cutting Tests on Plywood and Plexiglas
All results at no standoff,
Jet contained 833 p.p.m., Nalco 625 (solid polymer)

Test No.	Pressure (k.s.i.)	Nozzle Diam.(in.)	Feed Rate (in./min.)	Result
a) Plywood (1/2" thick 5 ply)				
1	43	0.012	90	penetrated 1/2"
2	43	0.007	90	penetrated 3 ply
3	43	0.005	90	penetrated 2 ply
b) Plexiglas (1/4" thick)				
4	43	0.012	30	cut cleanly through
5	43	0.012	60	cut roughly through
6	43	0.012	300	broke roughly through
7	43	0.012	900	cut deep
8	43	0.012	2040	cut deep
9	35	0.012	60	cut roughly through
10	35	0.012	300	cut deep
11	30	0.012	60	cut through intermittently
12	25	0.012	60	cut deep
13	35	0.005	60	cut deep
14	43	0.005	60	cut deep
15	43	0.005	8	cut cleanly through
16	43	0.007	60	cut through intermittently
17	43	0.010	60	cut cleanly through
18	43	0.010	300	cut roughly through
19	43	0.010	900	cut deep

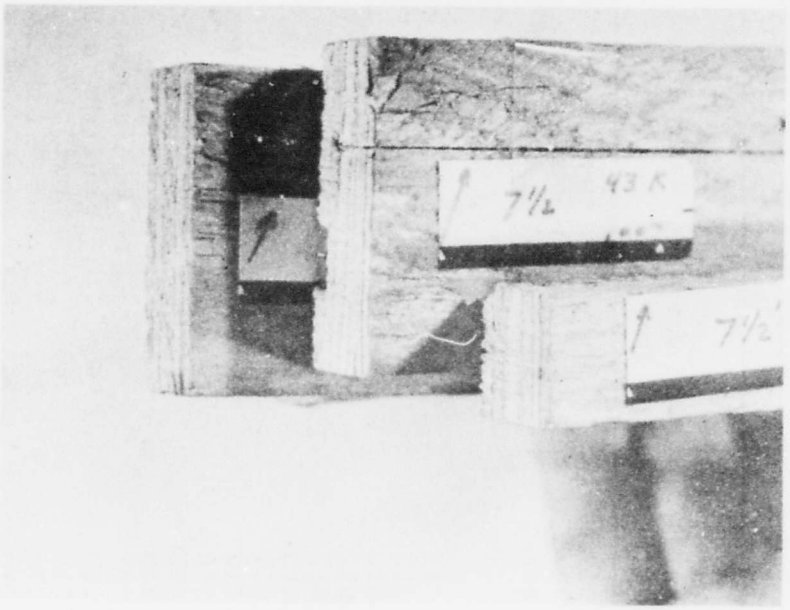

Figure 30. One-half in. plywood cut at 7-1/2 in./sec. and 43,000 p.s.i. Three nozzle diameters (0.005, 0.007, 0.012 in.).

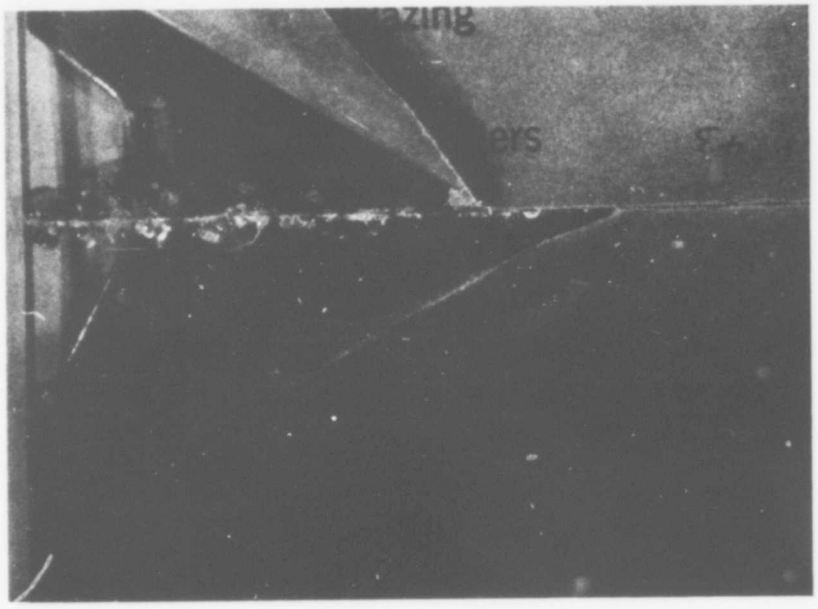

Figure 31. One-quarter in. Plexiglas cut but not penetrated by a 0.005-in. diameter, 43,000 p.s.i. jet at 5 ft./min.

Figure 32. One-quarter in. Plexiglas cut through by a 0.010-in. diameter, 43,000 p.s.i. jet at 5 ft./sec.

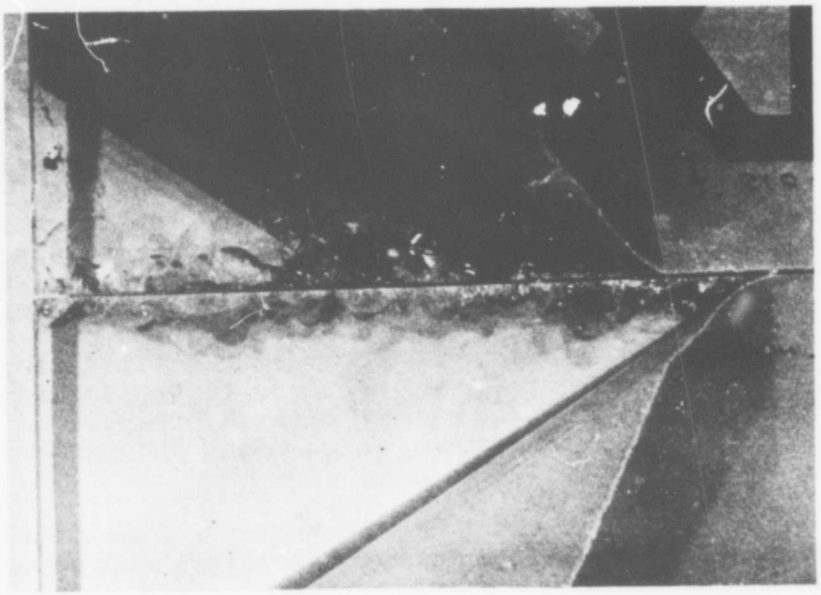

Figure 33. One-quarter in. Plexiglas cut through by a 0.012-in. diameter, 43,000 p.s.i. jet at 5 ft./sec.

as possible in the cutting of these materials in order to obtain a through cut. For example, in cutting 1/2-in. plywood at 43,000 p.s.i. nozzle pressure at a feed rate of 90 in./min. the 0.005-in. nozzle jet penetrated only two plies, the 0.007-in. nozzle jet penetrated three plies and the 0.012-in. nozzle jet cut through the five plies (Figure 30). The greater effectiveness in cutting of larger diameter jets at constant pressure is due at least in part to the larger amount of energy available in the cutting area.

Results from the test program and from the results of other investigations suggest that while it is relatively easy to cut wood (jet pressures as low as 2000 p.s.i. have been used), a large diameter (0.01-in. or larger) jet is most effective as well as a relatively slow traverse speed. In the cutting of Plexiglas, where the penetration mechanism is different, it is more important to have a high jet pressure (above about 30 k.s.i.). Here, too, a large nozzle diameter (about 0.01-in. diameter) and feed rates below 60-in./min. are most effective. While the jet continued to cut at higher feed rates, large scale fracturing of the target occurred. Where the jet was traversed slowly over the sample, allowing adequate time for jet cutting, the pressure was confined to the cut area and a clean cut resulted.

In the use of fluid jets for mine neutralization, confinement of the jet impact pressure to the desired area to be cut would avoid the danger of high pressure being transmitted beyond this area, which might induce detonation of the mine contents.

In other words, the jet must retain a high degree of cohesion so that it will penetrate the target and material can be removed without affecting adjacent and possibly sensitive material. Therefore, in addition to moderate traversing speeds, the nozzle must be relatively close to the material surface for cutting materials like Plexiglas. Close proximity to the cutting surface is not as important in the cutting of wood since, in this case, the material has a much lower threshold pressure to initiate penetration.

CHAPTER 4

Conclusions

1. The presence of viscoelastic additives in the jet fluid increases the coherency of high pressure turbulent water jets extruding into stagnant air. Polyethylene oxide polymer (Polyox FRA at 500 p.p.m.) was the most effective additive tested in this study. Several commercial polyacrylamide polymers were also quite effective.

2. In the high jet Reynolds Numbers range studied, the effects of jet pressure (velocity α pressure$^{1/2}$) and nozzle diameter on jet coherent length varied with Reynolds Number. In the Reynolds Number range of 60,000 to 210,000, jet pressure had little effect on coherent length while an increase in nozzle diameter caused an increase in jet length. At higher Reynolds Numbers an increase in both variables caused an apparent increase in jet coherent length. These results suggest that the quantity

$$\frac{L}{D(WE)^{1/2}}$$

reaches a (second) turbulent plateau at high Reynolds Numbers. A careful study of coherent jet length as a function of these two variables at high Reynolds Number is necessary to determine the exact relationships between

$$\frac{L}{D(WE)^{1/2}}$$

and Reynolds Number.

3. High pressure turbulent jets with viscoelastic polymer additives present offer no advantage in cutting soils at short (10-in.) standoff distances compared with pure water jets. The additives limit disruption of the jet, some of which are desirable for soil removal. However, at longer standoff distances (22 in. or more), where they prevent total disruption of the jet, the viscoelastic additive solutions are more effective in penetrating soils than pure water.

4. At a jet pressure of 2,500 p.s.i., a nozzle diameter of 0.06 in. and jet traversing speeds of 3 ft./sec. and 6 in./sec. with pure water, soil removal was achieved at a standoff distance of 5-1/2 ft. Using the same nozzle

at a jet pressure of 2,000 p.s.i. and the same traversing speeds, solutions of 500 and 1,000 p.p.m. of a polyacrylamide polymer (Nalco BX-254) gave more coherent jets which penetrated the soil well but which did not remove soil from the target tray as efficiently as pure water. Both the more coherent jets and the poorer splashing properties giving poorer soil removal are believed to be due to the high extensional viscosities of the polymer solutions. A study to find the optimum polymer types and concentrations for achieving coherent jets and effective soil removal needs to be carried out.

5. In high pressure jet cutting of solid materials, the presence of viscoelastic polymer additives increases cutting effectiveness.

6. For high pressure jet cutting of wood and Plexiglas, the largest nozzle diameter (at a fixed pressure) gave the best cut.

7. For jet cutting of Plexiglas, jet pressures above 30,000 p.s.i., very small standoff distances, and moderate traversing speeds (below 60 in./min.) are required for clean cuts of 1/4-in. material.

8. The interactions of nozzle design and jet traverse speed with the variables studied, viscoelasticity of the solution, jet pressure, and nozzle size, are important for system designs for practical applications. A more complete study to encompass all of these variables and to study them in more detail is required.

9. Solutions made with Nalco 625, an emulsion containing about 1/3 polyacrylamide polymer by weight, are easily prepared. The convenience of using this product warrants its inclusion in any test program in which the effect of polymer additives is to be studied for practical applications.

REFERENCES

1. London Sunday Times (1973), December 16, 1973, p. 33.

2. Wilkinson, A. (1874), The Ancient Egyptians, 2, p. 137.

3. Bowie, A.J., Jr. (1885), A Practical Treatise on Hydraulic Mining in California, D. Van Nostrand Co., New York.

4. Boyd, W.T. (1959), Mining & Transporting Coal Underground by Hydraulic Methods - A Literature Survey, U.S.B.M. IC 7887.

5. Green, J.H. (1971), "Effect of Polymer Additives on Nozzle Stream Coherence: a Preliminary Study," Naval Undersea Center, Tech. Note No. 504.

6. Anon (1973), "Engineering Corps Display," Tenesalem Post Weekly-Overseas Edition, Aug 13, 1974, p. 4.

7. Leinhard, J.H. and Day, J.B. (1969), "The Break-up of Superheated Liquid Jets," ASME paper no. 69-WA/FE-19, presented at the ASME Winter Meeting, Los Angeles, November 1969.

8. Miesse, C.C. (1955), "Correlation of Experimental Data on the Disintegration of Liquid Jets," Ind. & Engr. Chem., 47, pp. 1690-1701.

9. Leinhard, J.H. and Day, J.B. (1969), "The Break-up of Superheated Liquid Jets," ASME paper no. 69-WA/FE-19, presented at the ASME Winter Meeting, Los Angeles, November 1969.

10. Heubner, A.L. (1969), "Disintegration of Charged Liquid Jets," Jl. Fluid Mech., 38 (4), pp. 679-688.

11. Leach, S.J. and Walker, G.I. (1966), "The Application of High Speed Liquid Jets to Cutting," Proc. Roy. Soc. (London), 260A, pp. 295-308.

12. Zakin, J.L. and Chang, J.L., (1972), "Nonionic Surfactants as Drag Reducing Additives," Nature Physical Science, Vol. 239, p. 26.

13. Zakin, J.L., Poreh, M., Brosh, A. and Warshavsky, M., (1971), "Exploratory Study of Friction Reduction in Slurry

Flows," in Drag Reduction, Chem. Engrg. Prog. Symp. Series No. 111, Vol. 67, pp. 85-89.

14. Hoyt, J.W. and Taylor, J.J. (1974), "A Photographic Study of Polymer Solution Jets in Air," Proc. Intl. Conf. Drag Reduction, Cambridge, U.K., paper E3.

15. Phinney, R.E. (1973), "The Break-up of a Turbulent Liquid Jet in a Gaseous Atmosphere," Jl. Fluid Mech., 60, pp. 689-701.

16. Beutin, E.E., Erdmann-Jesnitzer, F. and Louis, H. (1974), "Material Behavior in the Case of High-Speed Liquid Jet Attacks," Proc. 2nd Intl. Symp. Jet Cutting Tech., Cambridge, U.K., paper C1.

17. Golden, M., et al (1969), "Break-up of a Laminar Capillary Jet of a Viscoelastic Fluid," Jl. Fluid Mech., 38 (4), pp. 689-711.

18. Summers, D.A. (1968), Disintegration of Rock by High Pressure Jets, Ph.D. Thesis, U. of Leeds, U.K.

19. Bryan, E.L. (1963), High Energy Liquid Jets as a New Concept for Wood Machining, Ph.D. Thesis, University of Michigan.

20. Lord Rayleigh (Strutt, J.J.) (1878), "On the Instability of a Cylinder of Viscous Liquid under Capaillary Force," Phil. Mag. 34, (207), pp. 145-154.

21. Lord Rayleigh (1878), "On the Instability of Jets," Phil. Mag., 36, pp. 4-13.

22. Bohr, N. (1909), "Determination of the Surface Tension of Water by the Method of Jet Vibration," Phil. Trans. Roy. Soc. (London), 209A, p. 281.

23. Weber, C. (1931), "Zum Zerkall eines Flussighkeitsstrahles," Zeit. Ang. Math. Mech., 2 pp. 136-154.

24. Pai, Shih-I, (1954), Fluid Mechanics of Jets, D. Van Nostrand Co., Inc., New York.

25. Leach, S.J. (1966), Unpublished information.

26. Merritt, G.E. (1969), "The Expansion of a Supersonic Parallel Flow into a Source Flow," AD 693 285.

27. Rupe, S.H. (1962), NASA Tech. Rept. No. 32-207.

28. Grant, R.P. and Middleman, S. (1966), "Newtonian Jet Stability," A.I.Ch.E. Jl., 12, (4), p. 669.

29. Lyshevskii, A.S. (1961), The Relationships in the Disintegration of Liquid Jets by Mechanically Operated Pressure Nozzles, Radaktsionno-izdatelskii odtel NPI, Novockerkass K.

30. Bridgeman, P.W. (1925), "The Viscosity of Liquids under Pressure," Proc. Nat. Acad. Sci., U.S., 11, p. 603.

31. Bowden, F.P. and Brunton, J.H. (1961), "The Deformation of Solids by Liquid Impact on Supersonic Speeds," Proc. Roy. Soc. (London), 263A, p. 433.

32. Lyshevskii, H.A. (1962), "Some Laws Governing the Cutting of Rock with a Liquid of Ultra-high Pressure," Ugol Ukrainy 6, (9), p. 28.

33. Vereschagin, L.E., et al. (1958), "On the Problem of the Break-up of High Speed Jets of Water," Sov. Phys. Tech. Phy., 4, (1), p. 38.

34. Okhrimenko, V.A. (1962), Hydro-monitor Operator in Coal Mines and Pits, State Scientific Technical Press of Literature on Mining, Moscow.

35. Yufin, A.P. (1965), Hydromechanisation, Moscow.

36. Shavlovsky, D.S. (1972), "Hydrodynamics of High Pressure Fine Continuous Jets," Proc. 1st Intl. Symp. Jet Cutting Tech., Coventry, U.K., paper A6.

37. Semerchan, A.A., Kusin, N.H., and Isagkov, V.K., (1963), "The Reaction of Electric Poles on Uninterrupted Liquid Jets," 6, (2), pp. 114-117.

38. Kuklin, I.S. and Shtukaturov, K.M. (1962), "Advances in the Methods of Studying the Structure of Hydromonitor Jets," Works of the Inst. of Min., Acad. Sci., USSR, (3), pp. 63-69.

39. Franz, N.C. (1972), "Fluid Additives for Improving High Velocity Jet Cutting," Proc. 1st Intl. Symp. Jet Cutting Tech., Coventry, U.K., paper A7.

40. Semerchan, A.A., et al. (1958), "Distribution of Momentum in a Continuous Liquid Jet of Supersonic Velocity," Soviet Physics, 3, pp. 1894-1903.

41. Shtukaturov, K.M. and Kuklin, I.S. (1962), "The Influence of the Initial Diameter and Jet Pressure on its Quality," Acad. Sci., USSR, Urals Branch, Works of the Mining Institute, (3), pp. 83-86.

42. Voitsekhovsky, V.B., et al. (1972), "On the Destruction of Rocks and Metals by High Pressure Jets of Water," Proc. 1st Intl. Symp. Jet Cutting Tech., Coventry, U.K., paper G8.

43. Zelenin, A.N., et al. (1958), "Rock Breaking with a Jet Stream under Pressure to 2000 Atm," in Problems in Mining, Moscow.

44. Farmer, I.W. and Attewell, P.B. (1965), "Rock Penetration by High Velocity Water Jet," Intl. Jl. Rock Mech. Min. Sci., 2, (2), pp. 135-153.

45. Matsumoto, K., et al. (1972), "High Pressure Jet Cutting," Proc. 1st Intl. Symp. Jet Cutting Tech., Coventry, U.K., paper B4.

46. Daniel, I.M., Rowlands, R.E., and Labus, T.J., (1974), "Photoelastic Study of Water Jet Impact," Proc. 2nd Intl. Symp. Jet Cutting Tech., Cambridge, U.K., paper A1.

47. Fowkes, R.S., and Wallace, J.J. (1968), "Hydraulic Coal Mining Research-Assessment of Parameters Affecting the Cutting Rate of Bituminous Coal," U.S.B.M. RI 7090.

48. Anon (1965), "Stone and Coal Cutting with Small High Pressure Water Jets," N.C.B. Rept. CEE, Bretby, U.K.

49. Anon (1974), Hydromechanical Coal Mining and Hydraulic Transportation-II (Mine Carl Funke), Schlussbericht des Steinkohlenbergbauvereins, Essen.

50. Garcia, R., Hammitt, F.G., and Hystrom, R.E. (1966), "Correlation of Cavitation Damage with Other Material and Fluid Properties," in Erosion by Cavitation and Impingement, ASTM STP 408.

51. Schweitzer, P.H. (1937), "Mechanism of Disintegration of Liquid Jets," Jl. Appl. Phys., 8, pp. 513-520.

52. Kuehn, --(1927), Der Motorwagen, (Berlin).

53. Tyler, E., and Watkins, F. (1932), "Experiments with Capillary Jets," Phil. Mag., 14 (94), pp. 849-881.

54. Tyler, E., and Wyatt, R. (1925), "The Characteristic

Curves of Liquid Jets," Proc. Phys. Soc., 37, pp. 297-312.

55. Haenlein (1932), Forsch. Ing. Wes., 4, p. 139.

56. Ohnesorge, (1936), Z. Agr. Math. Mech., 16, p.355.

57. Littaye, (1939), C.R. Acad. Sci., Paris, 208, p. 788.

58. Merrington, A.C. and Richardson, E.G. (1947), "The Break-up of Liquid Jets," Proc. Phys. Soc., 59, (331), pp. 1-13.

59. Richardson, E.G. (1954), "Mechanism of the Disruption of Liquid Jets," Appl. Sci. Res., 4A, pp. 374-380.

60. Misse, (1956), Voprosy Raketnoi Tekhniki, 5, (35).

61. Cooley, W.C. (1973), "Correlation of Data on Rock Disintegration by Liquid Jets," Spring Hill Conf. on Res. in Tunneling and Excavation Technology, Minn.

62. Rochester, M.C. and Brunton, J.H. (1973), "The Influence of the Physical Properties of the Liquid on the Erosion of Solids," CVED/C-MAT/TR10.

63. Sims, J.S., Jr., et al (1968), "Jet Delivery Optimization," Final Report R-4-23-68 on DOT Contract No. 7-35381.

64. Vlasov, S.A., et al (1973), "The Long Range Nature of Turbulent Submerged Jets of Polymer Solutions," Fluid Mechanics-Soviet Research, 2 (1), pp. 108-111.

65. Hoyt, J.W. and Fabula, A.G. (1964), "The Effect of Additives on Fluid Friction," Proc. 5th Symp. Naval Hydrodyn., p. 945, Bergen: Office of Naval Research, ACR-112.

66. White, D.A. (1967), "Velocity Measurements in Axisymmetric Jets of Dilute Polymer Solutions," Jl. Fluid Mech., 28 (1), pp. 195-204.

67. Gadd, G.E. (1965), "Turbulence Damping and Drag Reduction Produced by Certain Additives in Water," Nature, 206A (4983) pp. 463-467.

68. Hoyt, J.W., Taylor, J.J., and Runge, L.D. (1974), "The Structure of Jets of Water and Polymer Solution in Air," Jl. Fluid Mech., 63 (4), pp. 635-640.

69. Davis, J.T., and Young-Hoon, A.A. (1974), "Restrained Turbulent Jets of a Non-Newtonian Solution," Chem. Engrg. Sci., 29, pp.1115-1121.

70. Garner, F.H., Nissan, A.H., and Wood, G.F. (1950), Phil. Trans. Roy. Soc. (London), 243A, p. 37.

71. Cristy, G.A. and Brooks, C.B. (1970), Tunneling-An Annotated Bibliography, ORNL-HUD-17, Oak Ridge National Laboratory.

72. Cooley, W.C. (1974), "A Survey of Hydraulic Mining Technology," for U.S.B.M. (in preparation).

73. Richardson, C.A. and Thornton, W.A. (1973),"Jet Cutting Technology-A Bibliography," BHRA Fluid Engineering.

74. Summers, D.A. and Peters, J.F. (1974), Preliminary Experimentation on Coal Cutting in the Pressure Range 35-200 MN/m^2," Proc. 2nd Intl. Symp. Jet Cutting Tech., Cambridge, U.K., Paper H2.

75. Summers, D.A. and Peters, J.F. (1974), "The Effect of Rock Anisotropy on the Excavation Rate in Barre Granite," Proc. 2nd Intl. Symp. Jet Cutting Tech., Cambridge, U.K. , paper H5.

76. Chadwick, R.F. (1973), Continuous High-Velocity Jet Excavation-Phase II, Final Rept., ARPA Contract H0220067, Bendix Research Labs.

77. Conn, A.F. and Johnson, V.E., Jr. (1974), "Further Applications of the Cavijet Method," Proc. 2nd Intl. Symp. Jet Cutting Tech., Cambridge, U.K., paper A2.

78. Franz, N.C. (1974), "The Influence of Standoff Distance on Cutting with High Velocity Fluid Jets," Proc. 2nd Intl. Symp. Jet Cutting Tech., Cambridge, U.K.,paper B3.

79. Yugov, V.G. and Osipov, A.I. (1960), "The Use of High Speed Water Jets in Wood Cutting and Processing," Trans. Central Sci. Res. Inst. of Mech. & Eng. Req. of the USSR, 15 (6).

80. Kurko, M.C., Chadwick, R.F. and Kee, W.R. (1970), "Fluid Jet Developments and Applications in the Paper Industry," Proc. TAPPI Fall Conf., Portland, Maine.

81. Olsen, J.H. (1974), Personal Communication to Dr. David A. Summers.

82. Walstad, O.M. (1974), "Commercial Utilisation of the McCartney Fluid Jet Cutting Concept," Proc. 2nd Intl. Symp. Jet Cutting Tech., Cambridge, U.K., paper E2.

83. Various (1974), Proc. 4th Intl. Conf. of Rain Erosion and Associated Phenomena, Meersburg, W. Germany, May.

84. Mohaupt, U.H. and Burns, D.J. (1973), "Machining Unreinforced Polymers with High-Velocity Water Jets," Proc. 3rd SESA Intl. Conf. on Experimental Mechanics, Los Angeles, CA, May 13-18.

85. Mohaupt, U.H. and Burns, D.J. (1972), "Machining with Continuous Fluid Jets at Pressures of 2 to 7 Kbar," Proc. 1st Intl. Symp. Jet Cutting Tech., Coventry, U.K., paper G4.

APPENDIX I

Previous Work

Historical Development of Theory

Within the literature on water jet structure there is a constant intermingling of jet veolcity and jet pressure values as descriptions of the jet parameter. Strict terminological usage requires that pressure terms be used upstream of the nozzle and velocity terms downstream, where confinement is removed. Simplistically the relationship between jet pressure and velocity can be derived from Bernoulli's theorem, based on energy conservation. Because of the high pressures normally considered, height variations can be neglected and the relationship summarized as

$$v = \frac{2P}{\rho} \qquad 7$$

where ρ is the density of the jet fluid, P is jet pressure upstream of the nozzle and v the jet velocity at the orifice.

Where consideration is also given to fluid compressibility, Bryan (Ref. 19) has derived an equation for jet velocity from which he has plotted a curve correlating jet velocity and pressure (Figure 34). The experimental curve was derived from the results of Bryan's research using a high pressure intensifier for cutting wood (Ref. 19).

At low jet velocities the structure of the jet [Figure 35(a)] remains continuous across individual diameters and breakup occurs by sinusoidal contractions which ultimately increase in size to the point where the jet becomes a set of traveling, discrete particles (Ref. 20). This effect is due to capillary forces generating instabilities in the jet flow. Analysis of jet breakup under these conditions was studied by Rayleigh (Ref. 21), Bohr (Ref. 22), and Weber (Ref. 23) to obtain the coherent length, L_B, as

$$\frac{L_B}{D\sqrt{WE}} = \ln\left(\frac{D}{2\delta}\right)\left(1 + \frac{3\ WE}{RE}\right) \qquad 8$$

where the symbols are the same as those used in Chapter 2, and δ is the initial jet disturbance. Since, in most cases, Reynolds Number is much larger than Weber Number, we can approximate jet length as

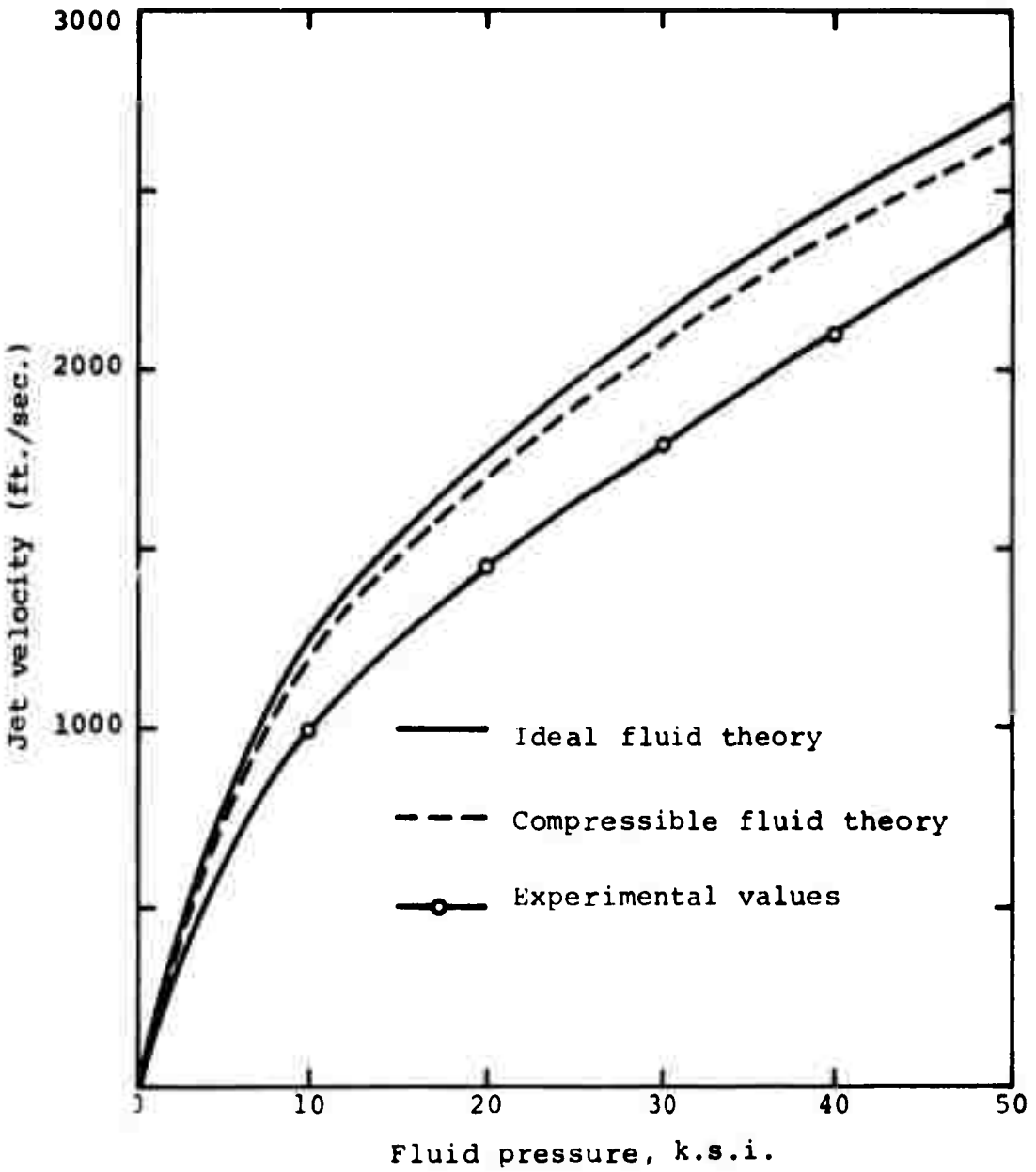

Figure 34. Variation in jet velocity with change in pump pressure (after Ref. 19).

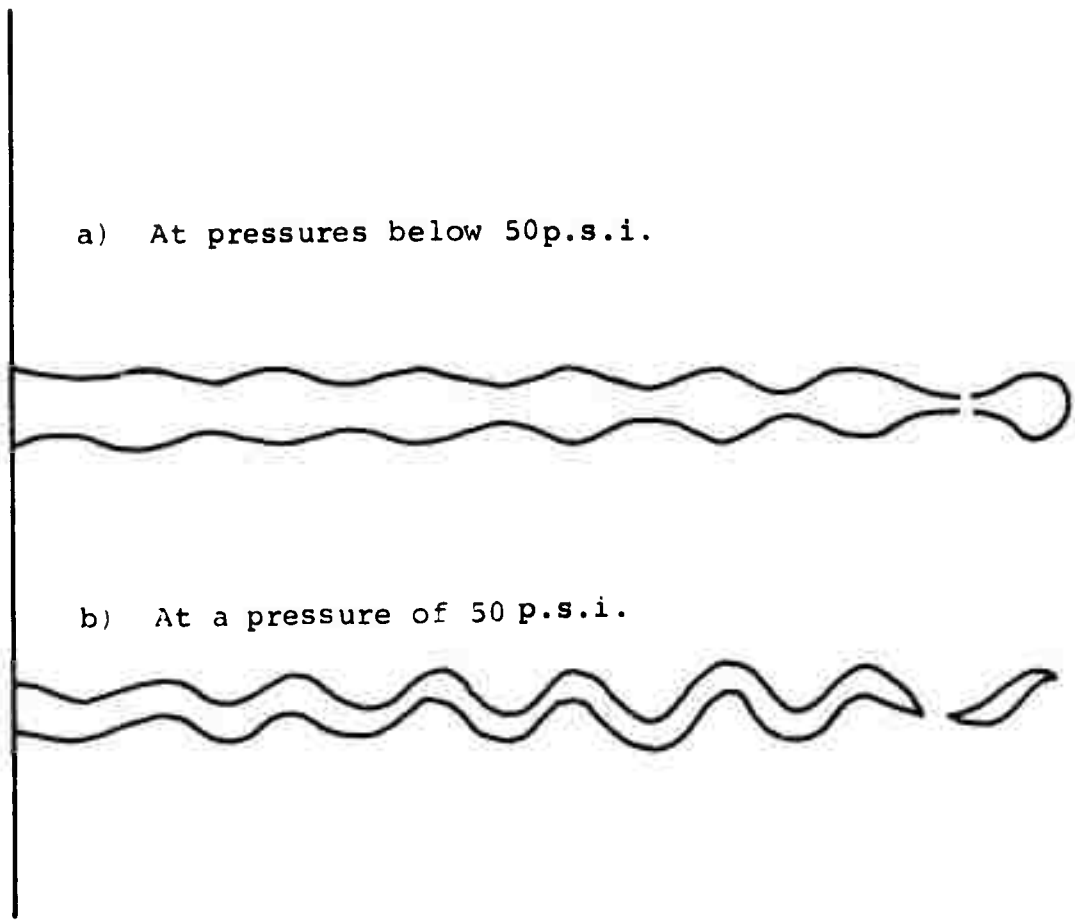

Figure 35. Forms of jet breakup at low velocities.

$$L_B = DWE^{1/2} \ln\left(\frac{D}{2\delta}\right) \qquad 9$$

Lienhard and Day(Ref. 9) state that in most cases $\ln(D/2\delta)$, the ratio of nozzle diameter to initial surface disturbance, can be taken as 12 ± 1 (Figure 36). As the jet velocity increases, the pattern of jet disintegration changes, and the jet structure ceases to be axisymmetrical. The jet structure assumes the shape of a wave form, of increasing amplitude with distance from the nozzle, leading ultimately to jet disruption (Figure 35(b)) . It is in this region where the axis of the jet deviates sinusoidally that Miesse (Ref. 8) has derived a relationship for jet length of the form

$$\frac{L_B}{D\sqrt{WE}} = 540RE^{-5/8} \qquad 10$$

The transition between the two forms of disruption is a function of Reynolds Number, in the same manner, but at a lower value, as the change from laminar to turbulent jet flow occurs. Normally, below a value for Reynolds Number of approximately 2100, laminar flow prevails and the sinusoidal oscillations lead to disruption by capillary forces. Above this Reynolds Number some of the oscillations will increase in aplitude without bound while others are damped (Ref. 24). The Reynolds Number at which the flow becomes turbulent depends on the jet flow pattern. With carefully controlled conditions such as a long, straight supply line and suitable nozzle, laminar flow may exist to much higher Reynolds Numbers.

In this range of Reynolds Numbers jet cohesive length reduces with an increase in velocity and the effect of wave distortion becomes more pronounced with higher velocity. Initially the waves are damped and axisymmetrical breakup still occurs but in a shorter length. If laminar flow continues beyond this stage, the transverse waves will increase in magnitude and the coherent jet length decreases until the point is reached where the surface waves are initiated at the nozzle. The jet will disrupt violently at this point.

In the more general case where turbulence occurs, vortices are formed under the jet surface. These vortices have a high angular velocity, sufficient to raise disturbances in the form of a standing wave at the surface. With an increase in overall jet speed this angular velocity also increases until it is sufficient to cause

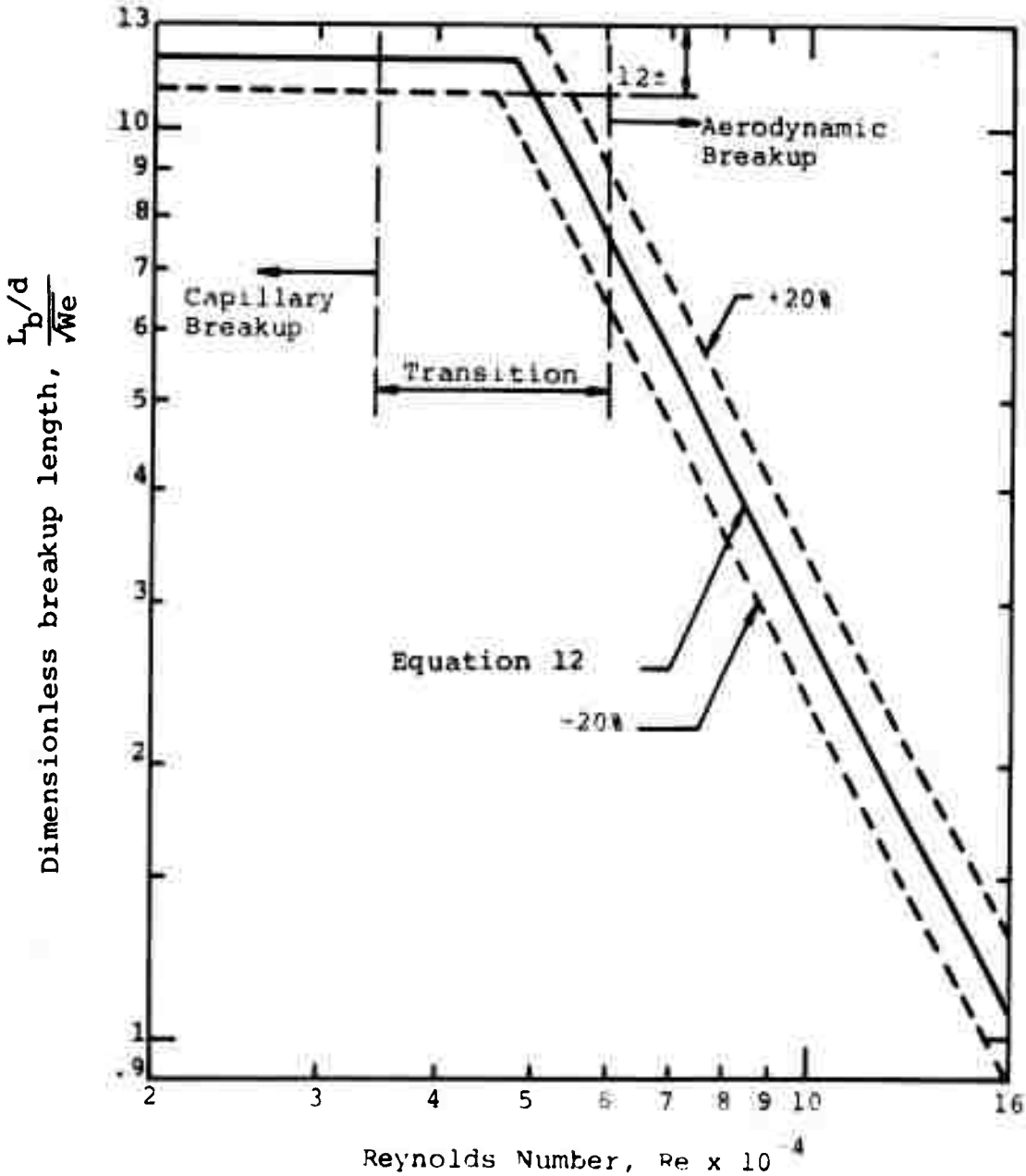

Figure 36. Variation in jet breakup length with Reynolds number (after Ref. 7).

the disruption of the surface. The droplets which are created develop a radial velocity which gives a steeper angle to the disrupted jet cone. This phenomena has been observed by Leach (Ref. 25) and Merritt (Ref. 26) and has been postulated by Rupe (Ref. 27) as being the fundamental cause of breakup.

As jet velocity continues to increase further, Grant (Ref. 28) has shown that in the range of 210 ft/sec. the jet coherent length will increase. He obtained a relationship between jet length, diameter and Weber Number

$$\frac{L_B}{D} = \left(7.68 - \frac{2.66\sqrt{WE}}{RE}\right) \sqrt{WE} + \frac{3\ WE}{RE} \qquad 11$$

but suggested that as the time of jet stability continues to reduce, the breakup is increasingly influenced by the radial jet velocity.

Lyshevskii (Ref. 29) has defined the length of the basic section in the same terms as Grant and the theoretical behavior of the jet within the range to first maximum length [where the jet flow is laminar (Eq. 11)] agrees well with his experimental findings. Beyond this point correlation is not good.

With a further increase in jet velocity the forces generated between the jet and the ambient fluid cause stripping of the outer layers of the jet and a radial erosion inward of the jet structure. This form of disruption is referred to as aerodynamic breakup.

Lienhard and Day (Ref. 9) examined jet breakup over a range of velocities through the transition from capillary to aerodynamic breakup and obtained the equation

$$\frac{L_B}{D\sqrt{WE}} = 2.75 \times 10^{10}\ RE^{-2} \qquad 12$$

as a best fit curve, as shown in Figure 22, for jet length under aerodynamic disintegration.

The analysis to date has considered only jet length as a parameter, a value which is not constant under normal pump operation but for which operational length may be defined as an average value.

When a liquid is subjected to a high pressure, the viscosity increases (Ref. 30) causing greater pressure

losses in the nozzle and may account for the discrepancy between the theoretical and experimental curves in Figure 34. Large pressure gradients occur in the vicinity of the nozzle throat and this complicates the problem. All of these factors must be included in any theoretical analysis which will lead to nozzle design parameters.

Experimental Considerations

Bowden and Brunton (Ref. 31) found that turbulence in the supply piping was a major factor affecting jet coherence beyond the nozzle exit. The jet structure is also influenced by nozzle design and smoothness, but other factors including straightness of the nozzle supply inlet, pressure variations and external factors such as properties of the surrounding medium also play a large part in jet cohesion. Investigators of jet structure under aerodynamic breakup (Ref. 32) generally divide the structure of the jet into three sections; a completely coherent or "basic" section, an "intermediate" section with a coherent core but surrounded by an expanding cone of droplets, and the "final" section where the jet is completely disrupted (Figure 37).

Vereschagin (Ref. 33) has shown that the volume of the pump manifold is a major parameter. When the jet is produced from a multi-piston pump, as is most common, pressure fluctuations are present in the manifold. Should these variations be carried through to the jet, then velocity will also vary, creating fast and slow sections. As a "fast" section overtakes a "slow" one, a "disc" of water is formed, standing out from the main stream. This disc is quickly eroded by the surrounding medium but will cause further interference as these drops are impacted by the stream which follows.

As jet velocity is further increased, shock waves will be initiated in the surrounding air, and at still higher velocities, within the jet. These in turn will also create or intensify the jet segmentation into "fast" and "slow" regions.

For a given pump system, however, the equipment behind the nozzle is generally of fixed geometry and the factors which can be controlled to give the best "throw", or effective jet length, are the nozzle geometry, the jet pressure, and the physical properties of the fluid.

Figure 37. Liquid jet structure at medium and high pressure. Length "a" is the basic length and "b" is the effective length (after Ref. 32).

Low Velocity, Large Diameter Flow

Russian investigators have been concerned with improvement of jet flow, particularly as it applies to the cutting of coal, rock, and soils. For example, in open pit mining the theoretical range of jet flight (L in meters) is given by

$$L = \frac{V^2}{2g} \sin 2\alpha \qquad 13$$

where V is in m/sec, α is jet inclination to the horizontal and g = 9.81 m./sec.^{2} (Ref. 34).

The jet is, as mentioned above, divided into three sections. The initial section of the jet is defined as that section over which the total impact force of the jet is reduced by a factor of 2 from that at the nozzle. For the operation of jets in surface mining the following relationships have been found to hold

Table IX. Length of the Initial Section of a Monitor Jet (ft.)with Jet Pressure (p.s.i.) (after Ref. 35)

Jet Pressure (p.s.i.)	Nozzle Diameter (ins.) 2.95	3.54	3.94	4.33
85	4.92	4.97	5.94	5.41
114	9.02	10.5	11.48	11.81
128	11.48	13.12	14.77	16.08
142	14.76	17.06	18.04	19.69

These jets, however, are extremely bulky and are only suited to operation in a permanent site with an adequate supply of water. In a more mobile operation it is necessary to use a higher pressure and lower flow rate to achieve the same effect. Under such conditions the dominant force causing jet breakup becomes aerodynamic, as mentioned above, and jet length is reduced with increasing pressure (Eq. 11). Yufin (Ref. 35) quoted Abromovitch as relating jet diameter to initial orifice diameter by the relationship

$$d = \frac{0.475\ \ell}{D} \qquad 14$$

and the length of the initial section is

$$\ell_o = 145\ D \qquad 15$$

Velocity at the end of the initial section is given by

$$V_\ell = \frac{145\ D}{\ell} \cdot V \qquad 16$$

where ℓ, d, and v_ℓ are length, diameter and jet velocity and diameter at the nozzle orifice. Russian experience (Ref. 24) has found that it is not effective to cut soil with the disrupted part of the jet and that the maximum useful length (L_u) is given by

$$L_u = 0.415^3 \sqrt{\alpha \cdot D \cdot P^2} \qquad 17$$

(P in meters of water head, D is in mm, and α is in degrees). This equation only holds, however, where jet parameters are: inclination angle (α) from 5-32 degrees nozzle diameter (D) of 0.2 to 2 in. and pressure (P) from 15 to 150 p.s.i.

Yufin has carried out experiments examining jet structure at pressures up to 20 p.s.i. with a 0.8-in. diameter nozzle. By measuring jet profiles he found that while overall jet energy may be increased by increasing jet pressure,at greater standoff distances the peak pressure is produced by the jet which initially had the lowest pressure (Figure 38).

For the pressures concerned, Yufin plotted specific pressure (measured value/initial pressure) against length values for various low pressures (Figure 39).

Intermediate Jet Pressure Studies

Shavlovsky (Ref. 36) examined jet structure at pressures up to 7000 p.s.i. with nozzle diameters from 0.04 to 0.143 in. and found that pressure in the initial section could be given by

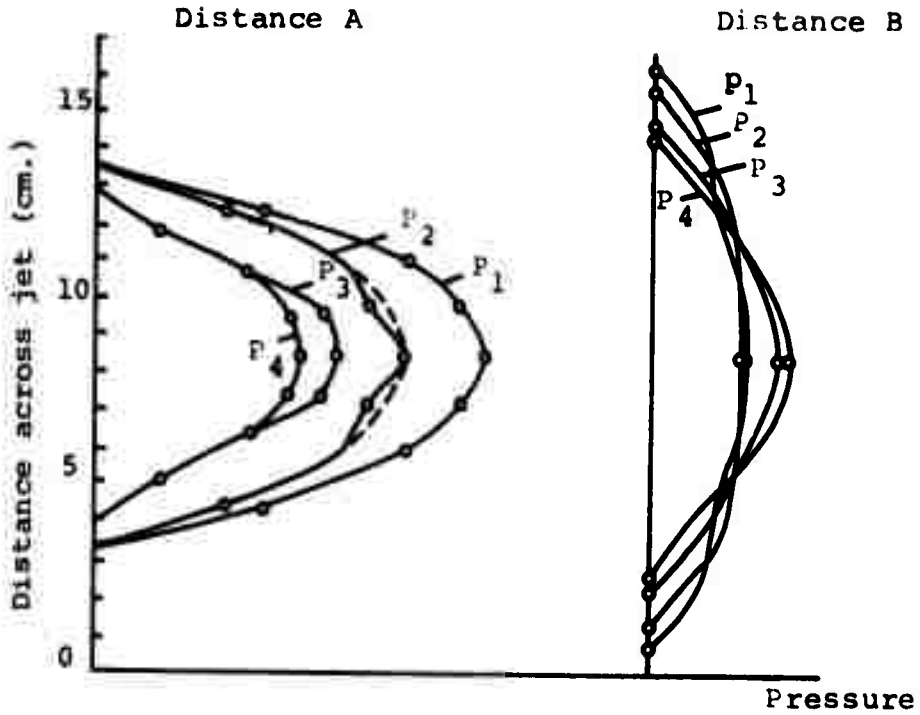

Figure 38. Relative jet pressure profiles with increasing pressure ($P_1 > P_2 > P_3 > P_4$) at two standoff distances (B > A) in front of a hydraulic monitor with a 35-mm. nozzle (after Ref. 35).

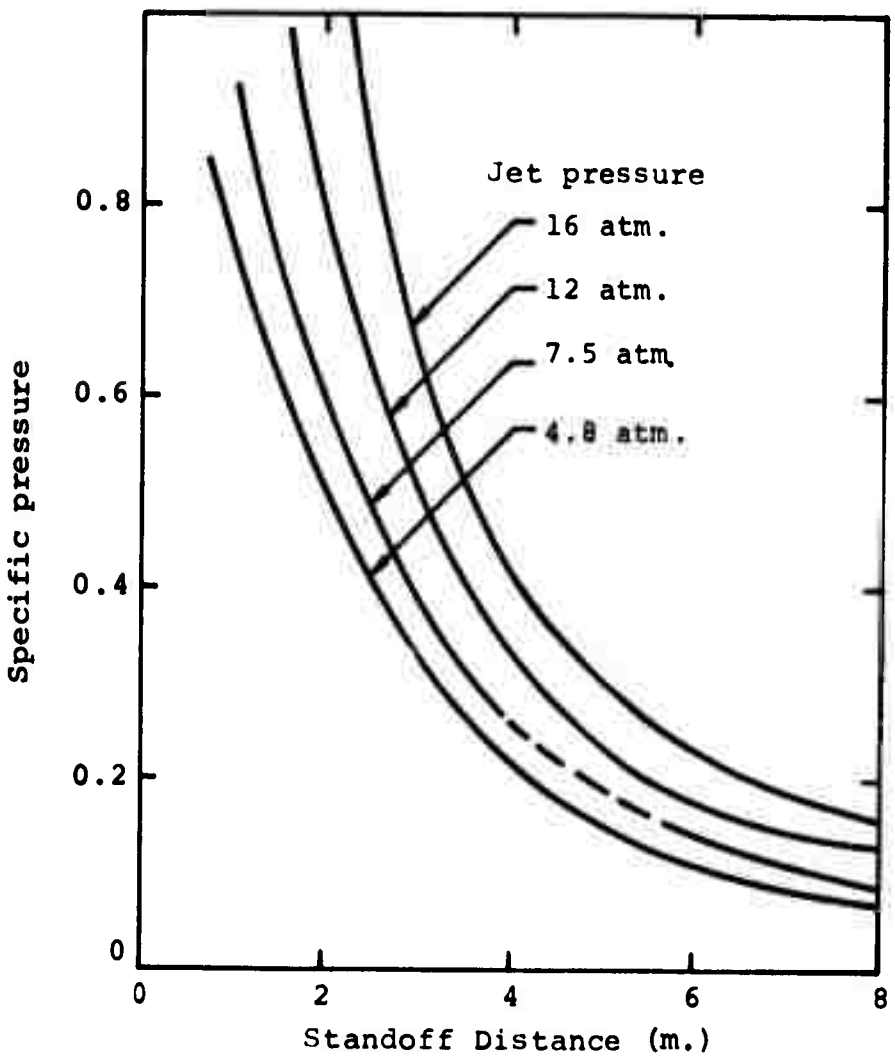

Figure 39. Variation in specific pressure with distance from a 2-mm. nozzle (after Ref. 35).

$$\frac{P_m}{P_o} = \left(\frac{\ell_o}{\ell}\right)^{A + B\left(\frac{\ell_o}{\ell}\right)} \qquad 18$$

Where P_m is the pressure at a distance ℓ from the nozzle, P_o is the initial jet pressure and ℓ_o is the length of the initial section of the jet. Where the units are metric

$$A = 85 \text{ to } 112$$
$$B = 68 \times 10^{-6}$$

and

$$\ell_o = A - B \times RE,$$

Re being jet Reynolds Number at the orifice. Pressure distribution across the jet was given by

$$\frac{P_x}{P_m} = e^{-\phi}\left(\frac{r_x}{r}\right) \qquad 19$$

Where P_x is the pressure at a distance r_x from the jet axis, n^x and ϕ are constants with n varying from 1.5 to 7 with an approximate value of 4 while ϕ is given by

$$\phi = 0.009\,\frac{\ell}{D} + 1.3 \qquad 20$$

Plots of the data obtained are shown in Figures 40 and 41.

The pressure distribution across the jet has been measured by Leach and Walker (Ref. 11) (Figure 42) and compared with a theoretical distribution given by the equation.

$$\frac{P_x - P_a}{1/2\rho\, U^2} = 1 - 3\left(\frac{x}{R}\right)^2 + 2\left(\frac{x}{R}\right)^2 \qquad 21$$

R is the jet radius at which the pressure is equal to atmospheric (P_a), and U is mean jet velocity. The result indicates that the jet reaches an asymptotic effective radius of 2.6 nozzle radii. Research investigators have

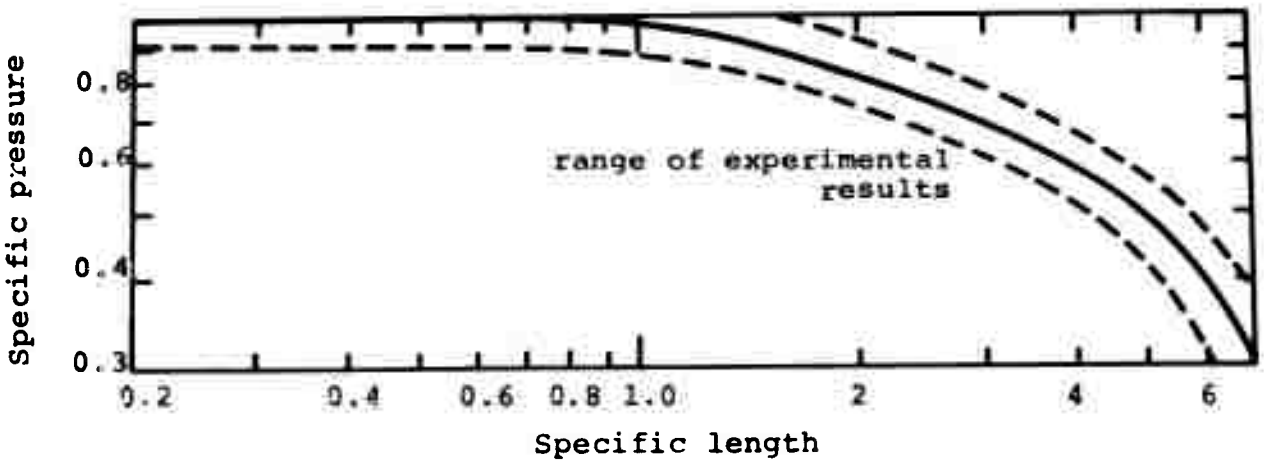

Figure 40(a). Specific jet pressure with specific jet length (length/initial section length) (after Ref. 36).

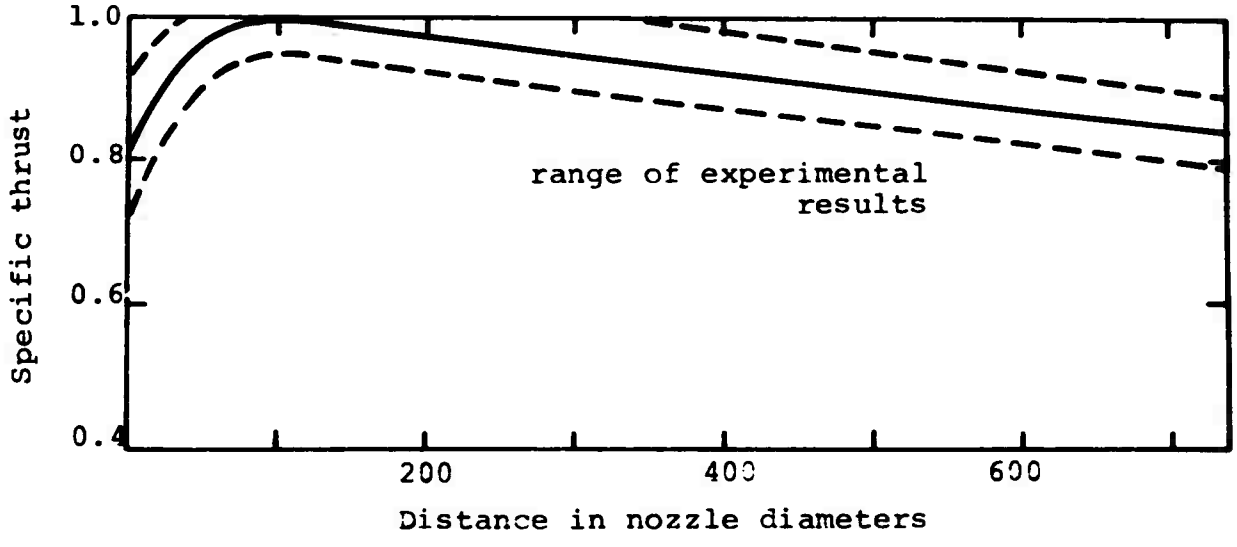

Figure 40(b). Specific jet thrust with distance from the nozzle (after Ref. 36).

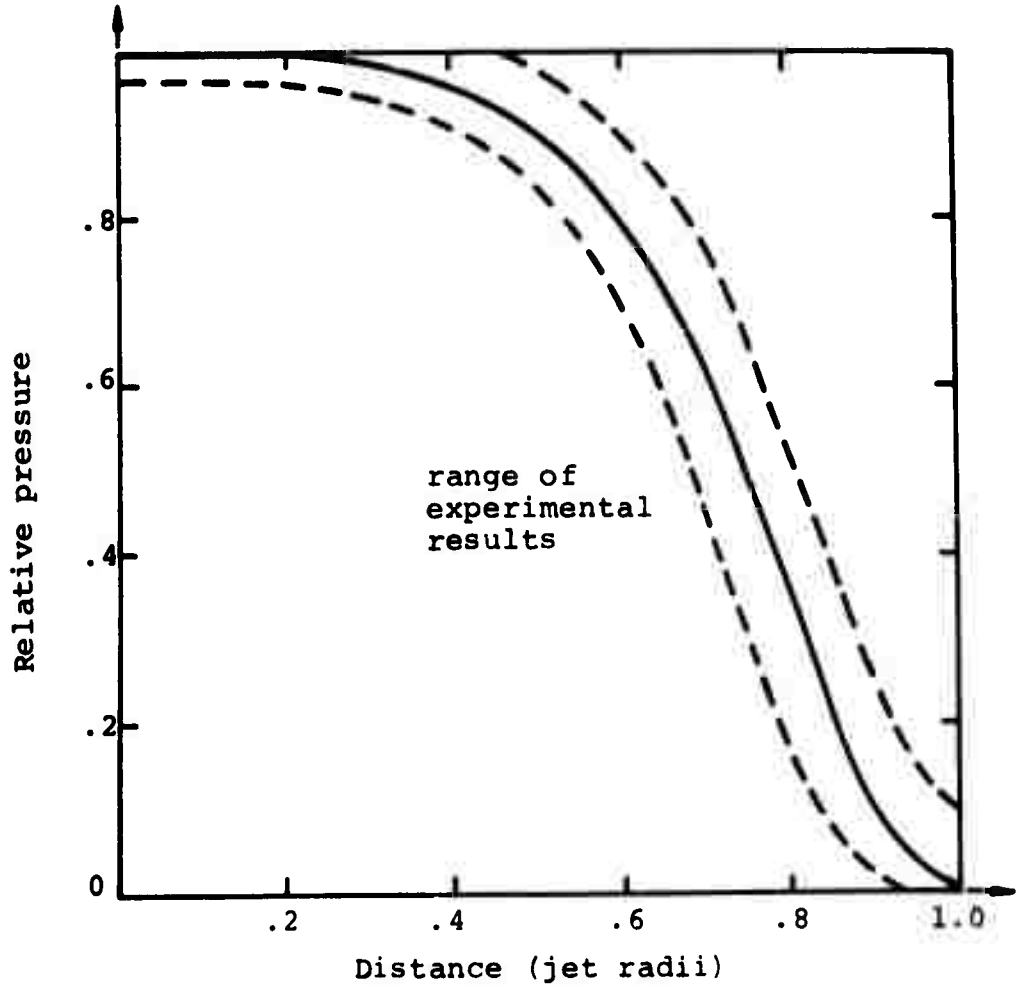

Figure 41(a). Pressure distribution across a jet stream nozzle diameter 2.17 mm., beyond the initial section (after Ref. 36).

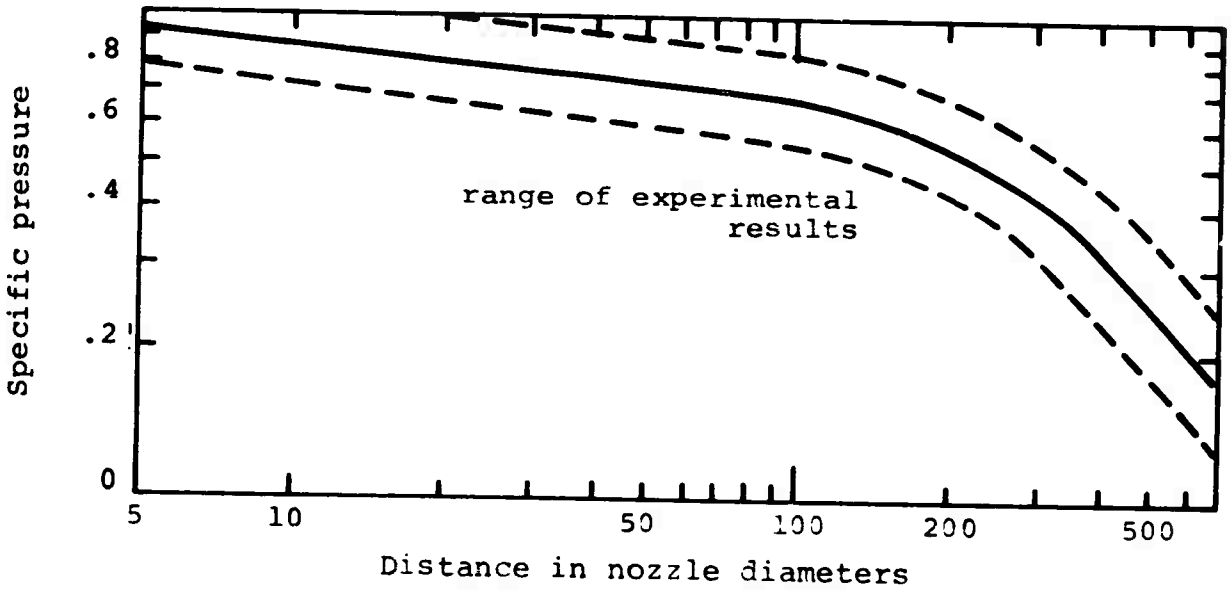

Figure 41(b). Specific jet pressure with distance from the nozzle (after Ref. 36).

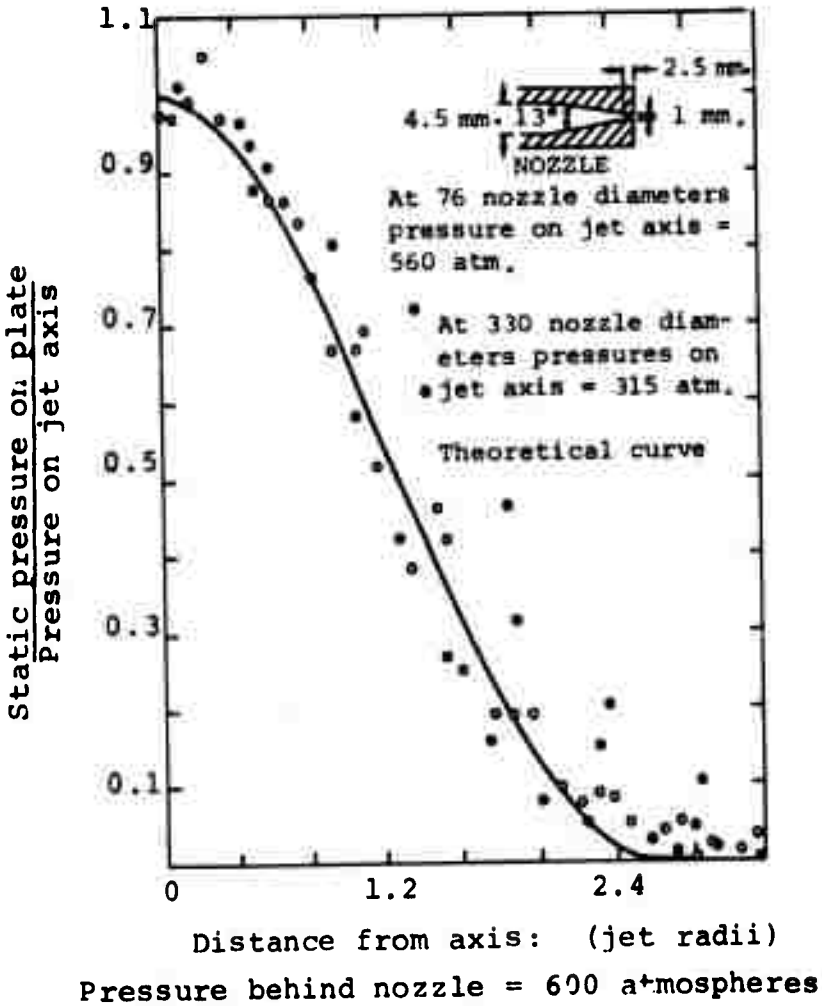

Figure 42. Pressure distribution across a jet, nozzle pressure 600 atmospheres (after Ref. 11).

found a value in excess of 3 for the relation of slot width to nozzle diameter but this can be explained by lateral flow and continued cutting as the jet flows back out of the excavation.

Lyshevskii has carried out experiments within the range of pressure (<10,000 p.s.i.) and with nozzle diameters (<0.06 in.) more suited to a mobile application. As with the research described herein, he found that the jet structure is difficult to distinguish using high speed photography due to the rapid disintegration of the outer layer of the jet into atomized droplets. Lyshevskii used the electrical contact method in order to overcome this problem. The method, useful only for water and conductive fluid applications, relies on passing a current into the jet and measuring the maximum distance down the jet at which this may be detected. In order to pass the current, it was found necessary to first acidify the water.

In initial nozzle studies, it was found that the coefficient of discharge of the nozzle varied with the jet pressure and nozzle diameter (Figures 43, 44, 45).

Experiments were then carried out to determine the coherent jet length using water and the electrical contact method (Figure 46).

It is interesting to note that the curve has two maxima and that as jet velocity increases above 50 m./sec. (240 p.s.i.) coherent jet length is reduced below 1.5 in. Lyshevskii (Ref. 29) found that at velocities up to 50 m/sec., at which the transition to aerodynamic disruption occurred, the jet length could be obtained from

$$\frac{L_B}{D} = 10.5\sqrt{WE}\ (1 + \sqrt{M}) \qquad 22$$

where M had a range of values from 0.2×10^{-4} to 33.4×10^{-4}. The length where the jet was destroyed by atomization (the aerodynamic breakup) was

$$\frac{L_B}{D} = 442(WE)^{-.71}\ \rho^{-1.21}\ M^{.308}. \qquad 23$$

The exact values of the constant and exponents were, however, found to be a function of nozzle shape. Lyshevskii also found that increasing the density of the medium at rest (by overpressuring the chamber) also reduced effective jet length (Figure 47).

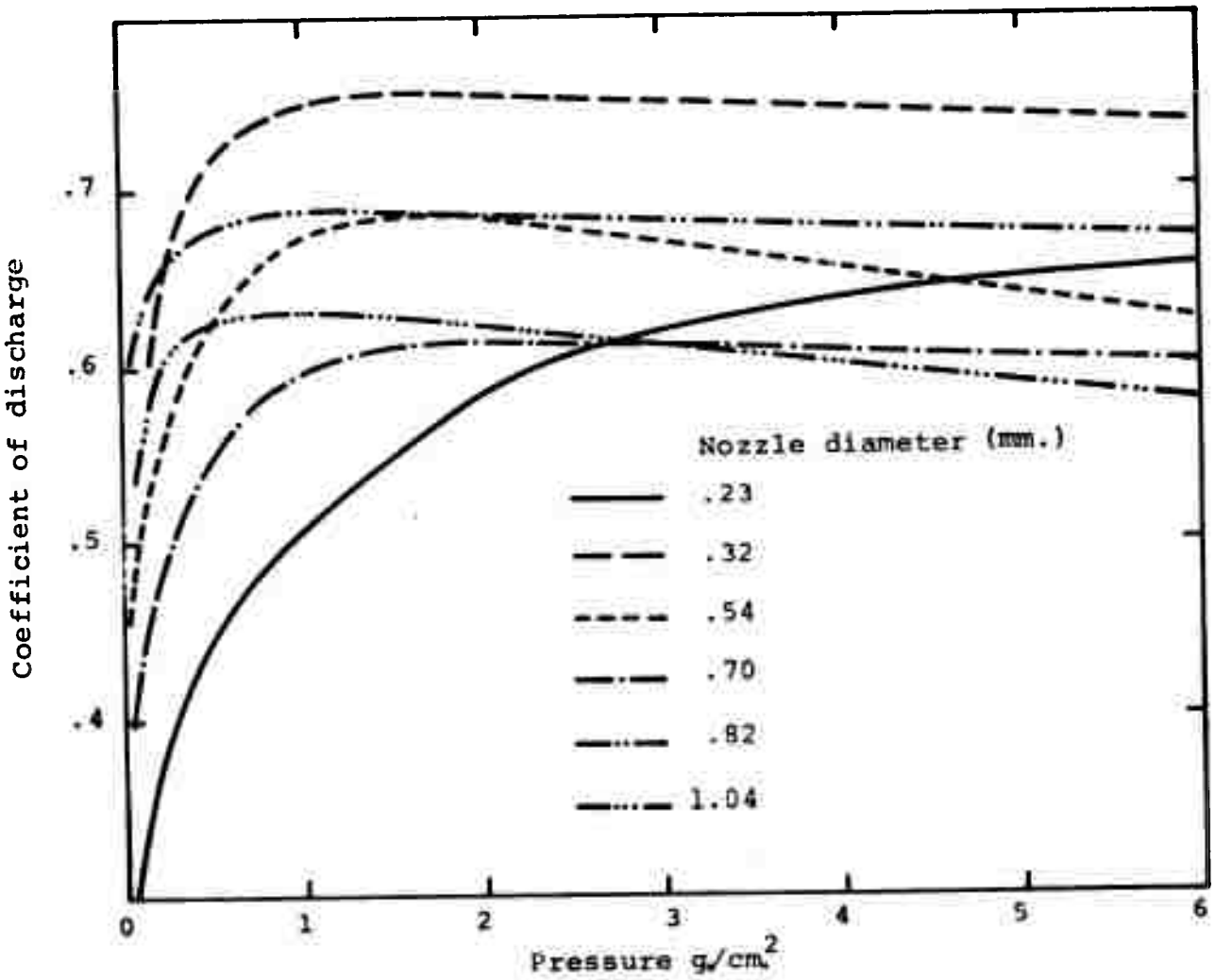

Figure 43. Variation in the coefficient of discharge with pressure and nozzle diameters (after Ref. 32).

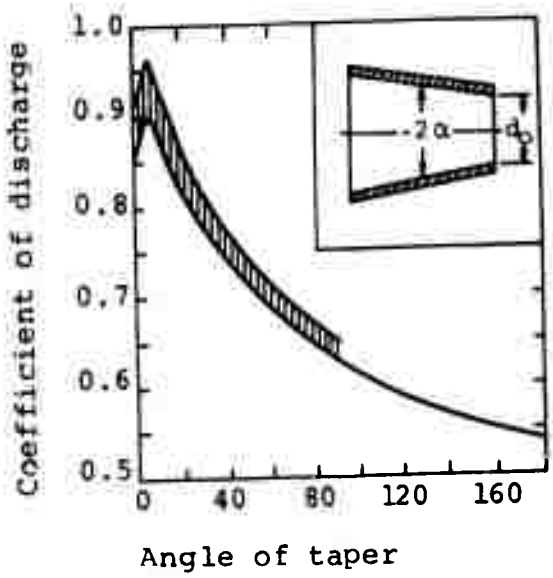

Figure 44. Discharge coefficient as a function of angle of taper (after Ref. 32).

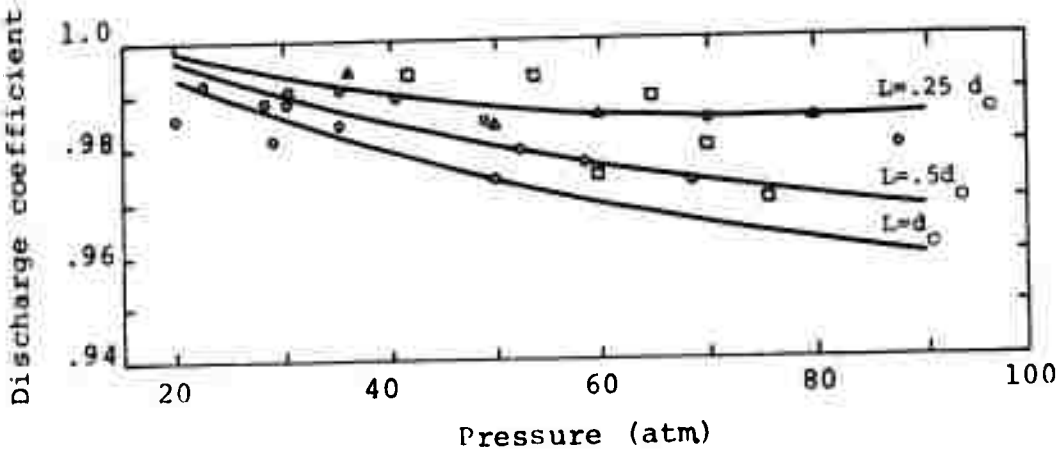

Figure 45. Discharge coefficient as a function of pressure and throat length (after Ref. 32).

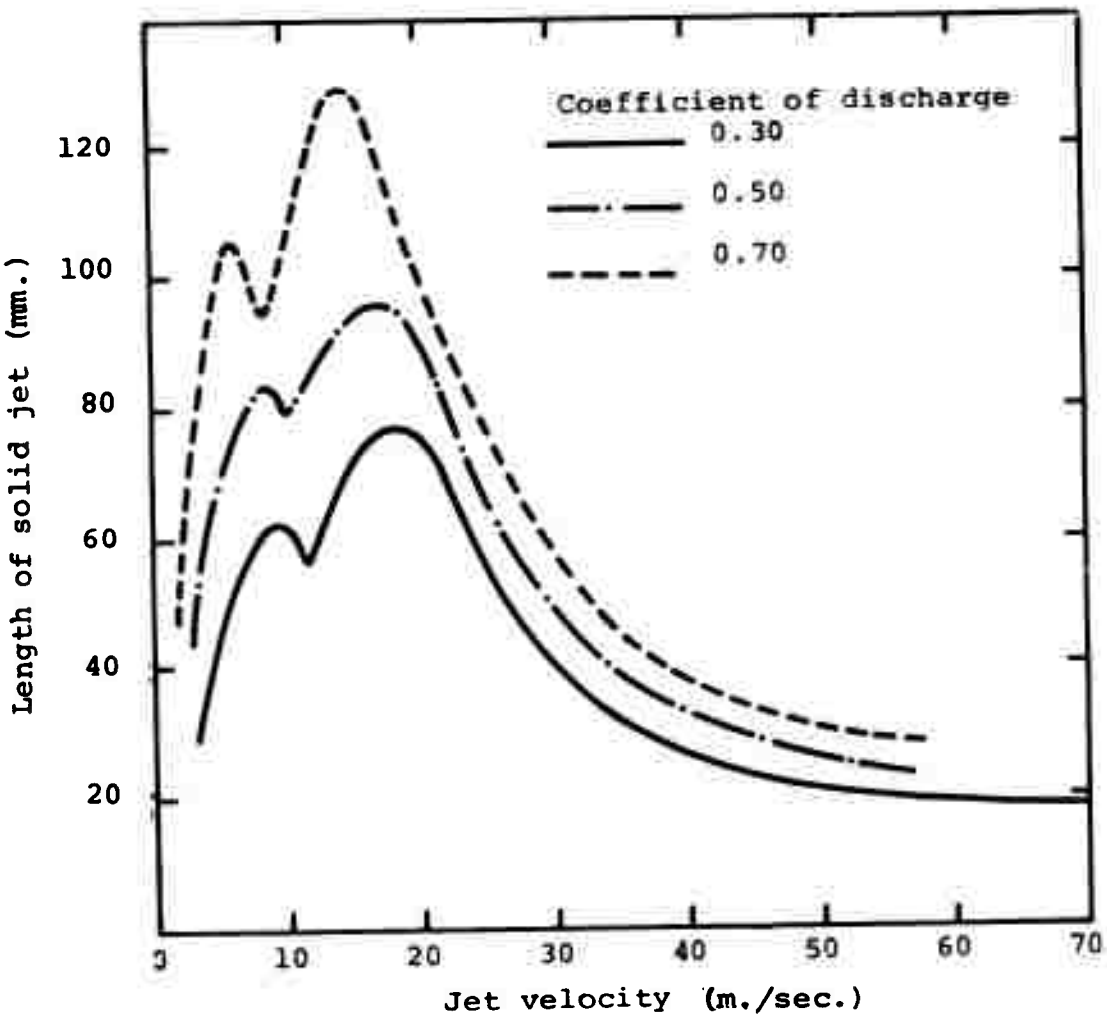

Figure 46. Correlation between coherent jet length and jet velocity at varying discharge coefficients (after Ref. 29).

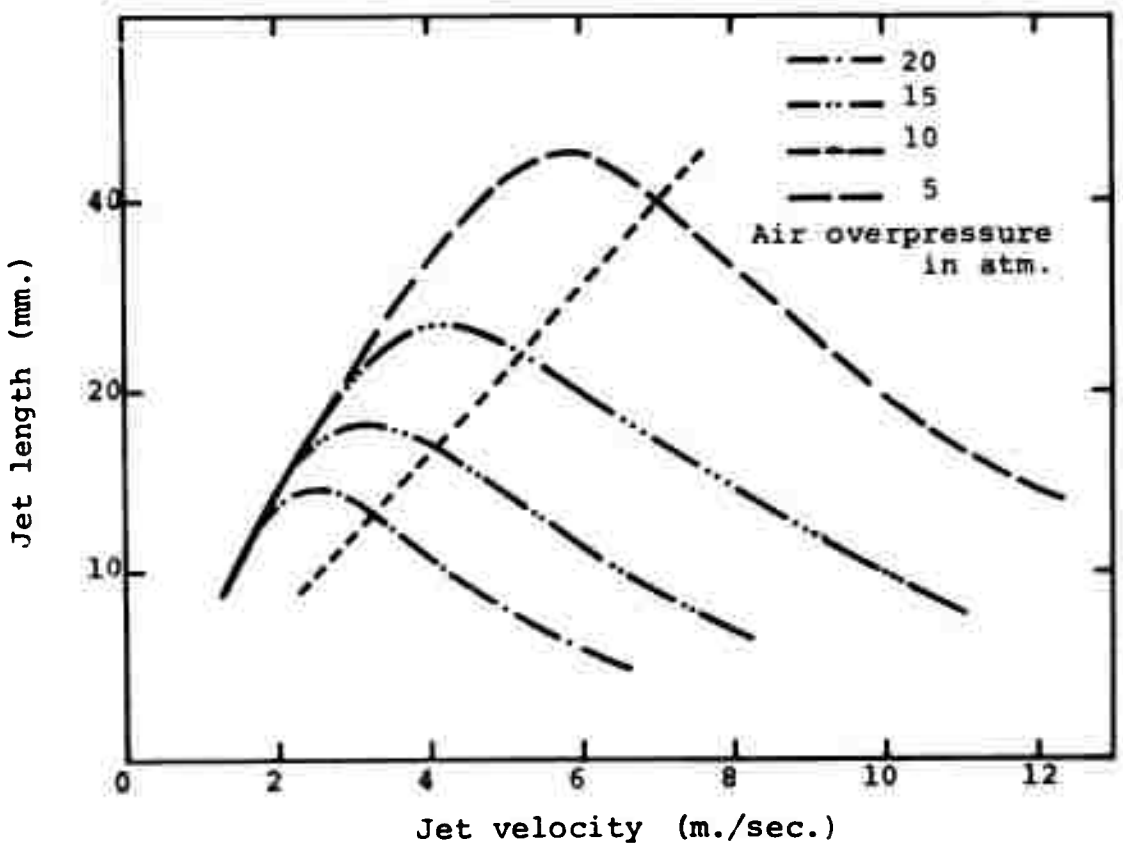

Figure 47. The effect of increase in ambient air pressure on coherent fluid length (after Ref. 29).

Vereshagin et al (Ref. 33) had carried use of this technique further, to pressure levels of 15,000 p.s.i., and found that jet length had 3 maxima as pressure was increased (for a 1-mm. diameter nozzle). The maxima occurred at approximately 5, 75, and 3,000 p.s.i. with a length of 7 in. being the maximum length obtained at pressure of 75 p.s.i. (Figure 48).

Although this technique does provide an indication of the effects of external forces on jet cohesion, its results are not reliable because of the use of the electrical contact method. Semerchan et al (Ref. 37) have shown that presence of an electrical charge within the jet stream affects jet cohesion and that charging a jet increased jet disruption linearly with charge value.

Kuklin and Shtukaturov (Ref. 38) had also used the same method to investigate jet structure and had defined the structure coefficient (a) as

$$a = \frac{d_c}{\ell} \qquad 24$$

where ℓ is the length of the initial section and d_c is coherent jet diameter at ℓ, where a is estimated as

$$a = 0.0066 + 1.26.10^{-8}RE. \qquad 25$$

Franz (Ref. 39) has also shown that as jet pressure is increased, jet width increases and the effective length of the jet is more rapidly attenuated (Figure 49). This is indicated by the respective depths of cut made by the jet with change in pressure (Figure 50).

Pressure distribution across the jet changes form as distance increases, as can be illustrated by curves given by Semerchan (Ref. 40) (Figure 51). Although for the most part, the overall total force exerted by the jet (Table X) stays much the same.

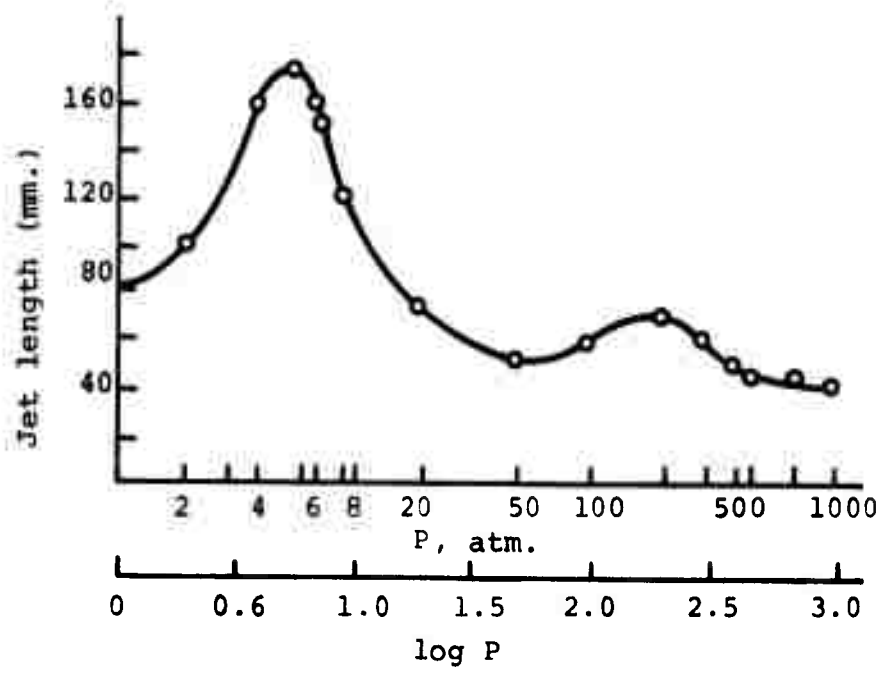

Figure 48. Variation in jet length with pressure (after Ref. 33).

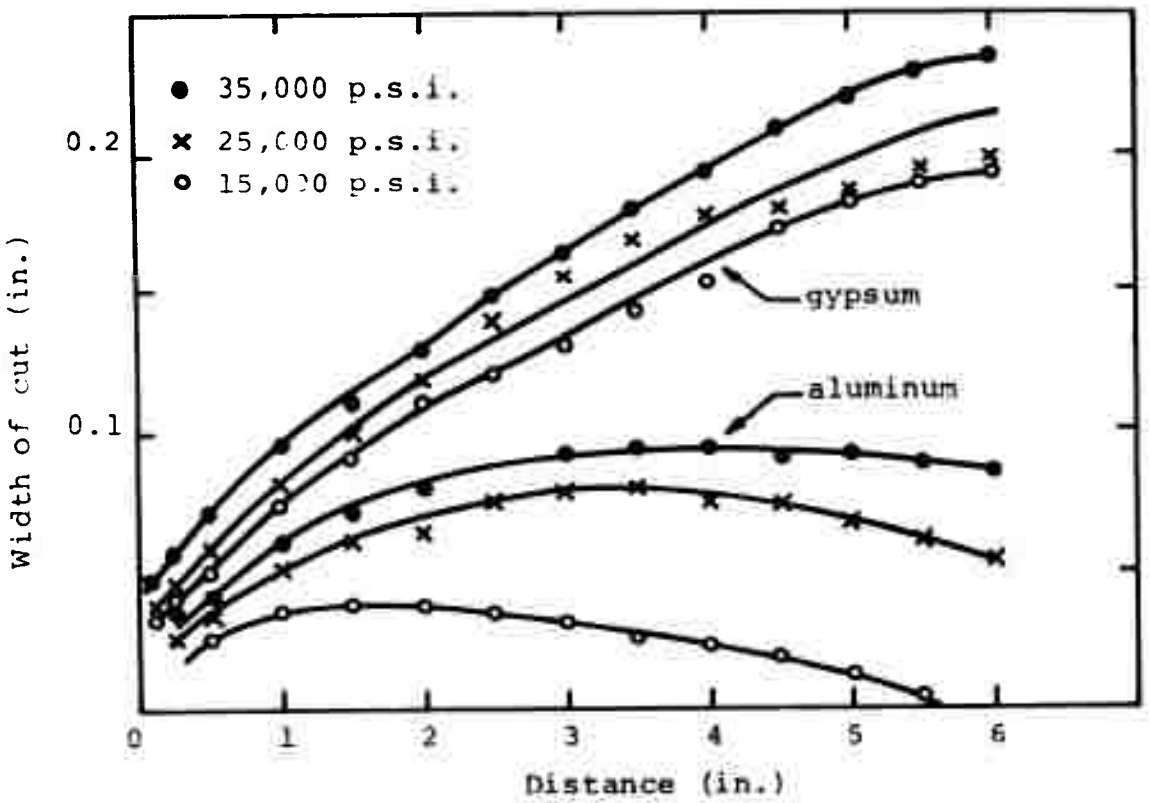

Figure 49. Slot width cut in gypsum and aluminum as a function of jet pressure and distance (after Ref. 39).

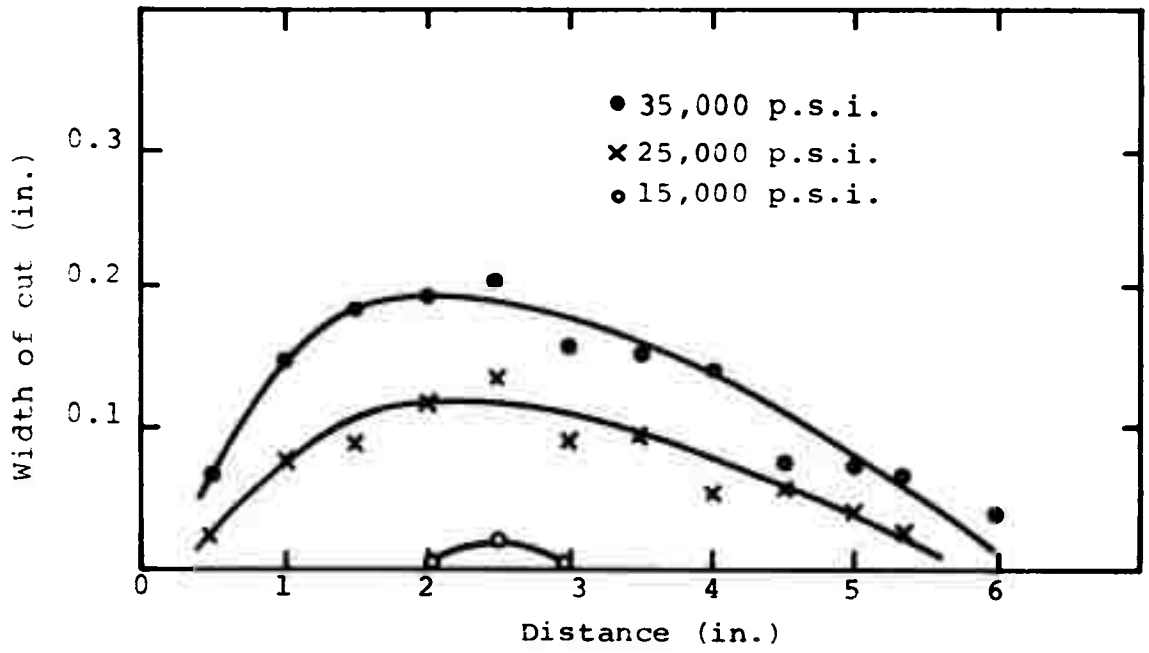

Figure 50. Depth of cut in aluminum as a function of jet pressure and distance (after Ref. 39).

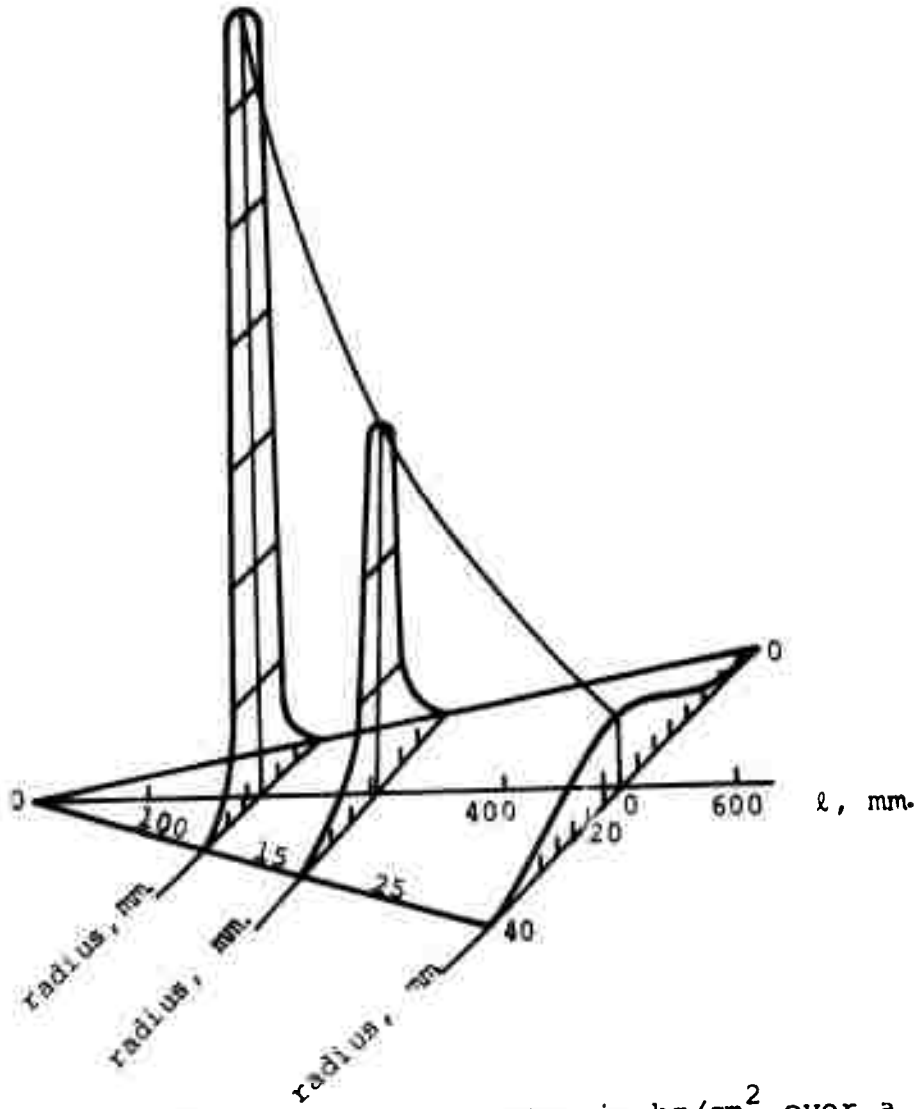

Figure 51. Distribution of momentum in kg/cm^2 over a jet issuing at 1500 atm. from a 0.595 mm. nozzle (after Ref. 40).

Table X. Total Force of Jet (kg.) (after Ref. 40).

Receiver Pressure, atm.	ℓ = 3 cm.	5 cm.	12 cm.	25 cm.	45 cm.
300	4.0	7.0	3.5	3.4	3.5
500	9.0	7.0	7.0	7.5	10.0
700	10.0	11.0	11.5	11.0	12.0
1000	15.0	14.0	14.0	15.5	15.0

The Effect of Nozzle Shape

There has been a considerable and continuing series of investigations relating to nozzle shape at all pressure levels at which water jets are used. Shtukaturov (Ref. 41) had shown that for large diameter jets the optimum length of the initial section is related to the diameter (Figure 52) and Voitshekhovsky et al (Ref. 42) have shown that the depth of cut obtained in granite is related to area of the nozzle (Figure 53), a conclusion also found by Zelenin (Ref. 43).

Water jet nozzles can, in general, be divided into two sections; a conic section reducing flow diameter from that of the feed pipe to that of the orifice and a straight section, or throat, at the orifice (Figure 54). Leach and Walker (Ref. 11) examined five combinations of shape (Figures 55, and 56) and the effects of change in cone angle (Figure 58) and throat length (Figure 59). The results indicated that a 13 degree conic section leading to a straight section of length equal to 2.5 nozzle diameters gave optimum results. It was interesting to note that the nozzles used gave improved results where the corners were left sharp, rather than being rounded, (Figure 57)

Farmer and Attewell (Ref. 44) have examined the effect of streamlining the conic section in comparison with a straight contraction, and contrasted the results with three other shapes (Figure 60). The tabulated results (Table XI) show that while a streamline nozzle of 20 degree half angle gave optimum results, a straight nozzle of 20 degrees included angle was also efficient and could be made much more easily.

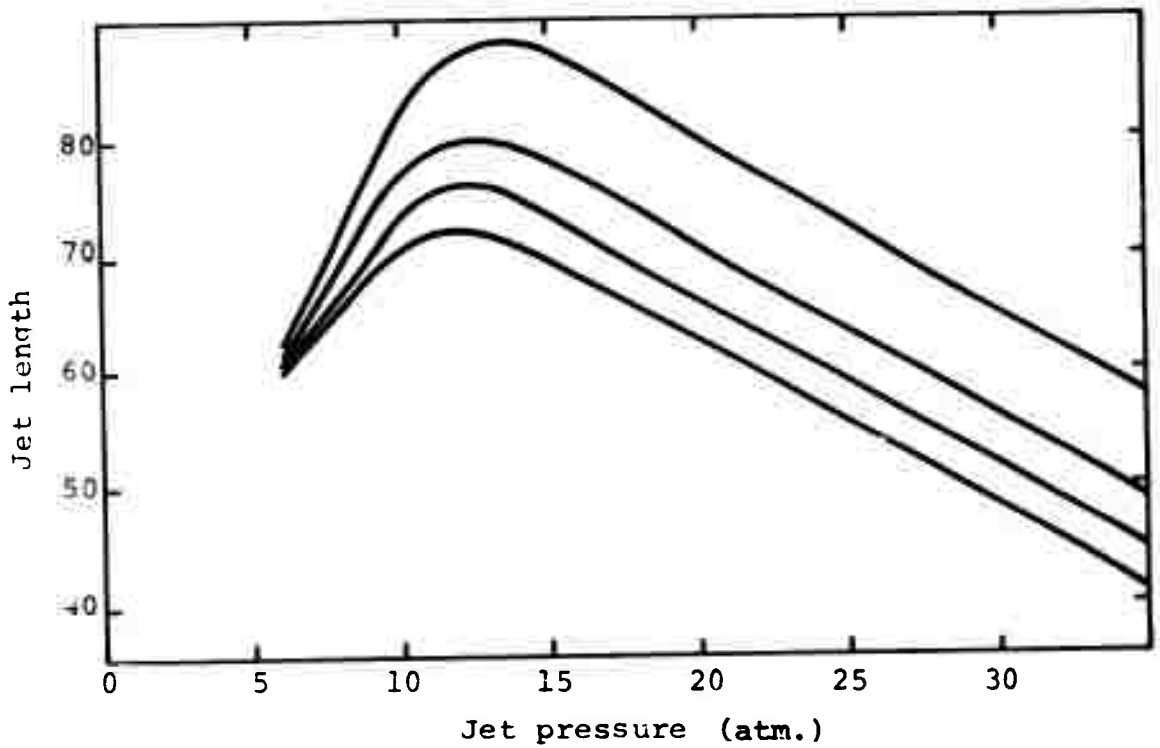

Figure 52. Variation in jet length with pressure for changing nozzle diameter (after Ref. 41).

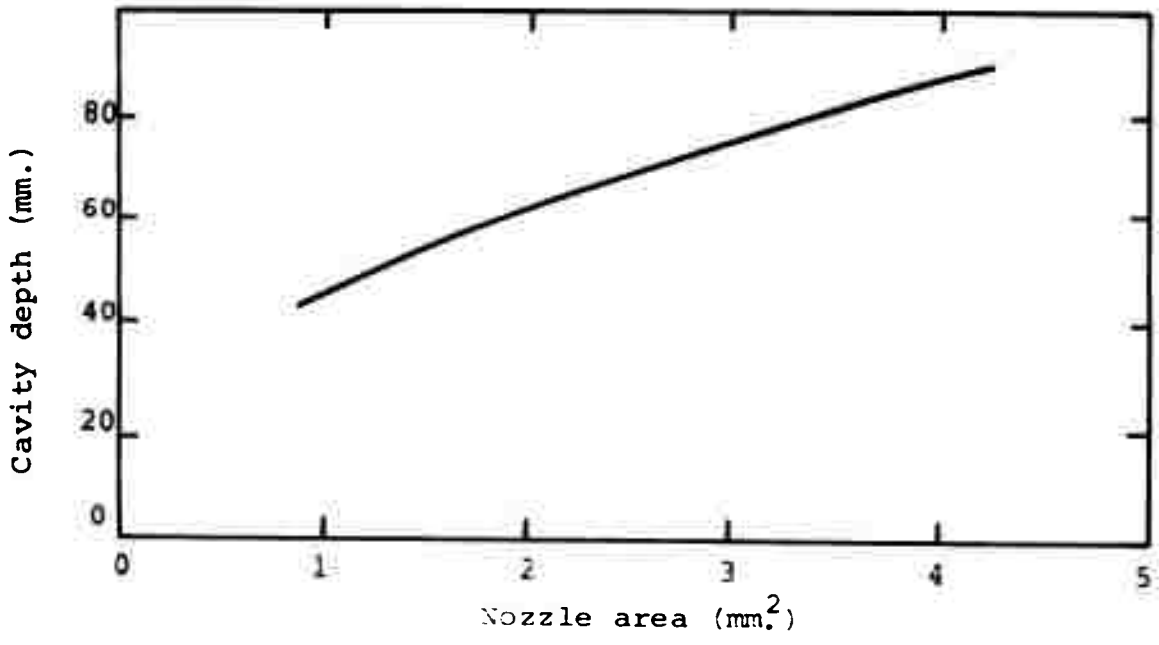

Figure 53. Variation in depth of cut in granite with nozzle area, at a jet pressure of 200 MN/m.^{2}.

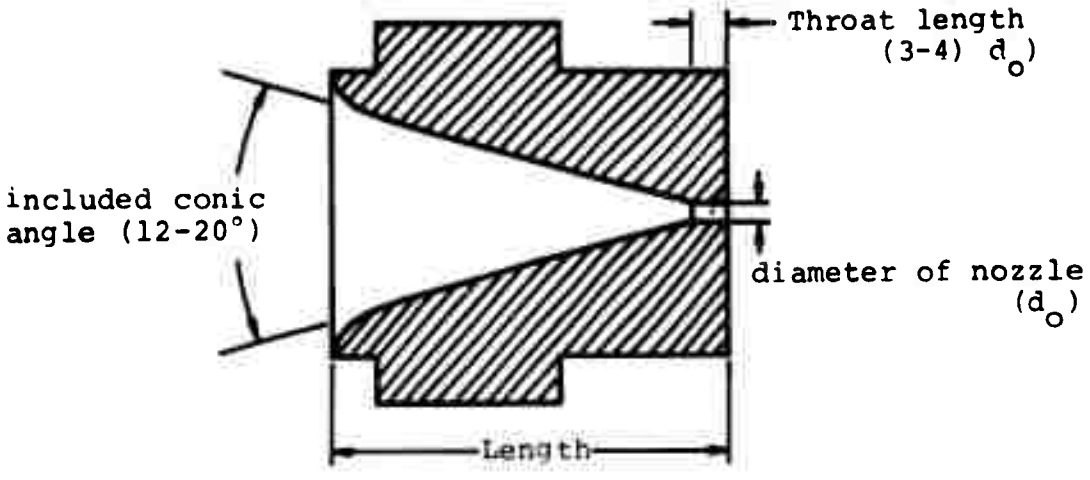

Figure 54. Typical nozzle geometry.

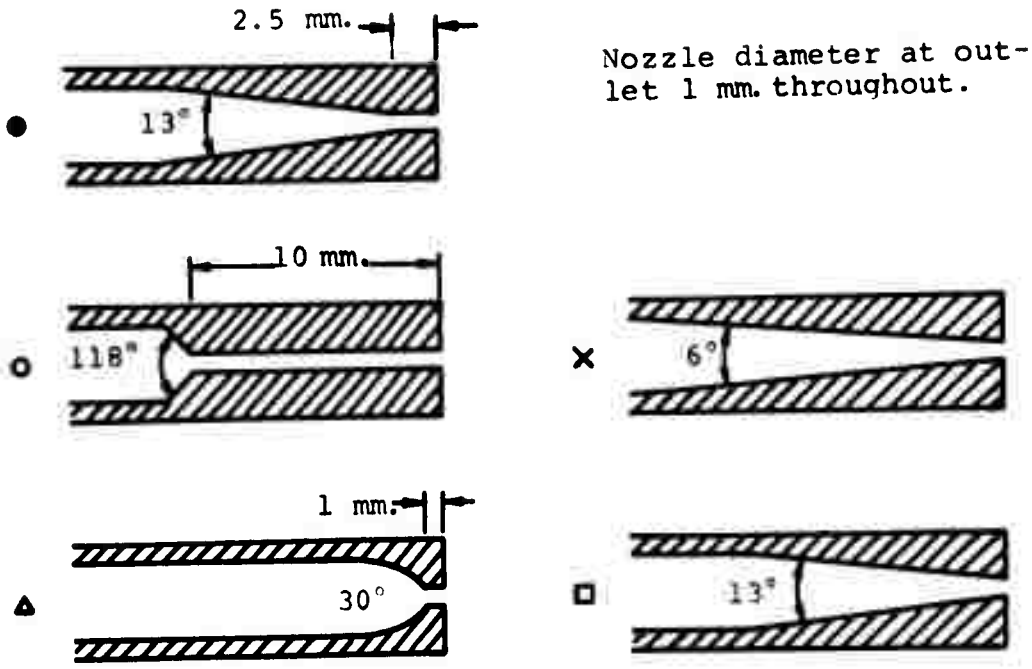

Figure 55. The five nozzle shapes studied by Leach (after Ref. 11).

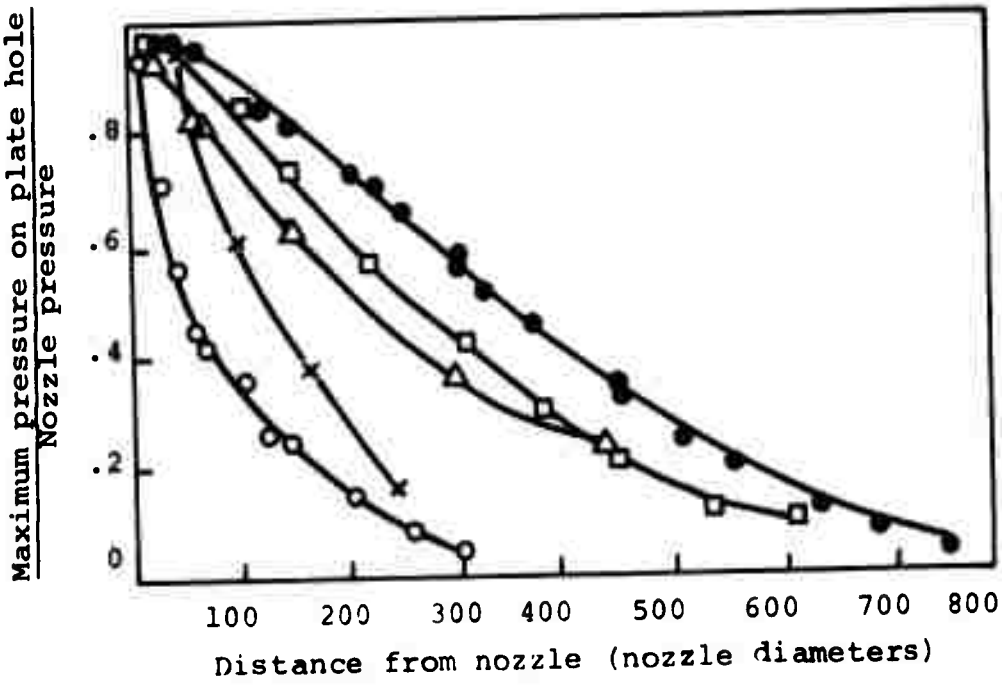

Figure 56. Effect of nozzle shape on performance (after Ref. 11) (for shapes see Figure 55).

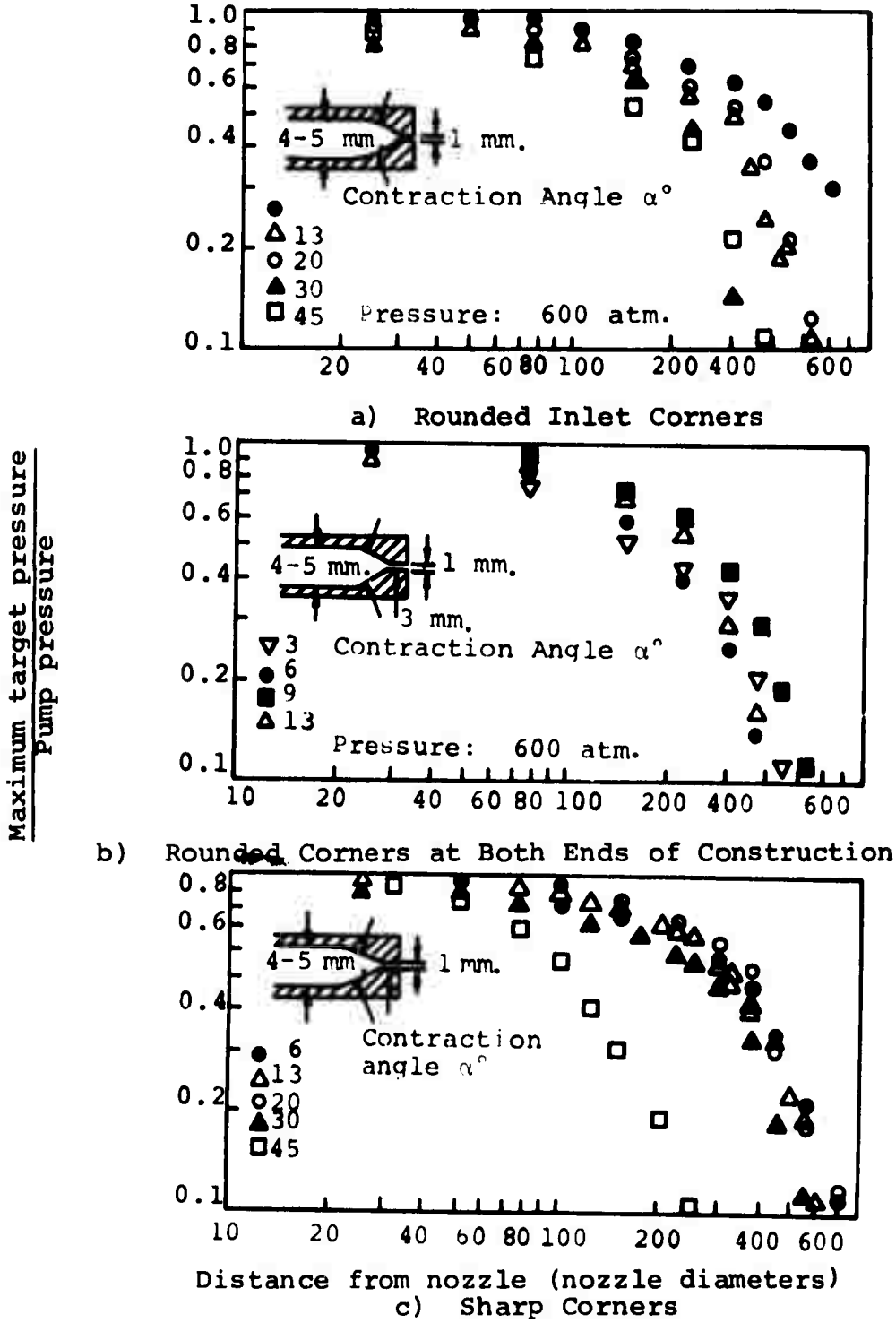

Figure 57. The effect of contraction angle on nozzle performance (after Ref. 11).

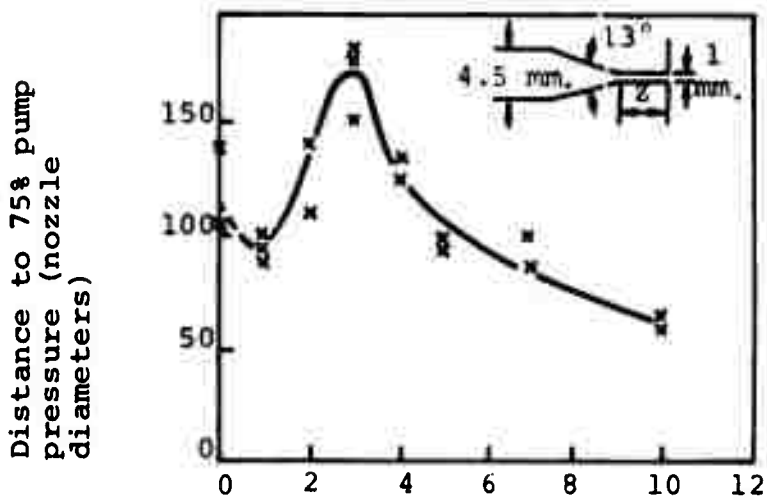

Figure 58. The effect of length of nozzle straight section on performance (after Ref. 11).

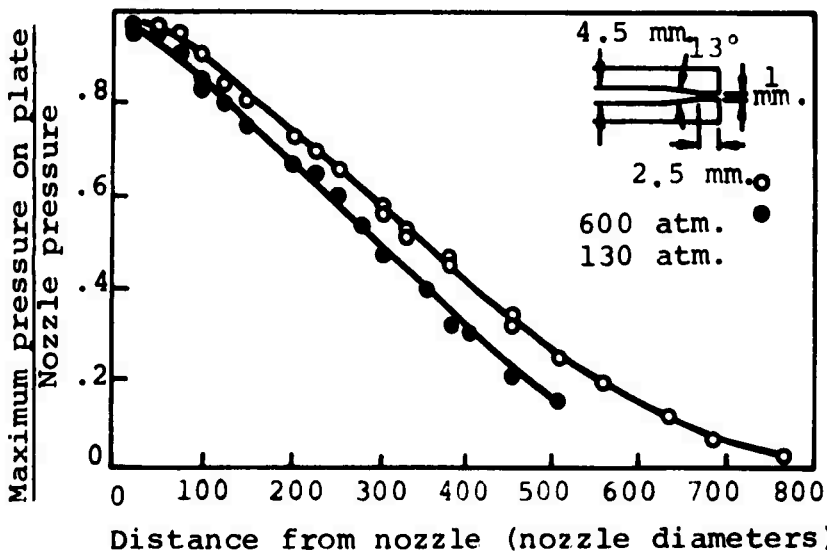

Figure 59. Variation of maximum pressure on plate hole with distance from nozzle, for pump pressure of 600 and 130 atmospheres (after Ref. 11).

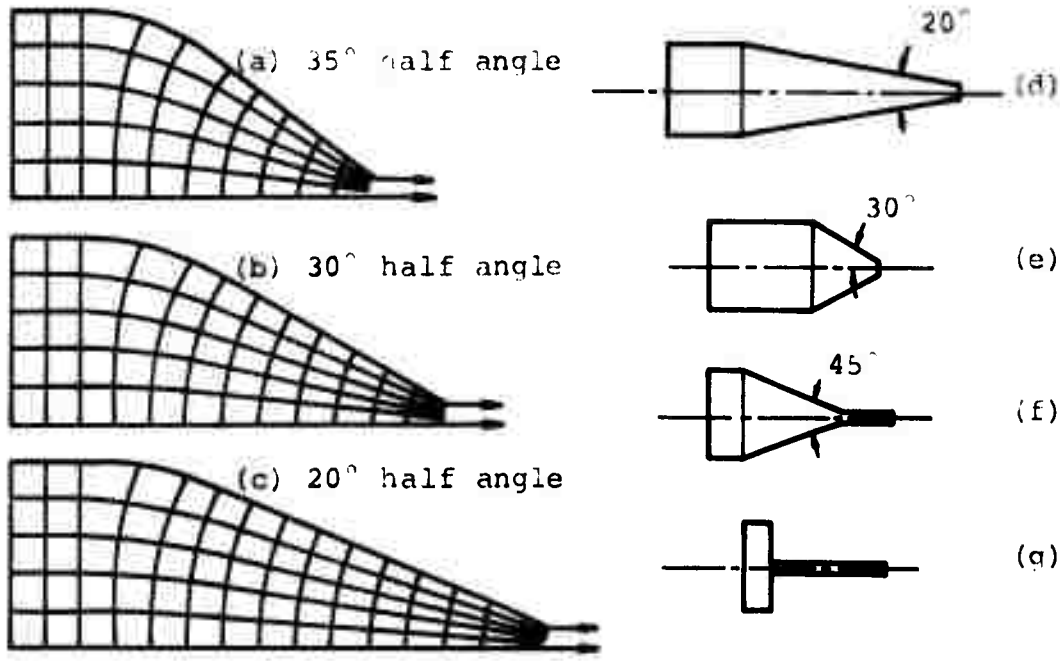

Figure 60. Nozzle designs. (a) to (c) streamline nozzle designs, (d) unstreamlined nozzle design, (e) to (g) experimental profiles (after Ref. 44).

Table XI. Maximum Jet Length for Various Nozzle Geometries (after Ref. 44).

Nozzle Device	Max. Jet Length (m.)
a	0.60
b	0.55
c	0.65
d	0.60
e	0.40
f	0.25
g	0.20

Voitsekhovsky et al (Ref. 42) tested twelve nozzle profiles (Figure 61) at a jet pressure of 200 MN./m.^{2} (29,000 p.s.i.) where the nozzle conic section was divided in two sections. Results were evaluated in terms of the angle of divergence of the emerging jet. It was found (Figures 62, 63) that the best results were obtained where the nozzle had a throat of length 3-5 times diameter and where the included inlet angle at the throat was 6 degrees (Nozzle 7 of Figure 61). Design formulas for this nozzle are

$$\frac{du}{dy} = \text{constant}$$

$$y = R \frac{D^2}{r^2 - D^2} \left(\frac{r^2}{D^2} - 1 \right) \qquad 26$$

where: u = flow rate

r = inlet diameter of nozzle (pipe diameter)

D = outlet diameter of nozzle (throat diameter)

R = nozzle diameter at a distance y from the inlet.

It should be noted that Figure 63 indicates that nozzles to be used at pressures between 100 and 200 MN./m.^{2}

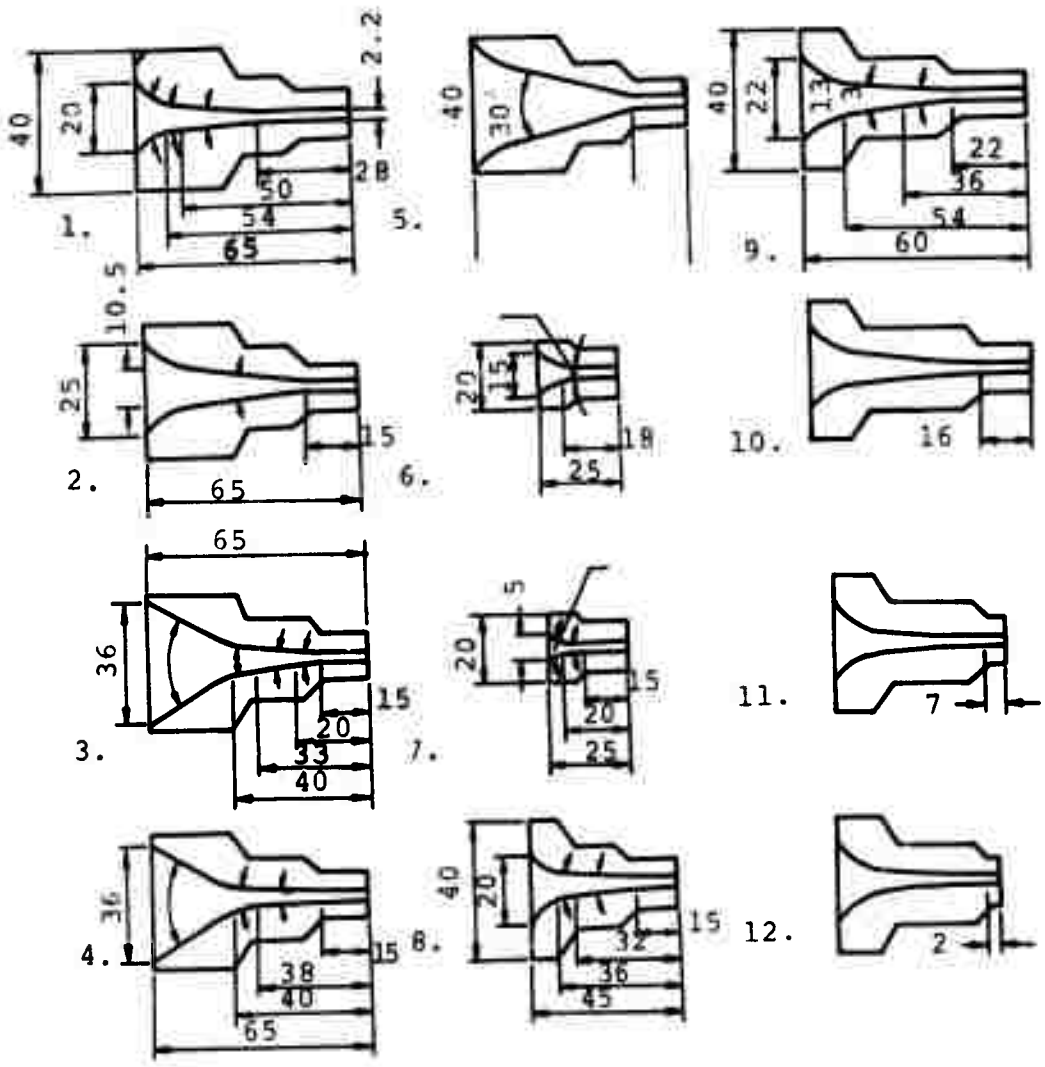

Figure 61. Profiles of experimental nozzles (after Ref. 42).

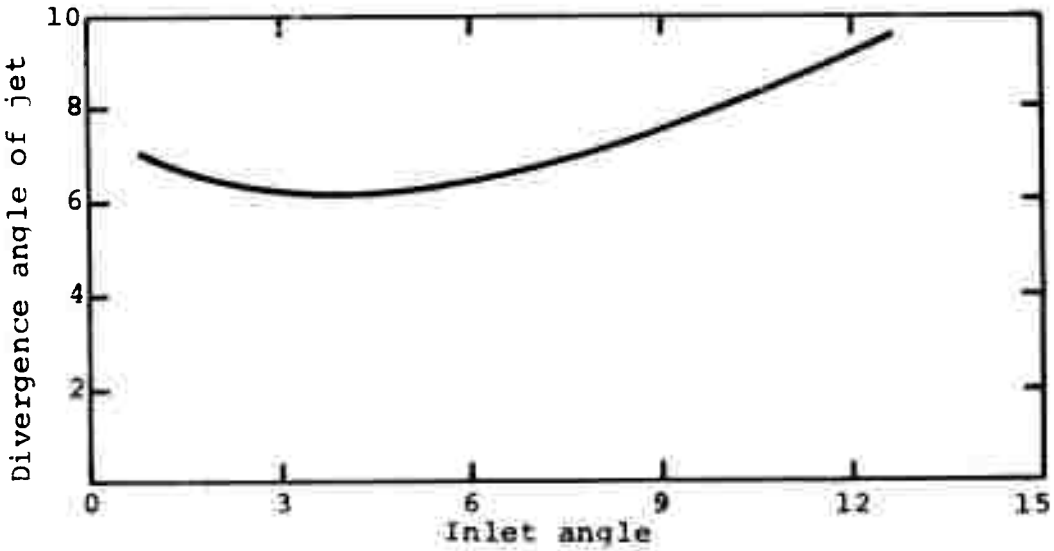

Figure 62. Angle of jet divergence with nozzle inlet angle (after Ref. 42).

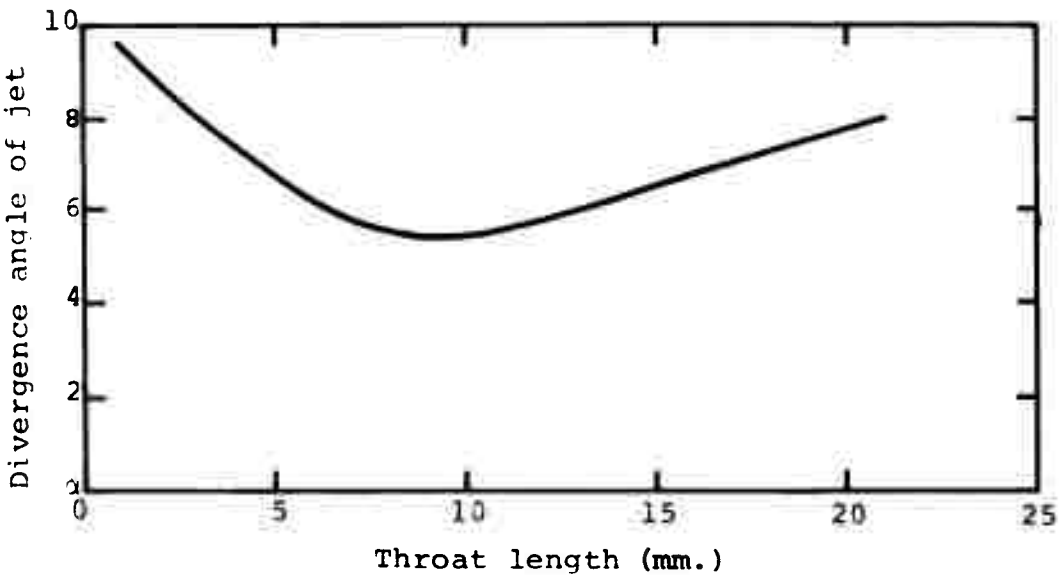

Figure 63. Angle of jet divergence with throat length (after Ref. 42).

(14,500 to 29,000 p.s.i.) require a smaller inlet angle and longer throat section than jets at lower pressure. At pressures up to 100 MN./m., Vereschagin (Ref. 33) had found that the nozzle design similar to that found optimum by Leach and Walker gave the best results.

Japanese investigators (Ref. 45) have investigated the change in coefficient of discharge with nozzle shape and found that a staged contraction of the jet gave improved results over a linear convergence (Figure 64). However, the improvement in discharge coefficient may be due to other factors since other investigators have claimed discharge coefficients of up to 0.98 (Figure 44).

The findings of these investigators corroborate the findings of Shavlovsky (Ref. 25) (Figures 65, 66) who found that a 4 nozzle diameter throat leading from a 14 degree conic section gave the optimum result. The conclusions have also been verified by Daniel et al (Ref. 46) at IIT Research Institute using explosively driven jets to attain jet velocities of up to 2.5 Km./sec(Figures 67 to 69).

The effects of jet nozzle shape have been studied by the U.S. Bureau of Mines (Ref. 47) for large diameter (3/8 in.) jets at pressures of up to 4,000 p.s.i. The experiments examined the pressure distribution of the pressure downstream from the nozzle (Figure 70) for a variety of nozzle geometries (Figure 71). Results showed that a 3D throat section with an 8 degree internal taper (16 degree included angle) gave the optimum result (Figure 72).

The change in jet pressure distribution with distance was also noted (Figure 73) and compared with theoretical curves based on the equations

$$P = Ae^{Br^2} \qquad 27$$

and

$$P = 3000e^{Br^2} \qquad 28$$

P is jet pressure, A and B are constants, and r is the jet radius (Figures 74, 75). It was found that the volume of coal removed by a water jet correlated with total jet force computed from this relation better than any other jet parameter.

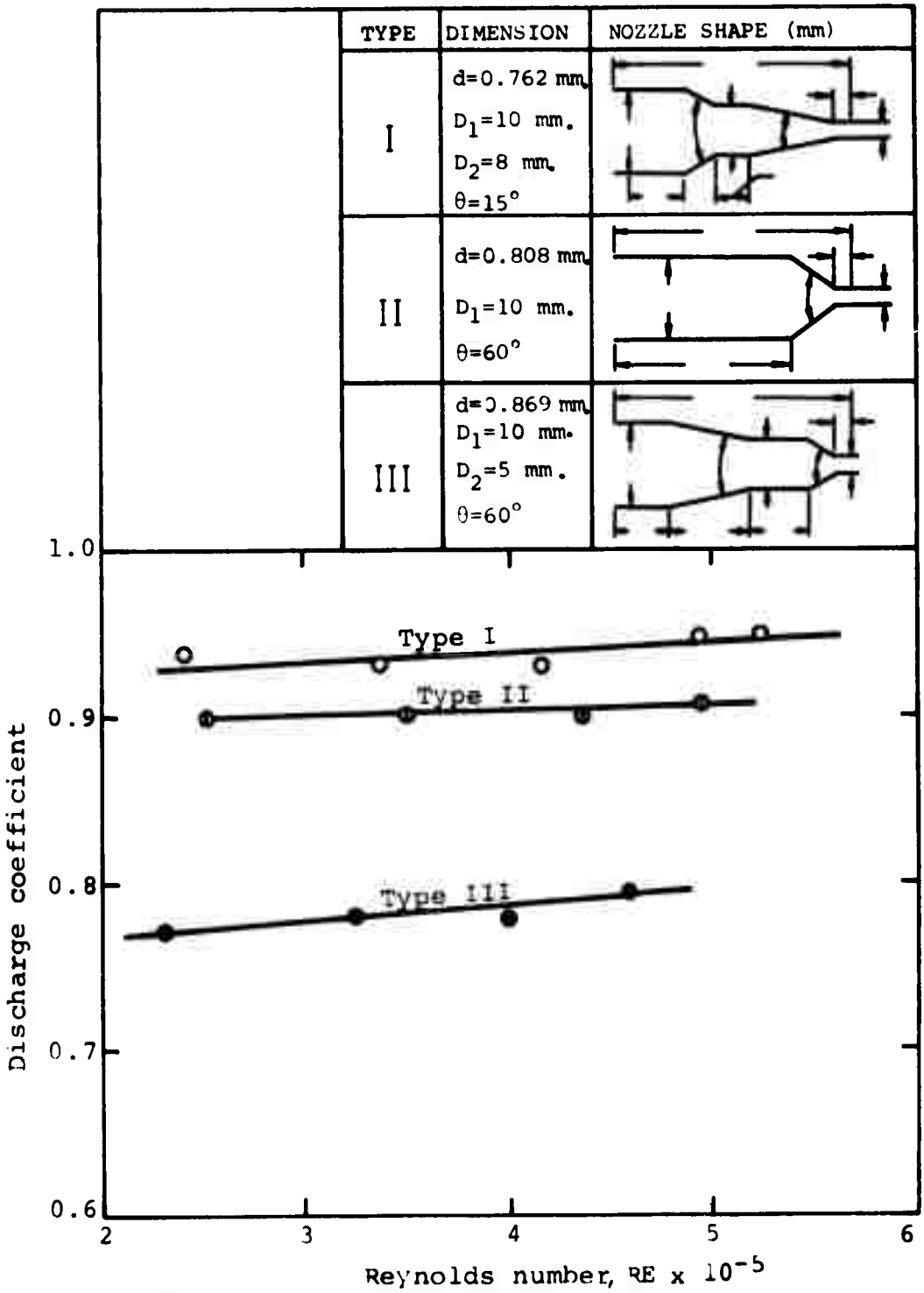

Figure 64. Coefficient of discharge for various types of nozzle (after Ref. 45).

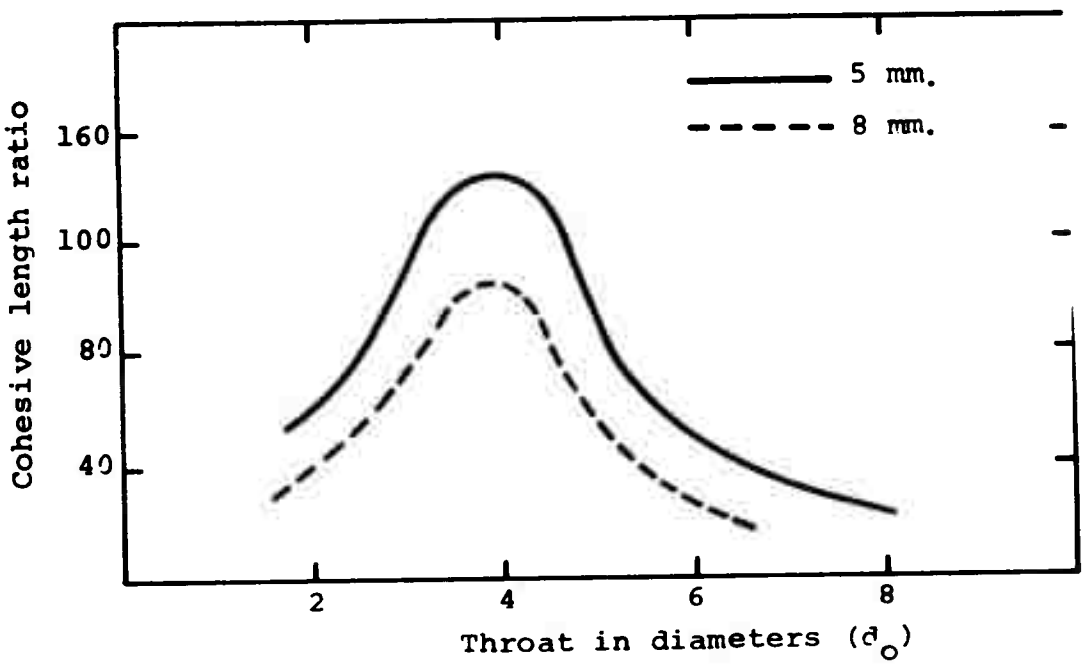

Figure 65. The effect of throat length on jet cohesive length (after Ref. 25).

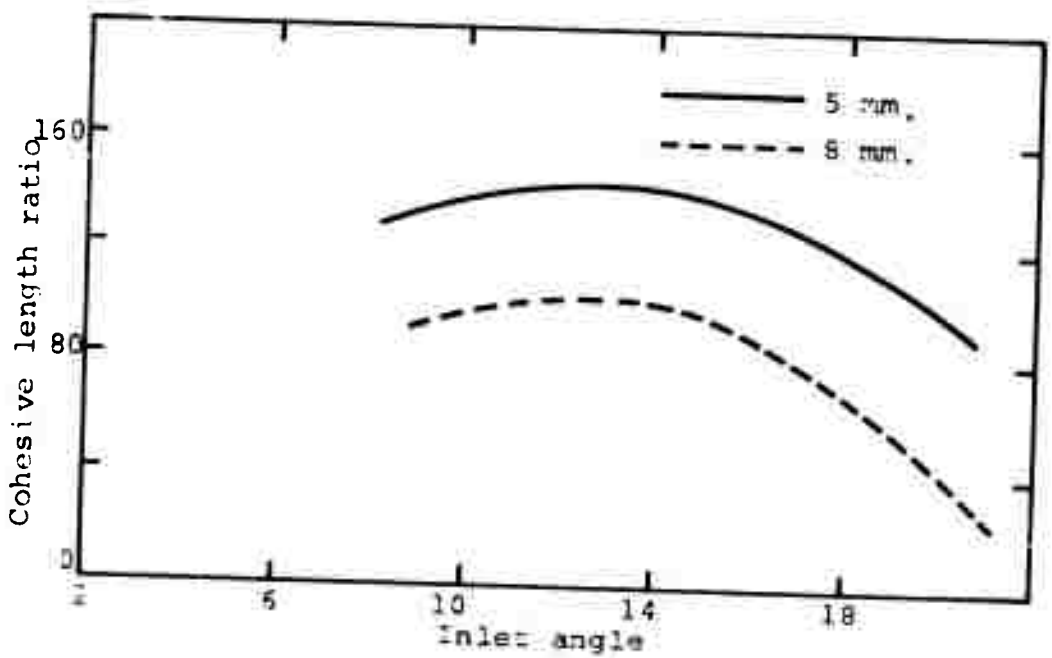

Figure 66. The effect of conic angle on jet cohesive length (after Ref. 25).

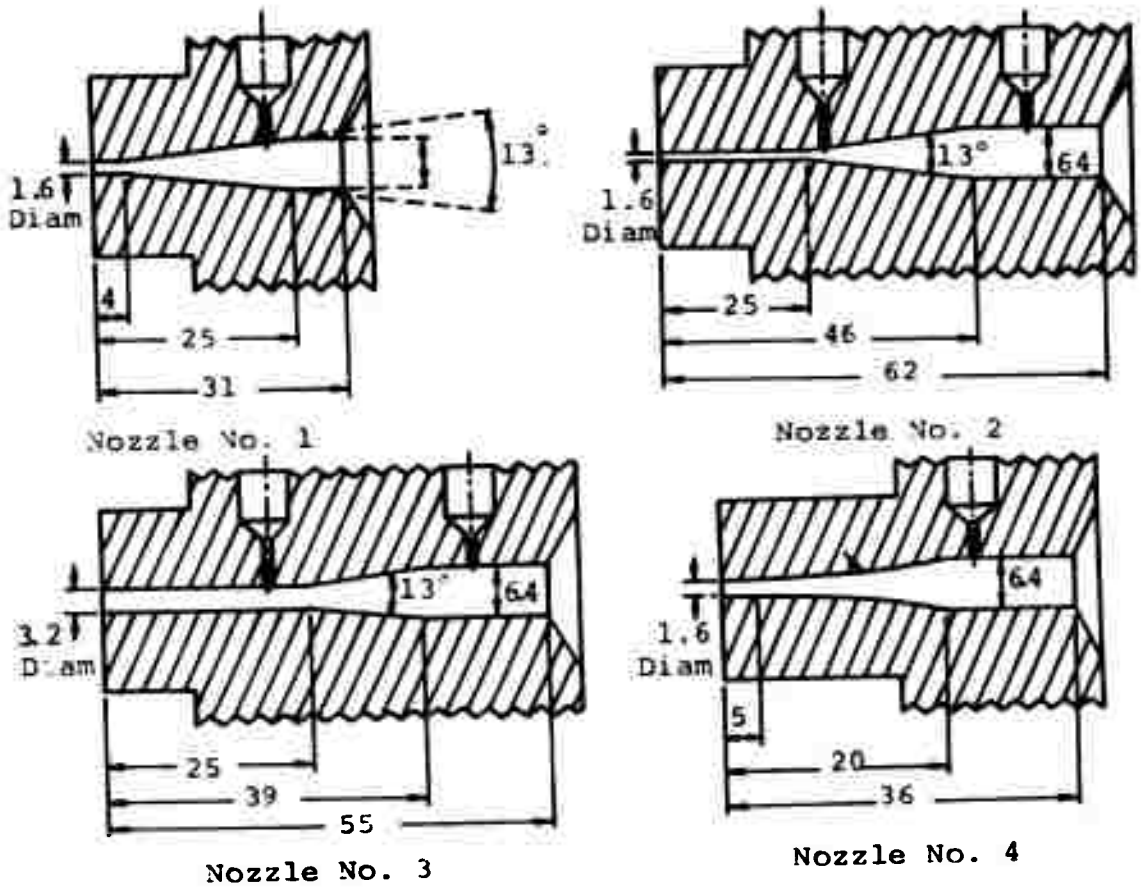

Figure 67. Nozzle geometries investigated by Daniel (after Ref. 46).

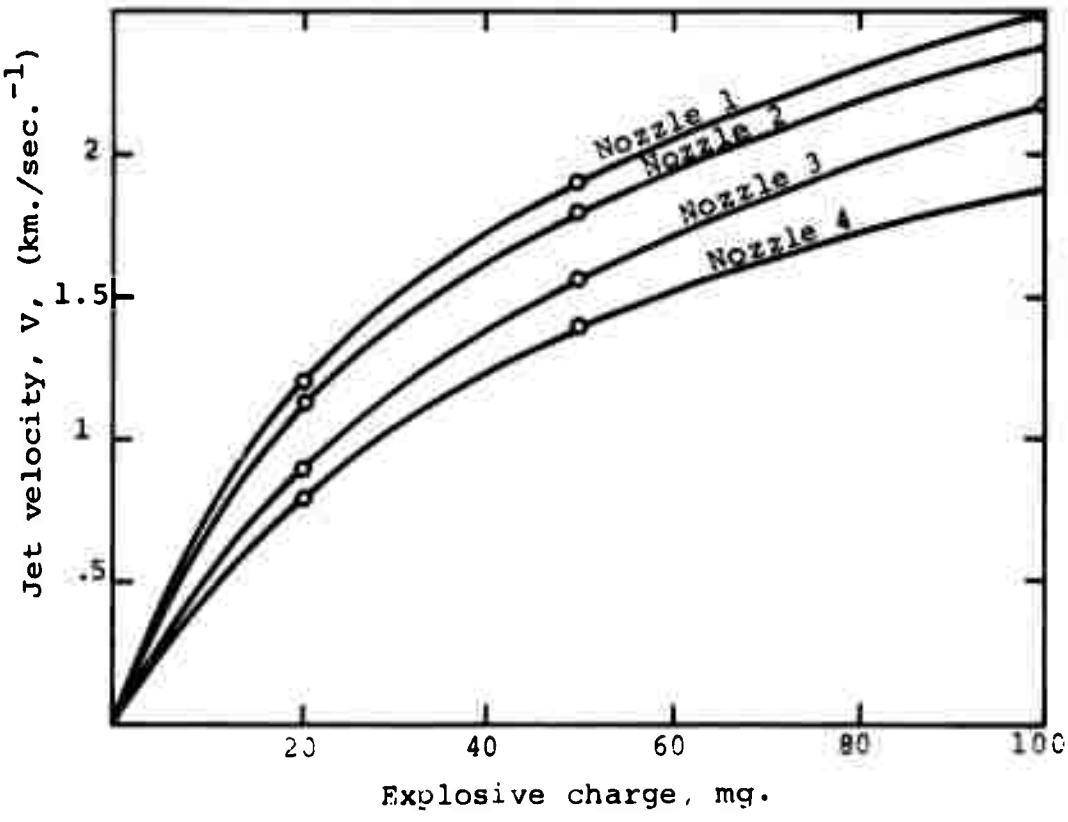

Figure 68. Jet velocity as a function of explosive charge for four different nozzles (after Ref. 46).

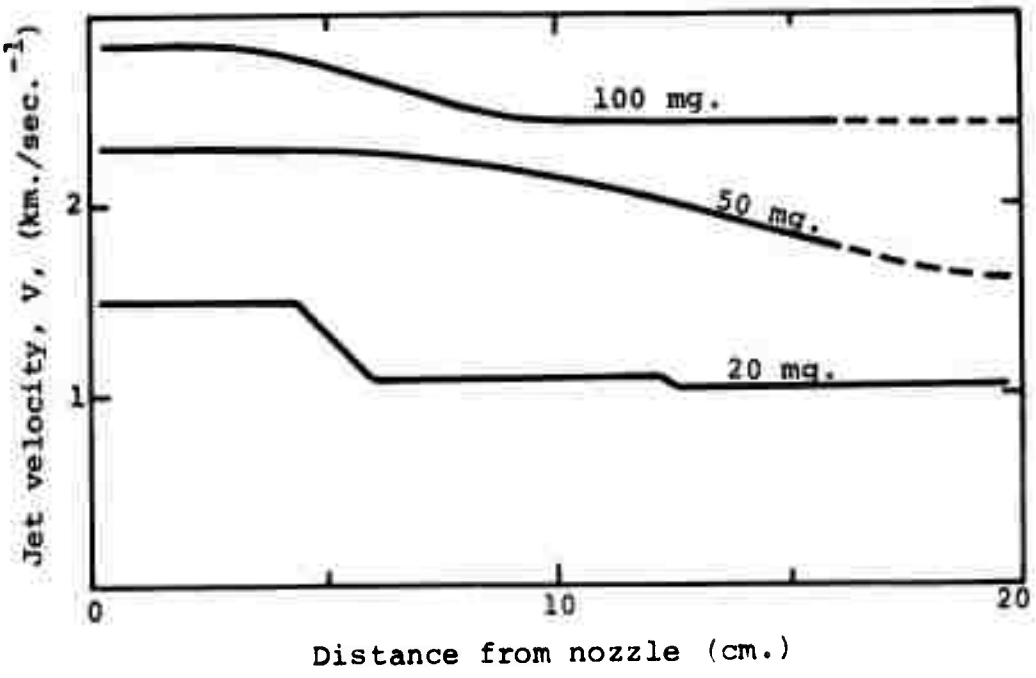

Figure 69. Jet velocity as a function of distance from nozzle No. 1 for various explosive charges (after Ref. 46).

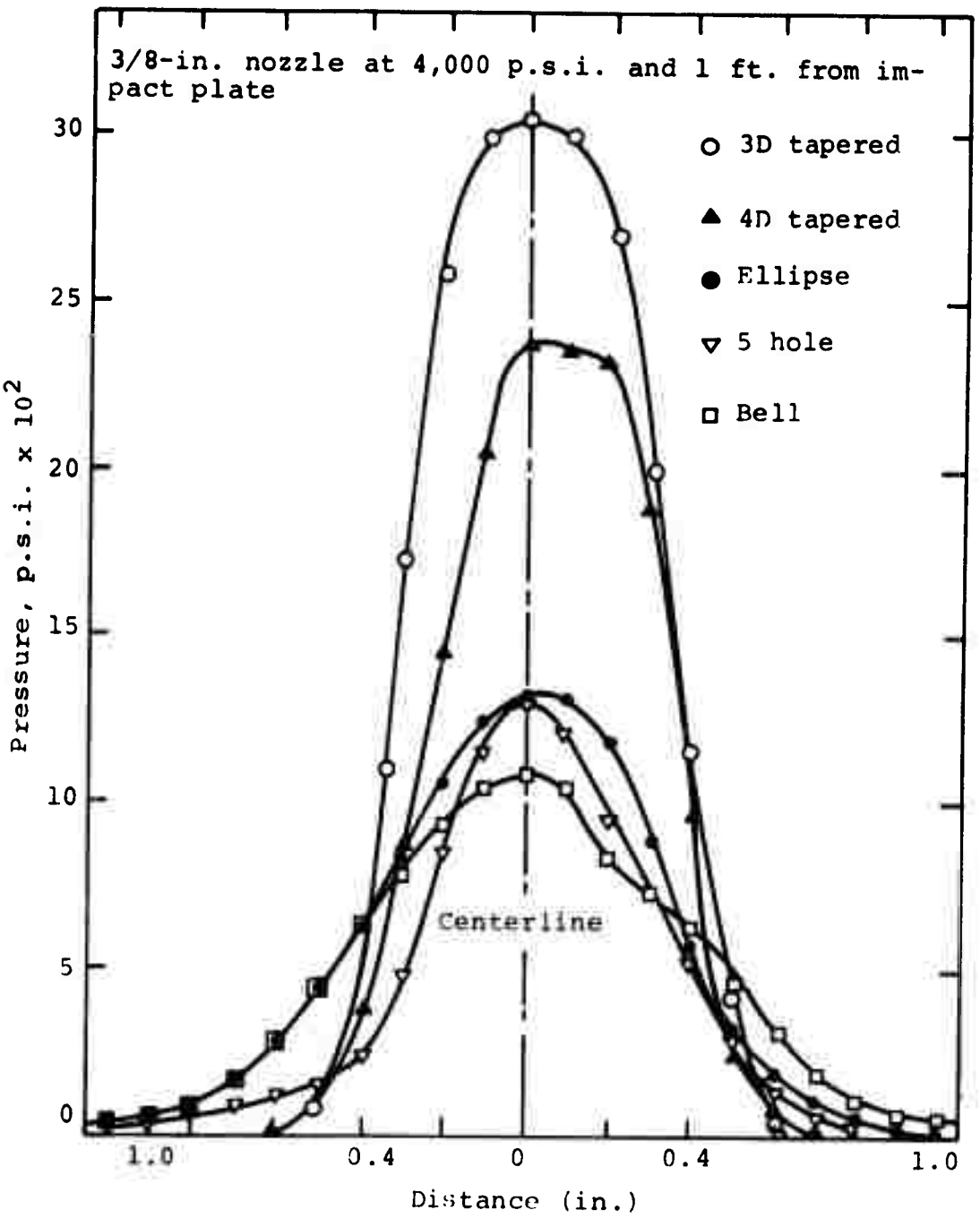

Figure 70. Pressure profile of jetstreams from various nozzle types used by U.S. Bureau of Mines (after Ref. 47).

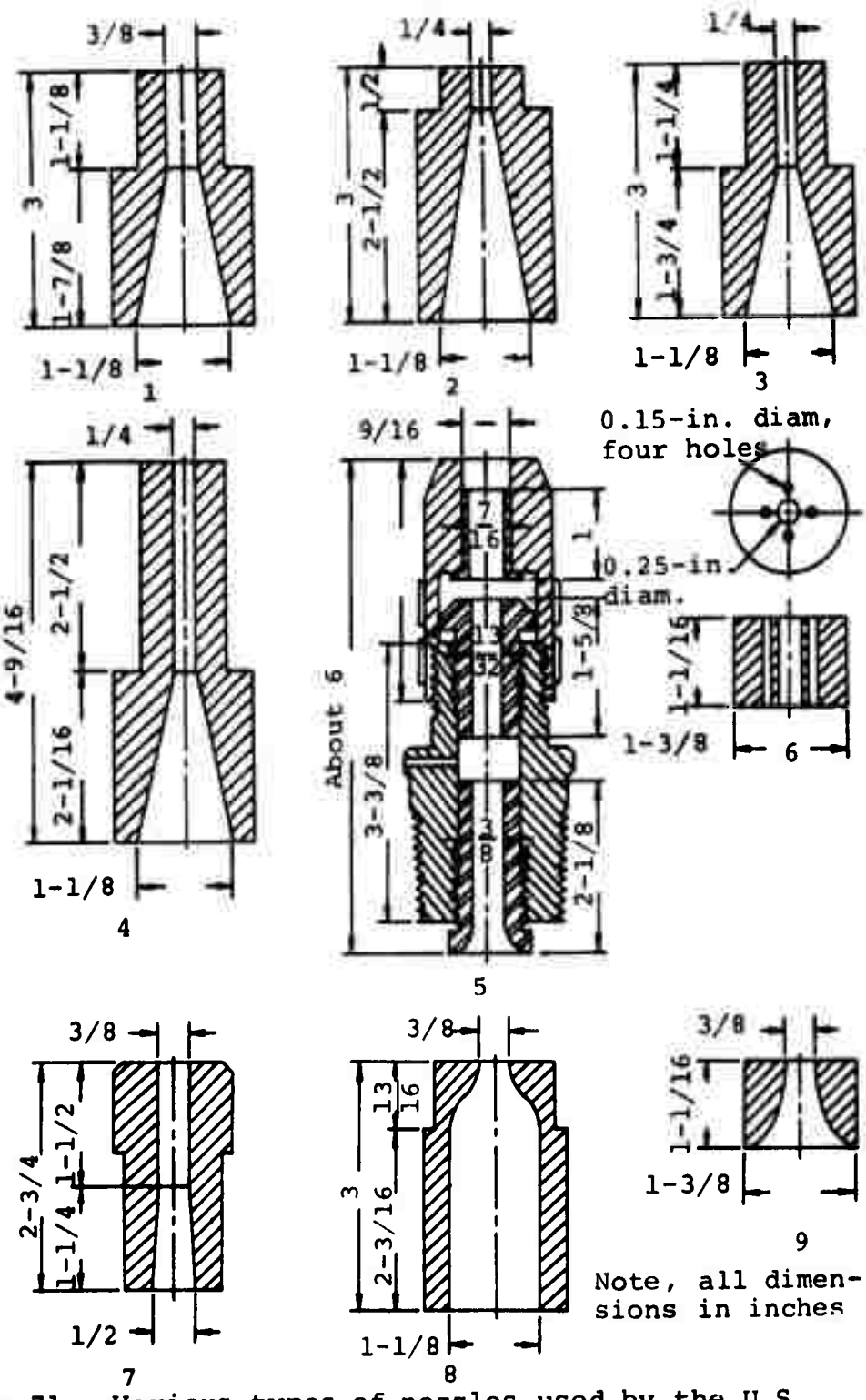

Figure 71. Various types of nozzles used by the U.S. Bureau of Mines (after Ref. 47).

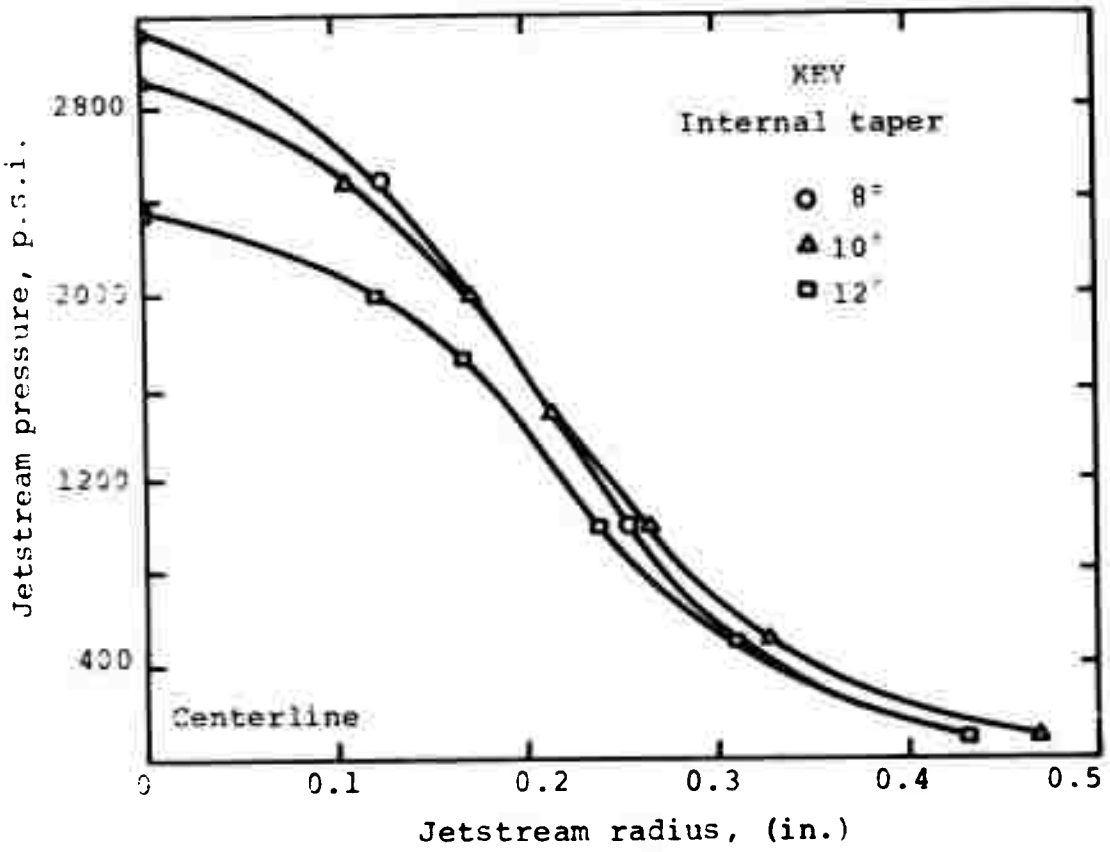

Figure 72. Pressure profiles of 1/4-in. 10D nozzle streams taken 1 ft. from impact (after Ref. 47).

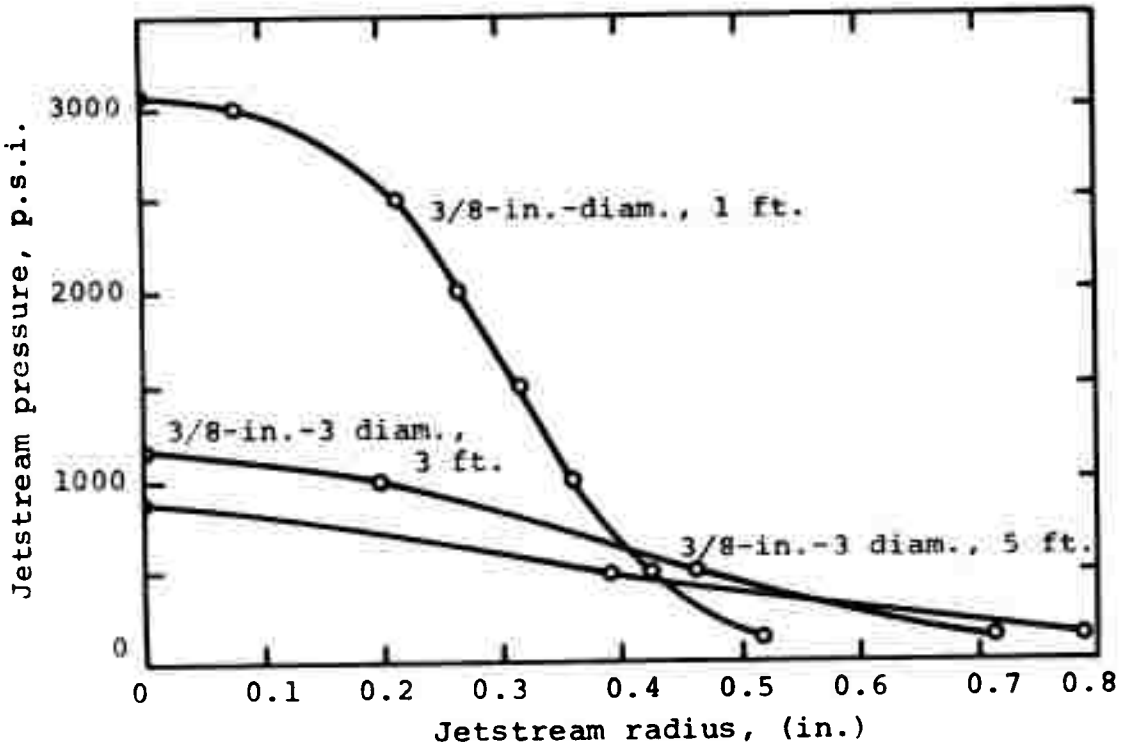

Figure 73. Pressure distribution of 3/8-in. diameter 3D nozzle at 1, 3, and 5 ft. from impact; 4,000 p.s.i. pump pressure (after Ref. 47).

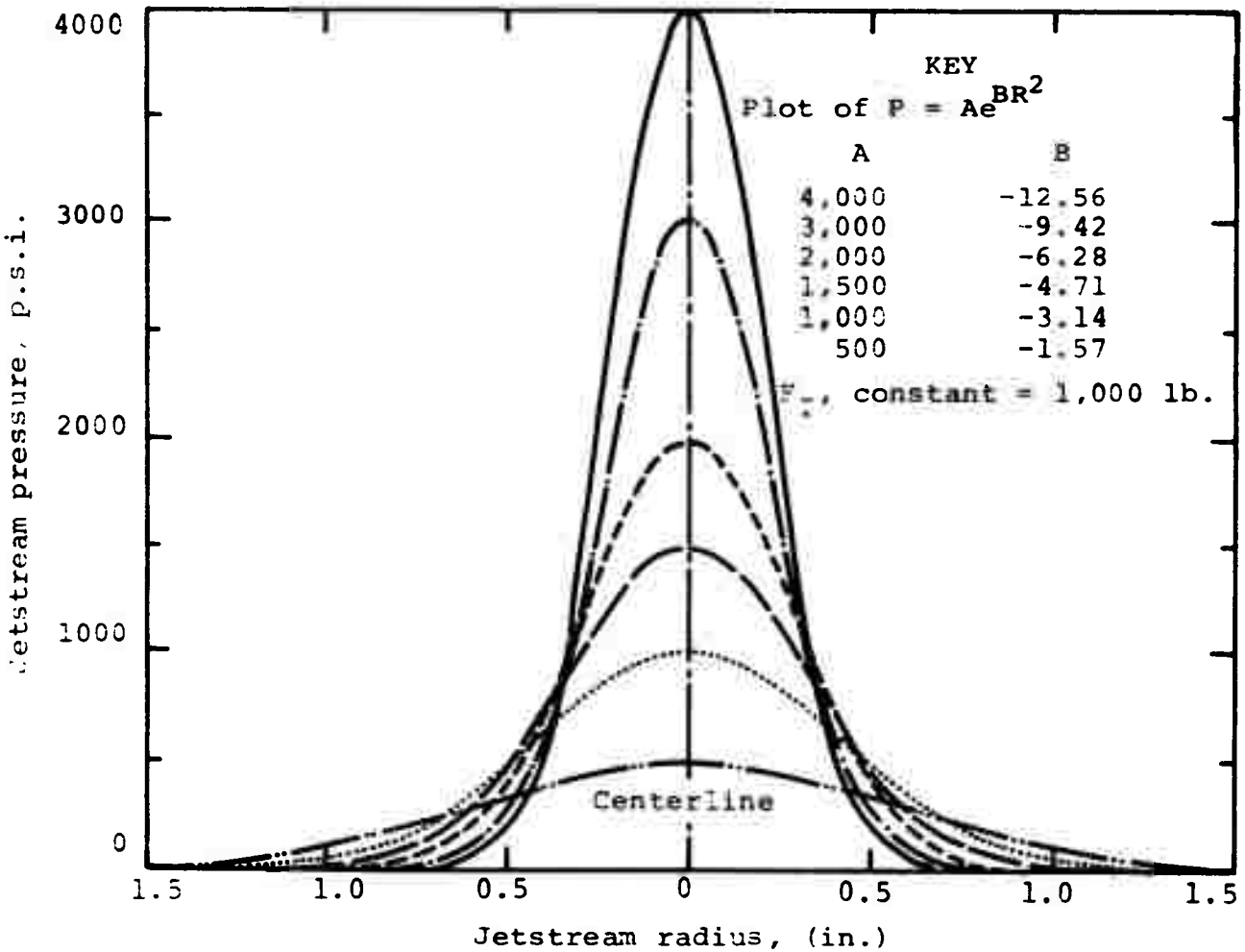

Figure 74. Pressure distributions of a jetstream with various maximum pressures and a constant total force (after Ref. 47).

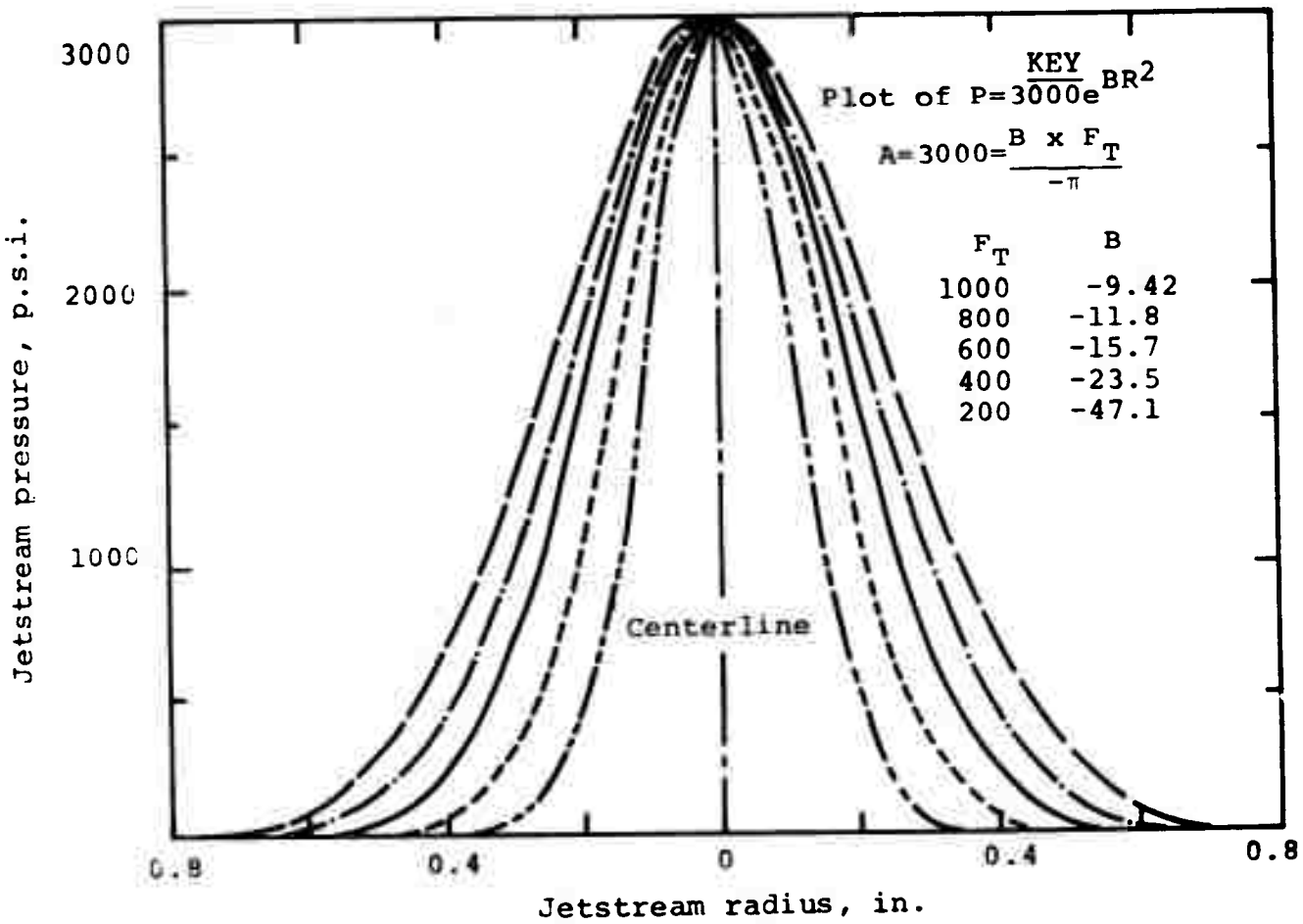

Figure 75(a). Pressure distributions of a jetstream with various total forces and a constant maximum pressure (after Ref. 47).

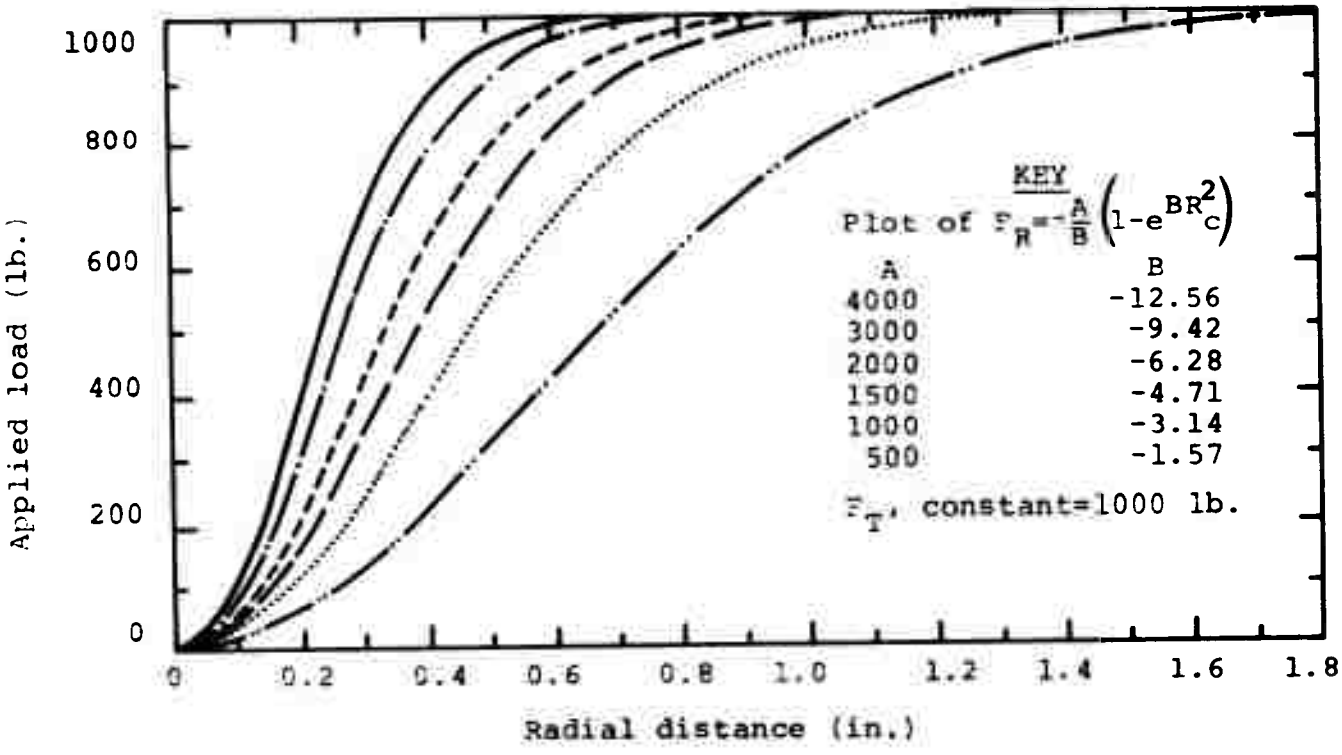

Figure 75(b). Force as a function of distance from the center of pressure for various maximum pressures (after Ref. 47).

National Coal Board investigators (Ref. 48) have also varied nozzle geometry and examined jet concentration with relative nozzle squareness (Figure 76). A conical taper was found to be the most effective shape although in comparisons among jets of various diameters, a smaller jet diameter appeared to give a better performance in cutting rock than equivalent large diameters (Figure 77).

More recently the German coal industry (Ref. 49) has studied various shapes and diameters of nozzles (Figure 78). Pressure profiles at various distances along the emerging jets were taken (Figure 79). The results indicated that a larger nozzle (from 20 to 25 mm. must be used if the jet is to cut at distances up to 45 feet from the nozzle (Figure 80). Tests were also carried out on the effect of wear (Figure 81) on nozzle effectiveness. For this reason, nozzles were made of hard metal rather than brass in order to improve life although brass initially took a better polish and, thus, improved jet structure (Figure 82).

Fluid Composition of the Jet

The erosion of materials by fluid impact has been related to the fluid density, surface tension, net positive suction head, bulk modulus, kinematic viscosity, and acoustic impedance ratio where there exists the possibility of having cavitation damage incurred during the impact (Ref. 50).

Schweitzer (Ref. 51) reviewed theories on the machanism of jet disruption in 1937. Kuehn (Ref. 52) had postulated that if viscosity forces influenced jet stability, then in a comparison between gas oil and kerosene, kinematic viscosity ratio 3.2:1, jet velocities to produce similar jet atomization would be in the same ratio. At low velocities the ratio was 2.5:1 but as pressure was increased this reduced to 1.7:1 apparently indicating a diminishing role of viscosity with increase in jet velocity.

At low jet velocities, Weber (Ref. 23) has shown that the wavelength of disruption increases for viscous fluids. Thus while it is 6D for glycerine, it is 22D for castor oil (D is jet diameter) from which the time to disruption of the jet, T, was computed as

$$T = K\left[\left(\frac{8\rho}{\sigma}\right)^{0.6} \cdot D^{1.5} + \left(\frac{6\mu}{\sigma}\right)\right]D \qquad 29$$

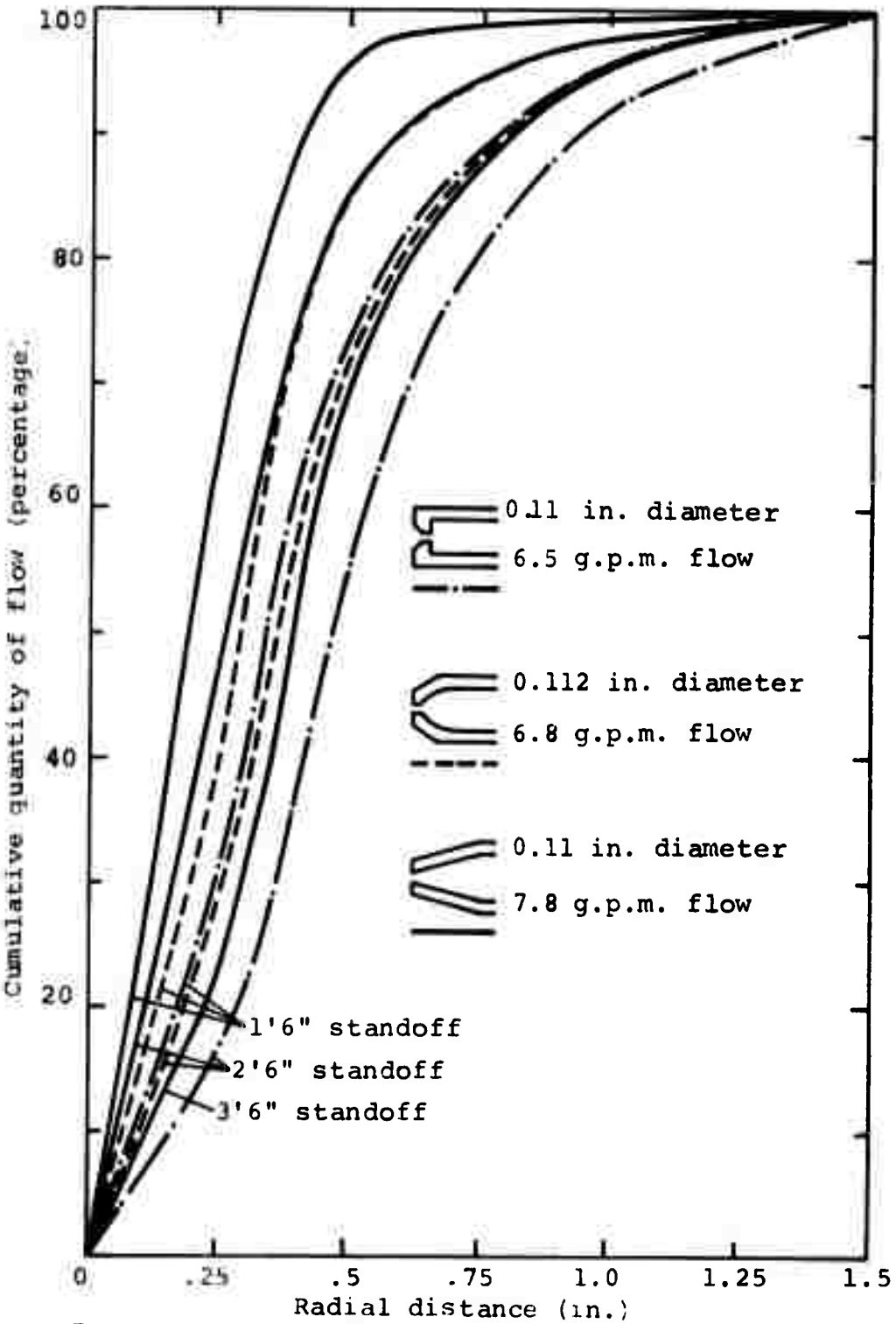

Figure 76. Jet volume distribution for various nozzle shapes at 1000 p.s.i. for three standoff distances (after Ref. 48).

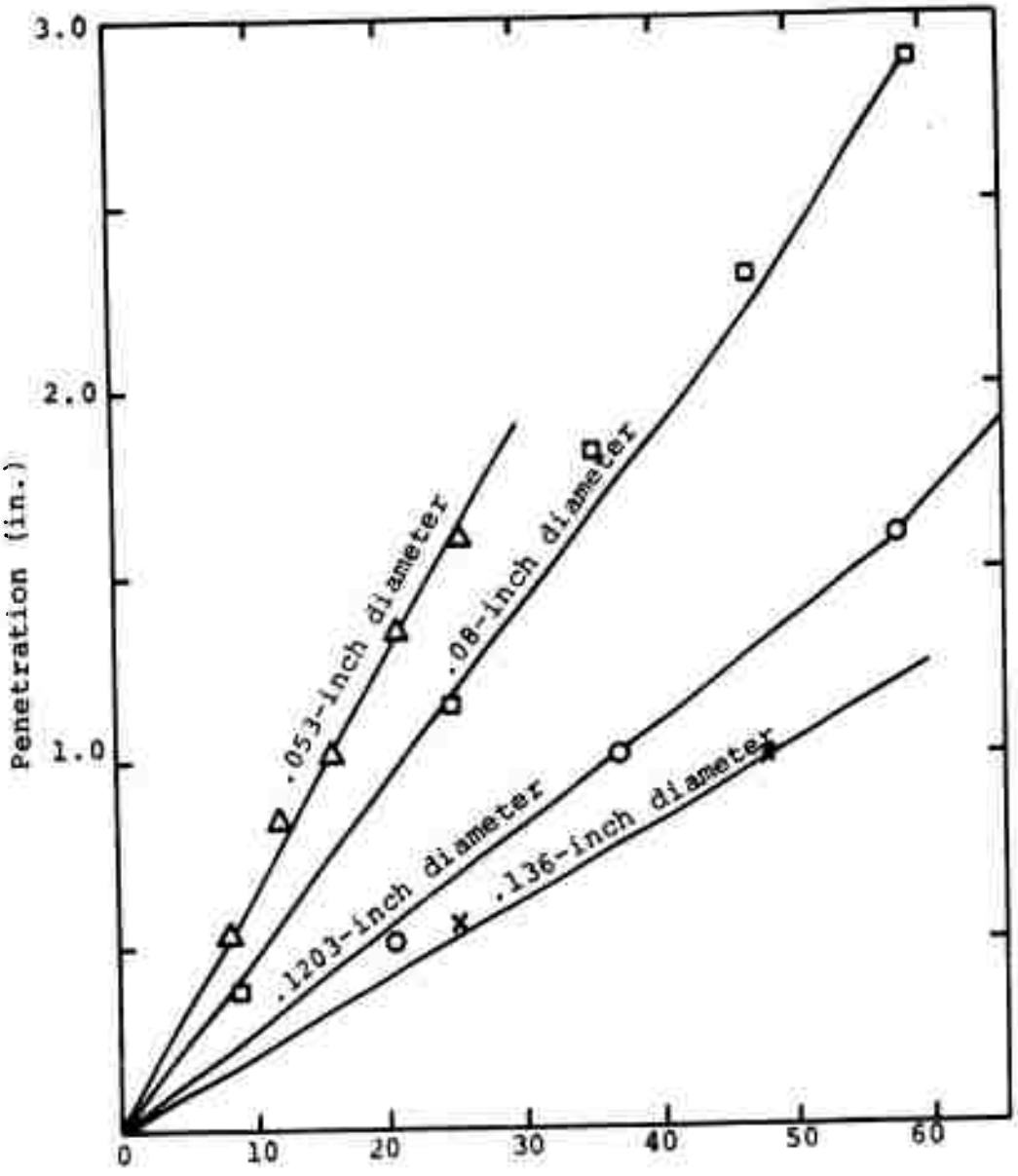

Figure 77. Penetration into sandstone as a function of jet horsepower and with change in nozzle diameter. Traverse speed 2.17 ft./min. (after Ref. 48).

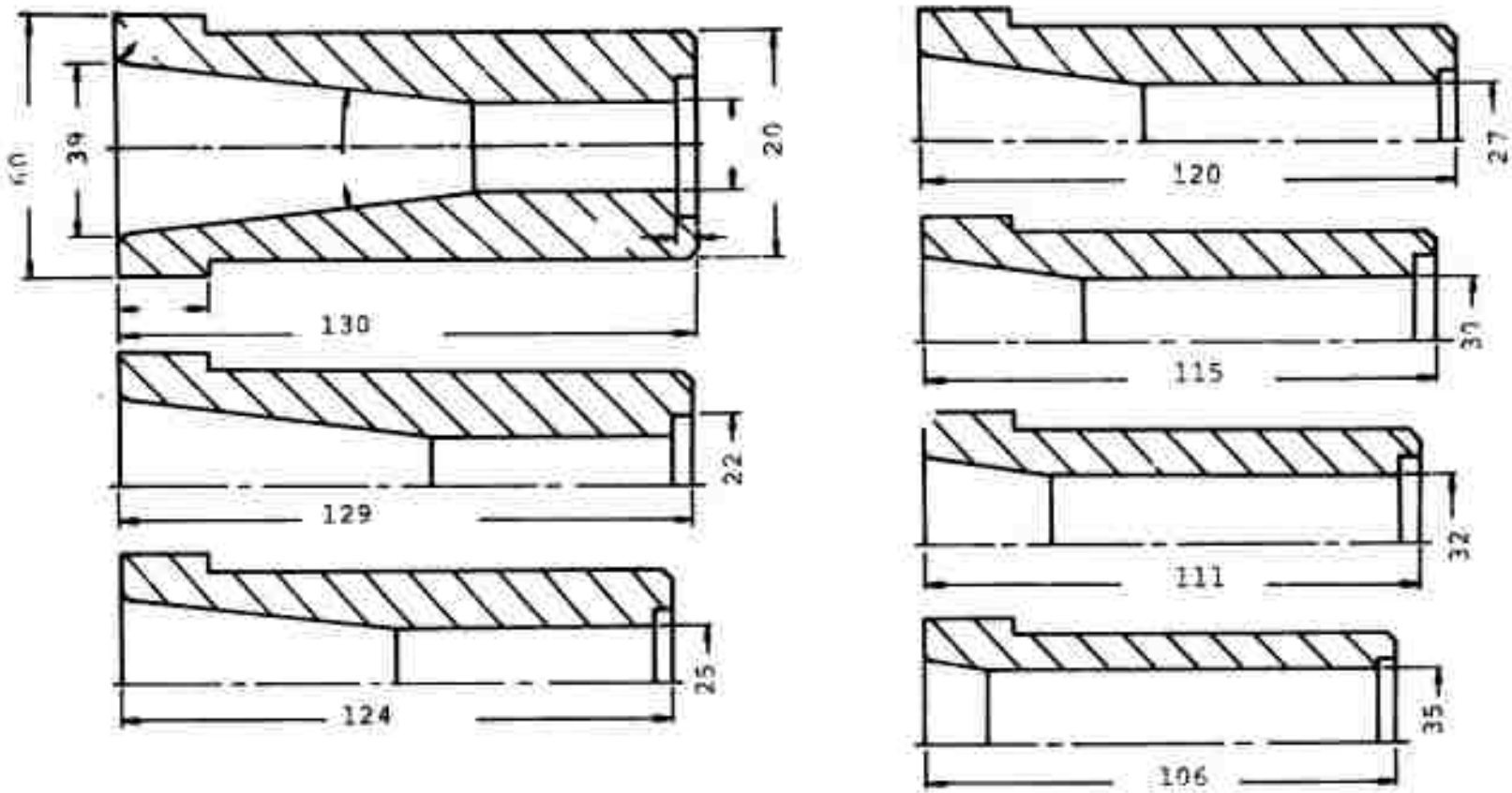

Figure 78. Nozzle shapes studied by German investigators (after Ref. 49). (Dimensions in mm.).

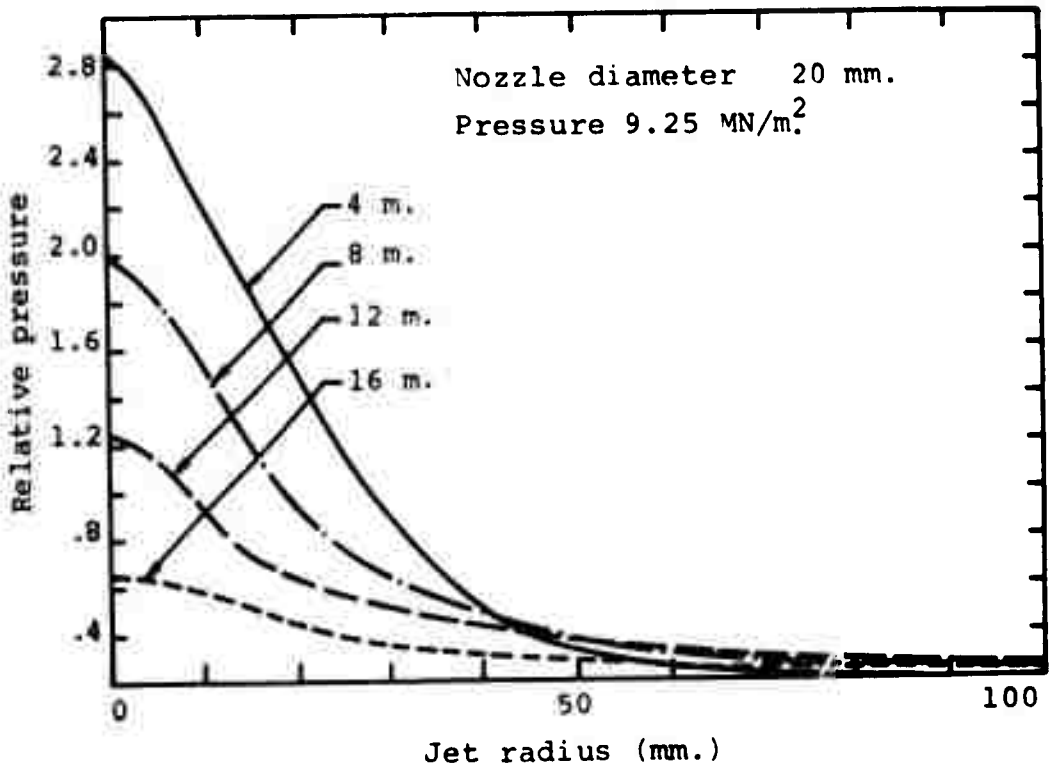

Figure 79(a). Variation in pressure distribution with distance (nozzle 1, Figure 78, after Ref. 49).

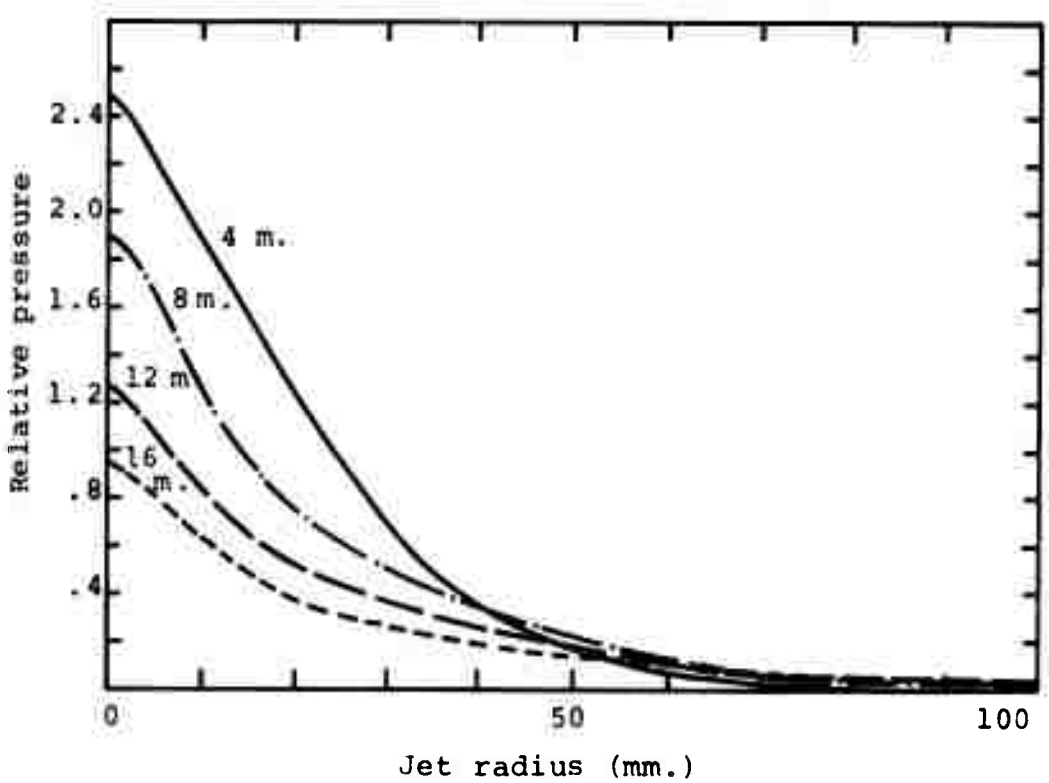

Figure 79(b). Variation in pressure distribution with distance (nozzle 2, Figure 78, after Ref. 49).

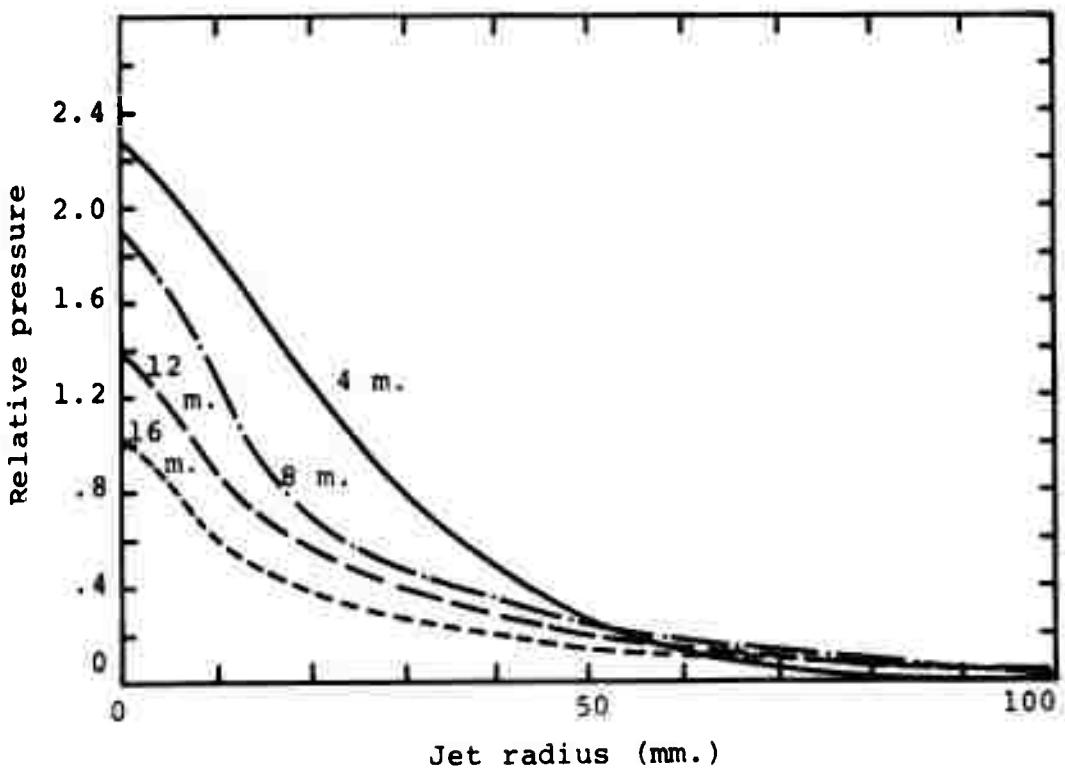

Figure 79(c). Variation in pressure distribution with distance (nozzle 3, Figure 78, after Ref. 49).

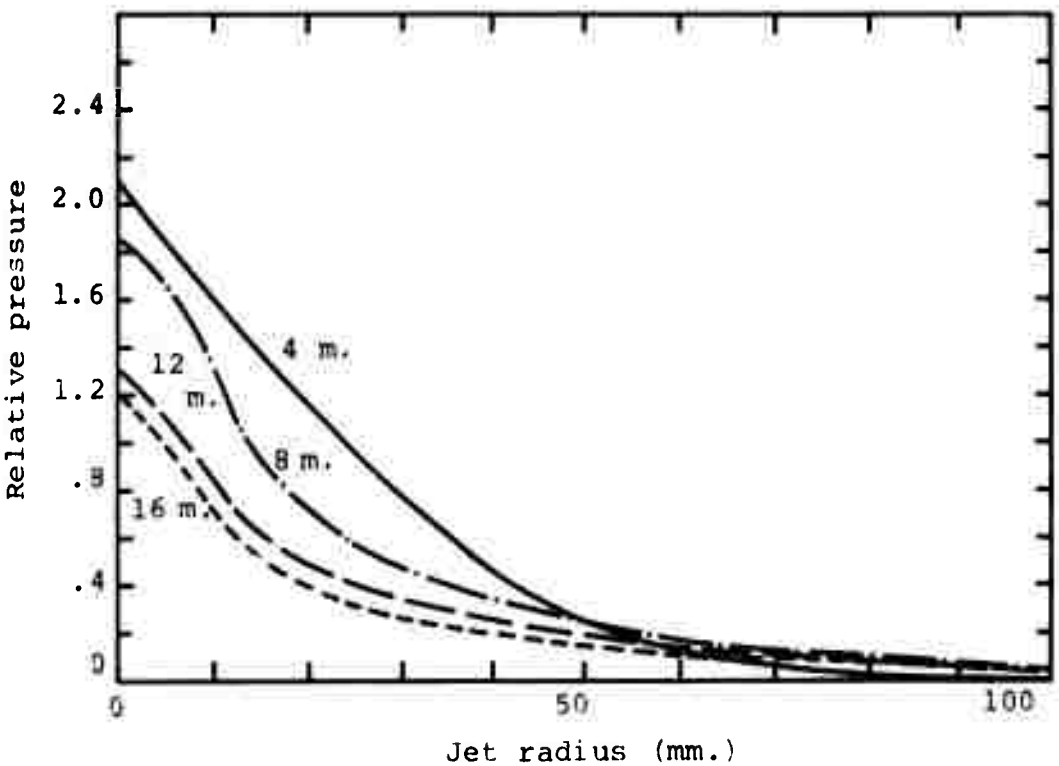

Figure 79(d). Variation in pressure distribution with distance (nozzle 4, Figure 78, after Ref. 49).

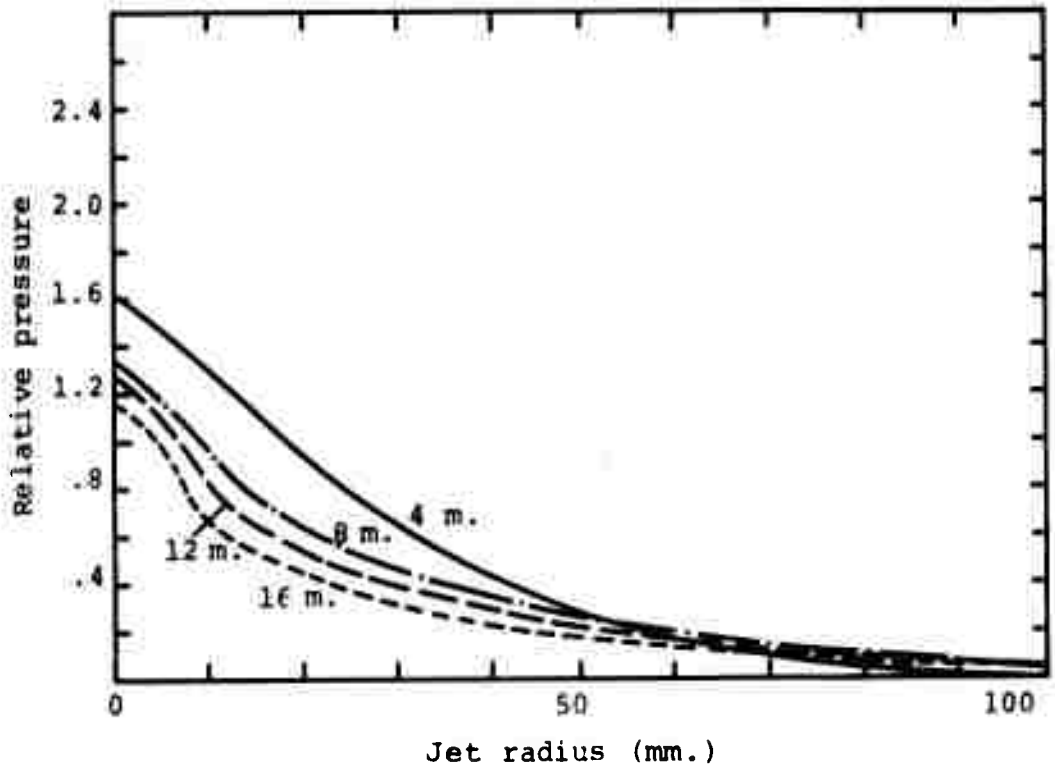

Figure 79(e). Variation in pressure distribution with distance (nozzle 5, Figure 78).

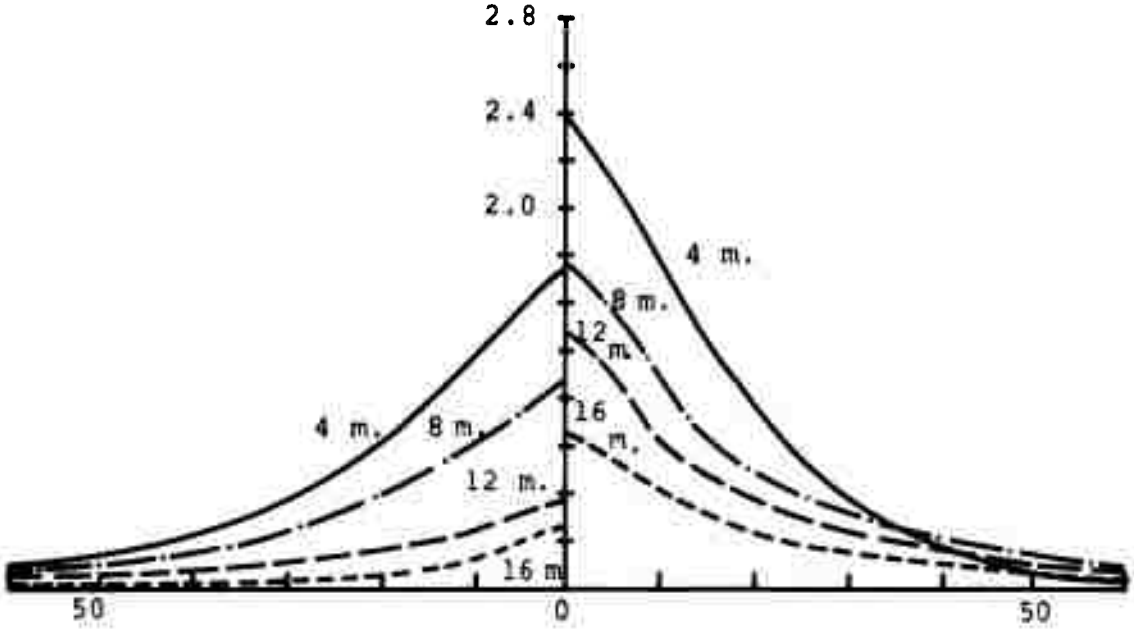

Figure 79(f) and 79(g). Variation in pressure distribution with distance. (Nozzles 6 and 7, Figure 78).

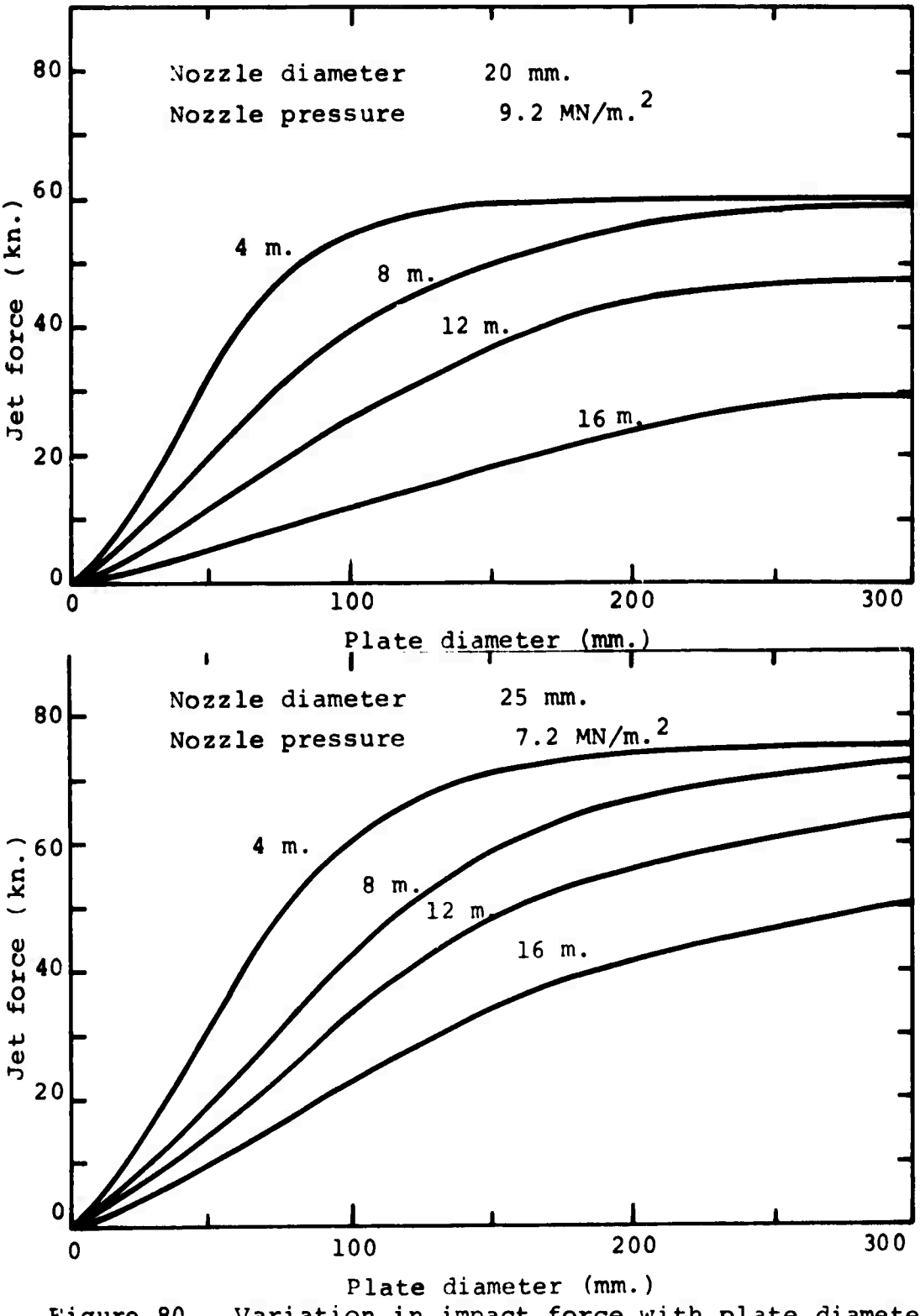

Figure 80. Variation in impact force with plate diameter (after Ref. 49).

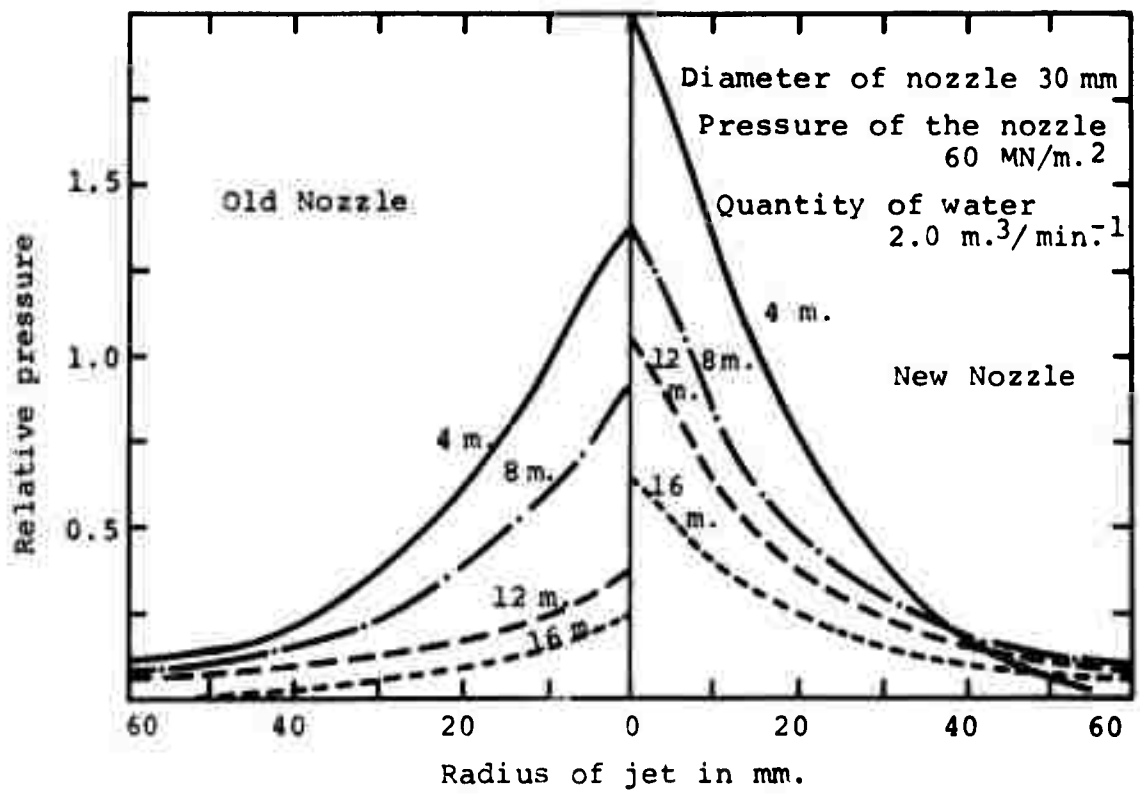

Figure 81. Influence of nozzle quality (after Ref. 49).

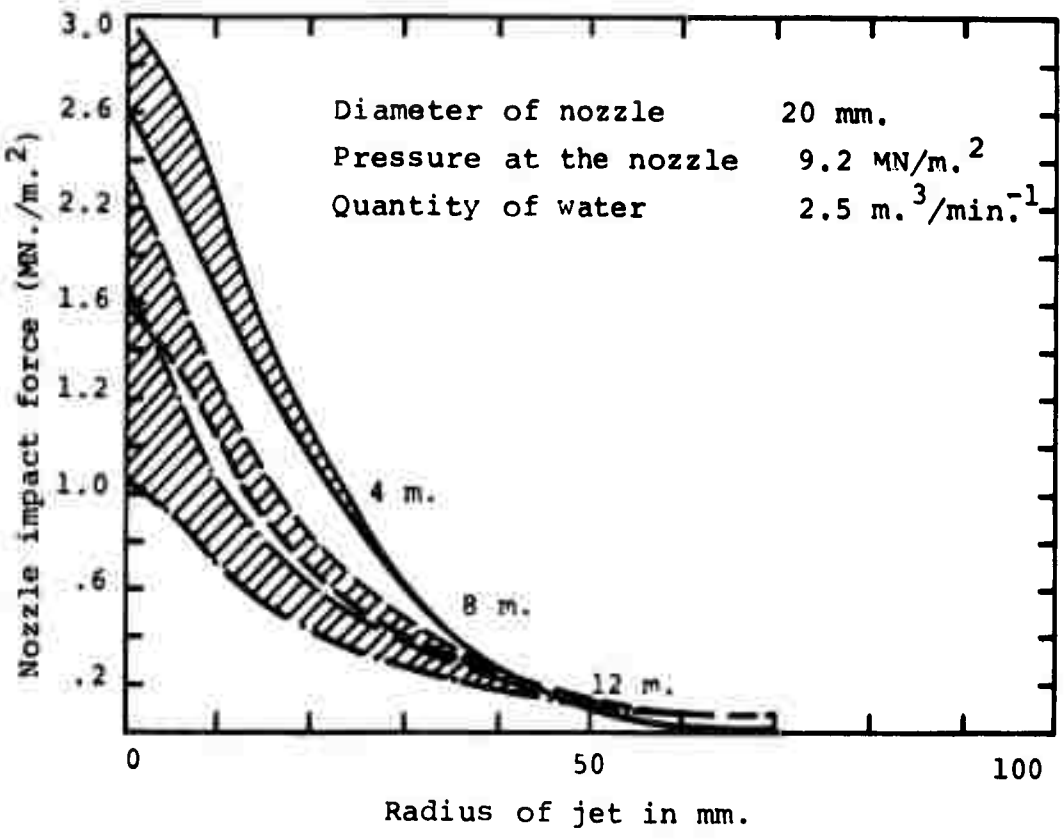

Figure 82. Influence of nozzle quality. Bands show variation in quality of jet with nozzle material (brass is lower curve, hard metal is upper curve) (after Ref. 49).

where K is a constant, μ is the coefficient of absolute viscosity, ρ is density and σ is surface tension. At low viscosity the first term is critical whereas at the higher fluid viscosities the second term becomes most important.

At greater velocities Schweitzer (Ref. 51) considered that disruption was, in part, due to turbulence within the jet. He examined the effect of change in jet pressure and ambient air pressure on the jet radius 14 in. from the nozzle for three oil jets (Figure 83) issuing through a 0.0135 in. orifice at pressures to 4000 p.s.i. Increasing jet viscosity improved jet stability (Figure 84). Schweitzer concluded that viscosity was the most influential of jet properties and that changes in surface tension values were of relatively minor importance at high jet velocities, except where the inner surface of the nozzle was rough.

Tyler and Watkin (Ref. 53) had identified the two maxima in jet cohesive length as pressure increases. Viscous and surface tension forces were identified as markedly influential on structure at these low velocities. In order to determine the effect of viscosity more clearly, various concentrations of treacle (a syrup) were added to water (Figure 85).

It was noted that there was an increase in the jet cohesive length with increase in viscosity. Tyler (Ref. 54) then went on to consider a range of fluids of varying viscosity (Figure 86) and obtained the curve from which the equation

$$\frac{L_B}{D} = V\sqrt{\frac{\rho D}{\sigma}}\left[1 + \frac{1}{1.095}\left(\frac{\sqrt{\sigma\rho D}}{\mu}\right)^{3/2}\right]\left(\frac{1}{Y}\right)\log\left(\frac{a}{a_o}\right) \qquad 30$$

was derived. A plot of such a relationship indicated the limiting condition of its validity (Figure 87).

Haenlein (Ref. 55) and Ohnesorge (Ref. 56) (1931) identified the disruptive aerodynamic breakup of high velocity jets to give a third maxima on the length-velocity curve. However, Littaye (Ref. 57) (1939) considered that, under normal laboratory studies, jet disruption by wave deformation was indeterminate and that there were generally only two major causes of disruption, capillary forces at low velocity and viscous forces at greater velocities.

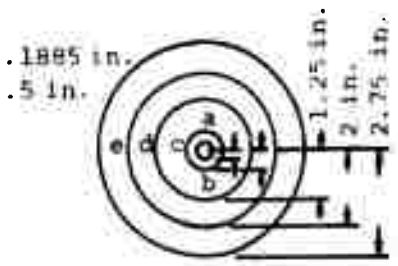

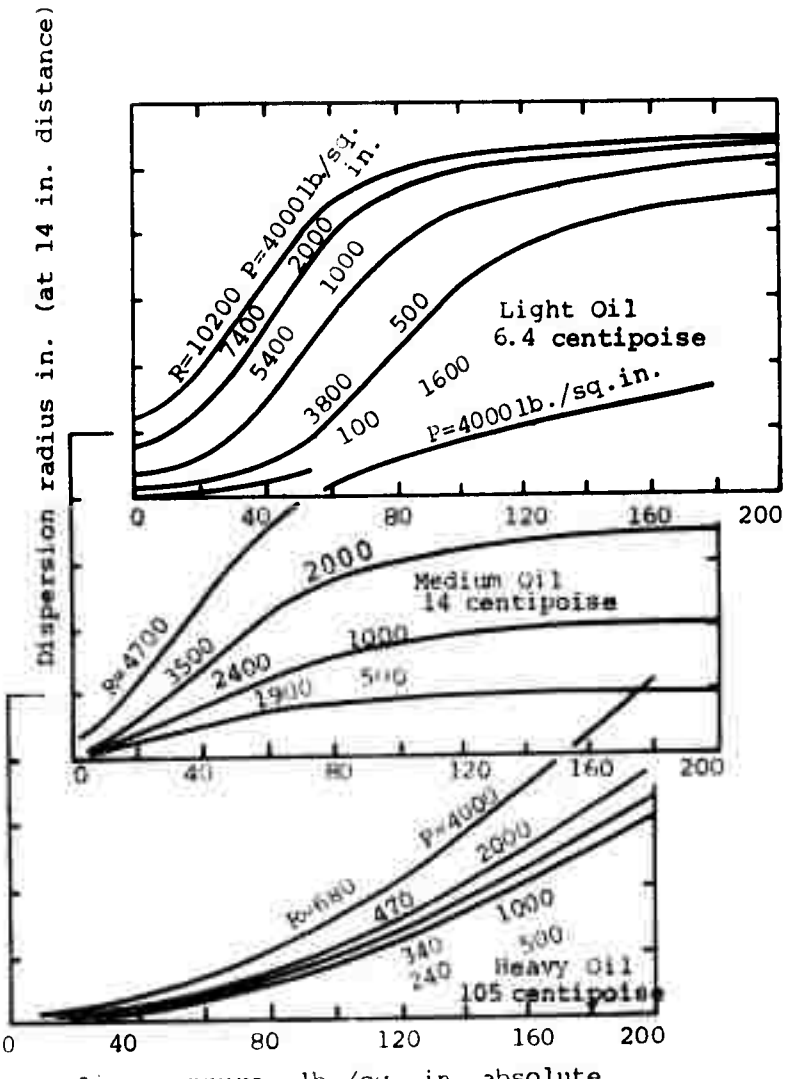

Figure 83. Variation in flow dispersion at 14 in. stand-off with change in air pressure for three oils (after Ref. 51).

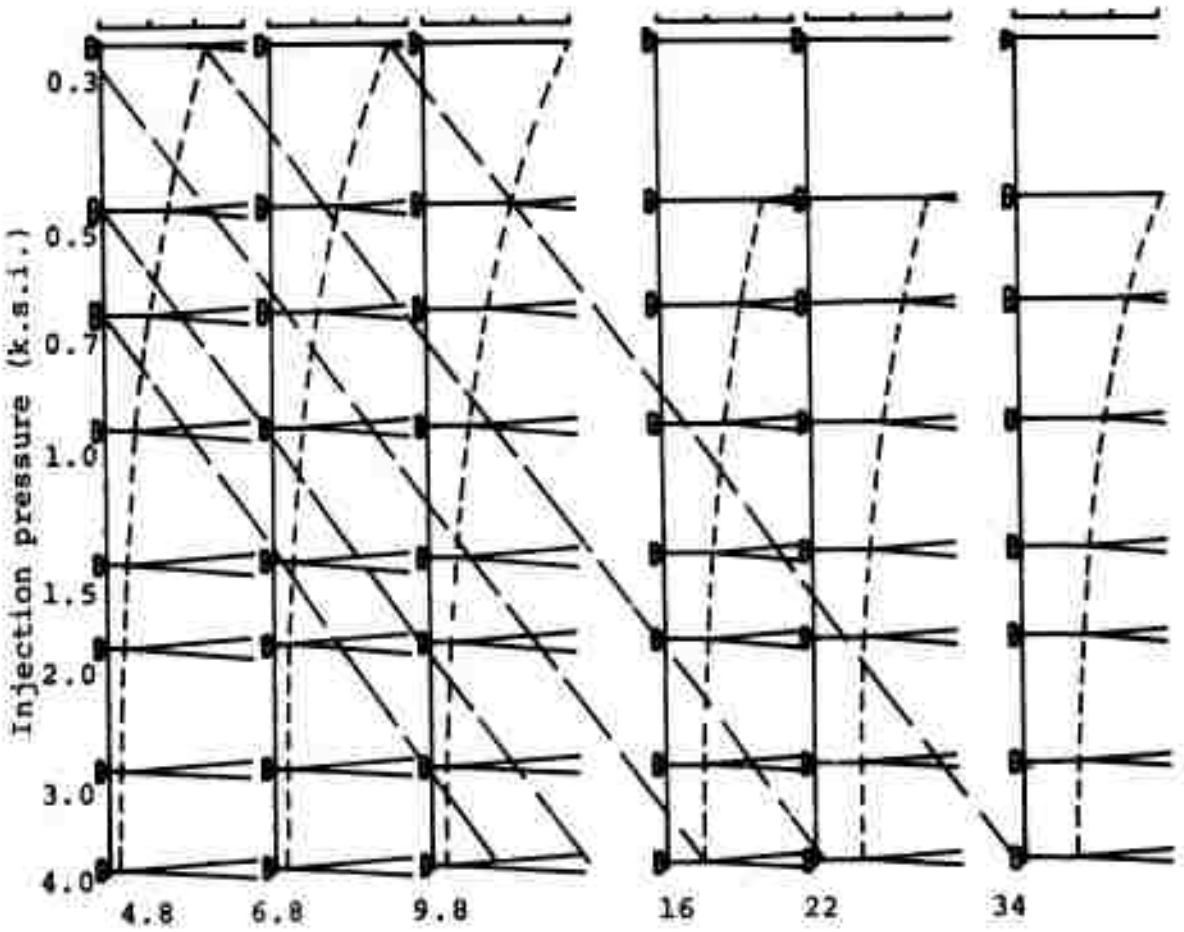

$$\text{Kinematic viscosity} = \frac{\text{Absolute viscosity (CP)}}{\text{density}}$$

Figure 84. Breakup distance and cone angle at various pressures and viscosities. The diagonal straight lines correspond to constant Reynolds numbers.

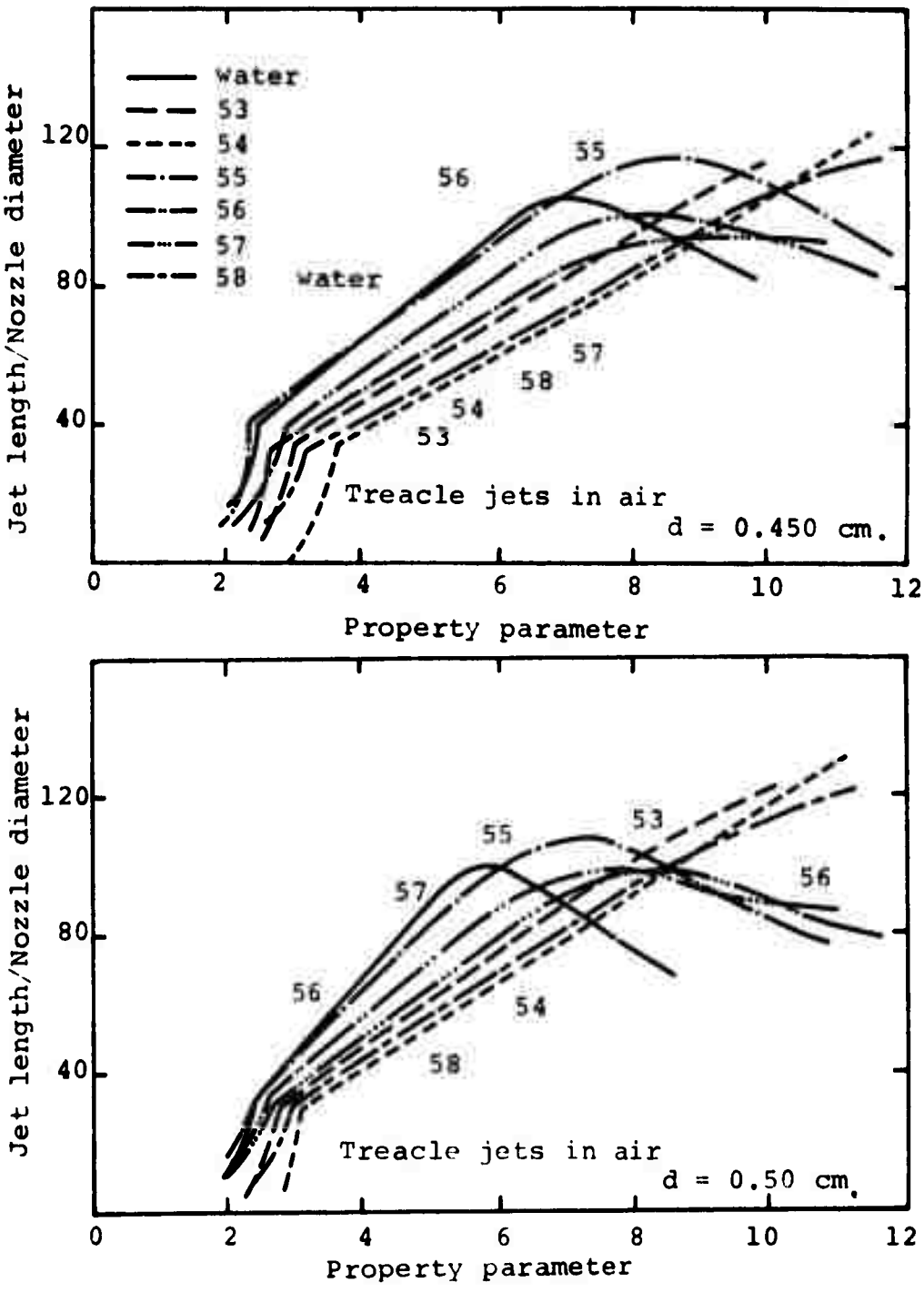

Figure 85. Variation in jet length with fluid properties for various treacle solutions at two nozzle diameters (after Ref. 53).

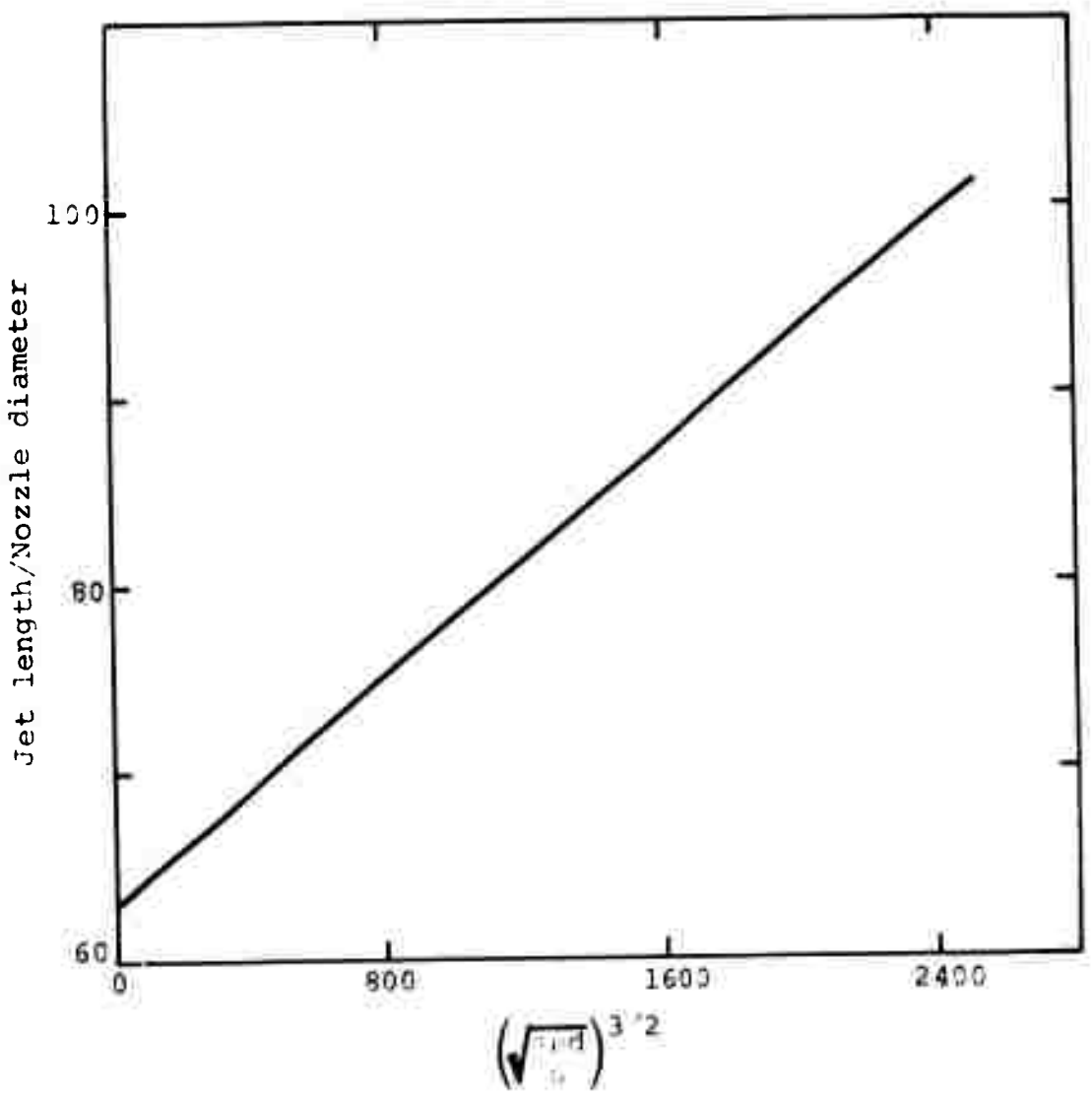

Figure 86. Variation in jet length with fluid properties (after Ref. 86).

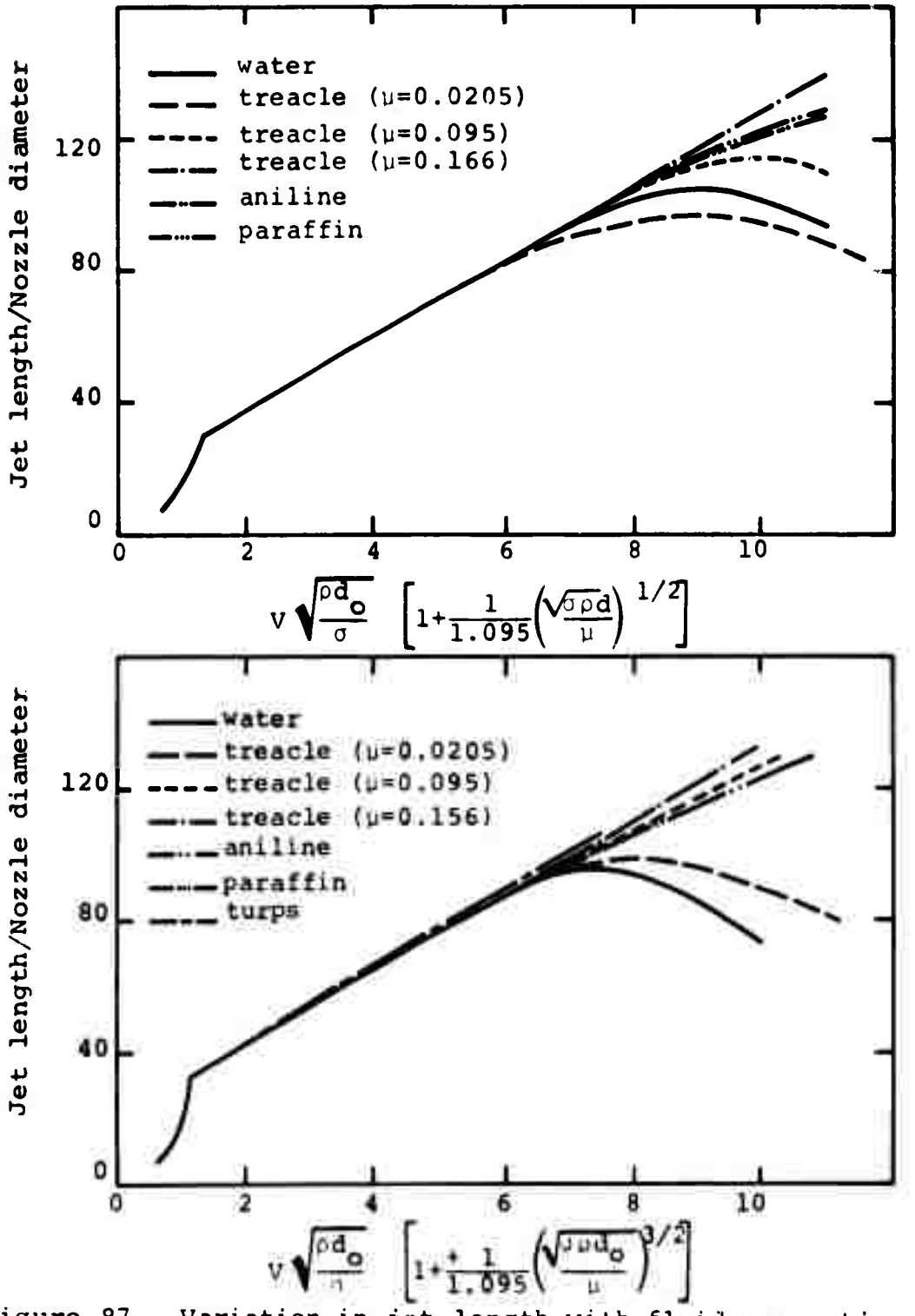

Figure 87. Variation in jet length with fluid properties for various fluids (after Ref. 54).

Merrington and Richardson (Ref. 58) evaluated stability of 11 liquids (Table XI). In evaluating the effects of viscosity, droplet size at the point of disruption was considered as the dependent variable (Figure 88). It was noted that for disruption to occur due to aerodynamic forces, there must be air friction and the jet must be turbulent. This conclusion was verified by Schneider (Ref. 51) and agrees with conclusions drawn by Lienhard and Day (Ref. 9) and discussed earlier in this text.

In comparing the length of jets at various jet velocities (Figure 89) to a maximum pressure of 1000 p.s.i., it became obvious that the relationships postulated earlier for jets of low viscosity did not hold where viscous jets were considered (Figure 90). It was found that for mercury the jet length was markedly dependent on the nozzle geometry (Figure 91). It was also discovered that the value of viscosity for rubber in gasoline (petrol) changed from a value of 0.5 poise when measured in an Ostwald viscometer to a value of 2-3 poise measured in jet flow. It was postulated that this is due to the relatively small value of the shearing forces present in the jet motion. Care must be taken, therefore, in evaluating viscosity data for non-Newtonian fluids.

Richardson carried this work further using high speed photography and found that "atomization" of jets issuing from a 2 mm nozzle occurred at a Weber Number of 30 (Ref. 59).

Misse (Ref. 60) examined jet breakup at higher velocity using jets of water and jets of liquid nitrogen, exhausting into atmospheric air and found that the length of the jet (Figure 92) could be given by

$$\frac{L_B}{2D} = 3480\ W_e^{-0.71} p^{-1.21} M^{0.308} \qquad 31$$

Leach and Walker (Ref. 11) examined the effect of change of jet fluid properties at higher velocities (Figure 93). The increase in viscosity, obtained by adding small quantities of sodium carboxymethyl cellulose to the water, improved the performance of the jet consistently over the length measured, whereas lowering the surface tension of the fluid by adding detergent reduced overall jet pressure out to 250 nozzle diameters, beyond which effectiveness was improved. However, it

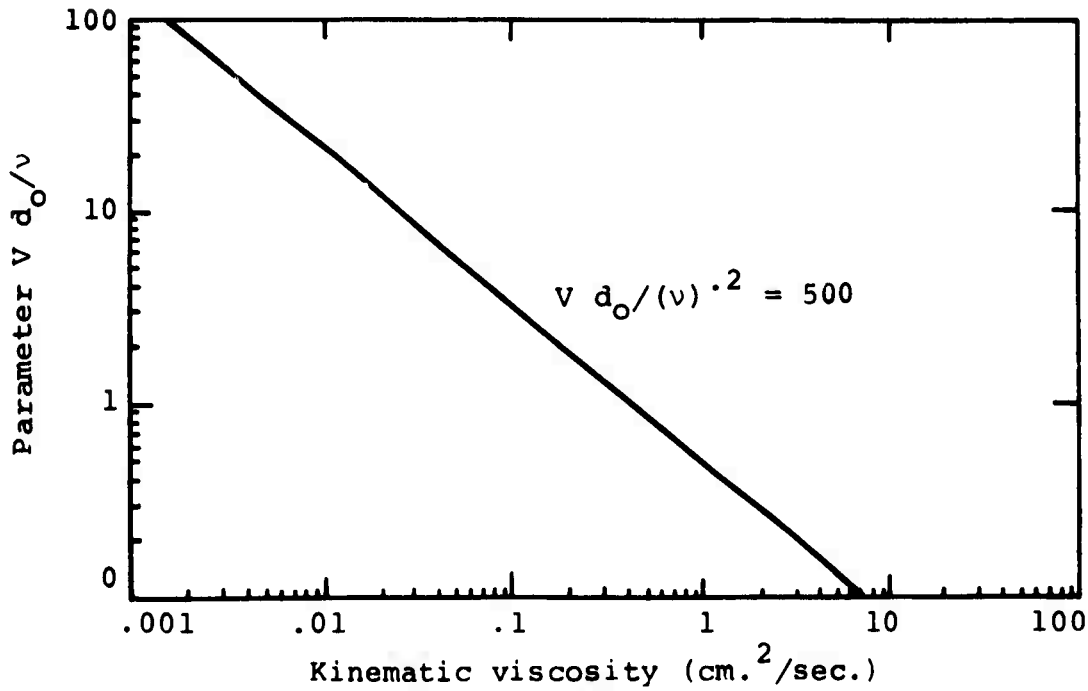

Figure 88. Variation in droplet parameter with kinematic viscosity (after Ref. 58).

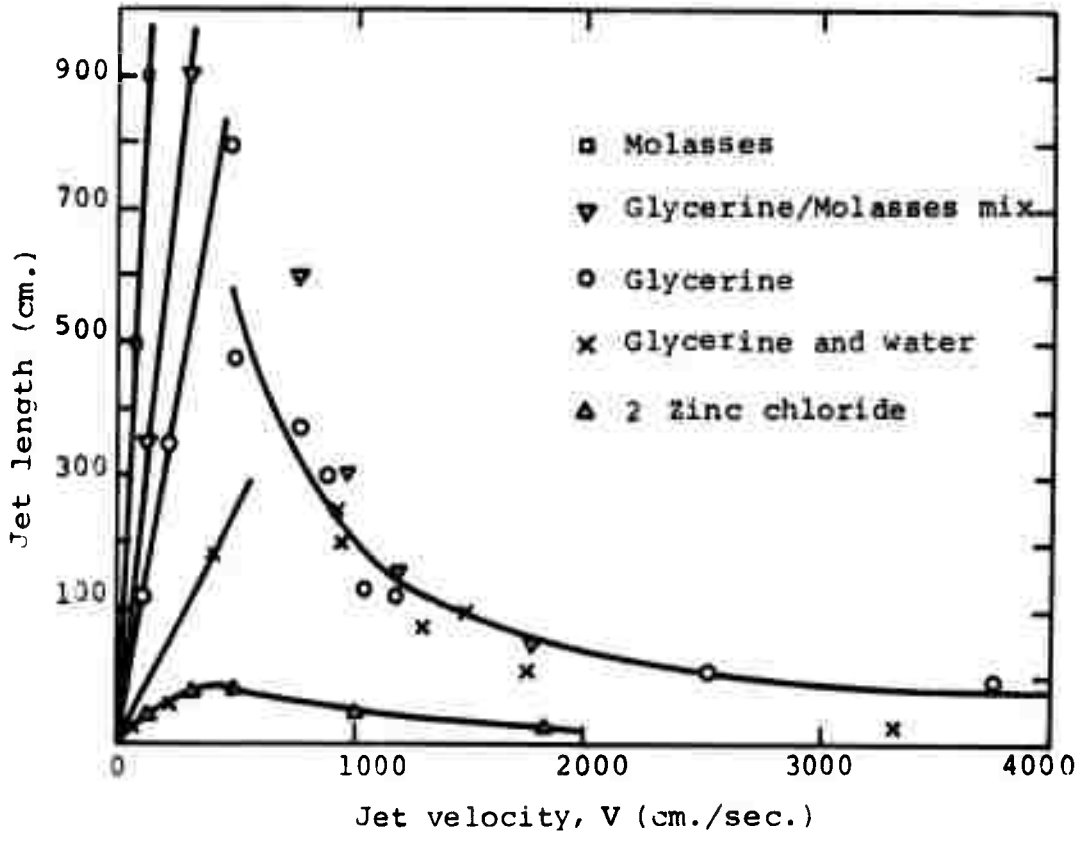

Figure 89. Variation in jet length with velocity (after Ref. 58).

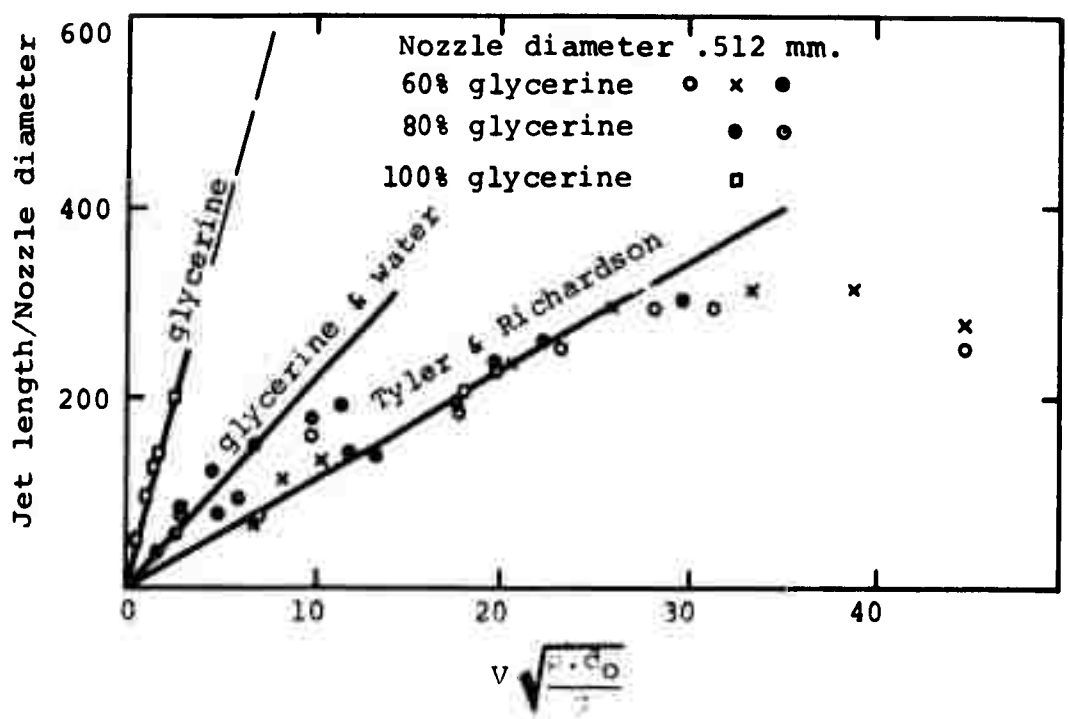

Figure 90. Variation in jet length with fluid properties for three glycerine concentrations (after Ref. 58).

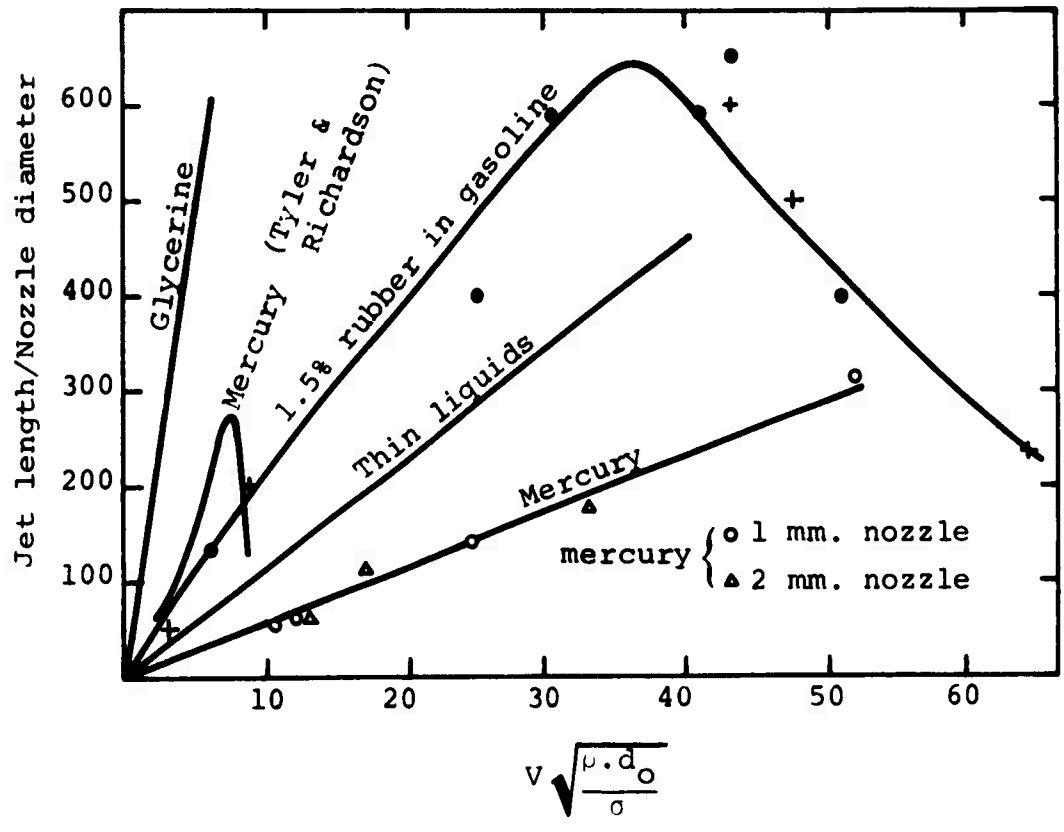

Figure 91. Variation in jet length with fluid properties (after Ref. 58).

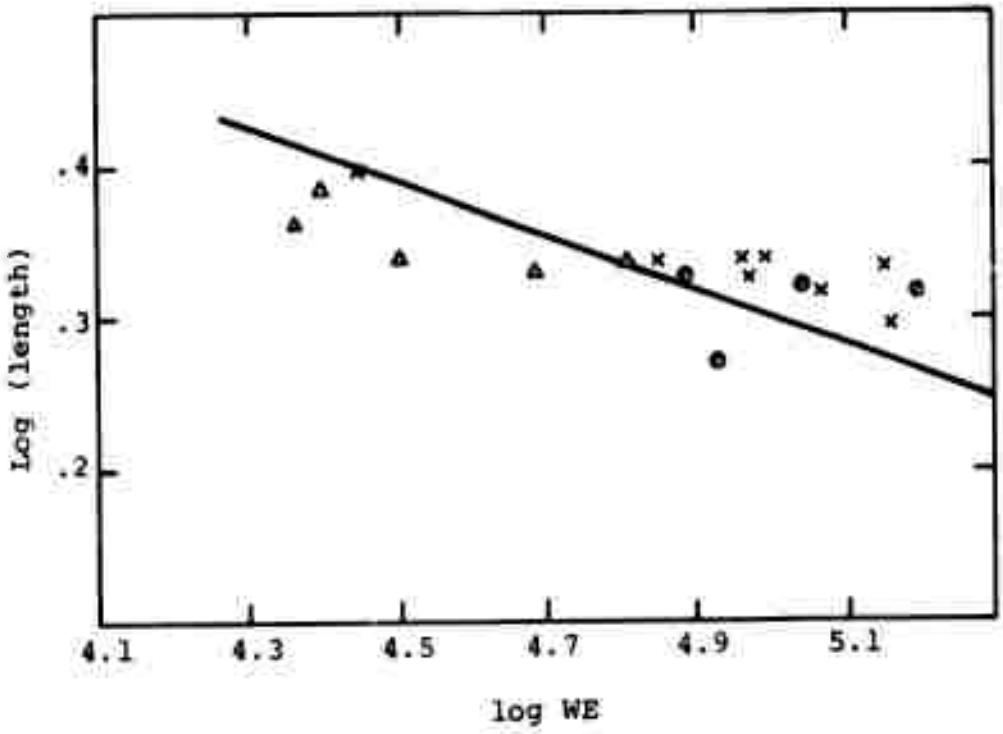

Figure 92. Variation in jet length with Weber Number for water and liquid nitrogen (after Ref. 10).

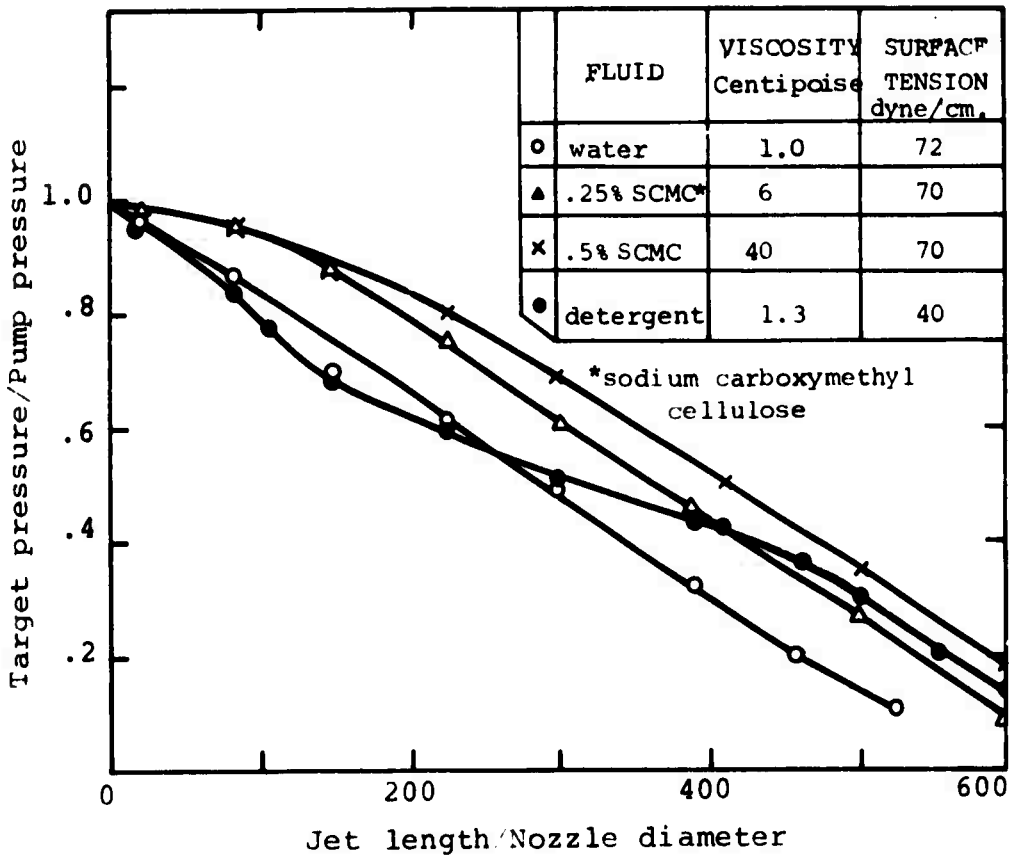

Figure 93. Variation in jet pressure with fluid properties (after Ref. 11).

should be noted that sodium carboxymethyl cellulose imparts viscoelastic properties to water, and such drag reducing solutions are known to improve jet cohesion as discussed below.

Semerchan (Ref. 40) varied the concentration of glycerine in a water solution from 0 to 40%, thus varying jet viscosity over three orders of magnitude.

Table XII. Viscosity Values for Glycerine-Water Solution

Viscosity of glycerine-water solution at t = 20°C					
Percentage Glycerine	0	10	20	40	100
Viscosity, cp	1.005	1.311	1.769	3.75	1499

The improvement in the performance of the high glycerine content jets (Figure 94) is stated as being because of the increase in cohesion effected by the increase in viscosity. In two photographs taken at the jet nozzle and given in the text, a pronounced improvement in cohesion is obtained at 15,000 p.s.i. where a pure glycerine jet is used rather than water. The effect in this case might, however, be due to a change in flow pattern from turbulent to laminar flow since the change in viscosity will change the Reynolds Number from 13×10^6 for water to 1×10^4 for glycerine.

Recently there has been an increase in the use of long chain polymers as a means of jet enhancement for cutting purposes. The initial interest was in the polymerized ethylene oxide compound known as Polyox*. Experiments carried out by and for the New York Fire Department showed that the use of small concentrations of the polymer in water increased the volume rate of flow for a given pump pressure and demonstrably increased the throw of the jet.

*A Union Carbide product

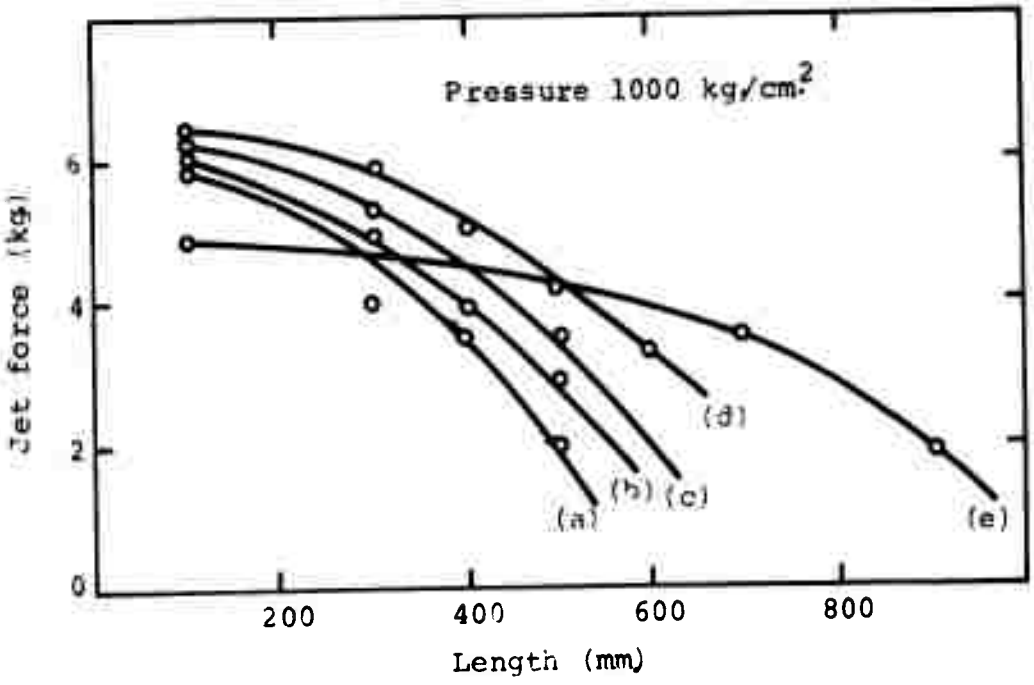

Figure 94(a). Jet force variation with standoff distance (after Ref. 40).

Fluids for both figures: a) water, b) 10% glycerine in water, c) 20% glycerine, d) 40% glycerine, and e) 100% glycerine.

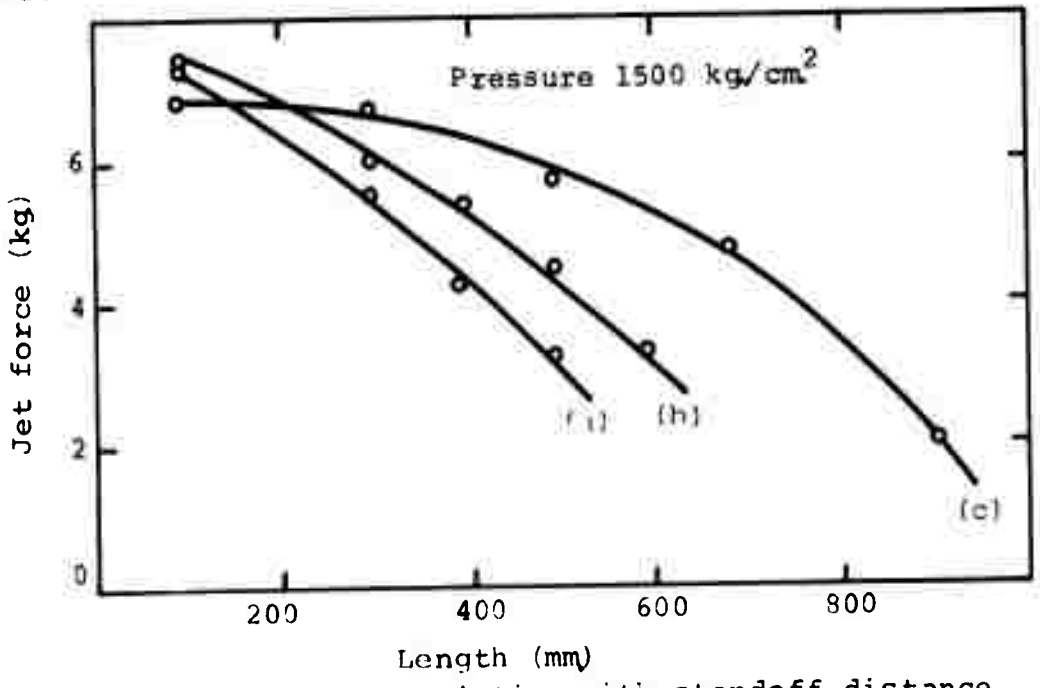

Figure 94(b). Jet force variation with standoff distance (after Ref. 40).

Summers (Ref. 18) showed that, in the cutting of sandstone, the addition of 0.1 percent Polyox improved jet performance with distance (Figure 95) and that the improvement was consistent over a range of pressures (Figure 96).

Franz (Ref. 39) found that the cutting ability of a Polyox solution for use in wood carving was improved as the polymer concentration increased to a definable maximum, whereas the addition of glycerine to the water reduced the effectiveness of the jet (Figure 97). It is interesting to note that this agrees with the theory developed by Cooley (Ref. 61) who postulated that decreasing viscosity would improve jet cutting ability, because the fluid would be more readily able to penetrate miscrofissures in the target material, and thus weaken it and induce failure.

This conclusion is further borne out by studies carried out at the University of Cambridge (Ref. 62) (Figure 98) and by Franz who found a reduction in the fluid retained by the target when Polyox was used instead of water (Figure 99). At low concentrations there is little change in viscosity where Polyox is added to water (Ref. 63) but as concentration level is increased viscosity also increases (Figure 100). Concurrently there is a reduction in the friction coefficient of the fluid, a reduction which grows with increase in Reynolds Number (Figure 101).

Franz states that this drag reduction might explain the relatively minor changes in flow rate achieved at higher polymer concentrations where the increase in viscosity could otherwise be expected to reduce the flow (Figure 102). He also found that increasing concentrations of Polymer reduced the amount of wetting of the target material.

The change in jet diameter with distance as polymer concentration increases has been studied by Sims (Ref. 63) who showed a clear improvement in cohesion of the jet (Figure 103). Care in the use of the polymer should be noted, however, since it does age (Figure 100b). The lack of cognisance of this by early investigators (including the present author) may have had some effect on the data obtained.

A problem in correlating jet studies with those carried out for polymers in pipelines is indicated by Vlasov et al (Ref. 64). An apparent feature of certain polymer additives is that while reducing flow disturbances near smooth surfaces, as in pipelines, they work to the opposite effect in free jet turbulence.

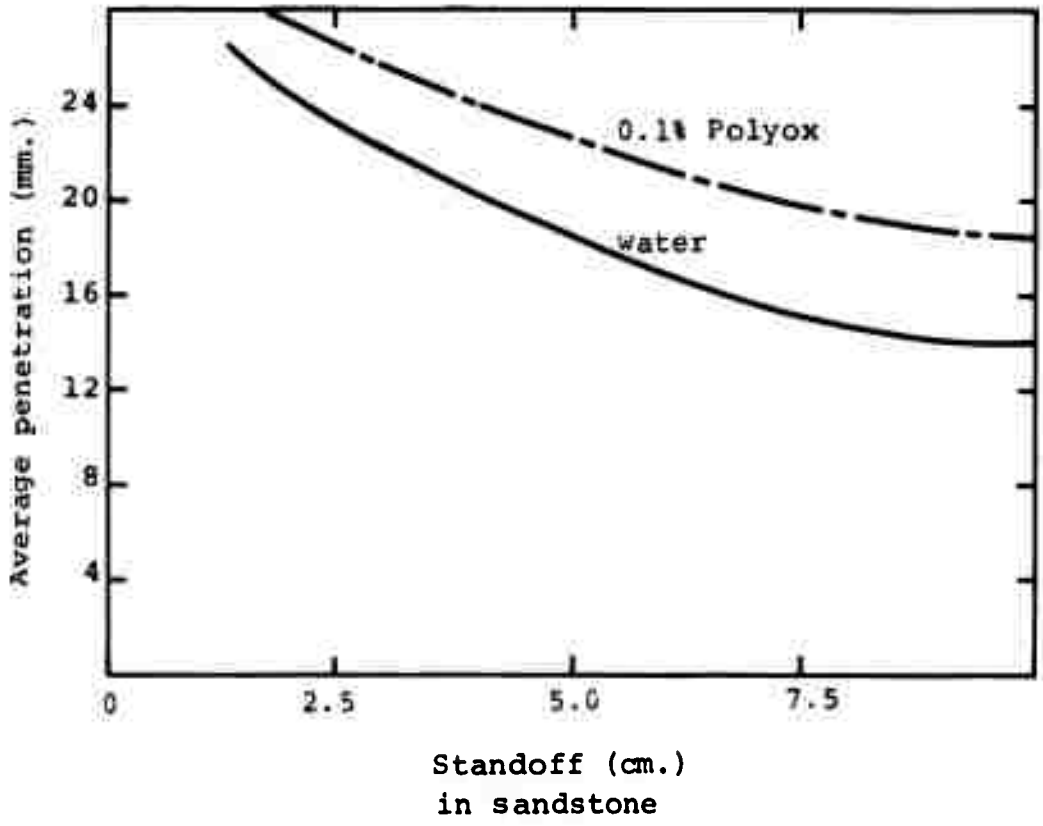

Figure 95. Variation in penetration in sandstone with standoff distance showing the effect of Polyox (after Ref. 18).

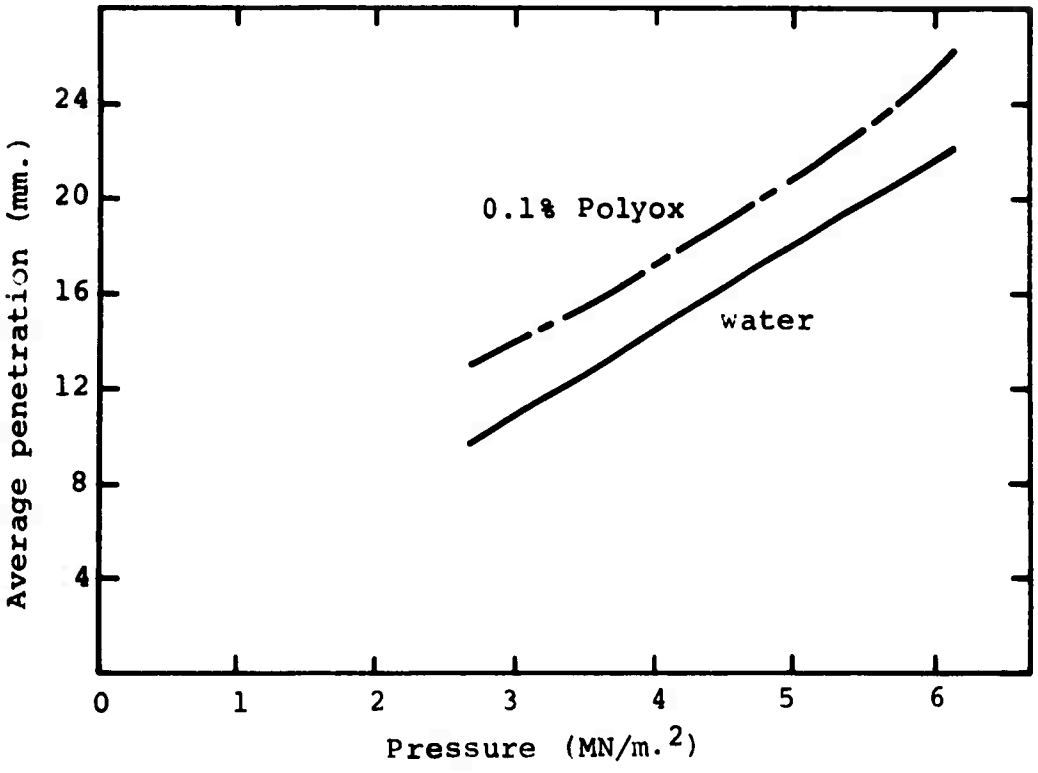

Figure 96. Variation in penetration in sandstone with pressure showing the effect of Polyox (after Ref. 18).

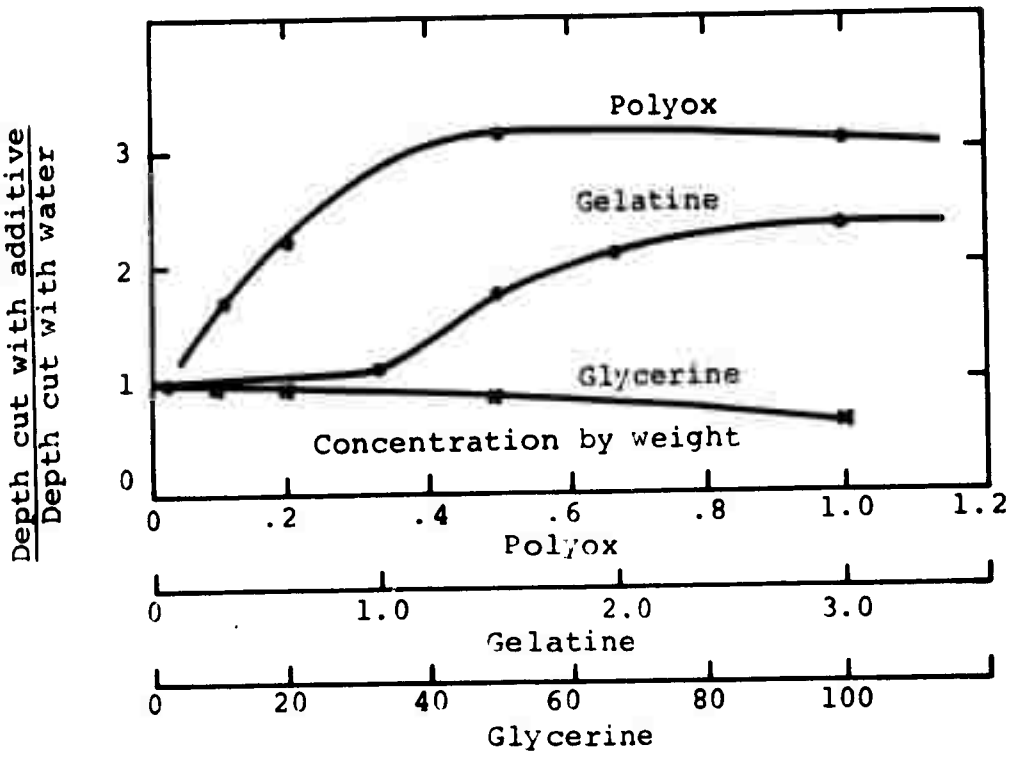

Figure 97. Variation in relative penetration in wood with additive concentration for three additives (after Ref. 39).

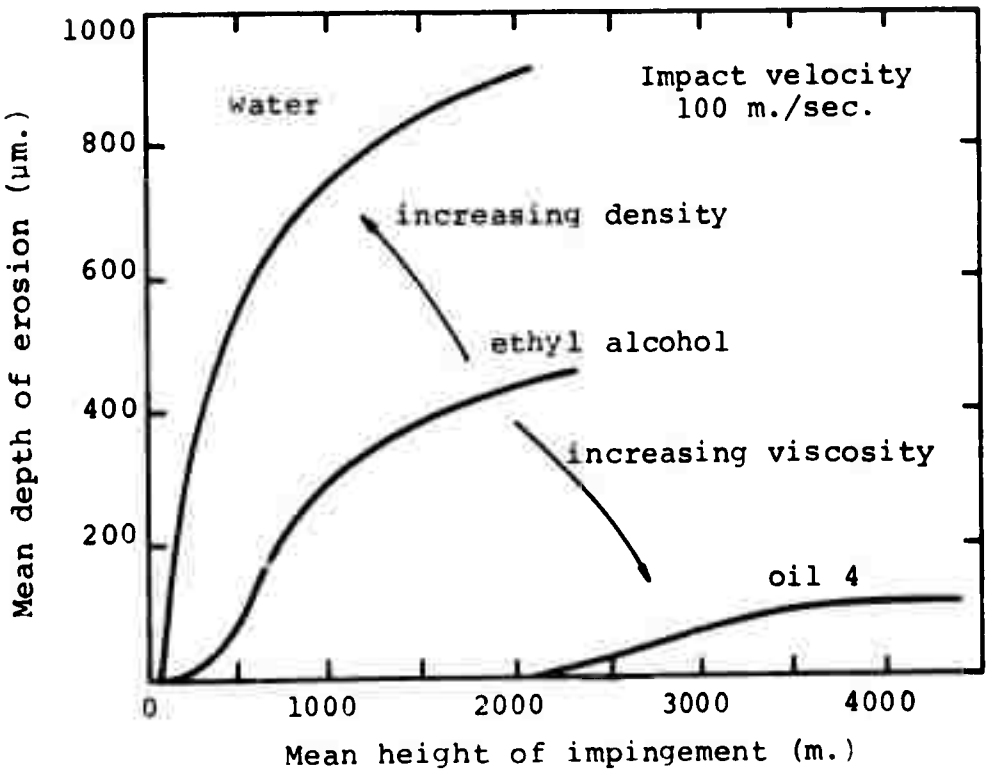

Figure 98. Variation in penetration with time for three fluids of varying properties (after Ref. 62).

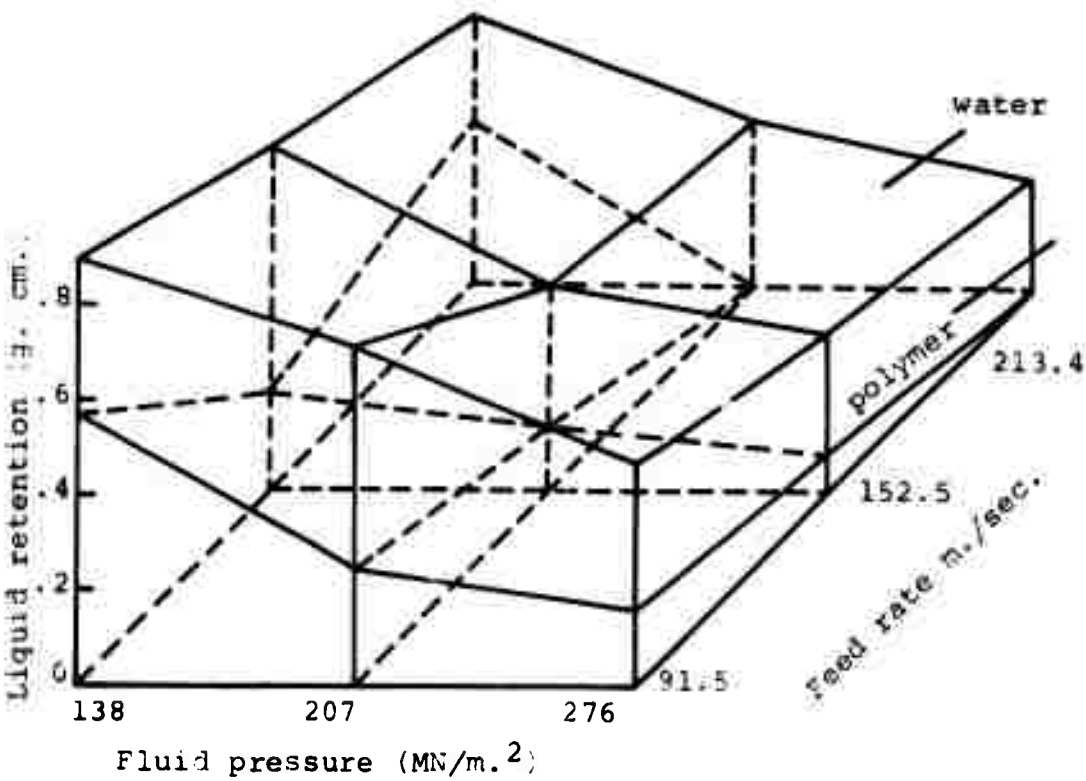

Figure 99(a). Variation in liquid retention for 0.49 Kg./m.^{2} corrugated board.

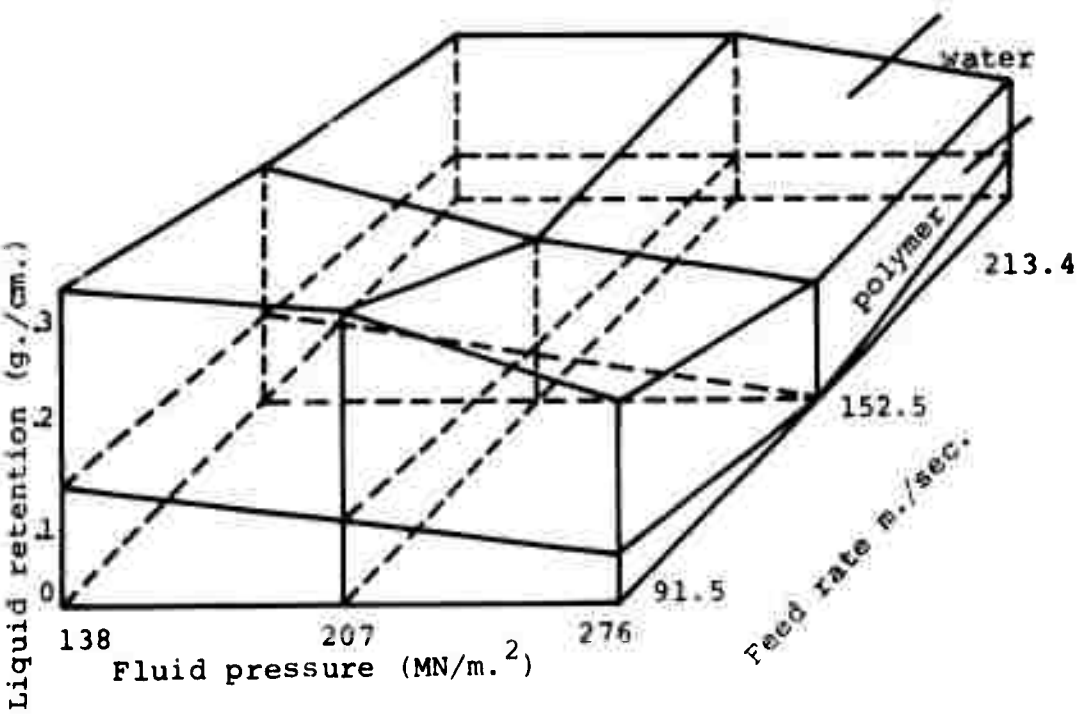

Figure 99(b). Variation in liquid retention for 0.44 kg./m.^{2} corrugated board showing the effect of Polymer (after Ref. 39).

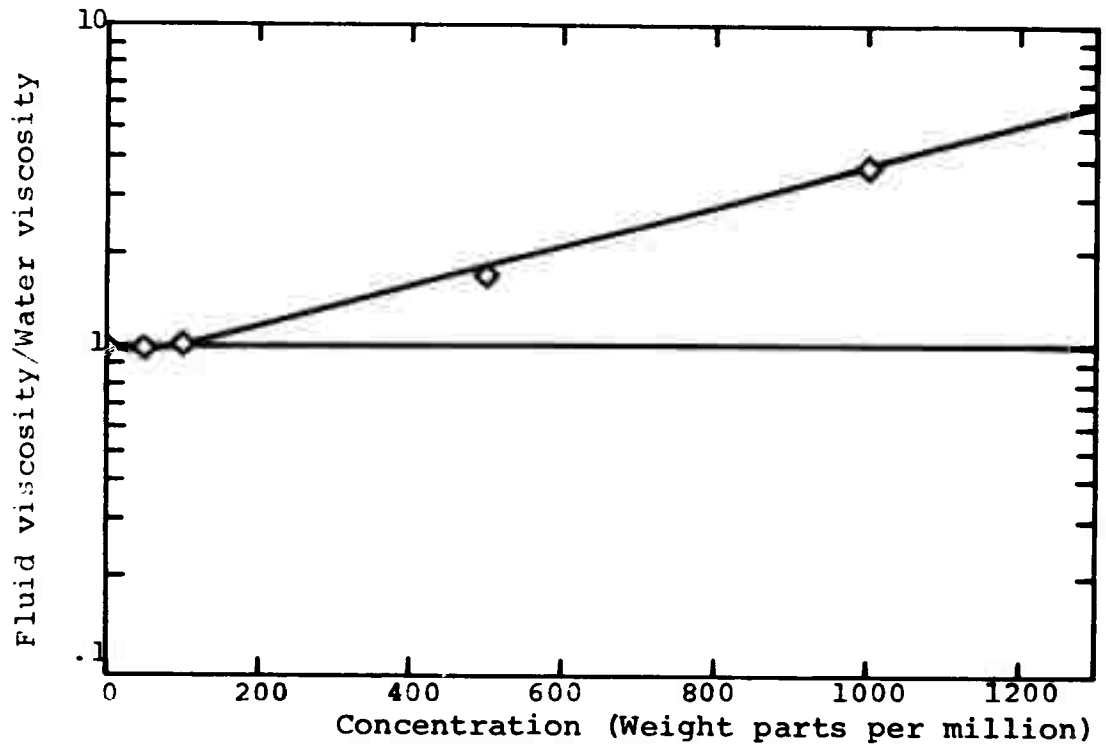

Figure 100(a). Change in relative viscosity with polyox concentration (after Ref. 63).

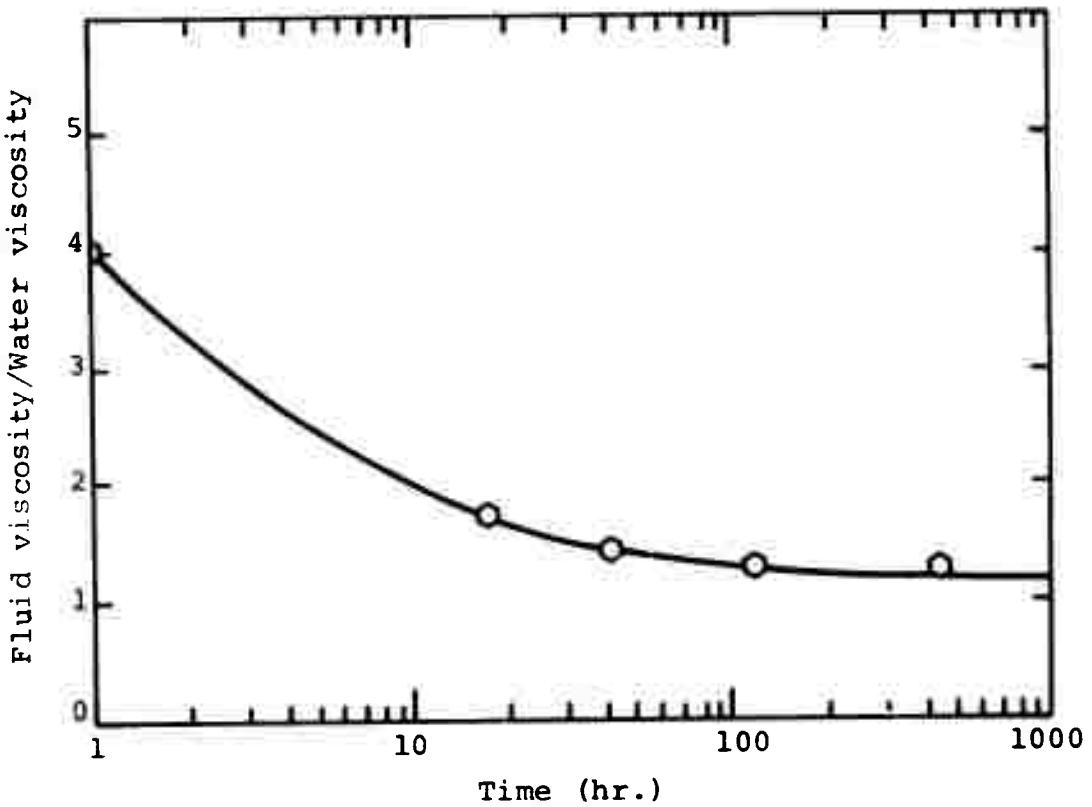

Figure 100(b). Change in viscosity of a Polyox solution with time (after Ref. 63).

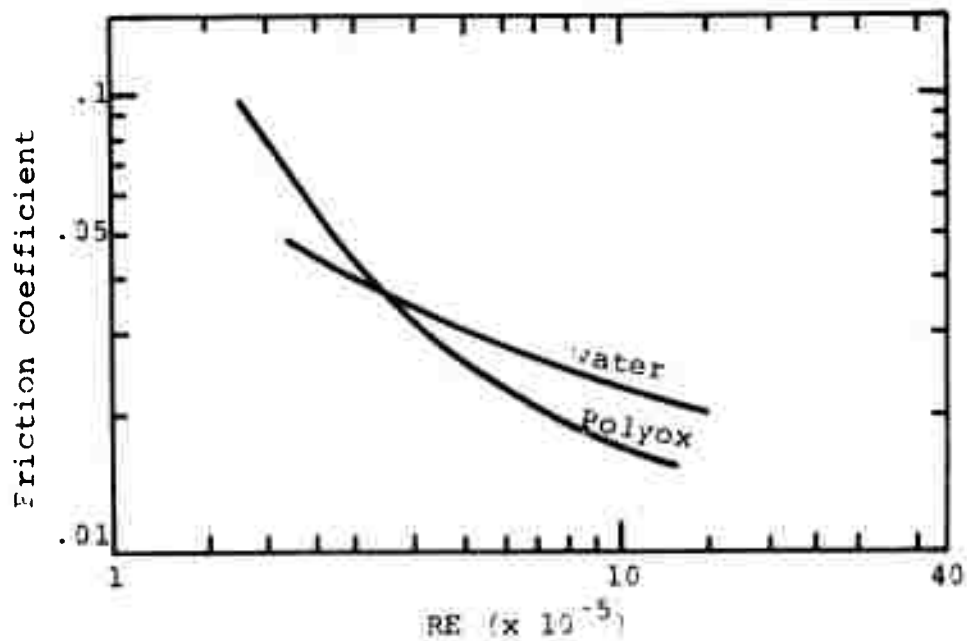

Figure 101. Variation in friction coefficient for water and Polyox solution with Reynolds Number (after Ref. 39).

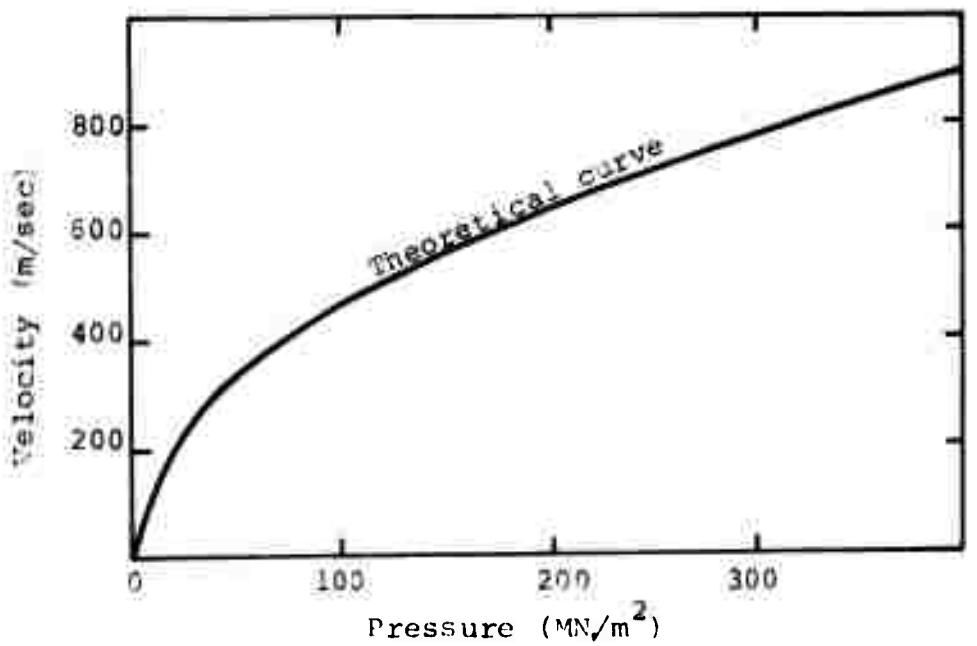

Figure 102. Theoretical and measured jet velocities for water and Polyox solutions (after Ref. 39).

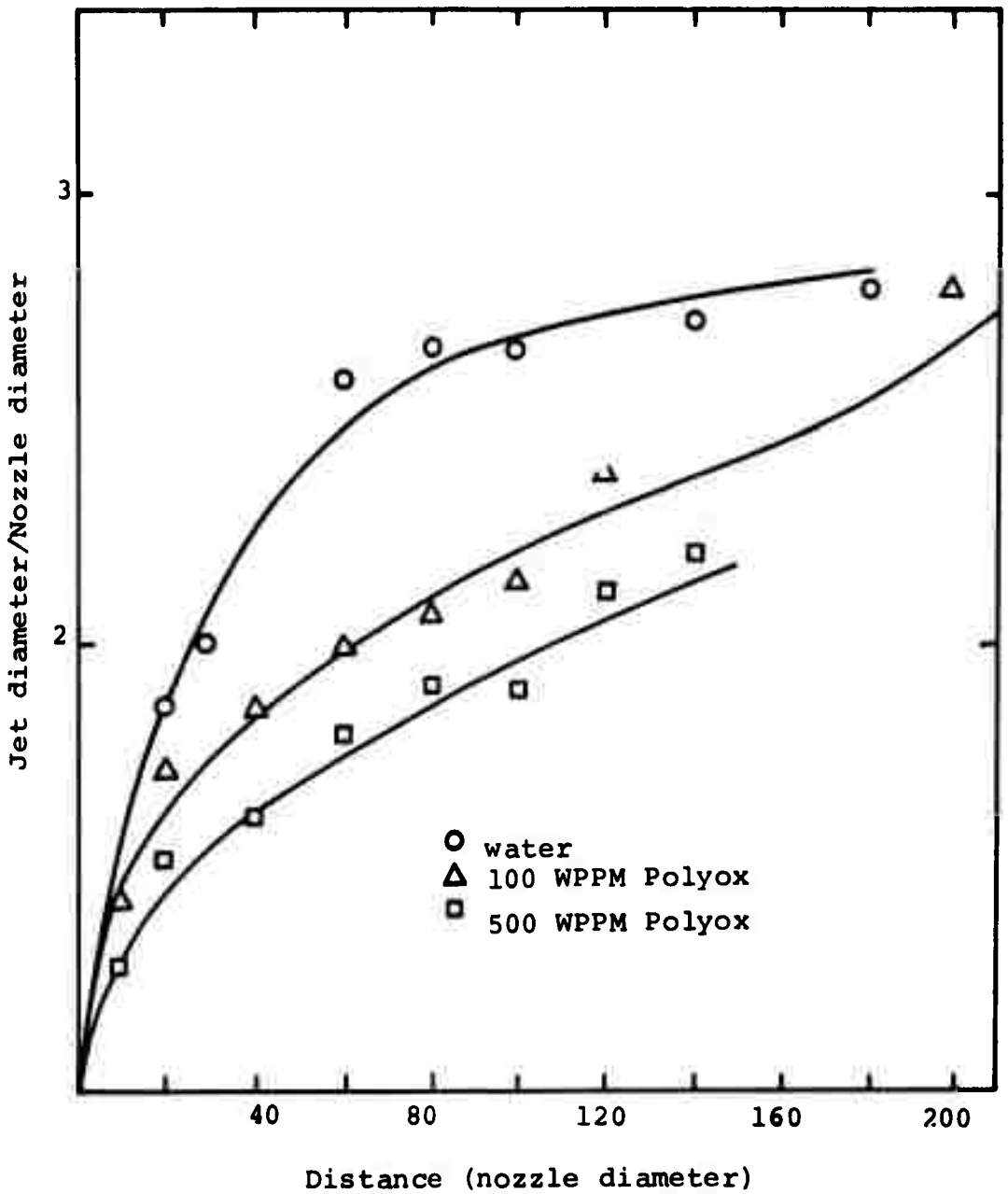

Figure 103. Variation in jet diameter with distance downstream (after Ref. 63).

Studies by Hoyt and Fabula (Ref. 65) have indicated that the long chain linear polymers of high molecular weight are better friction reducers than branched polymers. White (Ref. 66) measured the velocity profiles of jets issuing into ambient surroundings of the same fluid by means of a traversing Pitot tube. Relative comparisons of Polyox and water, Guar Gum, Hydroxyethyl Cellulose (HEC) and Polyox of three molecular weights showed that Guar Gum and HEC did not affect jet stability (Figure 104). The addition of Polyox did decrease jet velocity at greater standoff distances (Figure 105) (note that U_m is the maximum jet velocity at a distance x from the nozzle where U_o is the mean emerging velocity), although the pressure profile apparently remains similar at all standoff distances and for all fluids (Figure 106). White postulates that the elasticity of vortices in the flow is a potential cause. He also emphasized that while 150 p.p.m. solution of Guar Gum and a 50 p.p.m. solution of Polyox had similar effects in pipeline flows, their effects in free turbulent flows are different. It should be noted, however, that turbulent velocity profiles of viscoelastic fluids measured with Pitot tubes have inherent errors so that detail of the profiles may be unreliable. Thus, White's conclusions are open to question.

Gadd (Ref. 67) has proposed that the change in fluid properties is due to an increase in the viscoelasticity of the flow and consequent reduction in the number of eddies generated on the surface of the jet. The increased stability of the jet is thus explained as being due to a reduction in jet turbulence, a necessary condition for aerodynamic breakup as stated earlier.

In the analysis of the behavior of fluids such as those containing Polyox, the viscoelastic and viscoinelastic behavior of the flow must be considered. In such an analysis Goldin et al (Ref. 17) draw attention the the fact that while most analyses assume instantaneous stress release as the jet issues from the nozzle, in reality this relaxation may be displaced downstream, thus strongly affecting subsequent jet stability. Golden thus questions his own analysis and any use of viscoelastic theory since there is a two component constituency in the disturbances of the jet. Additional normal stresses imposed on viscoelastic fluids during pipeline flow must also be released upon the exhausting of the jet, a phenomenon that can be neglected for Newtonian fluids, and which also count a against use of linear viscoelastic theory. In the experimental study described in the paper, fluids of various viscosities were considered, with relationships between viscosity and shear rate established (Figure 107).

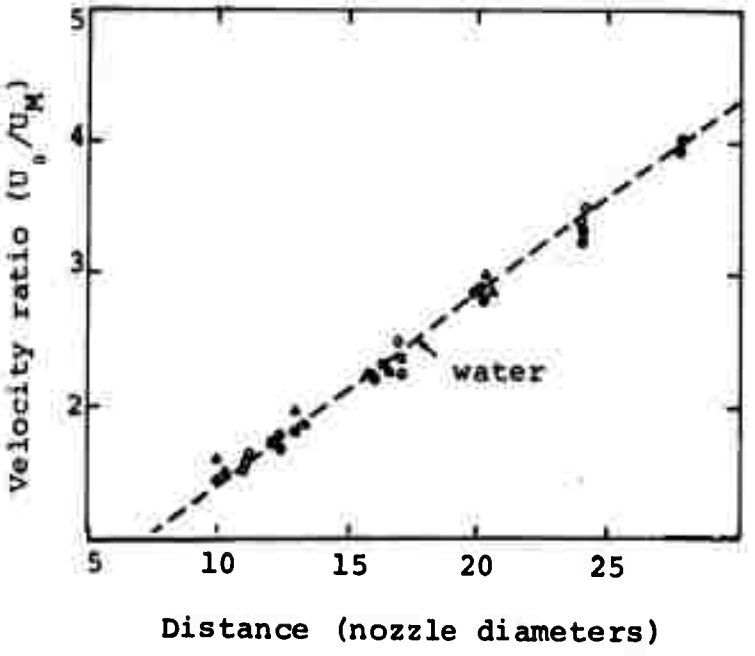

Figure 104. Centerline velocities for 75 p.p.m. Guar Gum, ● ; 150 p.p.m. Guar Gum, O ; and 200 p.p.m. HEC, ▲ with distance (after Ref. 66).

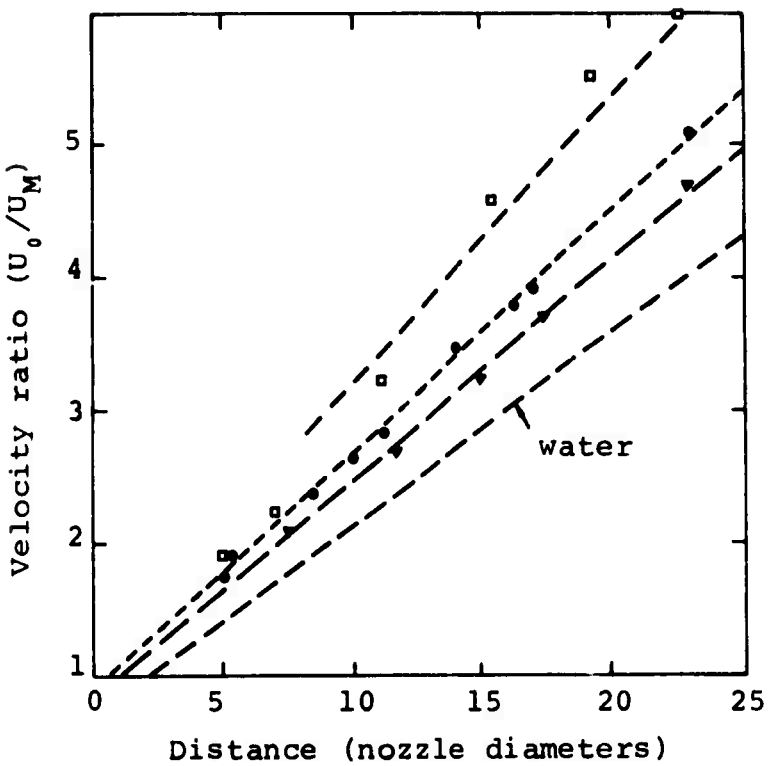

Figure 105. Centerline velocities for 50 p.p.m. of Polyox solutions, □ , 1.9×10^6 M.W., ● , 1.2×10^6 M.W. and ▲, 1.1×10^6 M.W. with distance (after Ref. 66).

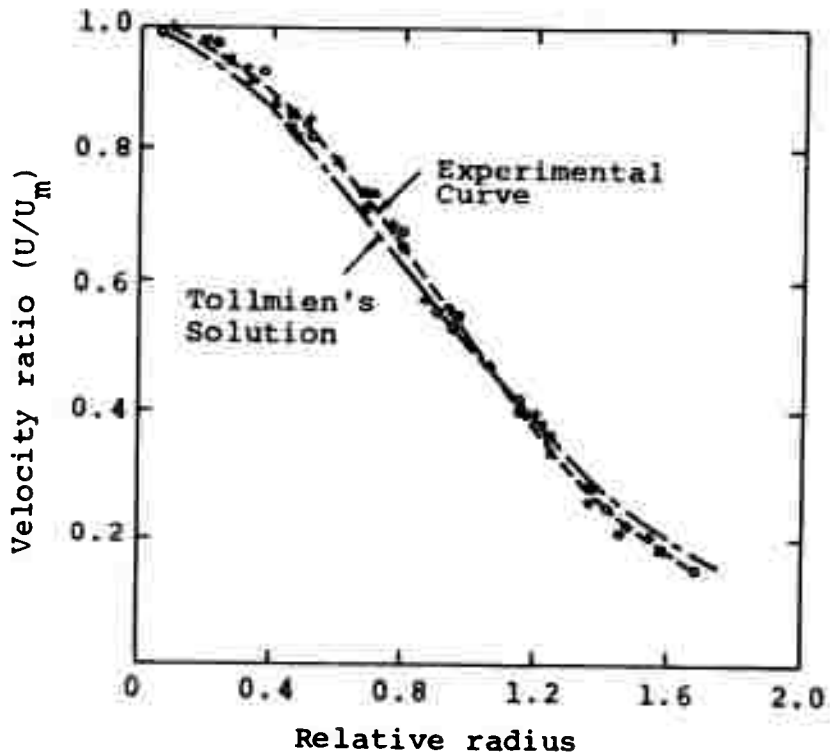

Figure 106. Variation in velocity profile for 50 p.p.m. Polyox solution at standoff distances from 10 (▲) to 30 (●) nozzle diameters (after Ref. 66).

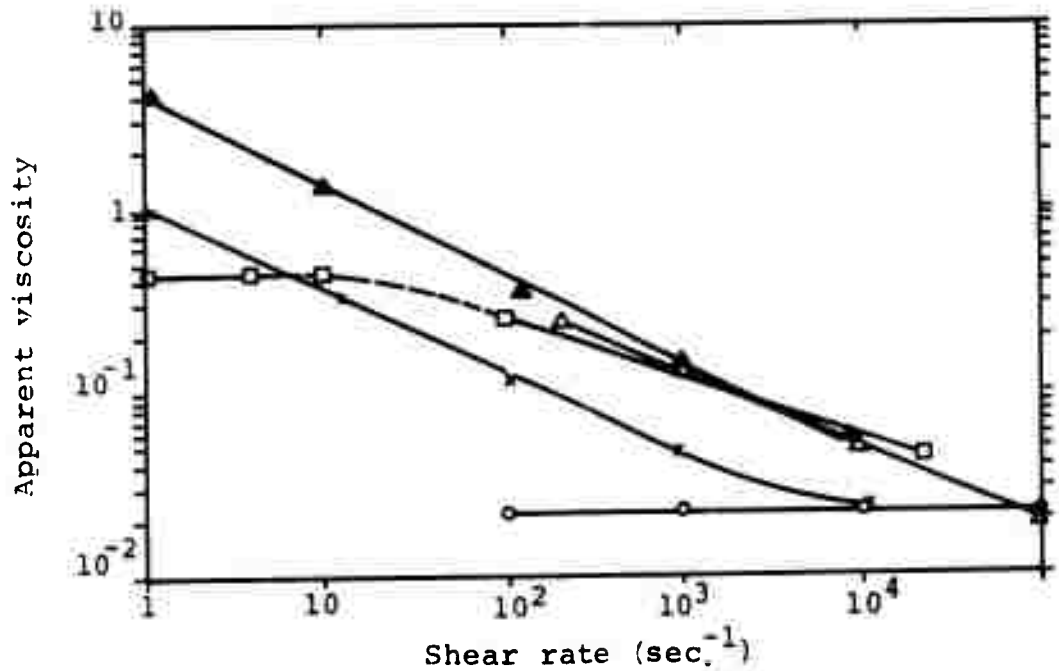

Figure 107. Published data of apparent viscosity vs. shear rate for various fluids. O, 0-5% Guar Gum; X, 0-05% Separan AP 30; ▲, 0.25% Separan AP-30, Δ, 0.25% Separan; □, 0.25% sodium carboxymethyl cellulose (after Ref. 17).

From photographs Goldin observed that Carbopol, a viscoinelastic fluid which does not give drag reduction, gave a lower jet cohesive length in comparison with water (Figure 108) down to only 40 percent at the maximum differential, in capillary and oscillatory disruption. But the Carbopol was able to withstand aerodynamic forces and produced a more coherent jet at higher jet velocities.

Goldin's results confirmed that, in the velocity range where capillary forces act, jet behavior was accurately predicted by Weber's analysis of Newtonian fluids which predicts that the length:diameter ratio is proportional to $(\text{diameter})^{1/2}$ at low viscosities and independent of diameter at high viscosity. The Carbopol behaved like an inviscid fluid, since coherent length increased both with velocity and diameter (Figure 109).

For Separan a similar result was obtained at low diameter (Figure 110) but as diameter increased the ratio became independent of diameter (Figure 111). It was concluded that this was because as diameter increased, shear force within the jet was reduced.

Goldin found no wave formation (the intermediate disruption phenomenon) for highly elastic fluids, but rather found that, even where the jet was sensibly disrupted the particles remained attached to each other by thin threads. In discussion of this, Goldin quotes the work of White (Ref. 66) who showed that viscoelastic materials can undergo a sharp increase in elongational viscosity when subjected to stretching flows.

More recently, Hoyt, Taylor and Runge (Ref. 68) have used a novel photographic technique to observe large diameter (1/8 in.-1/2 in.) jets moving at 50 p.s.i. containing measured concentrations of Polyox. Estimates of the Reynolds Number of the flow, and the equivalent surface tnesion of the solutions are also given (Figure 112). It is shown, by contrasting the behavior of Polymer solutions with that of detergent solutions of equal surface tension, that surface tension is not the cause of the change in behavior.

Photographs taken of the jet show a change in the solid section of the jet, as found by earlier investigators and this could be a viscoelastic effect.

Hoyt and Taylor have updated this research (Ref. 14) and increased the range of fluid studied to include jets containing asbestos fibers and heated jets. Concentra-

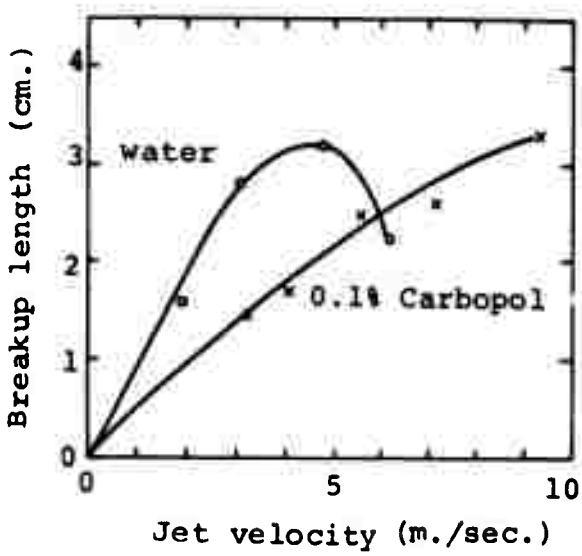

Figure 108. Variation in breakup length of two fluids with jet velocity (after Ref. 17).

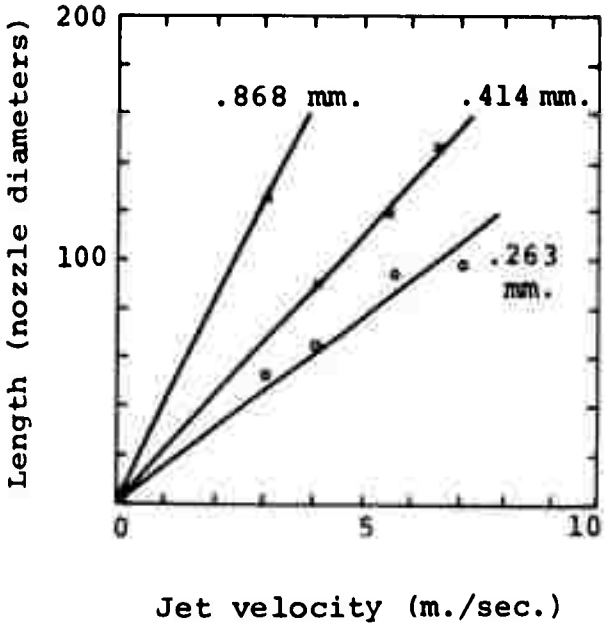

Figure 109. Variation in breakup length of 0.1 percent Carbopol with velocity for three nozzle diameters (after Ref. 17).

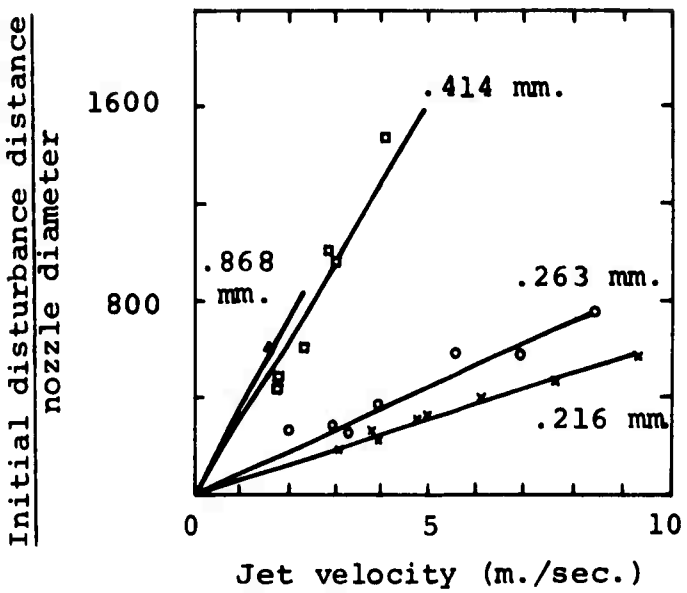

Figure 110. Variation in disturbance distance with velocity at four nozzle diameters (after Ref. 17).

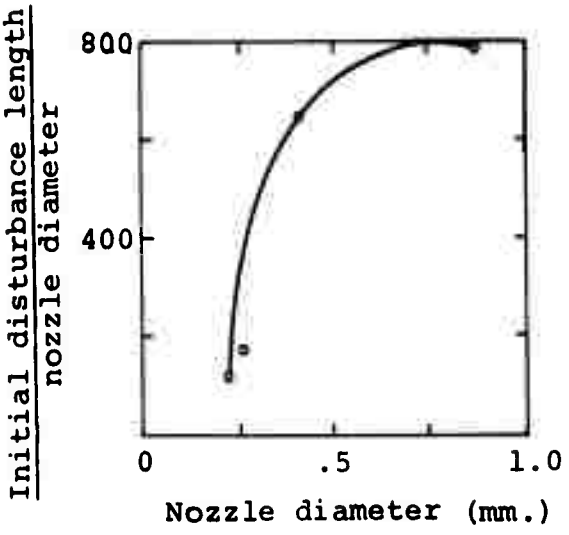

Figure 111. Variation in length with nozzle diameter for 0.25 percent Separan at 4 m./sec. (after Ref. 17).

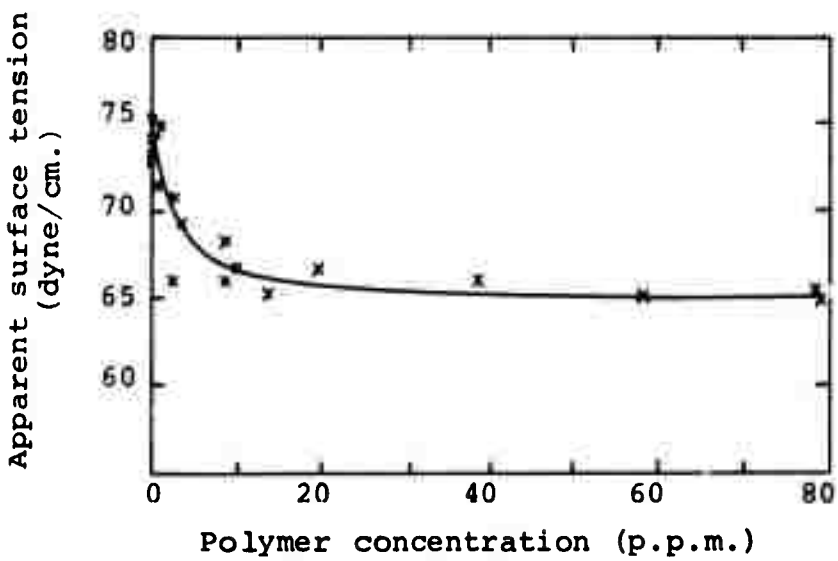

Figure 112. Measured air-liquid surface tension of polyethylene oxide solutions (after Ref. 68).

tions of 50 and 100 p.p.m. of Polyacrylamide, 100 and 500 p.p.m. Guar Gum, 100, 500 and 2,000 p.p.m. Carbopol and 5 p.p.m. concentration of asbestos were photographed as they issued from nozzles of diameters 1/8, 1/4, and 1/2 in. In all cases an increased polymer concentration produced a smoother jet as it issued from the nozzle. Hoyt and Taylor associate this result with an earlier transition to turbulence for the fluid in the presence of polymers. A similar result was obtained by heating the nozzle and thus locally raising the Reynolds Number. It was found that jets could be made coherent at a standoff distance of 2 meters where 100 p.p.m. Carbopol for the 1/8-in. diameter nozzles were used. However, in all cases the jets were disrupted within 3 meters of the nozzle. Hoyt and Taylor surmise that filament formation and viscoelasticity of the polymer are the causes of increased jet stability.

Davis and Young-Hoon (Ref. 69) examined the structure of jets at Reynolds Numbers over 7000. Garner, Nissan, and Wood (Ref. 70) had shown that the addition of polymers increased the lower velocity of atomization from 20 m./sec. to up to 60 m./sec. Davis and Young-Hoon used flash photography to examine jets issuing at velocities below this limit, but at Reynolds Number up to 25,000. An elongational viscosity was introduced into a theoretical analysis of the stability of eddies on the jet surface. The authors conclude from the study that initial disturbances in the jet are caused by nozzle and fluid properties before the orifice is reached and the disruption of the disturbances is controlled by the ambient conditions beyond the nozzle. The addition of the polymer therefore causes a viscoelastic restraint to the growth of the disturbance thus smoothing and cohering the jet.

It should perhaps be noted that the theoretical and experimental analysis only affects jet breakup at velocities below aerodynamic disruption. Once this occurs, the surface tension effects which are considered in this analysis, no longer appear to play as important a role in cohesion.

Material Cutting

The review of previous investigations has to date covered mainly the theories which relate to jet structure and stability. The primary objectives of most investigations are, however, to improve the ability of a water jet to excavate some target material, or to cut a required

Table XIII. Volume Flow and Pressure Required to Mine Soil Materials (after Ref. 33).

Soil Type	Subclassification	Height of Bench (ft.) 10-15		15-45		above 45	
		q	p	q	p	q	p
1	Preloosened and not bedded	5	43	4.5	57	3.5	71
	Fine grained sand	5	43	4.5	57	3.5	71
	Powdered sand		43		57		71
2	Light sandy loam	6	43	5.4	57	4	71
	Friable loess		57		71		85
	Peat		57		71		85
	Medium Grained Sand		43		57		71
	Various-size grained sand		43		57		71
3	Medium sandy loam	7	57	6.3	71	5	85
	Light loam		71		85		100
	Compact loess		85		100		114
	Coarse grained sand		43		57		71
	Heavy sand loam		71		85		100
4	Medium and heavy loam	9	100	8.1	114	7	128
	Lean flowing clay		100		114		128
5	Sandy gravel	12	57	10.8	71	9	85
	Semi fat clay		114		142		170
6	Sandy gravel	14	71	12.6	85	10	100
	Heavy clay		145		170		200

q is the flow rate in ℓ/min.
p is pressure in p.s.i.

path in that material. The vast amount of literature which has been published on jet cutting has been compiled into several reviews (Refs. 71, 72, 73) and its volume precludes detailed review in this report. The material cutting portion of this investigation centered on the investigation of the ability of the water jets to cut several soil types and an evaluation of the ability of a jet to cut wood and Plexiglas.

Soil Excavation

The use of water jets for soil excavation is perhaps the oldest use of jets, and some of the historical detail has been covered in the opening remarks of the Introduction. Russian engineers have provided most of the information and the practical applications of the hydraulicking method, which is used for overburden removal in strip mining of coal and the removal of the coal itself. Further, hydraulicking provides a ready method of removing overburden without the extensive use of expensive equipment. The productivity figures quoted in Table XIII indicate the usefulness of the method in operations involving large volume material removal rate. In the book Hydromechanization by Yufin (Ref. 35), the development of hydromechanization in Russia is described, tracing its usage from 5 percent of the excavation work for the Moscow canal in 1934, to date. From 60-70 percent of the earthmoving in the Don, Volga, and Dnieper Rivers hydraulic engineering projects was affected by hydromechanization with the moving of around 100 million cubic meters of earth.

The jets used for the removal of soil and soil-like overburden require relatively low specific pressures (Table XIV).

Table XIV. Required Pressure to Remove Overburden Material (after Ref. 35).

Classification	Material	Pressure (p.s.i.)
1	Sandy Loam	9
2	Medium Loam	32
3	Heavy Loam	56
4	Sandy Clay	82
5	Clay	114
6	Argeillaceous and Arenaceous Shales	142

In mining these materials from the solid, production standards have been achieved (Table XV) from which outputs, or volume produced, can be calculated.

Such jets, however, are extremely bulky and are only suited to operation in a permanent site with an adequate supply of water. In a more mobile operation, it is necessary to use a higher pressure and lower flow rate to achieve the same effect.

The quantities of earth removed by the hydraulic excavation equipment is large, and the equipment is accordingly massive and unsuitable for rapid movement. Nevertheless, the results obtained illustrate the potential application of the system. The results given show that there is little need to go to the higher cutting pressures which have proved necessary in the excavation of harder materials. Further experience which has been gained in coal excavation is relevant to the removal of soils also.

In an experiment carried out to determine optimum jet parameters for cutting coal, Summers and Peters (Ref. 74) investigated the range of pressure from 5,000 to 25,000 p.s.i. and the variation in nozzle size from 0.02 to 0.04 inches. The results of their research showed (Figures 113, 114) that there was no advantage to be gained by increasing nozzle pressure but rather that for a given horsepower it was better to increase the diameter of the nozzle of the jet. Similar conclusions were also obtained in cutting granite both by the authors cited (Ref. 75) and by Chadwick and Kurko (Ref. 76).

The Cutting of Wood

The potential of water jets as a means of cutting wood has been the subject of investigation in this country (Ref. 77), in Canada (Ref. 78), and in the Soviet Union (Ref. 79). The most comprehensive studies have, however, been carried out by Bryan (Ref. 19) at the University of Michigan. The advantage of using high pressure jets small cross section, lies in the very thin slice of material which is removed by the jet in cutting, much less than is used by conventional cutting methods such as revolving saw blades and the like. Bryan used simple factorial experiments to study the effects of nine variables. Considered were fluid pressure, standoff distance, wood grain direction, moisture content, jet diameter, wood species, angle of incidence, feed rate, and the number of passes of the jet over the sample. Bryan initially

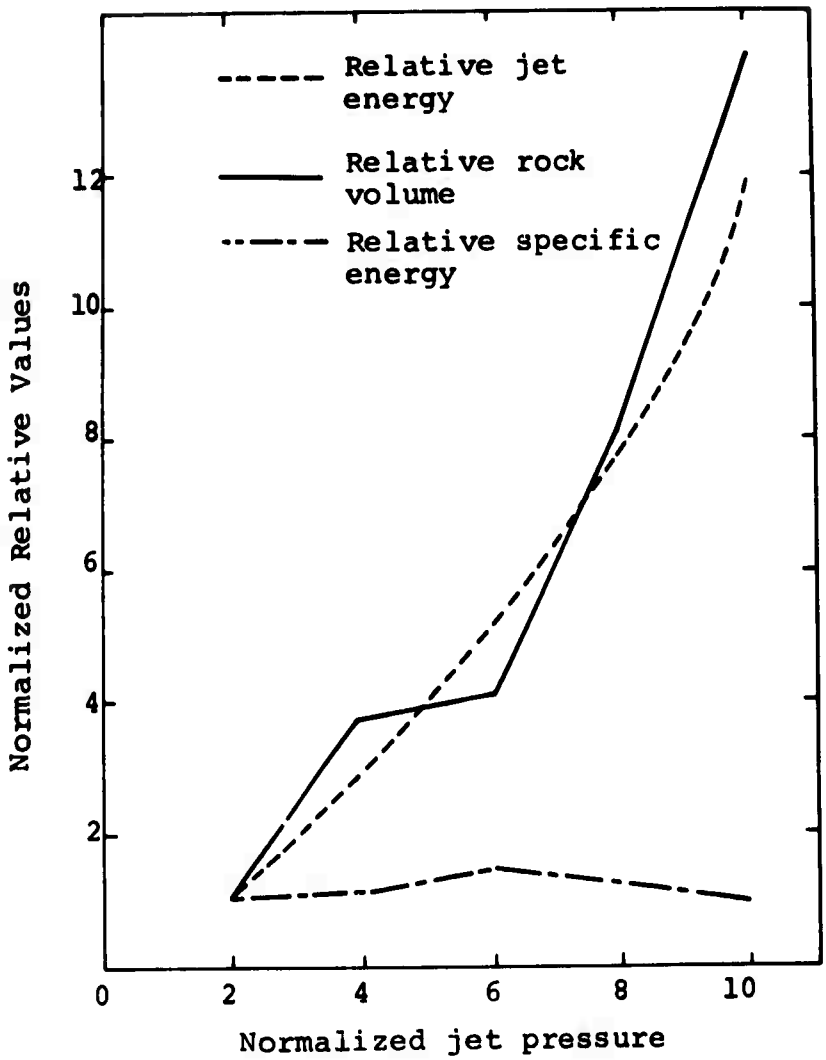

Figure 113. Variation in jet energy, rock removal, and specific energy with jet pressure (after Ref. 74).

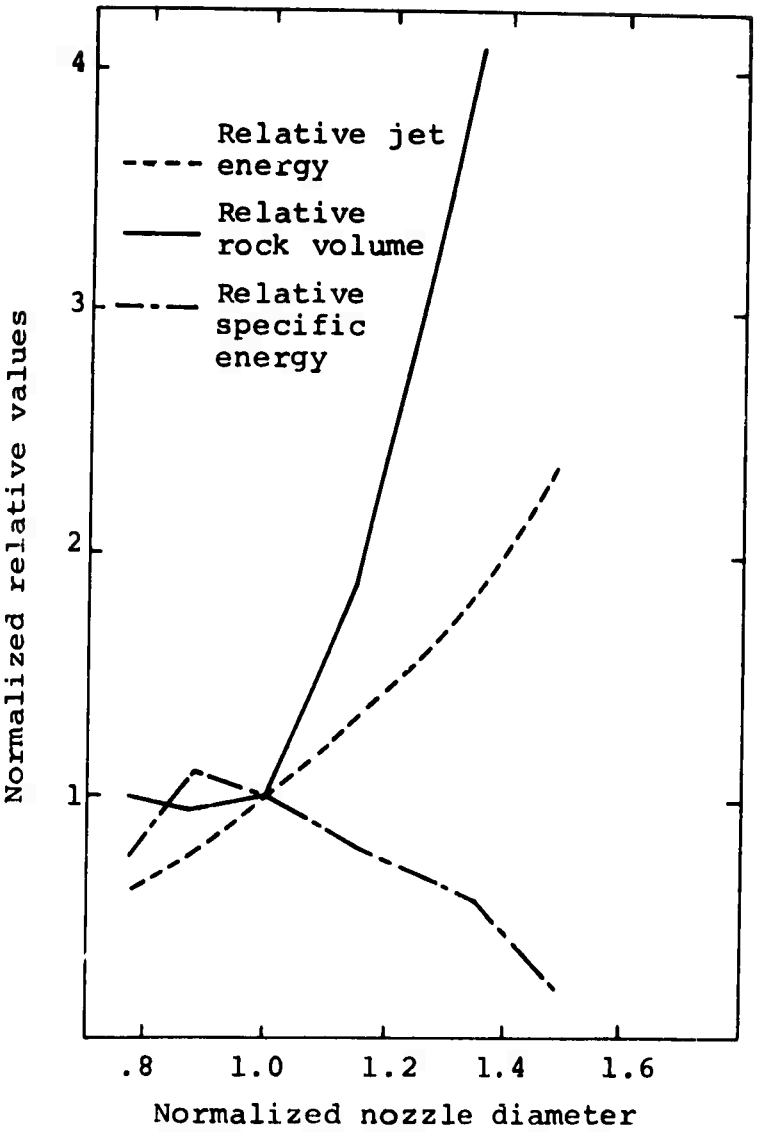

Figure 114. Variation in jet energy, rock removal and specific energy with nozzle diameter (after Ref. 74).

Table XV. Output per hour for a Single Hydraulic Excavator (cu. yd.*).

Soil Type	Water Volume** (gal./min.)	Bench Height (ft.) up to 15	15-30	30-45	over 45
Fine grained sand, light sandy loess, medium loess	1600	73	80	87	110
	2400	110	123	132	166
	3200	146	159	176	220
	4000	183	201	220	274
	4800	219	240	265	331
Medium grained sand, light loam, medium loess	1600	50	68	73	87
	2400	96	101	110	132
	3200	124	134	147	176
	4000	157	169	183	221
	4800	188	202	220	263
Coarse grained sand, heavy sandy laom, arenaceous clay compact loam	1600	49	52	56	62
	2400	73	78	84	96
	3200	98	105	110	123
	4000	122	129	138	157
	4800	146	155	166	188
Sands with up to 40% gravel, clay with up to 15% gravel, semifat clay	1000	37	38	40	44
	2400	54	58	59	66
	3200	73	79	80	87
	4000	92	95	99	110
	4800	109	115	120	132
Sand with over 40% gravel, fat clay, siltstones and argillites	1600	21	23	30	27
	2400	33	34	37	41
	3200	44	47	49	54
	4000	54	58	61	68
	6800	61	70	73	81

*Note--this table is computed assuming a Russian effective working shift of 6 hrs.
**to nearest 100 gal.

measured the relative pressure drop within the first inch of standoff from the nozzle for four nozzle diameters (Figure 115) and over a range of jet pressures (Figure 115). A series of tests of static penetration, i.e., no relative movement between the nozzle and the sample, indicated the same form of the penetration time curve as has been found by others (Table XVI) (Figure 116).

Table XVI. Direct Penetration of Jets in Wood, Inches (after Ref. 19)

Wood Species	Nominal Duration of Jet Action, seconds 1/2	3	5
Sugar Maple	0.24	0.30	0.30
Douglas Fir	0.25	0.38	0.*
Red Oak	0.47	0.50	0.47
Yellow Poplar	0.51	0.54	--
Redwood	0.50	1.17	*

*Specimen ruptured as a result of internal pressure

The conclusions from the study are summarized in the attached figures (Figures 117 to 126) and can be detailed as follows.

Jet penetration is increased with jet pressure and nozzle diameter although there does appear to be a limiting pressure above which increase in pressure is less effective (Figure 120). This may be due to more rapid jet disintegration at the higher pressures. The jet effect was found to be more directly related to the total force of the jet.

Change in the type of wood tested appeared to have little effect on the ability to cut when the jet was traversed across the specimen (although this was not the case where the nozzle and specimen were held static). It was found that a change in the moisture level altered the

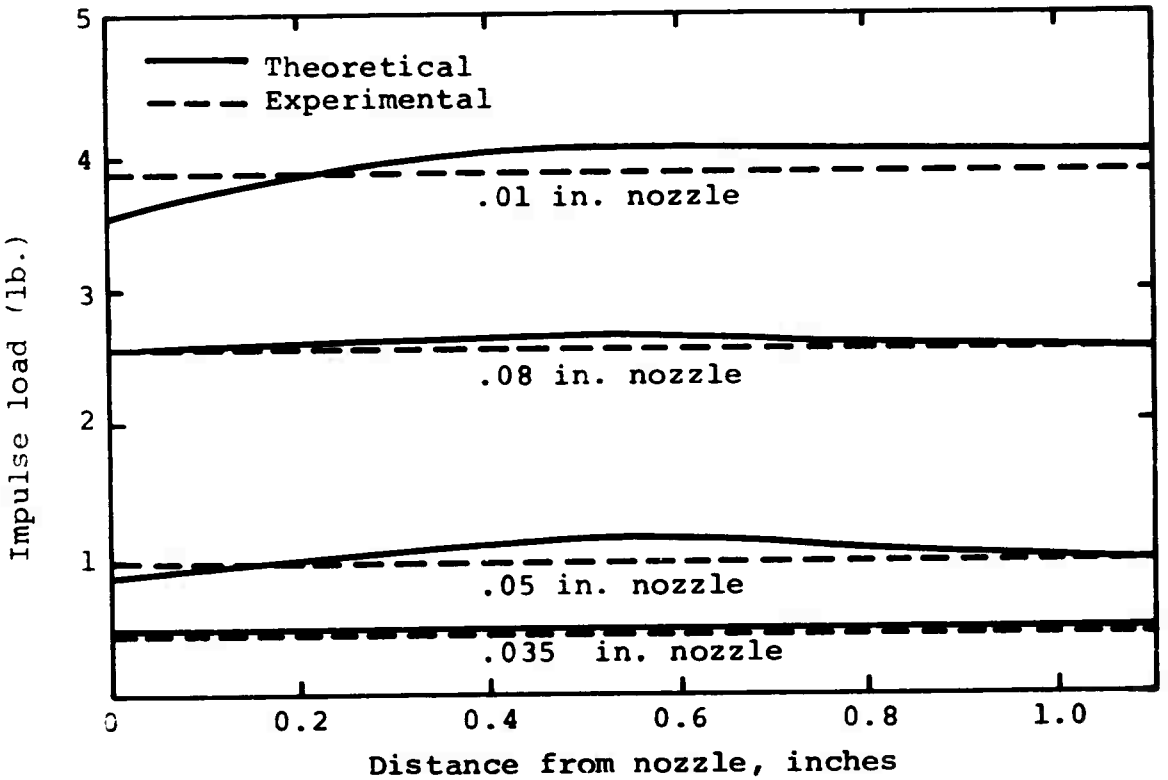

Figure 115(a). Jet force vs. distance from nozzle for four nozzle sizes.

(The solid lines connect experimental points and the broken lines are theoretical force levels based on empirically determined jet velocity, pressure level = 30,000 p.s.i.).

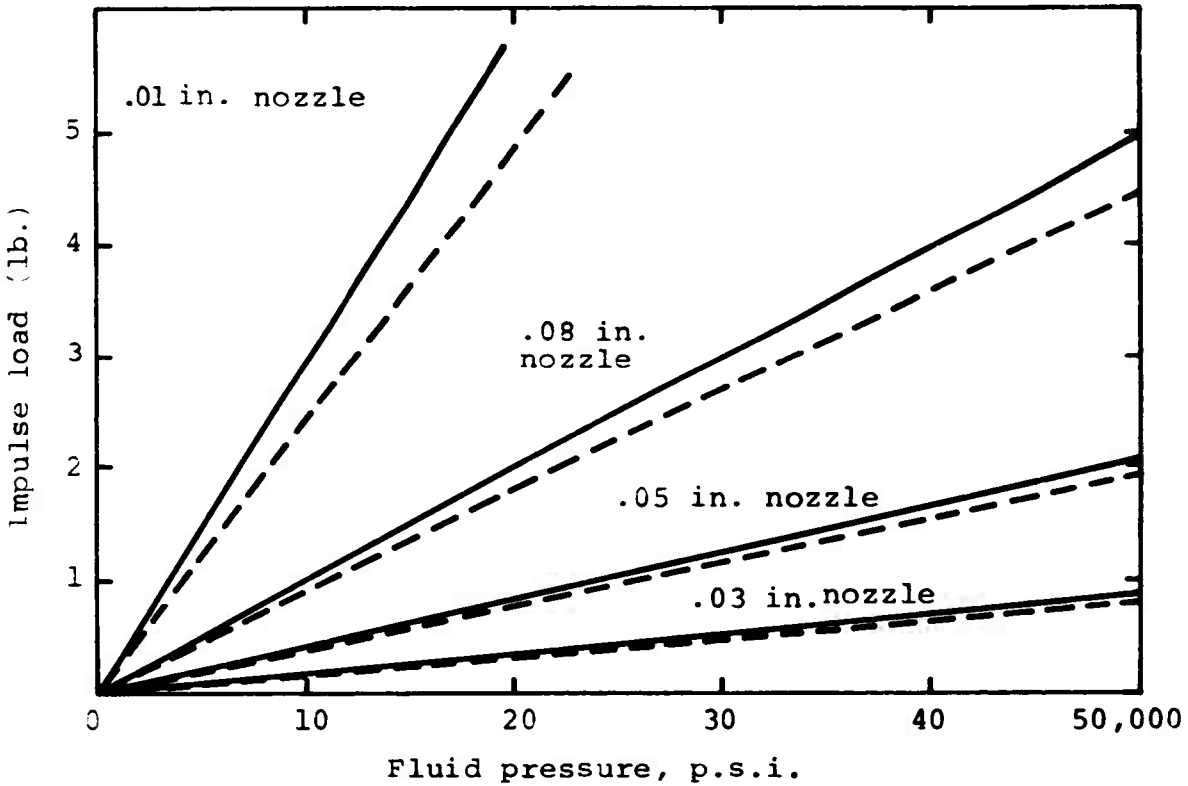

Figure 115(b). Relationship between fluid pressure and jet force for four nozzle sizes (after Ref. 19).

(The solid lines connect experimental points and the broken lines are theoretical force levels based on empirically determined jet velocity, pressure level = 30,000 p.s.i.).

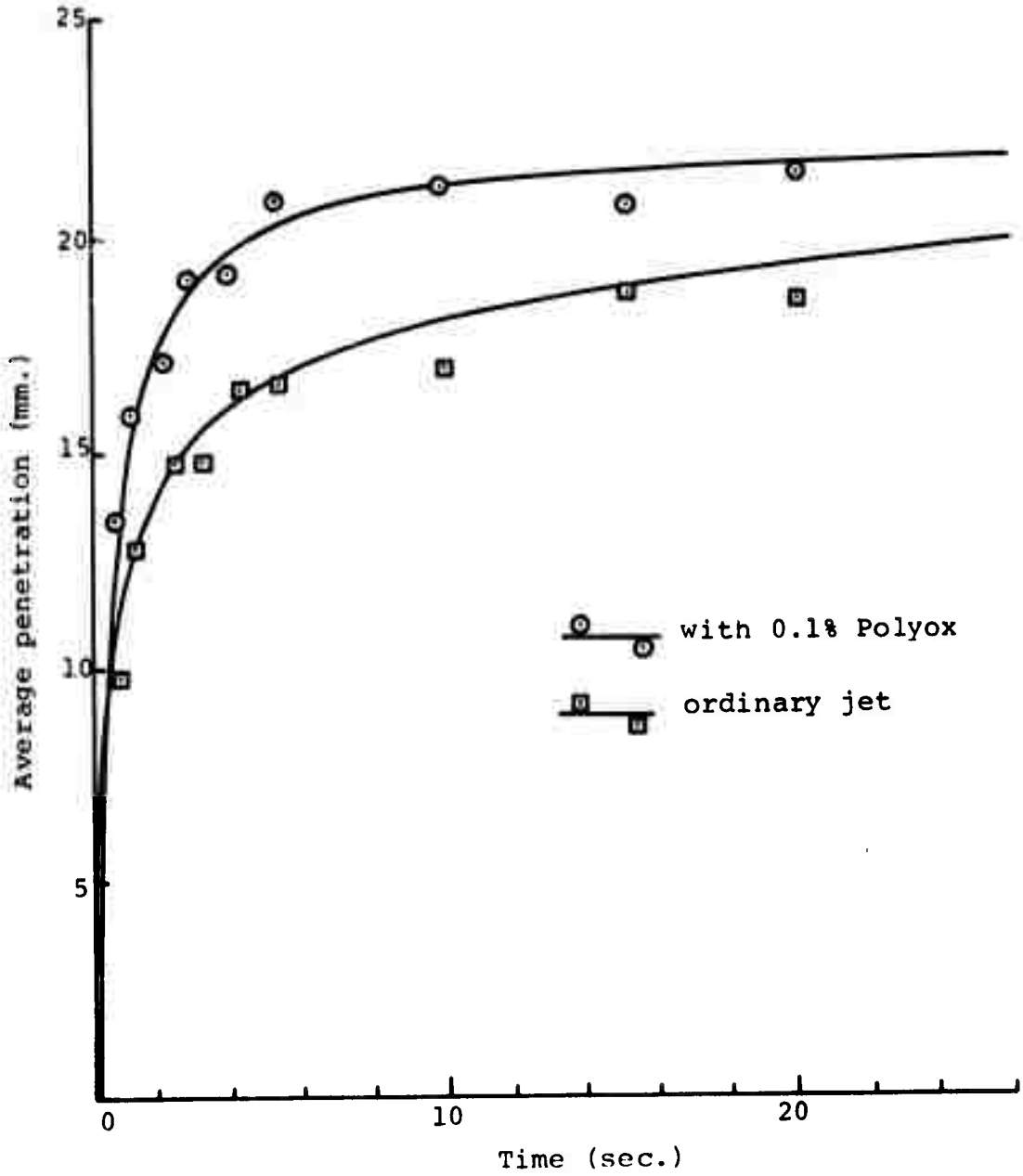

Figure 116. Variation in jet penetration into sandstone with time (after Ref. 18).

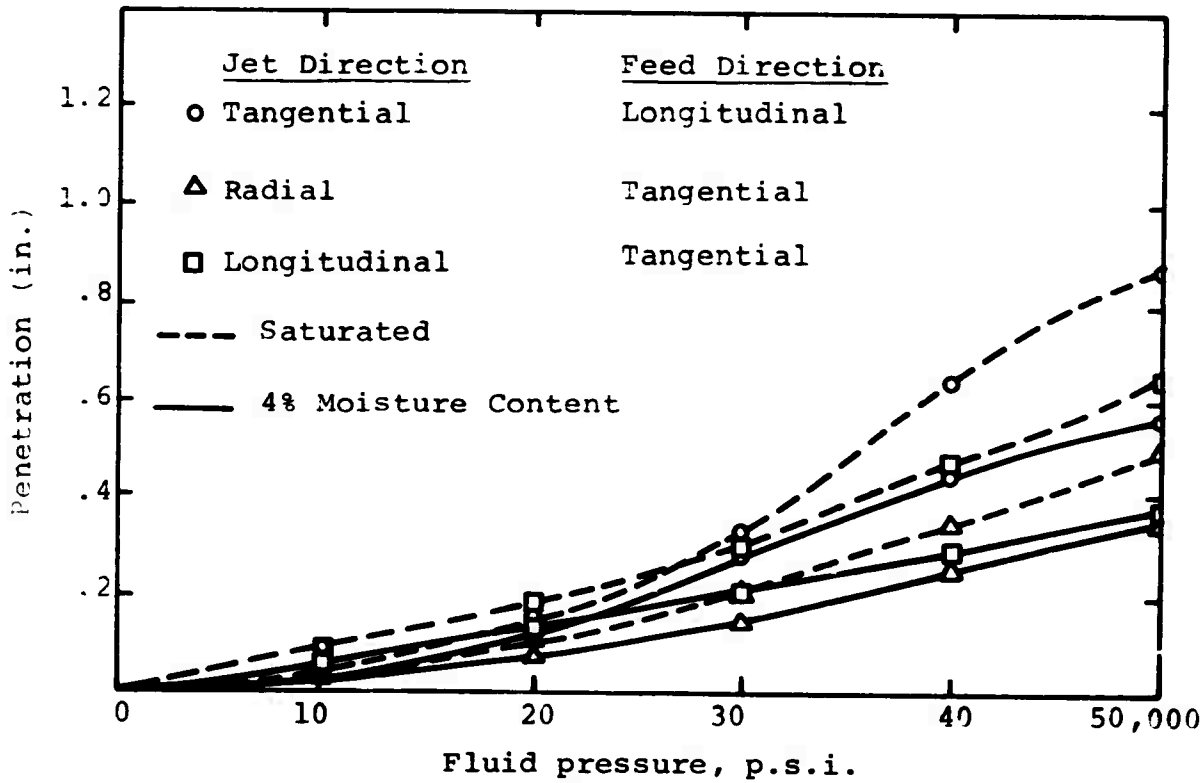

Figure 117. Variation in jet penetration in wood with fluid pressure for three grain orientations and two moisture conditions (after Ref. 19).

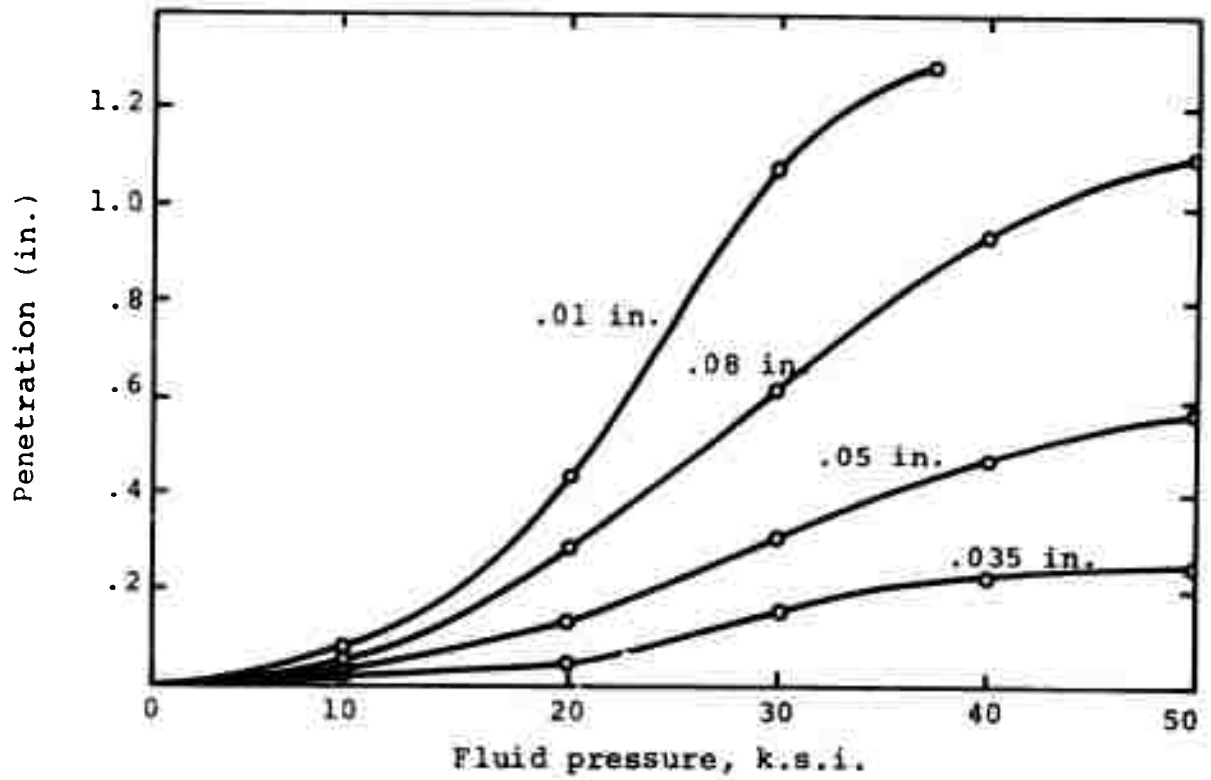

Figure 118. Variation in jet penetration with pressure for four nozzle sizes (after Ref. 19).

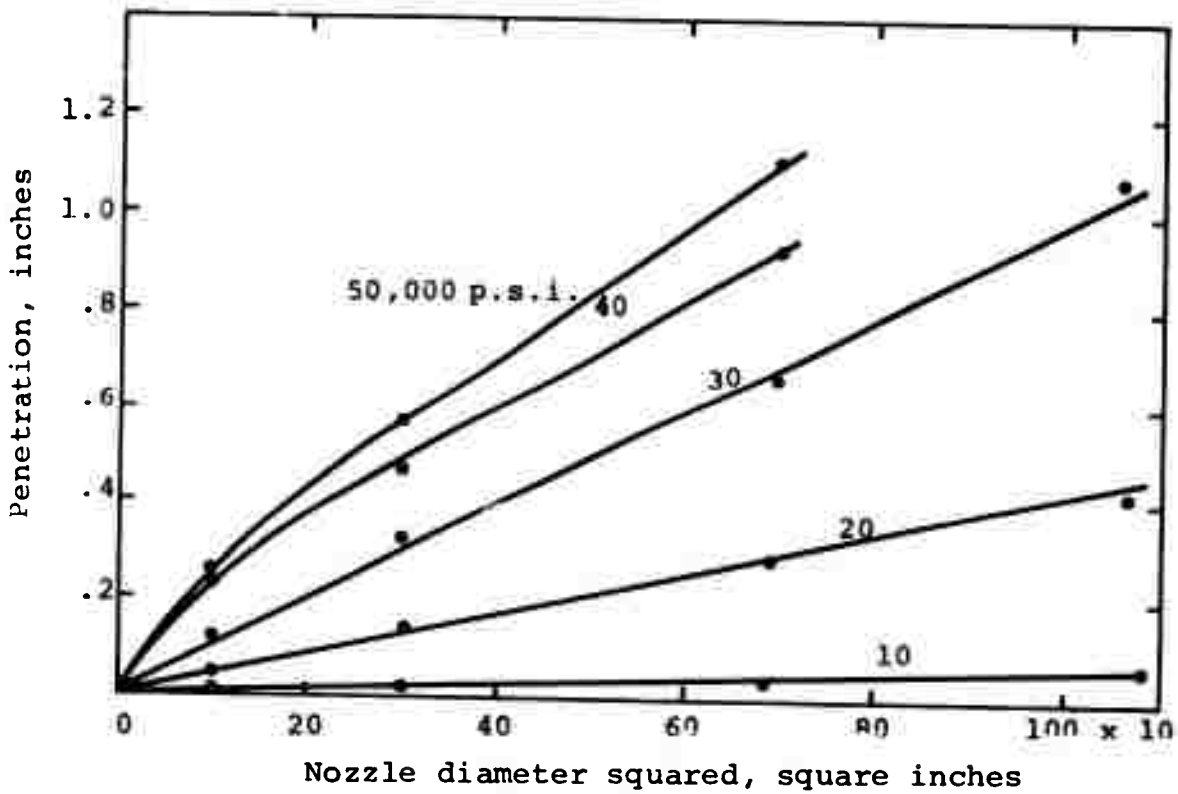

Figure 119. Variation in penetration with (nozzle diameter)^2 for five pressure levels (after Ref. 19).

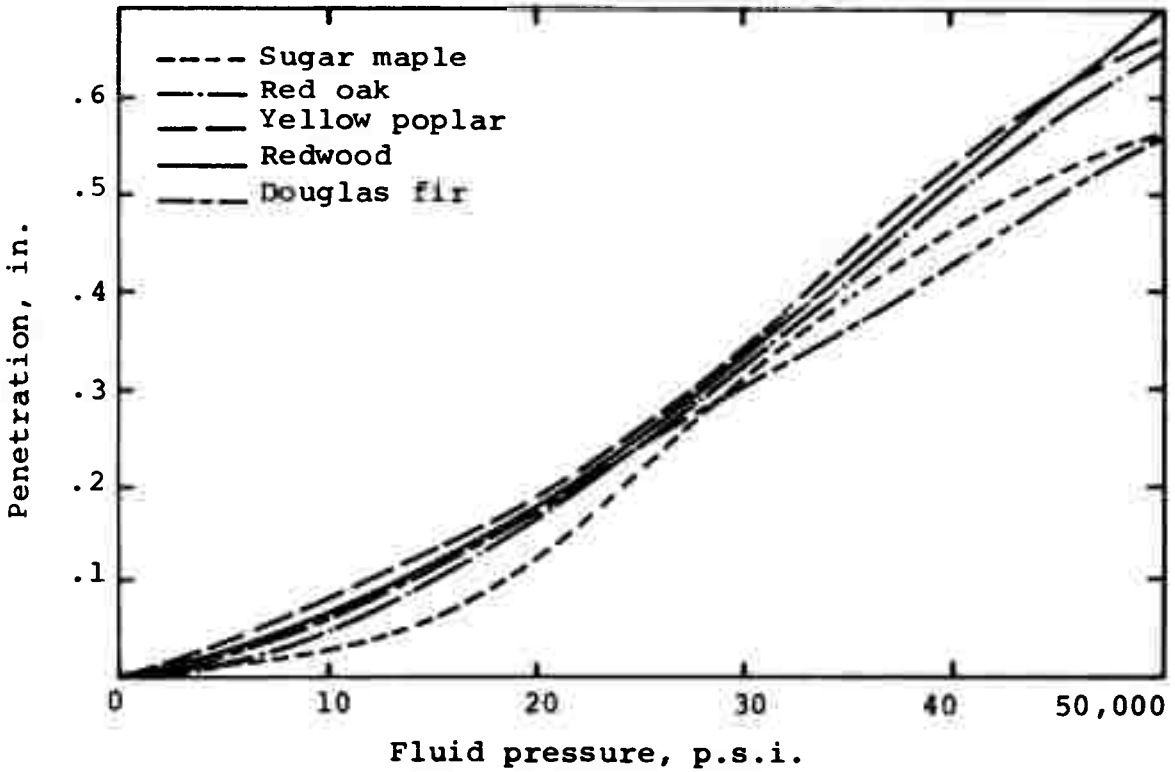

Figure 120. Variation in penetration with pressure for various woods (after Ref. 19).

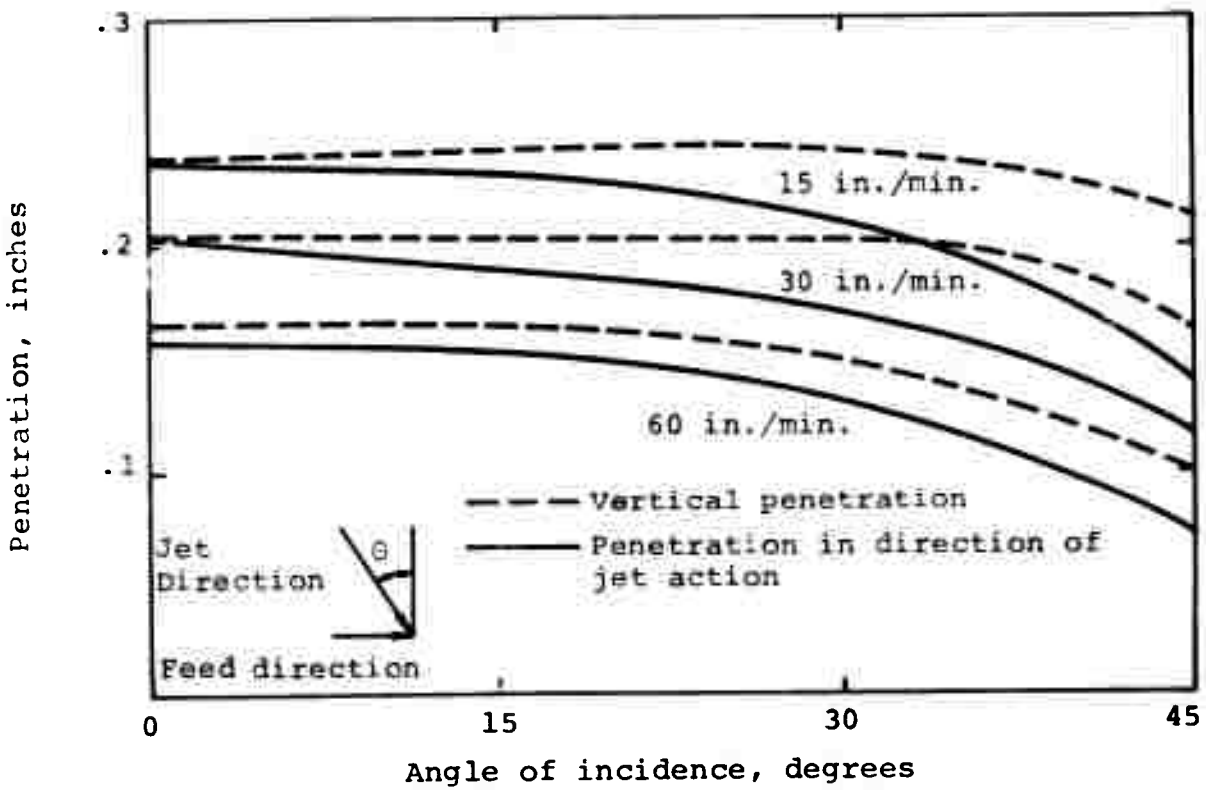

Figure 121. Variation in penetration with angle of impact for three feed rates (after Ref. 19).

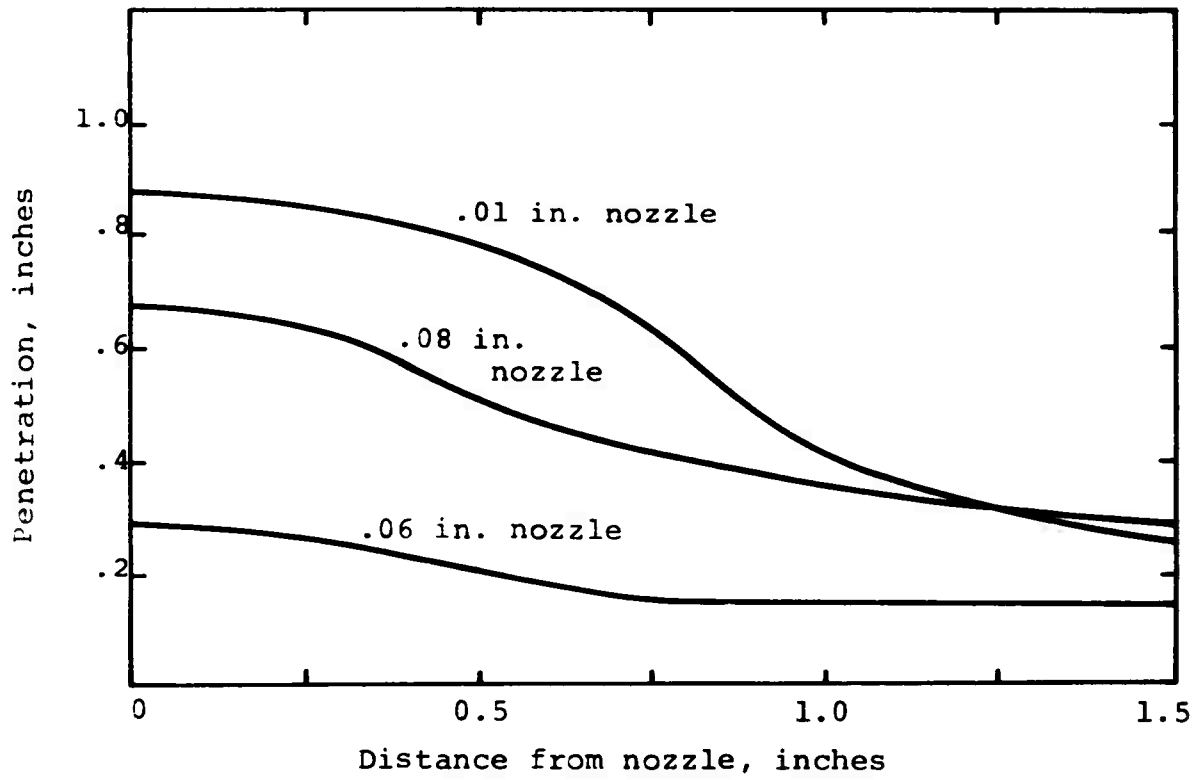

Figure 122. Variation in penetration with standoff distance for three nozzle sizes (after Ref. 19).

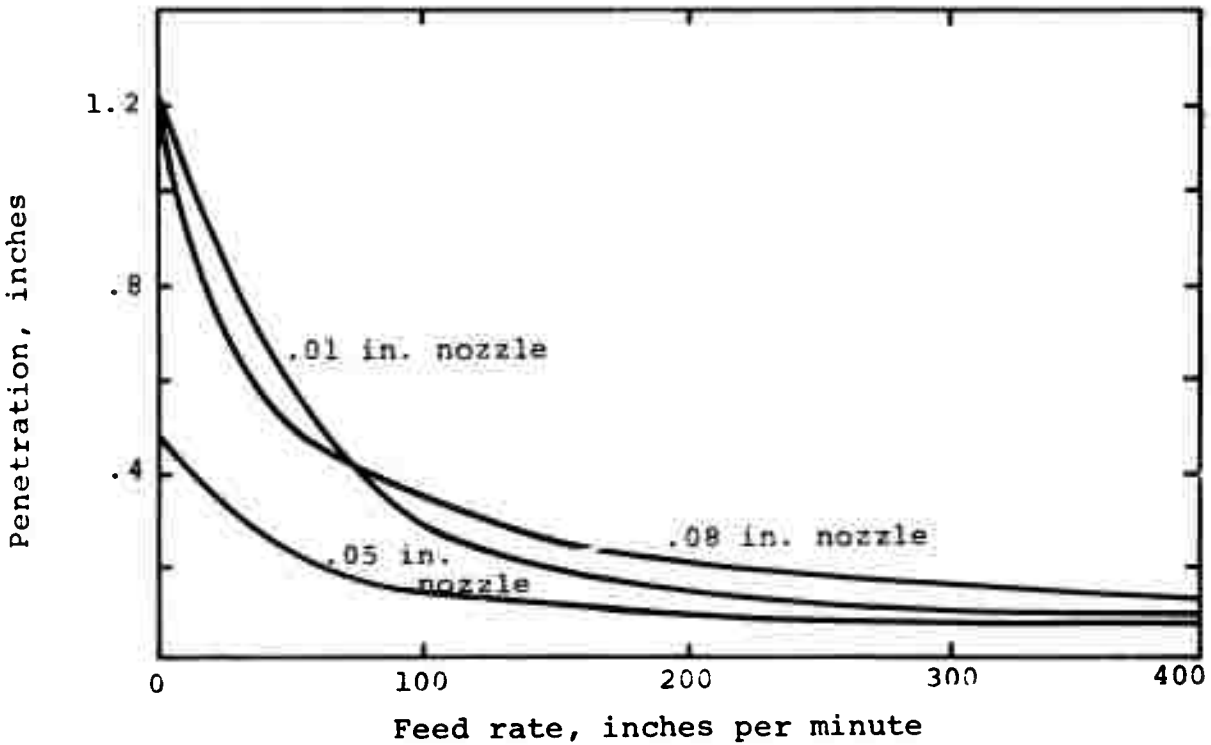

Figure 123. Variation in penetration with feed rate for three nozzle sizes (after Ref. 19).

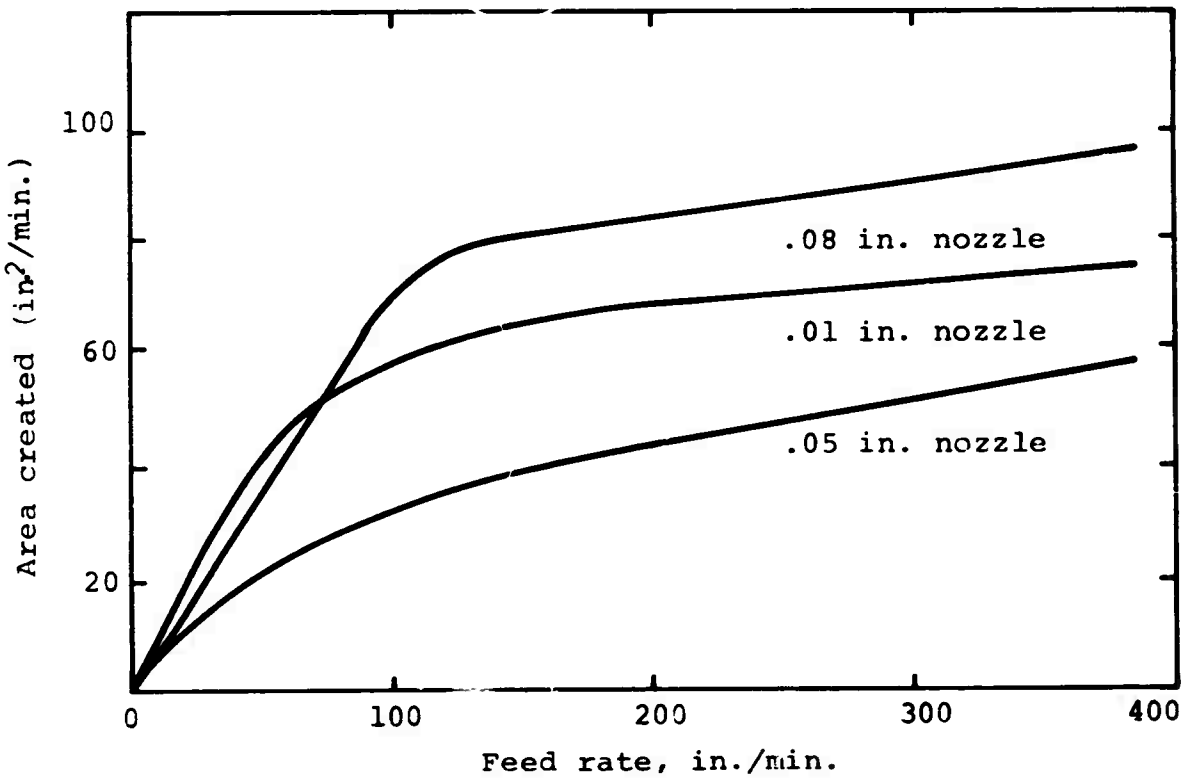

Figure 124. Variation between cut area and feed rate, for three nozzle sizes (after Ref. 19).

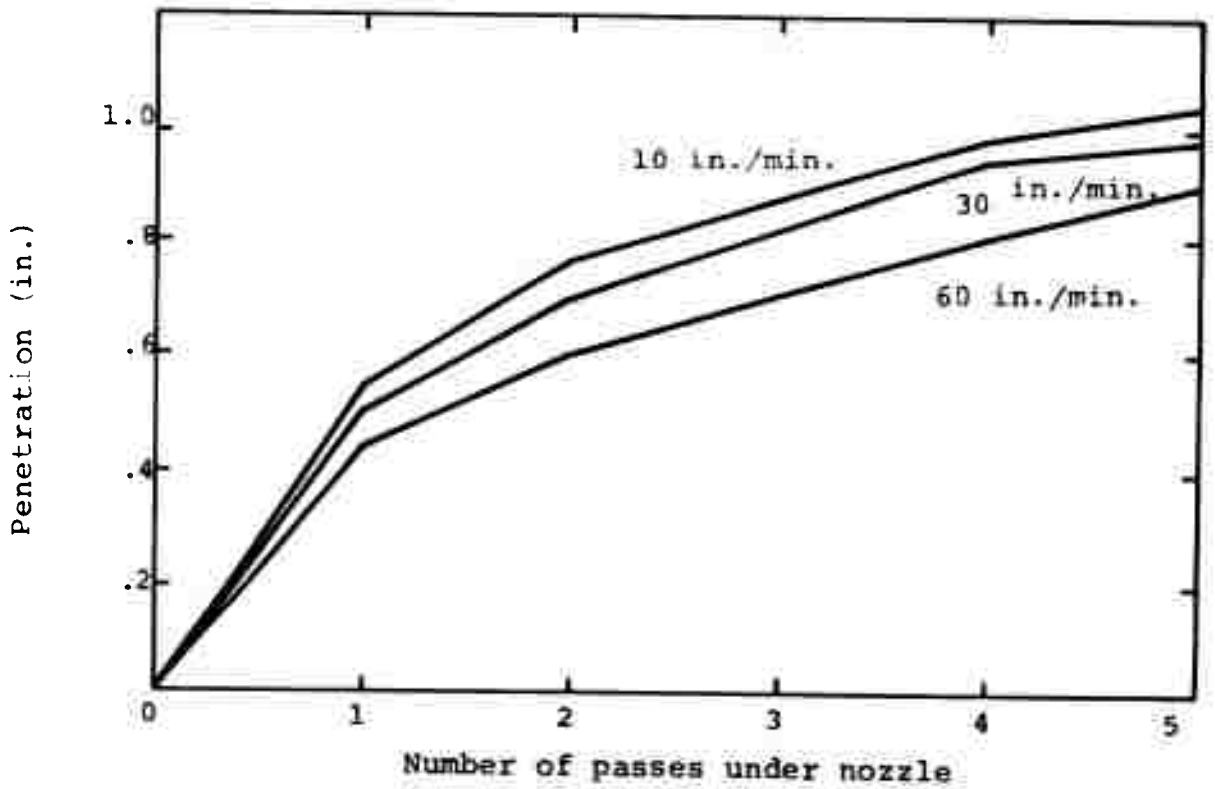

Figure 125. Variation in penetration with number of passes (after Ref. 19).

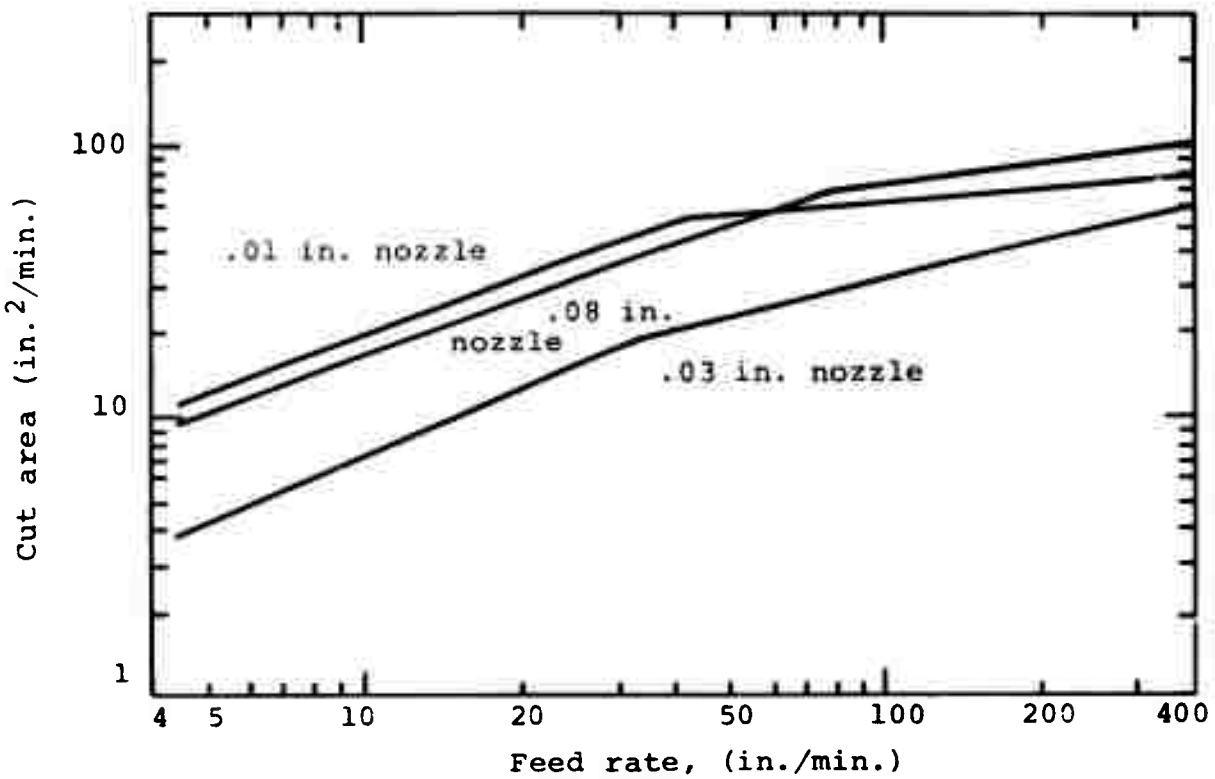

Figure 126. Variation between cut area and feed rate (after Ref. 19).

penetration characteristic. Bryan speculated that the wet wood being more dense, would be more difficult to cut, however in the event it proved easier to cut. He postulated that this is due to the tendency of the wood to swell when wet. Where the wood is intially dry this swelling inhibits penetration, whereas when wet the swelling has already occurred. Summers considers it also possible that the presence of the moisture in the wood acted, under impact, as a series of fluid wedges. The structure of the wood was found to affect impact and the jet cut most effectively when traversed along the wood, cutting the fibers apart in their weakest direction.

The change in penetration with angle of impact can be explained in terms of the relative change in wood grain orientation relative to the impacting jet axis.

There was a marked decrease in jet cutting effectiveness as the target was moved away from the nozzle (Figure 122), although the effect varied somewhat with nozzle diameter.

A similar effect was found between depth of cut and traverse velocity (Figure 123), where the shape of the graph is modified by nozzle diameter, depth reducing exponentially with velocity.

For the three nozzles considered, a computation of the form

$$Y = ae^{bx}$$

on the results yields values of 1.1, 3.09 and 4.66 for 'a' and -.44, -.51 and -.62 for 'b' with nozzle diameters 5, 8, and 10 mils respectively. (A regression correlation 0.97 was obtained for each line).

Since the time Bryan wrote his thesis there have been a number of studies carried out commercially, notably by Bendix (Ref. 80), Flow Research (Ref. 81), and McCartney Mfg. Co. (Ref. 82), on the feasibility of using high pressure jets to cut such material. McCartney is currently marketing a system which has been installed and is being used commercially by Alton Box Board.

The Cutting of Plexiglas

Plexiglas has been used as a target material for several jet impact studies, and because of its use in aircraft

has also been used in high speed rain erosion studies by Air Force investigators (Ref. 83). Daniel at IIT Research Institute (Ref. 46) has examined the growth of fractures under single pulsed jet impact at jet velocities up to 2800 m./sec. Mohaupt and Burns (Ref. 84) have used continuous jets at pressures of up to 60 k.s.i. to cut Plexiglas, polycarbonate, acetal (Delrin) and, in earlier work (Ref. 85), a phenolic sheet. The results of their experiment (Figures 127 to 130) were sufficient for development of a theory of cutting, which has recently been modified to include considerations of nozzle diameter not included in the original analysis. It is interesting to note that at low traverse speeds, below 0.1 in./sec., there was local melting of the polymer around the impact point. This melting was due to the inability of the heat to dissipate adequately.

Based on the results of the experiments, the following equation for cutting depth (h) has been proposed.

$$h = \frac{P_0 - P_1}{\frac{C_1}{(D)^{1.3}} + (C_2 D + C_3)\frac{u}{q}} \qquad 32$$

where the values of the constants are obtained from the tabe, D is nozzle diameter, q is jet flow rate, and u is traverse velocity. P_0 is jet pressure at the nozzle and P_1 is the pressure at which cutting is initiated. It should be noted that Mohaupt and Burns (Ref. 84) found this value of pressure was dependent on nozzle diameters.

Table XVII. Values of the Constants for Equation 32, Derived from Experimental Values (after Ref. 84).

Material	Delrin	Plexiglas	Poly-Carbonate
C_1	.0804	.0595	.0885
C_2	62.6	15.7	7.95
C_3	-.0935	.156	0.335

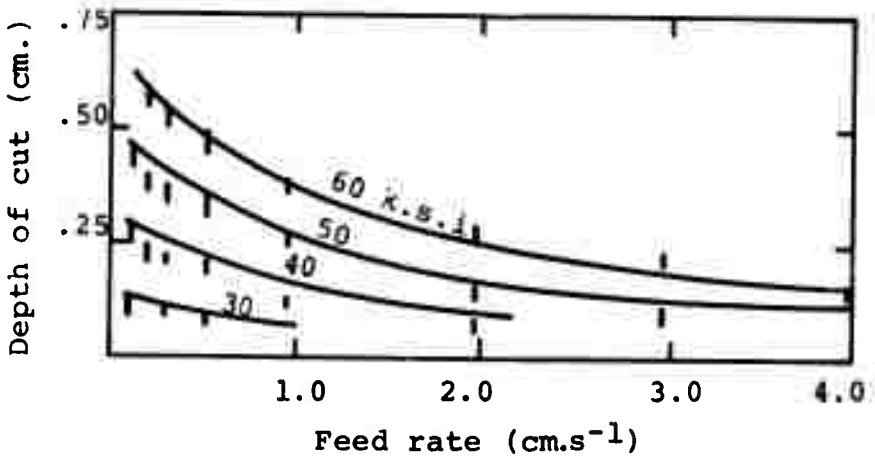

Figure 127(a). Delrin sheet cut with a nozzle of 0.076-mm. diameter (after Ref. 84).

| is the experimental result, the curves are the theoretical predictions.

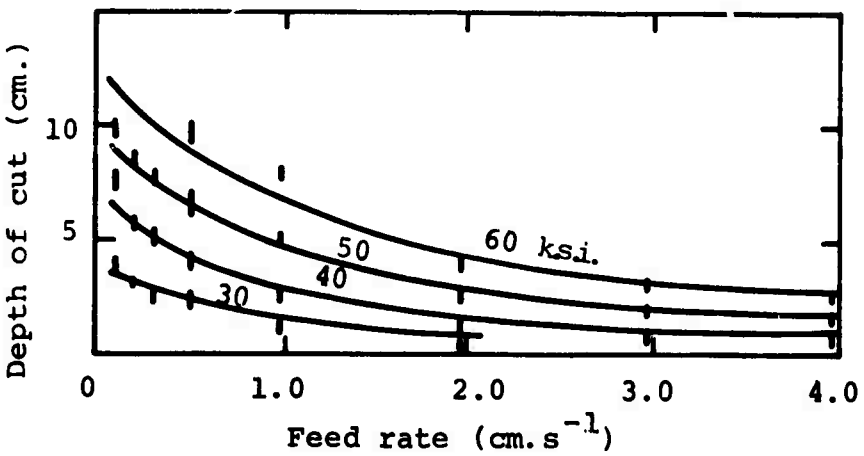

Figure 127(b). Delrin cut with a nozzle of 0.127-mm. diameter (after Ref. 84).

| is the experimental result, the curves are the theoretical predictions.

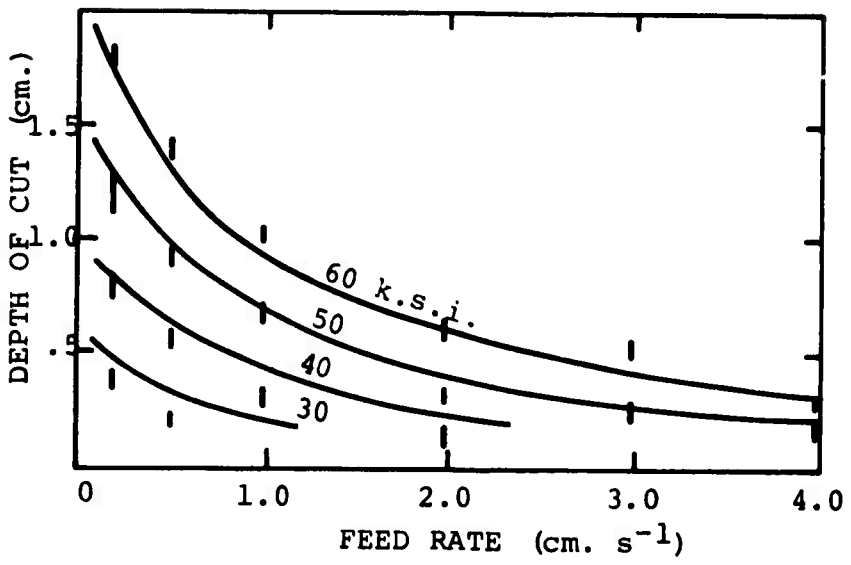

Figure 127(c). Delrin cut with a nozzle of 0.178-mm. diameter (after Ref. 84).

| is the experimental result, the curves are the theoretical predictions.

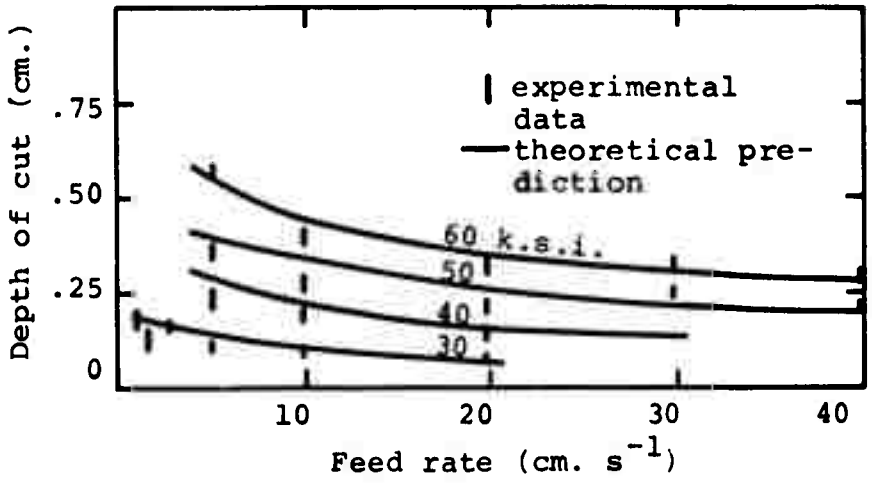

Figure 128(a). Polycarbonate cut with a nozzle of 0.076-mm. diameter (after Ref. 84).

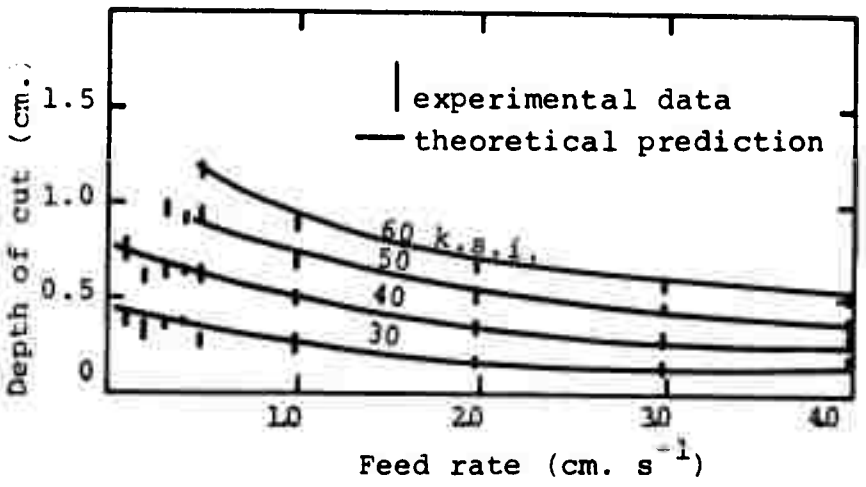

Figure 128(b). Polycarbonate cut with a nozzle of 0.127-mm. diameter (after Ref. 84).

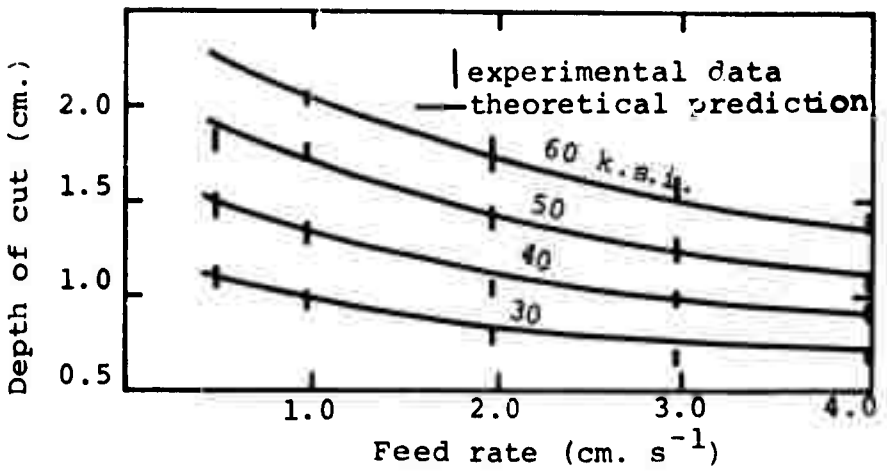

Figure 128(c). Polycarbonate cut with a nozzle of 0.178-mm. diameter (after Ref. 84).

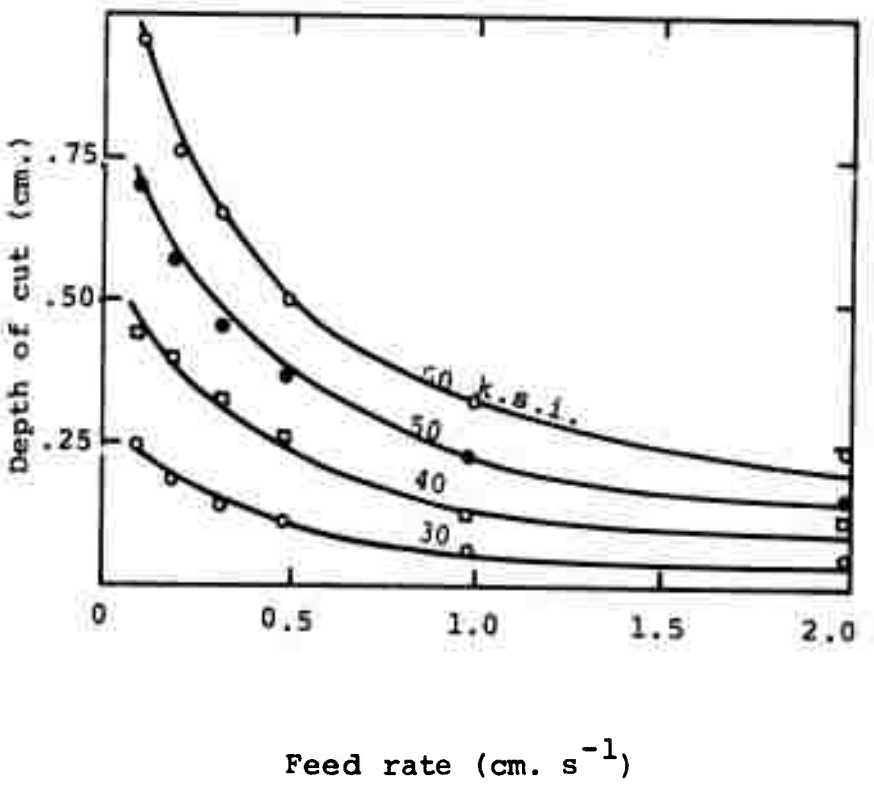

Figure 129(a). Plexiglas sheet cut with a nozzle of 0.075-mm. diameter (after Ref. 84).

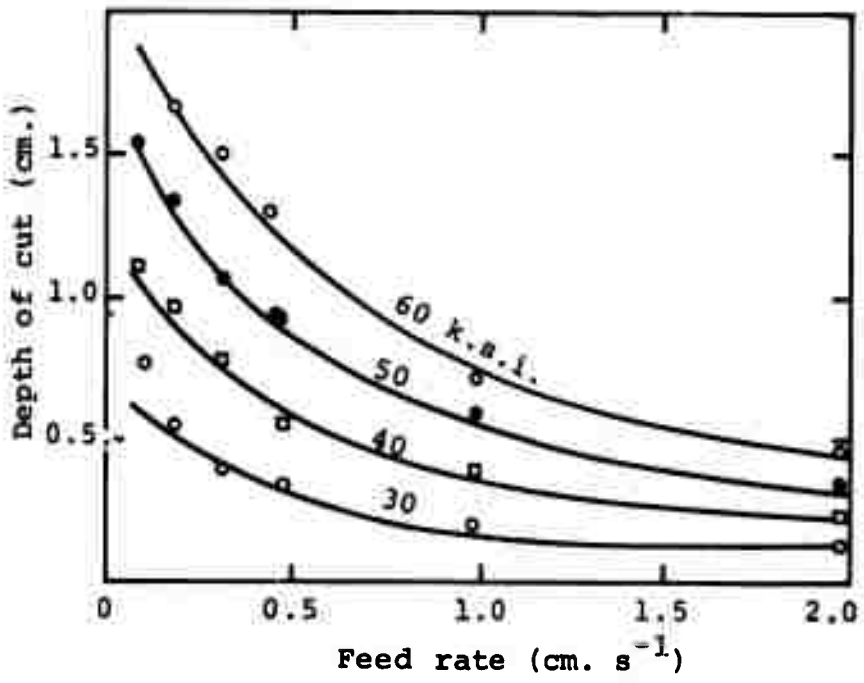

Figure 129(b). Plexiglas cut with a nozzle of 0.127-mm. diameter (after Ref. 84).

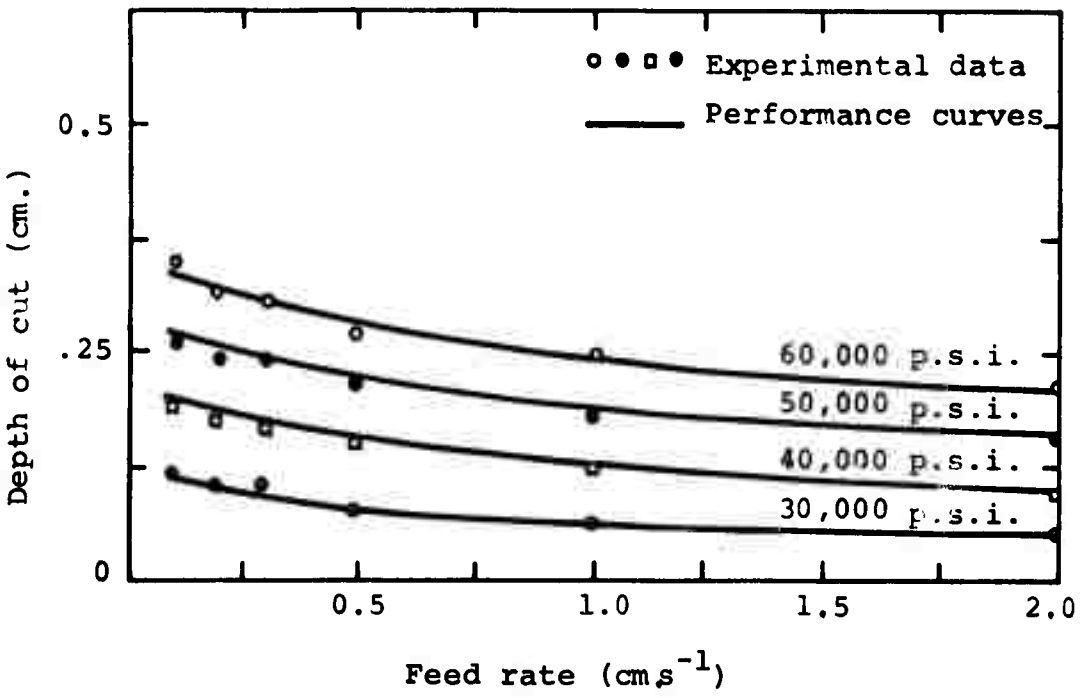

Figure 130(a). Phenolic sheet cut with a nozzle of 0.076-mm. diameter (after Ref. 85).

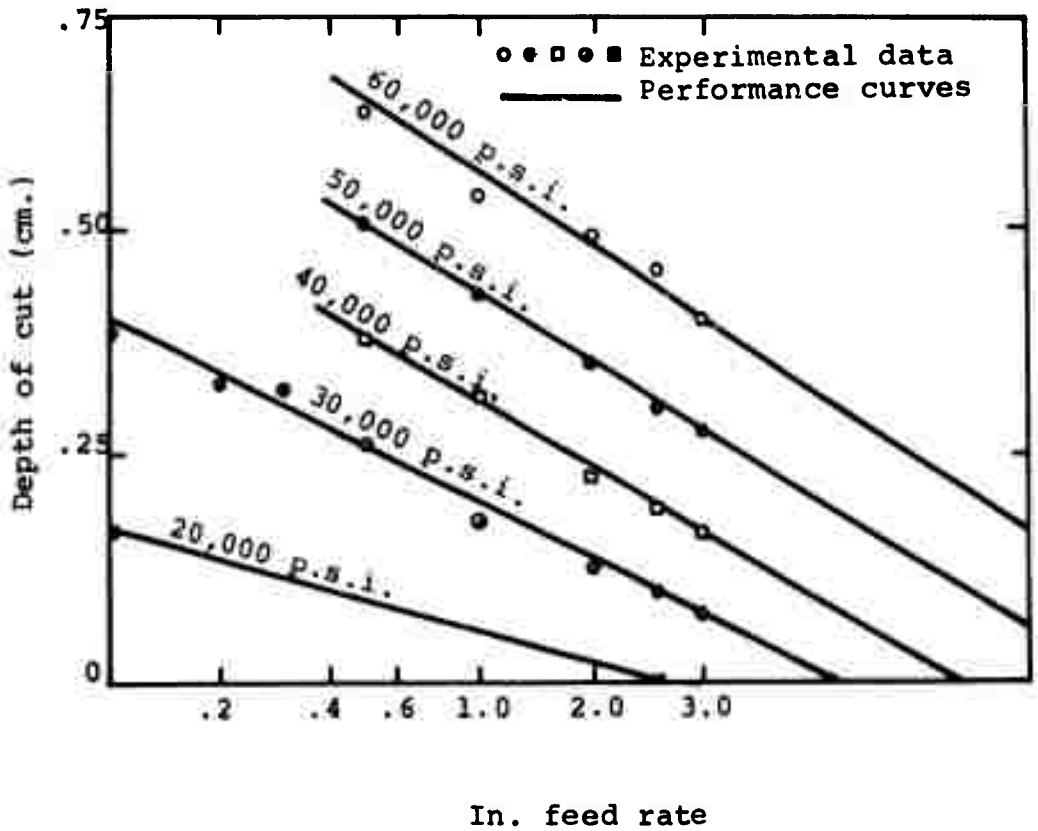

Figure 130(b). Phenolic sheet cut with a nozzle of 0.076-mm. diameter (after Ref. 85).

APPENDIX II

Test Procedures

Test procedures for the pressure profiling studies, the photography of the jet structure at McCartney and the soil cutting tests at McCartney and Rolla are herein described.

1. Pressure Profiling Studies at Rolla

The fluid was supplied by a 75 hp Kobe pump unit through a 9/16-in. outer diameter stainless steel pressure pipe to the nozzle assembly. This was clamped to direct the jet along the axis of a lathe bed toward the central chuck. The clamping device contained two sets of Allen screws to adjust the inclination of the nozzle and was screw-mounted for vertical height adjustment. A pressure transducer was fixed to the travelling carriage of the lathe and oriented such that the jet axis was parallel to the axis of the transducer. A shield consisting of a hardened steel plug with a 0.02-in. central hole was threaded over the end of the transducer. The pressure transducer was connected to give the vertical component (y-axis) on an x-y recorder. An LVDT (linear variable differential transformer) indicator unit was clamped to the lathe with the plunger springmounted against the carriage which carried the pressure transducer. The signal from the LVDT was fed to the x-y recorder to give the horizontal component (x-axis).

The carriage was advanced to locate the face of the transducer shield at the required distance from the face of the nozzle. The pump was started and the pressure raised to the required level. The carriage was fed across the lathe until the readout on the x-y recorder indicated a maximum value, which located the central plane of the jet. The carriage was returned to this position. The height and inclination of the jet nozzle was re-adjusted until the readout from the pressure transducer indicated a new maximum. The center of the jet was now aligned with the center of the transducer. The transducer carriage was traversed out of the jet, a fresh piece of recording graph paper was inserted in the x-y recorder and the transducer was traversed at a slow constant speed through the jet. The carriage was advanced to a new location and the procedure was repeated. It was found necessary to realign the location of the jet and transducer axes for each reading, because of the variation in jet path from the horizontal.

2. Jet Photography at McCartney

The nozzle at the McCartney installation was oriented to direct the jet vertically downward. An expanded form shield laid over a collecting container was found sufficient as a receptor for the jet, the foam was located at a distance of 3 ft. from the nozzle.

A standard 35 mm. reflex camera fitted with a single 50 mm. lens and closeup attachment was used to obtain a record of each jet, the image being recorded on Kodak Tri-X film. The camera was tripod mounted at a distance of 9 in. from the jet axis. This enabled accurate relocation of the camera after it was removed for reloading. A General Radio Strobetac was used as a light source and set to give a flash duration of 0.8 μsec. The source was either directed to front light the jet or by location behind the jet, it was directed onto a ground Plexiglas screen which provided backlighting for the jet.

Two camera positions were established, with equivalent light positions such that the first and third 9-in. sections of the jet were clearly recorded. For each fluid concentration the procedure was to first mix a 5 gal. solution and place this in the pressurized supply tank leading to the McCartney pump. The camera was loaded and the lightproof frame surrounding the test section was closed. The pump was switched on and raised to the required pressure at which point the camera shutter was opened, the flash source triggered, and the shutter closed. The sequence of taking photographs for each jet fluid was standardized such that both front and backlit pictures of the jet for either of the two locations were recorded on the same film. In this manner, since the camera and jet positions remained constant, the scale, which is clearly seen when the jet was front lit, also held for the equivalent backlit pictures.

3. Soil Testing at McCartney

It was apparent, from the little effect which the series of jet structure tests had had on the target foam, that tests beyond a standoff distance much over 2 ft. with the nozzle sizes useable at McCartney would yield little effective result. Concurrently, preliminary tests showed that at a small standoff distance 1.25 in. the jet penetrated but, due to cut narrowness and infilling by subsequently cut material, little soil removal occurred. Two distances of test were accordingly chosen, 10 ins. and 22 in.

The soil sample was first loosely filled into the retaining frame and half the sample tamped down using an impacting hammer and a wooden platen to distribute the impact load. The consolidated section was refilled and further compacted until the two halves were filled to a standard height. The variation in height was achieved by a platform which was located beneath the retaining frame raising the carriage and reducing the standoff distance.

The frame was wheeled, but since the weight of the sample was too great for the available driving system it was manually driven under the cutting jet. Although this introduced a greater possibility of error into the system, nevertheless this method was felt sufficiently accurate for these exploratory tests since the true slot dimension was concealed by the subsequent re-entry of ejected material.

The speed of advance was determined by timing the traverse of the sample under the jet. Measurements were made over the central section of the sample away from the initial impact point since, due to the large inertia of the box, traverse velocity was quite steady after movement began. Where traverse velocity departed from the required value the experiment was repeated.

The procedure was to locate the edge of the sample frame under the jet nozzle and raise the jet pressure, while bypassing the nozzle. When the required pressure level was reached the flow was directed through the nozzle and the sample traversed under the jet. The pressure was then reduced and the pump shut off. Measurements of the slot dimension were made at inch increments down the slot and averaged. Depth was measured from a wire stretched over the slot at the height of the sides, to the surface of the material. This gave an effective slot depth although in many cases the initial slot depth was up to 2 ins. deeper, a depth reduced by the deposition of subsequent ejecta.

4. Soil Testing at Rolla

The soil testing at Rolla was modified so that the jet could be traversed over the sample rather than the converse. Jet fluid was supplied to the nozzle through a rotatable coupling so that this could be effected. The sample was retained in a steel frame located so that as the jet issued from the nozzle the standoff distance was 5 ft. 6 in. (Figure 25). The nozzle was traversed by hand over

the sample surface, since the purpose of the experiment was qualitative rather than quantitative. (The test was to show if jets could move soil at this distance rather than to parameterize the performance.) The pump was started, the pressure raised to the required level, the nozzle traversed over the surface, and the pump shut off. Measurements of the slot cut were made in the same manner as for the tests at McCartney.

The nozzles used in the tests at UMR were of the simple cone and straight section type as illustrated in Figure 55 of Appendix I. The conic angle was 18 degrees included, and the throat length was three times the nozzle diameter.

APPENDIX III

Method of Mixing

For the chemicals, Dow AP-30, Dow AP-273, Jaguar, Alfonic Ethoxylate 1214-60, Polyhall 654, and Polyox, the additive was slowly added to a solution while the solution was stirred by a rotating brass rod.

The mixing procedure of α-Napthol and CTAB is to fill two tanks equally with sufficient water that when combined, the solutions will be at the required weight percent. Transfer the required amounts of α-Napthol and CTAB to the tanks. Agitate. (If only one agitator is available, start with the α-Napthol). While continuing to agitate the fine suspension of α-Napthol, drain the CTAB tank into the α-Napthol tank. Agitate one to two hours. A screen may be necessary for this test due to incomplete solubilization of the α-Napthol.